Fall 12-2020

Not Too Hot, Not Too Cold, But Moderately Variable: The Influence of Environmental Variability on Coral Thermal Tolerance

Courtney Nicole Klepac
Old Dominion University, cklep001@odu.edu

NOT TOO HOT, NOT TOO COLD, BUT MODERATELY VARIABLE: THE INFLUENCE OF ENVIRONMENTAL VARIABILITY ON CORAL THERMAL TOLERANCE

by

Courtney Nicole Klepac
B.S. December 2008, Texas A&M University at Galveston
M.S. August 2014, Florida Atlantic University

A Dissertation Submitted to the Faculty of
Old Dominion University in Partial Fulfillment of the
Requirements for the Degree of

DOCTOR OF PHILOSOPHY

ECOLOGICAL SCIENCES

OLD DOMINION UNIVERSITY
December 2020

Approved by:

Daniel J. Barshis (Advisor)

David Gauthier (Member)

Richard Zimmerman (Member)

Mikhail Matz (Member)

ABSTRACT

NOT TOO HOT, NOT TOO COLD, BUT MODERATELY VARIABLE: THE INFLUENCE OF ENVIRONMENTAL VARIABILITY ON CORAL THERMAL TOLERANCE

Courtney Nicole Klepac
Old Dominion University, 2020
Advisor: Dr. Daniel J. Barshis

Anthropogenic climate change is causing an increase in the frequency and severity of marine heat waves, resulting in declining health of coral reef ecosystems worldwide. Coral bleaching events – the breakdown in symbiosis between the coral host and their intracellular photosynthetic algae – are increasingly common in recent years and contribute to widespread losses in coral cover. However, bleaching and heat stress responses vary across spatial scales both within and among coral species. Coral populations native to highly variable environments can have greater bleaching resistance than corals from more stable habitats and corals transplanted into these variable reef sites can increase their thermal tolerance, providing promising evidence for the ability of corals to cope with rapid climate change. This dissertation investigates the physiological and genetic response of two massive corals, *Porites lobata* and *Goniastrea retiformis,* from a Moderately Variable (MV) and a Low Variability (LV) pool transplanted into a Highly Variable (HV) pool on Ofu Island in American Samoa. Paired transplant and native ramets were exposed to an acute thermal stress every six months (for 1.5 yrs) to evaluate changes in thermal tolerance. For both species, photosynthetic efficiency and chlorophyll loss following acute heat stress did not differ between ramets transplanted into the HV pool and respective native pool. Surprisingly, HV *P. lobata* exhibited the greatest bleaching susceptibility compared to MV and LV natives and there was no effect of acute heat stress on MV *P. lobata*. Genetic and gene expression patterns indicate shared responses to heat stress in the coral host, yet population-level differences were observed in response to acclimatization to a novel environment and symbionts had distinct variation in reacting to heat stress. During this study, Ofu's backreef temperature regime surpassed historical records and fine scale temperature variation across reefs may have contributed to increased susceptibility of HV *P. lobata*. These results represent a stark contrast with other research on coral tolerance in

variable environments, potentially underscoring species-specific mechanisms and regional thermal anomalies that may be equally important in shaping coral responses to extreme temperatures.

To the woman, deathly afraid of water, but wholeheartedly supported my love of it. My grandmother Caley Nell Klepac gave me more than my initials, she championed whatever I was passionate about and loved to hear all my stories. I dedicate my dissertation to her and continue to strive for great accomplishments in her memory.

ACKNOWLEDGEMENTS

I would first like to thank my advisor, Dr. Dan Barshis, for his guidance, support, and compassion throughout my doctoral journey. His unique and innovative approaches to executing research and making sense of the complexities of nature are an inspiration and have taught me more during my dissertation than I ever could have imagined. To my committee members (past and current): Drs. David Gauthier, Mark Butler, Mikhail Matz, and Richard Zimmerman, thank you for your constructive suggestions and challenging me to be a more critical scientist. Each of you have taught me in your own respective field that little details always matter and the importance of a clear, informative Figure.

I also must recognize those who assisted in my research, members from Old Dominion University sequencing facility and computing cluster, University of Santa Barbara sequencing facility, National Park of American Samoa (NPSA) staff, and the American Samoa Department of Marine and Wildlife Resources. A special thank you to Deb and Ben Malae and Tongan Mike – without your company and assistance, remote field work with limited resources would have been a failure. There were countless occasions where your personal connections, vehicles, gasoline, duct tape, and towels saved the day and for that, this research is indebted to you. Appreciation is also warranted for others: Mark Schmedik, Kaho Tisthammer, and Robert Richmond for use of your freezers, Caroline Rising-Maxie for always making sure my samples will make it to the U.S. and that I drink enough wine before the red-eye flights home. An additional thank you to my undergraduate research assistant Caroline Haymaker for bravely traveling with me to Ofu Island, learning to snorkel in some hairy conditions, and being my research sidekick for the laborious setup of my second chapter.

To my dearest friend, Hannah Aichelmann, one of the brightest coral scientists I know and look up to. Sharing two years side-by-side in the Barshis lab did wonders for my productivity, critical thinking and overall well-being. We bounced ideas and analyses off of each other, shared many wine bottles to ‘whine’ about research woes, and made the time to go on epic through-hiking adventures. I cherish our friendship and admire your capacity to be an outstanding scientist and true friend, and hope we get to work together again one day!

To my immediate and extended family, although my career goals took me away from countless visits, weddings, and holidays in central Texas, you have always given so much love and support from afar for my passion to pursue coral reef biology.

This research was funded by a grant awarded to Dr. Dan Barshis from the National Oceanographic and Atmospheric Administration - Coral Reef Conservation Program (NA15NOS4820080), and scholarships awarded by the Women Diver's Hall of Fame, and ODU's Biology Department. Field research was conducted under the American Samoan Government's Department of Marine and Wildlife Resources permit and a NPSA permit # NPSA-2015-SCI-0012.

TABLE OF CONTENTS

Page

LIST OF TABLES

Page

LIST OF FIGURES

Page

CHAPTER 1

INTRODUCTION

The Coral-Algal Symbiosis

Scleractinian corals are ecosystem engineers responsible for building and supporting highly productive and biodiverse coral reef habitats. Coastal areas and island nations rely heavily on local reefs for food, shoreline protection, and as a source of income through tourism and harvesting (Moberg and Folke 1999). The trophic and structural success of tropical reef building corals is attributed to the mutualistic symbioses between corals, dinoflagellates of the family Symbiodiniaceae (Muscatine and Porter 1977; Trench 1993; Stat et al. 2006; LaJeunesse et al. 2018), and a plethora of other unicellular taxa. This symbiotic association is centered around nutrient exchange, whereby Symbiodiniaceae translocate photosynthetically fixed glucose in exchange for inorganic nitrogen, phosphorus, and carbon (Yellowlees et al. 2008) and can account for up to 100% of the coral energy needs (Muscatine and Porter 1977). Within the coral gastroderm a specialized organelle, the symbiosome, houses Symbiodiniaceae, providing protection from herbivory, as well as stable intracellular pH by concentrating dissolved inorganic carbon for photosynthesis (Barott et al. 2015; Tresguerres et al. 2017). Moreover, the coral host modulates resident Symbiodiniaceae populations by adjusting their light environment and cellular densities (Schlichter and Fricke 1990; Jones and Yellowlees 1997; Smith et al. 2013).

The dynamic resource exchange in the coral-algal partnership is predominantly determined by Symbiodiniaceae performance, which is dependent on light and thermal thresholds (Rowan and Knowlton 1995; Hoegh-Guldberg and Jones 1999; LaJeunesse et al. 2010). Symbiodiniaceae is subdivided into nine genera (previously Clades [A-I]; Pochon et al. 2004; LaJeunesse et al. 2018), where diverse physiologies within and among species affect overall coral growth and performance (Baker 2003; Little et al. 2004; Berkelmans and Van Oppen 2006; Abrego et al. 2008). Moreover, the identity and abundance of Symbiodiniaceae genotypes affects the ecological functioning of the symbiosis (e.g., stress tolerance, latitudinal distributions, etc.). For example, it has been shown that particular species, namely from the genus *Durusdinium* (previously clade D), enhance heat stress resistance and aid in recovery (Buddemeier and Fautin 1993; Baker 2003; Ulstrup et al. 2006; Oliver and Palumbi 2011). Local environmental factors influence the underlying eco-

physiology of specific coral-Symbiodiniaceae combinations, contributing to persistence under current conditions and determining survival under a changing climate.

Coral Bleaching

In the past three decades, increased global sea surface temperature resulting from climate change has led to a widespread decline in tropical coral reefs (Hughes et al. 2003; Baker et al. 2008). Although many factors can contribute to coral stress (i.e. changes in salinity, sedimentation and/or pollution, high irradiances; Goreau 1964; Gleason and Wellington 1993; Van Woesik et al. 1995; Brown 1997), increases in seawater temperatures of ~ 1-2 °C above the mean summer maximum of a given area are the leading cause of coral bleaching and mortality events (Hoegh-Guldberg 1999; Jokiel 2004; Donner et al. 2005). For instance, the mass coral bleaching event of 1998 led to the mortality of 16% of the world's coral reefs (Wilkinson 2000), and current projections estimate reef losses up to 60% by 2030 (Wilkinson 2006). Coral bleaching is a breakdown of the symbiotic relationship, whereby extended periods of stress cause substantial loss of symbiont cells (Brown 1997) and/or significant reductions in photosynthetic pigments *in hospite* (Douglas 2003). Evidence suggests that bleaching begins with damage to symbiont photosynthetic machinery (Lesser 1996; Fitt et al. 2001). Unless the symbiotic exchange of nutrients can be re-established via the uptake of healthy Symbiodiniaceae from the water or cryptic populations, coral mortality will result (Hoegh-Guldberg 1999; Jokiel 2004). It is therefore crucial to gain a better understanding of the physiological and molecular mechanisms responsible for coral bleaching mortality and survival.

Adaptation and Acclimatization in Thermal Tolerance

Previous studies consistently demonstrated a tight correlation between coral bleaching incidences and higher-than-normal sea temperatures (Goreau and Hayes 1994; Brown 1997), leading to the consensus of a regional bleaching threshold at ~1 °C above mean summer maxima (Jokiel and Coles 1990; Hoegh-Guldberg 1999). Recently however, a growing body of research supports widespread variation in coral bleaching thresholds. Bleaching susceptibility differs across space and time, where bleached and unbleached corals are side by side and previous exposure can change subsequent phenotypic and genetic responses, respectively (Berkelmans and Willis 1999). Coral bleaching can also vary among conspecifics and symbiotic associations, resulting in different

bleaching thresholds (Baird and Marshall 2002; Coles and Brown 2003; Abrego et al. 2008; Howells et al. 2016).

Given variable bleaching susceptibility, there are three possible outcomes for corals following exposure to frequent thermal stress: mortality, adaptation, or acclimatization (Gates and Edmunds 1999; Hughes et al. 2003; Weis 2010b; Edmunds et al. 2014). Adaptation refers to genotypic shifts in coral populations, where natural selection acts on an individual's trait(s) that increase fitness over evolutionary timescales. Corals are long-lived organisms, therefore adaption from novel mutations over many generations may be too slow to keep pace with climate change impacts (Hughes et al. 2003), and literature illustrating contemporary coral adaptation to warming temperatures is scant. Acclimatization refers to an organism adjusting its phenotype in response to multiple environmental factors during its lifetime (Prosser 1973) and is considered a promising mechanism for withstanding the impacts of climate change (Somero 2010b).

Around the globe, many reef environments contain corals living at, near, and sometimes surpassing regional bleaching threshold limits (Coles 1997; Craig et al. 2001; Riegl et al. 2011). Thermally variable or extreme habitats, such as shallow backreef pools and the Persian/Arabian Gulf, regularly experience high temperatures that typically bleach conspecifics from milder, or well-mixed environments. Acclimatization to brief, but frequent high water temperature pulses during summer months (Coles 1975; Palumbi et al. 2014) can give an organism a performance advantage over another not exposed to that environment (Leroi et al. 1994; Huey et al. 1999; Oliver and Palumbi 2011). Additionally, corals from milder environments can also acquire improved thermal tolerance when exposed to repeated heat pulses at levels similar to those experienced by thermotolerant corals (Edmunds 2014; Palumbi et al. 2014). Coral populations able to employ acclimatization strategies to withstand novel environments and persist under long-term selective pressures are potential representatives for climate change survival.

Ofu Island – A Natural Laboratory

The reefs of Ofu Island, American Samoa serve as a natural laboratory, as there is no nearby anthropogenic influence to confound or exacerbate environmental effects. Over a decade of research on reefs in the National Park of Ofu confirms that certain coral populations have enhanced bleaching resistance and broad acclimatization to particular environmental thresholds (Craig et al. 2001; Smith et al. 2007, 2008; Oliver and Palumbi 2009, 2010, 2011; Barshis et al. 2010, 2013; Palumbi et al. 2014; Bay and Palumbi 2015; Seneca and Palumbi 2015; Bay et al. 2016). Ofu

backreef sites occur at a similar depth (0.5-3m at low tide) but have distinct temperature regimes (Figure 2.1). The highly variable (HV) pool experiences temperatures as high as 35 °C, with daily fluctuations up to 4-5 °C and temperatures as low as 24.5 °C (Craig et al. 2001), whereas the moderately variable (MV) pool ranges from 32-25 °C (Bay and Palumbi 2014). The expected bleaching threshold for the Samoa region is 30.19 °C (http://www.coralreefwatch.noaa.gov), and the HV and MV pools surpass this threshold 3.6% and 0.96% of the time, respectively (Bay et al. 2016). In addition to temperature fluctuations, other environmental stressors such flow, solar radiation, dissolved oxygen, and nutrient concentrations (Craig et al. 2001; Smith et al. 2007) are more dynamic within the HV pool, especially during summertime low tides.

Despite environmental variability, coral species diversity is moderately high on Ofu Island. Of the 85 total species, 79 are found in the MV pool while 52 are found in the HV pool (Craig et al. 2001). However, most coral thermotolerance research on Ofu has been focused on two species of the branching, environmentally sensitive coral genus *Acropora* (Oliver and Palumbi 2011; Barshis et al. 2013; Palumbi et al. 2014; Bay and Palumbi 2015). These studies demonstrated that corals originating from, or acclimated to, the HV pool have increased thermal tolerance compared to conspecifics from the MV pool <1 km away. In addition to these studies, research in American Samoa has also examined Symbiodiniaceae diversity in *Acropora* spp.*, Pocillopora* spp.*, Leptoria, Pavona,* and *Millepora* (Oliver and Palumbi 2010) as well as skeletal characteristics, protein expression, and genetic structure in the massive coral *Porites lobata* following a reciprocal transplant experiment between a backreef pool and nearby forereef (Smith et al. 2007; Barshis et al. 2010). Despite this growing body of work, bleaching resistance has yet to be determined for massive corals from the backreef environments on Ofu Island, and it is unknown whether corals from MV and LV have a similar suite of responses to increased temperatures as HV corals.

Research Overview

Central to predicting the survival of coral reefs is whether corals are able to acclimatize and/or adapt in their upper stress tolerance limits to match or exceed the rate of global climate change. Globally, many coral reef populations naturally possess and/or can acquire increased thermal tolerance in high thermal variability environments in comparison to corals from more stable reefs, but this body of research is generally restricted to branching coral genera. Biological traits such as colony morphology, growth rate, and reproductive mode separate branching from

massive coral species into “competitive” and “stress-tolerant” life-histories, respectively (Darling et al. 2012). Large, slow growing massive corals are thought to be more thermally tolerant to chronically variable and disturbed habitats than branching species given life-history traits such as increased tissue thickness and energy surplus (Edmunds and Davies 1989; Loya et al. 2001; van Woesik et al. 2011). For my dissertation, I sought out to validate the suggested tolerance of massive coral species and whether enhanced bleaching tolerance is accessible to additional Ofu Island coral species other than from the genus *Acropora*? The aim of this dissertation is to characterize the thermal tolerance and underlying mechanisms of stress tolerance in two massive scleractinian coral species by integrating field ecology, organismal physiology, genetics and transcriptomics, as well as environmental temperature regimes.

Chapter 2: Reduced thermal tolerance of massive coral species in a highly variable environment

The well-studied backreefs of Ofu Island serve as a natural laboratory to investigate coral thermal tolerance and possible mechanisms underlying bleaching susceptibility. It is unknown whether massive coral species from contrasting backreef environments can also acclimatize to the conditions of the Ofu Highly Variable (HV) pool and increase their bleaching tolerance. To characterize the ability and timeline of thermal tolerance modifications of two massive coral species, *Goniastrea retiformis* and *Porites lobata*, ramets from two nearby backreef populations were transplanted into the HV pool, and physiological and symbiont genetic assemblage responses to transplantation and acute heat stress were measured at 6 and 12 month time scales. I found that corals transplanted into the HV pool did not have improved thermal tolerance, and most surprising was reduced tolerance in HV *P. lobata* under acute heat stress.

Chapter 3: Exploring the Scale of High-Resolution Thermal Variability and its Relationship with Bleaching Susceptibility

Increased thermal variability has a positive relationship with coral bleaching resistance, yet the findings from Chapter 2 illustrate a reduced tolerance in massive corals originating from the HV pool. Discrepancies in the way researchers measure and attribute chronic thermal heat stress with coral bleaching potentially undermines our understanding of how small-scale thermal conditions influence heat stress responses. Here, temperature metrics for each backreef pool are compared against regional sea surface satellite temperature data in attempt to characterize which

metrics likely correlate with physiological traits in the massive coral *Porites lobata.* In addition, physiological responses to acute heat stress and transplantation were again characterized and correlated to natural bleaching stress responses of donor colonies with the aim of understanding how small-scale thermal variability, natural, and experimental heat stress is related to coral bleaching responses. Although *in situ* calculations of thermal variability and cumulative heat loading was greater in the HV environment in comparison to the MV and LV pools, this did not translate into population-level differences in natural bleaching responses. In addition, various calculated temperature metrics correlated with *P. lobata* traits, where greater variability had a positive relationship with coral growth but a negative relationship with photophysiology and HV corals again demonstrated reduced thermal tolerance in comparison to MV and LV native corals.

Chapter 4: Population-specific gene expression patterns in response to acute heat stress and novel reef environments

Gene expression studies offer a mechanistic link between genetic and physiological responses to environmental change. Underlying molecular mechanisms in coral thermal tolerance could corroborate observed site-specific differences in *P. lobata* coral growth and physiological tolerances following transplantation and acute heat stress responses. This chapter compared population-level genetic differentiation and transcriptomic profiles of *P. lobata* and *in hospite* Symbiodiniaceae from six transplant groups to investigate potential gene expression differences in response to heat stress and transplantation. While the coral host demonstrated a largely shared response to acute heat stress with subtle differences in gene expression patterns in response to transplantation, their algal symbionts revealed much stronger differentiation in gene expression based on site of origin, corroborating the photophysiological results observed in the first and second chapters. The number of differentially expressed genes in coral host and symbiont from the HV pool were greater than MV corals and symbionts, which could suggest a greater response to acute heat stress thus contributing to reduced tolerance observed at the physiological level.

CHAPTER 2

REDUCED THERMAL TOLERANCE OF MASSIVE CORAL SPECIES IN A HIGHLY VARIABLE ENVIRONMENT

Published July 22, 2020 in the Proceedings of the Royal Society B 287: 20201379.
http://dx.doi.org/10.1098/rspb.2020.1379

Introduction

The frequency and magnitude of environmental variation is increasing in the upper ocean (Pachauri et al. 2014) as our global climate rapidly warms. Environmental variability strongly influences organismal physiology and behavior (Gilchrist 1995; Parmesan 2006), community assemblages (Levin and Paine 1974), and ultimately the integrity of ecosystems (Baker et al. 2008). Impacts of climate warming are further magnified in marginal/extreme environments, such as low, high, or highly variable temperature, pH, and/or CO_2 sites (Boyd et al. 2016; Camp et al. 2018). However, a number of studies show organisms in variable environments may have enhanced tolerance compared to those in more moderate habitats due to acclimatization or adaptation (Sgro et al. 2010; Oliver and Palumbi 2011; Palumbi et al. 2014; Kenkel et al. 2015; Schoepf et al. 2015). Alternatively, warm-adapted species in these extreme environments may be particularly at risk since they live closest to their upper thermal limit and may have limited acclimation capacity (Stillman and Somero 2000; Stillman 2003; Somero 2010a). Although these populations have likely evolved the greatest thermal tolerance, it is possible an increased cost is involved maintaining this tolerance (Stillman 2003) compared to other populations with lower tolerances (Calosi et al. 2008). Such a trade-off is critical for understanding the susceptibility of these populations to climate change.

Tropical reef-building corals live close to their upper thermal limits and are particularly sensitive to periods of elevated sea surface temperatures (Coles et al. 1976; Heron et al. 2016). Despite coral vulnerability to climate impacts, marginal and extreme reef habitats contain assemblages of corals that have acclimated and/or adapted to survive near or at their thermal thresholds (Craig et al. 2001; Riegl et al. 2011; Schoepf et al. 2015; Camp et al. 2017). Resident coral populations in these environments are continuously exposed to highly variable abiotic

conditions, yet coral diversity remains high (Craig et al. 2001) and upper temperature tolerances are significantly higher than conspecifics from higher latitudes (Coles et al. 1976) or less variable environments (Oliver and Palumbi 2011; Howells et al. 2013; Kenkel et al. 2013b; Palumbi et al. 2014; Kenkel et al. 2015; Schoepf et al. 2015; Camp et al. 2017; Barshis et al. 2018). Mechanisms that contribute to high heat tolerance result from increased prevalence of heat tolerant photosymbionts (Durusdinium spp. family Symbiodiniaceae; Oliver and Palumbi 2010; but see Howells et al. 2016; LaJeunesse et al. 2018), modifications in gene regulation (Barshis et al. 2013; Kenkel and Matz 2016), adaptive divergence between coral populations (Barshis et al. 2010; Kenkel et al. 2013b; Bay and Palumbi 2014; Dixon et al. 2015; Howells et al. 2016), and/or potential epigenetic contributions to thermal tolerance (Dixon et al. 2015; Putnam and Gates 2015). As a result, highly variable habitats have become popular natural laboratories to understand the capacity of and mechanisms underlying coral stress tolerance (Palumbi et al. 2014; Barshis et al. 2018; Camp et al. 2018).

One such system that has been extensively studied is the network of backreef pools within the National Park of American Samoa on Ofu Island. These backreef pools are nearly identical in species diversity and percent live coral cover, yet have distinct differences in small-scale environmental variability driven by tidal cycle and pool size (Craig et al. 2001; Smith et al. 2007; Oliver and Palumbi 2011). Coral populations from two pools – a small, highly variable (HV) and a larger, moderately variable (MV) pool – exhibit both fixed and acclimatory responses to highly variable temperatures that contribute to enhanced thermal tolerance (Palumbi et al. 2014). However, much of the research examining coral resilience in Ofu and elsewhere has been conducted on thermally susceptible branching corals, such as *Acropora spp.* (Loya et al. 2001; Middlebrook et al. 2008; van Woesik et al. 2011; Howells et al. 2013; Palumbi et al. 2014; Thomas et al. 2018). Thus, there is scant evidence on whether massive, more stress-tolerant corals exhibit similar responses to increasing environmental variability (Brown et al. 2015; Barshis et al. 2018).

Additionally, evidence of tolerance trade-offs in organisms from highly variable habitats has been documented in intertidal porcelain crabs (Stillman and Somero 2000; Stillman 2003) and snails (Tomanek and Somero 1999), diving beetles (Calosi et al. 2008), and seaweeds (Davison and Pearson 1996), but the potential negative impacts of extreme environments are largely unknown for tropical reef-building corals. Broadly, trade-offs in stress tolerance can result in reduced fecundity (Hoffmann et al. 2003; Muller-Landau 2010) and growth (Davison and Pearson

1996; Calosi et al. 2013), changes in basal gene expression (Hoffmann et al. 2003), transgenerational effects on offspring size and metabolism (Burgess and Marshall 2011), and a limited scope for further acclimation to warmer temperatures (Stillman 2003; Calosi et al. 2008). For corals, the few documented consequences of elevated heat tolerance trade-offs involve reduced lipids, growth, and eggs size (attributed to hosting Durusdinium; Jones and Berkelmans 2011; Cunning et al. 2014) and reduced larval size (Putnam and Gates 2015). However, we don't know whether similar or extensive trade-offs apply to corals in naturally extreme environments, and what the implications would be for future reef habitats in a warming world.

Here, the scope for thermal tolerance was tested in two dominant massive coral species, *Porites lobata* and *Goniastrea retiformis* in the Ofu backreef during an extremely warm year. I compared growth, bleaching sensitivity, and endosymbiont species assemblage (Symbiodiniaceae) of coral samples transplanted into the HV pool compared to corals in the neighboring MV and an additional nearby backreef pool of lesser thermal variability, the LV pool. Corals were exposed to controlled, acute heat stress experiments at six- and twelve-months following transplantation to determine whether massive corals can increase their upper thermal limits similar to branching corals in this extreme environment.

Materials & Methods

Coral collection & transplantation

In July 2015, corals were sampled from three backreef sites (HV, MV, and LV) within the National Park of American Samoa of Ofu Island (14.1780765° S, 169.660109° W). Thirty colonies (n = 5 genets per site/species) of two common massive coral species, *Porites lobata* and *Goniastrea retiformis*, were sampled to remove 24 cores/ramets from each genet in each site (n = 360 cores total per species). Cores were affixed to nylon bolts with Z-Spar, Splash Zone marine epoxy (Carboline Company, St Louis, MO), measured for initial buoyant weight, secured to transplant grids (~36 – 40 cores per grid), and then returned to the respective native backreef site for one week of recovery. Ramets were then divided equally and transplanted into either the HV pool common garden or returned to the native reef site (n = 12 cores/genet/site/species; Figure 2.1). Transplant grids were secured via rebar and cable ties at similar depths ≥.5 m above the sand substrate. During January 2016, the LV native sample grid was dislodged by a cyclone but found

a few days later and re-secured, precluding the six-month native versus transplant pairwise comparisons.

Environmental data

HOBO Pendant temperature loggers (Onset Computer Corp., Bourne, MA) were also deployed on most native and transplant grids at all three backreef sites. Loggers were programmed to collect temperature data every 15 min. At each experimental time point, salinity at each site was measured using a refractometer.

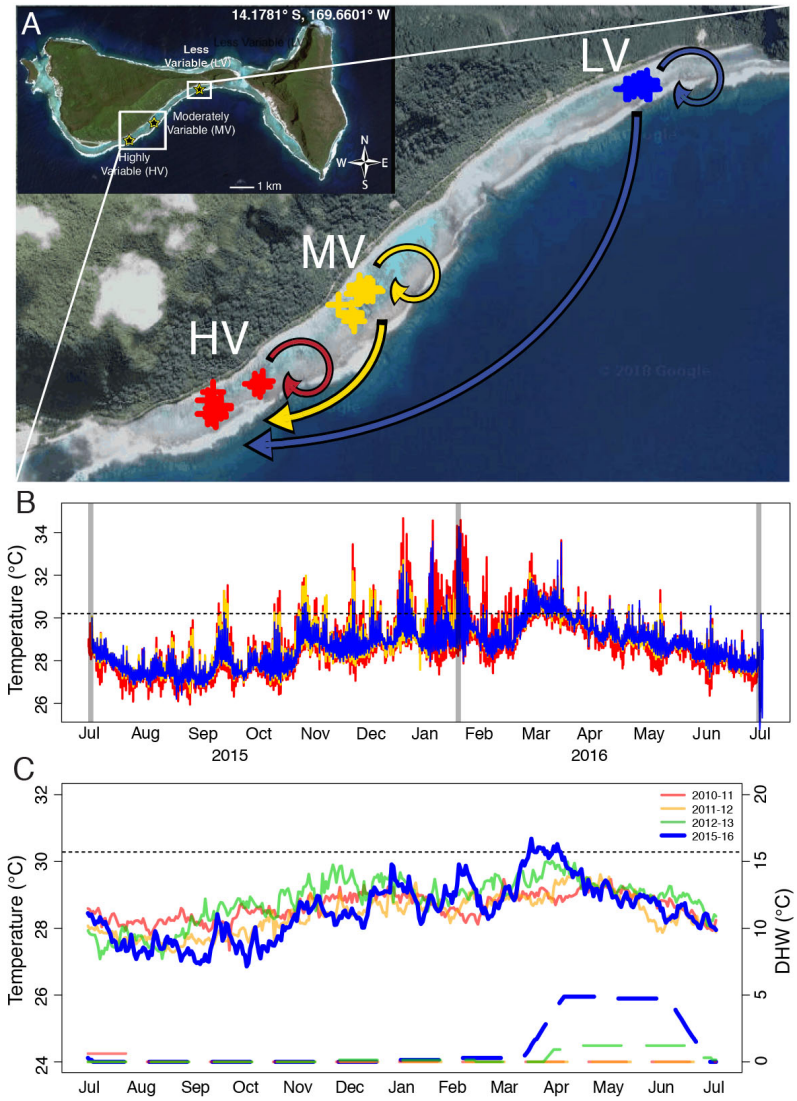

Figure 2.1. (A) Map of Ofu Island, American Samoa. Arrows display transplant experiment design within three backreef pools – HV (red), MV (gold), LV (blue). (B) *In situ* site temperatures during the study period. Vertical gray lines represent start of experiment and data collection time points. (C) Comparison of NOAA CRW 5km Ofu Island sea surface temperatures (solid lines) and Degree Heating Weeks (DHW; dashed lines) during years 2010-2012 (Palumbi et al. 2014) and 2015-2016 (this study). Dotted line represents the regional bleaching threshold, 30.2 °C (NOAA-CRW 2017).

Coral nubbin growth

At each time point – six months (January 17-18, 2016) and twelve months (July 9-11, 2016) after transplantation – 2 ramets per genet per species were collected from the grids in each backreef pool (5 genets * 2 ramets = 10 ramets per species * 2 species = 20 ramets/origin_destination * 5 origin_destination [LV_LV, LV_HV, MV_MV, MV_HV, and HV_HV] = 100 ramets total). Cores

were scrubbed (Dremmel, Racine, WI) to remove algal and epiphyte growth prior to buoyant weight measurements. Coral growth was calculated by subtracting initial weight from final weight and then further divided by the number of weeks since transplantation to determine weekly growth rate.

Heat-stress assays

Coral nubbins were placed in our Coral Bleaching Automated Stress System (CBASS), constructed from Coleman 24 L Party Stacker Coolers™ as head and sump tanks (42 L volume per treatment), resulting in four experimental tank systems – two heat and two control. A pump provided a flow of 88.9 mL sec^{1} to each head tank, which was also fitted with 6 LED bulbs (Phillips PAR38 LED; 500 ± 20 μM photons m^{-2} s^{-1} as measured via a Li-COR Li192 spherical quantum sensor) and 12 hr 7a.m. light/7p.m. dark photoperiod. A flow-through drip system provided 9 L hr^{-1} of local seawater throughout the duration of the experiment.

Following previous experiments by Palumbi et al. (2014), 60 ramets (~30 cm^3; 4 from each genet) were randomly assigned to one of two control and two heat treatment tanks (n ~ 10-15 ramets $tank^{-1}$) and then subjected to an Arduino-based customized temperature controlled ramp program (Klepac and Barshis 2020b) regulating two 60 W chillers and two 150 W titanium heaters. All ramets from a single species were assayed in one day, with the second species assayed the following day. Beginning at 11:00 a.m., temperature increased over 3 hrs from 28 to 36.5 °C for *P. lobata* to 35.5 °C for *G. retiformis*, followed by a 3 hr incubation at the maximum temperature, then a ramp down to 28 °C where they were held for 16 hrs (Figure A1). The control tank was set to remain stable at 28 °C for 22 hrs. The two maximum temperatures were chosen: based on preliminary trials intended to elicit a > 50% bleaching response across all experimental fragments, to represent acute thermal exposures above the local bleaching threshold, and to be ~1 °C above the HV pool's mid-day low tide average maximum temperature.

Symbiodiniaceae physiology under heat stress

To capture the relative photosynthetic efficiency of PSII of *Symbiodiniaceae* during the acute assays, maximum quantum yield (F_v/F_m) was measured using a pulse amplitude modulation (PAM) fluorometer (Junior-PAM, Walz, Germany). Instrument settings were as follows: Measuring Light Intensity = 6; Saturation Intensity = 12; Saturation Pulse Width = 0.6 s; Gain = 2. Following 30 min of dark-adaptation, tops of coral ramets were measured in triplicate at 0 hrs

and 21 hrs (during recovery). F_v/F_m values were normalized over the course of the experiment ((21hr – 0hr)/0hr) were used for statistical analyses to correct for between ramet variation in starting values. F_v/F_m values measured at the end of each assay were used for plotting for simplicity to allow for easy comparison to previous studies.

Following acute heat stress experiments, coral tissue was airbrushed from the skeleton using 35PSS artificial unfiltered seawater, and the resulting slurry was homogenized, centrifuged, and resuspended in 5 mL of seawater. For chlorophyll determination, slurry samples were homogenized using 90% acetone, a glass tissue homogenizer, and a 25 mm GF/F filter, and then stored at 4 °C for 24 hrs. Absorbance spectra was measured using an Ocean Optics Spectrometer (Largo, FL), and cellular chlorophyll *a* and *c* values calculated using the Jeffrey and Humphrey (1975) equation. Total chlorophyll (*a* + c) absorbance was normalized to acetone volume and then scaled to the surface area of each nubbin, measured using the paraffin wax method (Veal et al. 2010). Remaining pigment content, or chlorophyll retention, was calculated as the ratio of total chlorophyll ((heat – control)/control; μg cm^{-2}) in heated to control samples.

Symbiodiniaceae genotyping

Symbiodiniaceae was characterized from both native coral host colonies and corresponding HV pool transplanted replicates at 6 (January) and 12 months (July). A small (1 cm^2) fragment was sampled from 5-10 individuals per site, totaling 15 samples for *G. retiformis* and 15 for *P. lobata*, (collection permit #NPSA-2015-SCI-0015). Samples were incubated for 1-1.5 hour at 65 °C in a 1% SDS in DNABuffer (protocols.iodx.doi.org/10.17504/protocols.io.dyq7vv; Baker and Cunning 2016a) and then transported back to Old Dominion University. Genomic DNA was extracted from the archived coral samples using a guanidinium-based extraction protocol (Baker and Cunning 2016a) and quantified spectrophotometrically. A 350 bp segment of the internal transcribed spacer region 2 (ITS2) rDNA was used for amplification. The ITS2 region was amplified using Symbiodiniaceae specific primers, ITS-Dino-forward (5′-GTGAATTGCAGAACTCCGTG-3′) (Pochon et al. 2001) and its2rev2-reverse (5′-CCTCCGCTTACTTATATGCTT-3′) (Stat et al. 2009). Each primer also contained a universal linker, for downstream incorporation of Illumina adapters and barcodes during the second round of PCR, and four degenerate bases, denoted as N. The forward (‘5′-GTCTCGTCGGCTCGG + AGATGTGTATAAGAGACAG + NNNN) and reverse primer linker (5′-TCGTCGGCAGCGTCA + AGATGTGTATAAGAGACAG + NNNN) preceded the ITS2

forward and reverse primer sequences. PCR reactions (20 µL) consisted of the same reagents and volumes used for coral host PCR, except 0.2 µL of 10 µM forward and reverse primers was used. PCR cycles were run using the following profile: 95 °C for 5 min, followed by 22-37 cycles of 95 °C for 40s, 59 °C for 2 min, 72 °C for 30s, then a final extension of 7 min at 72 °C. For each sample, PCR cycle checking (Quigley et al. 2014) of final cycle number was verified when a faint band appeared following 1% EtBr agarose gel electrophoresis. Once cycle numbers were obtained, samples were amplified again to their specific cycle number and collectively checked on a gel to verify equal band intensity. Individual samples that did not amplify by 35 cycles were removed from analysis.

PCR products were cleaned with ExoSAP-IT prior to a second series of PCRs to incorporate sequencer primers and unique barcode sequences to each sample using Illumina's Nextera XT Adapter Kit (Kenkel et al. 2013b; Green et al. 2014). Following this barcoding PCR, samples were visualized on a 1% EtBr agarose gel and pooled based on band intensity. The resulting pool was again run on a 1% stained gel for 30 min, the target band excised, then cleaned using a QIAquick® Gel Extraction Kit (QIAGEN, MD). The pooled sample was prepared for sequencing with Illumina's 250bp paired end MiSeq Reagent Nano Kit v2 and sequenced on ODU's Illumina MiSeq. Samples were sequenced in two batches, the first in February and the second in November 2017.

The first ITS2 Mi-Seq sequencing run yielded 485,867 raw reads from 78 samples, averaging 6,299 reads per sample. The second sequencing run yielded only 2,554 forward raw reads from 58 samples, averaging 44 reads per sample. Therefore, we incorporated only the forward reads with the initial sequence data. Sequenced raw reads were demultiplexed of barcodes, adapters, linkers, and trimmed to remove ITS2 primers and degenerate bases. Distinct amplicon sequence variants (ASVs), a similar, but higher-resolution analog of traditional Operational Taxonomic Units (OTUs) were identified and a resulting abundance count for each sample produced using the R program DADA2v1.16 (Callahan et al. 2016). After filtering and denoising, DADA2 produced a total of 363,141 reads that were collapsed into 185 amplified sequence variants (ASVs). After filtering, denoising, and pooling positively correlated ASVs, DADA2 produced a final read abundance table containing 13 unique ASVs (Table A4). Each ASV representative sequence was identified by BLASTN comparisons in NCBI's GenBank of nucleotide reference databases (Table A4).

Symbiodiniaceae ASV abundance analysis used the R package MCMC.OTU as described in Green et al. (2014). Samples were first subset by coral host species, and then outlier ASV's and samples with low sequence coverage were identified and removed. Rare ASVs representing < 0.1% of the global sum of counts were discarded. Remaining ASVs were run through the MCMC.OTU model, with fixed effects for origin site, destination site, and time. Pairwise differences between all fixed effect combinations were calculated and adjusted using false discovery rate (FDR). Count data were further filtered to retain ASV's detected in > 10% of all samples, then normalized and log-linear hybrid transformed prior to performing Principal Component Analyses (PCA) to visualize differences in symbiont communities between reef site and time. A PERMANOVA was carried out on transformed ASV counts using the *adonis* function of the R package VEGAN (Oksanen et al. 2011).

Statistical analyses

All statistical analyses were performed using R.3.4.3 (R Development Core Team 2017). Daily maximum, minimum, mean and daily range of temperatures were calculated from the *in situ* data, further divided into seasons: winter (July 2015-October 2015 and April 2016-July 2016), and summer (October 2015-April 2016), and tested using ANoVA, with site and season as fixed effects. *Post hoc* comparisons of significant effects were tested using the lsmeans function (Lenth and Lenth 2018). We collected time series data from the NOAA Coral Reef Watch global 5km product for Ofu Island (NOAA-CRW 2017) – sea surface temperature (SST), sea surface temperature anomalies (SSTA), and degree heating weeks (DHW) – from 2010-2012 and 2015-2016. These years were chosen to compare Ofu temperatures between previous 'normal' years - the Palumbi et al. (2014) study (2010-2012) - and recent mass bleaching years. ANoVA (lm function; Bates et al. 2007) and Tukey's post-hoc comparisons (lsmeans) were used to determine whether SST, SSTA, and DHW differed between the aforementioned years.

For each coral species, differences in weekly growth, total chlorophyll, and normalized F_vF_m were evaluated with respect to time point (levels: winter and summer), origin (levels: HV, MV, LV), transplantation (levels: HV common garden, native MV and LV), and treatment (levels: heat and control). Sample sizes for each factorial group (origin*transplantation) were five (n = 5 genets), with an occasional reduction to 4 or 3 genets due to sample loss (Exact sample sizes for each variable/comparison are in Tables 2.2-2.3). Effects were tested using a mixed model ANoVA, where time, a combined origin_destination site variable (due to the unbalanced design [i.e., not all

origins in each destination]), and treatment were modeled as fixed factors, and colony identity was nested within experimental tank designation as a random factor. Multiple comparisons across factors and interaction terms were assessed *post hoc* using general linear hypothesis testing and multiple comparisons (glht function; Hothorn et al. 2016) for linear mixed effects models, specifying Tukey's test. To satisfy model assumptions, normality was examined using the shapiro.test and homoscedasticity via the bartlett.test in R, as well as plotting residuals.

Results

Anomalously high Ofu temperatures

In situ backreef temperatures of Ofu Island reveal greater daily maximum and lower minimum temperatures, and consequently a greater daily range in the HV pool than the MV and LV pool (Figure 2.1B & A2; Table 2.1, A1), specifically during the summer. Thermal anomalies were calculated as the total number of days during the experimental duration (July 2015 to July 2016) when temperatures exceeded the NOAA CRW 50km regional bleaching threshold of 30.2 °C (NOAA-CRW 2017). The HV pool had a total of 125 days in which the daily maximum exceeded the bleaching threshold, versus 93 and 81 days over the threshold for the MV and LV pools respectively. Moreover, the HV pool had 72 and 27 days above 31 and 32 °C, versus 38 and 8 for the MV pool, and 33 and 12 days for the LV pool. In contrast to daily fluctuations and high temperature events, overall mean temperature did not differ among the three pools (Figure A2C; Table 2.1, A1).

Table 2.1. 2015-2016 Ofu Island backreef pool seasonal temperature summary. All variables are mean ± 1SD, except maxDTR (Daily Temperature Range). Winter spans April-October 2015, and Summer spans October 2015-April 2016.

Site	Season	Water Temperature (°C)								
		Mean	SD	Max	SD	Min	SD	DTR	SD	maxDTR
HV	Winter	28.12	0.76	28.81	0.95	27.53	0.81	1.29	0.72	4.045
	Summer	29.19	0.63	30.64	0.9	28.34	0.68	2.3	0.82	6.484
	Annual	28.63	0.94	29.68	1.51	27.91	0.91	1.77	1.19	
MV	Winter	28.02	0.72	28.57	0.83	27.7	0.73	0.88	0.51	3.307
	Summer	29.15	0.78	30.13	1.08	28.61	0.8	1.51	0.92	4.572
	Annual	28.66	0.9	29.4	1.19	28.23	0.86	1.17	0.82	
LV	Winter	28.22	0.77	28.8	0.85	27.88	0.85	0.92	0.42	3.335
	Summer	29.15	0.79	30.05	1.17	28.68	0.79	1.37	0.95	5.714
	Annual	28.66	0.9	29.4	1.19	28.26	0.88	1.14	0.76	

Annual temperatures also differed over the course of our study, where 2015 had greater max, min, and average *in situ* temperatures in comparison to 2016 (Figure 2.1C). In comparison to temperatures of the previous study by Palumbi et al. (2014) (e.g. a non-bleaching year), this study had a greater number of Degree Heating Weeks (DHW) than 2010, 2011, and 2012 (Figure 2.1C, Table A1). 2015 had up to 8 DHW over five months (6 months prior to the first sampling point), 2016 had ≤ 5 DHW that spanned four months, while 2010 had ≤ 3 DHW over 2.5 months (Figure 2.1C). In addition, SST and SSTA from 2016 were higher than in 2011-2012, as well as 2015.

Coral host growth over time

For both coral species, weekly growth rate was influenced by the two-way interaction between origin_destination transplant site and time. Averaged across both time points, *P. lobata* from the HV pool grew ~2.5 times more than MV and LV corals transplanted into the HV pool (Figure 2.2A; Table 2.2, A2). By July 2016, growth was greatest in HV corals, and MV and LV

native corals grew twice that of transplanted paired ramets. Additionally, growth of native *P. lobata* ramets was higher in July than January (Figure 2.2A). For *G. retiformis*, weekly growth in July 2016 was 2-3 times higher in corals native to the MV pool compared to MV transplants and both LV groups (Figure 2.2D; Table 2.2, A3), but not different than corals native to the HV pool. Similar to *P. lobata*, there were no growth differences in January. Growth of *G. retiformis* native to the MV pool was two times greater in July than January (Figure 2.2D; Table 2.2, A3).

Symbiodiniaceae photophysiology under acute heat stress

Photophysiological responses of *in hospite* Symbiodiniaceae following heat stress varied by coral host species. For *P. lobata*, acute heat stress reduced F_v/F_m (calculated as loss normalized to starting value; see Methods) for HV and LV natives and MV and LV corals transplanted into the HV pool ($p < 0.0001$; Figure 2.2B, denoted with "*"). However, MV native *P. lobata* were not affected by acute heat stress (Table 2.3, A2), and F_v/F_m values were ~1.2-1.8 times higher in MV heated corals than heated HV and LV corals for both time points (Figure 2.2B; Table A2). For *G. retiformis* there were no differences in F_v/F_m values among native and transplanted groups, nor was there an effect of heat treatment in January. Photochemical efficiency of heat-treated samples varied by a time and treatment interaction, with higher F_v/F_m values in January than July, but only for MV heated corals ($p < 0.0001$; Figure 2.2E, Table 2.3, A3). For both species, there were no significant tank effects.

Total chlorophyll (a + c) differed by either native pool or time. For *P. lobata*, native LV corals had ~2 times higher control than HV and MV corals during January (time*origin_destination*trt $p = 0.047$; Figure 2.2C; Table 2.3, A2). In January, acute heat stress reduced total chlorophyll values in LV and HV corals (Table 2.3, A2). Similar to F_v/F_m, there was no effect of treatment on total chlorophyll content in *P. lobata* from the MV pool (Figure 2.2C; Table 2.3, A2). For *G. retiformis*, there was an interactive effect of treatment and time, where total chlorophyll control values were greater in July than January ($p < 0.0001$; Figure 2.2F; Table 2.3, A3). Similar to F_v/F_m, there was no effect of treatment in January, but heat stress reduced total chlorophyll values in MV and LV corals transplanted into the HV pool in July ($p \leq 0.0001$; Figure 2.2, denoted with "*").

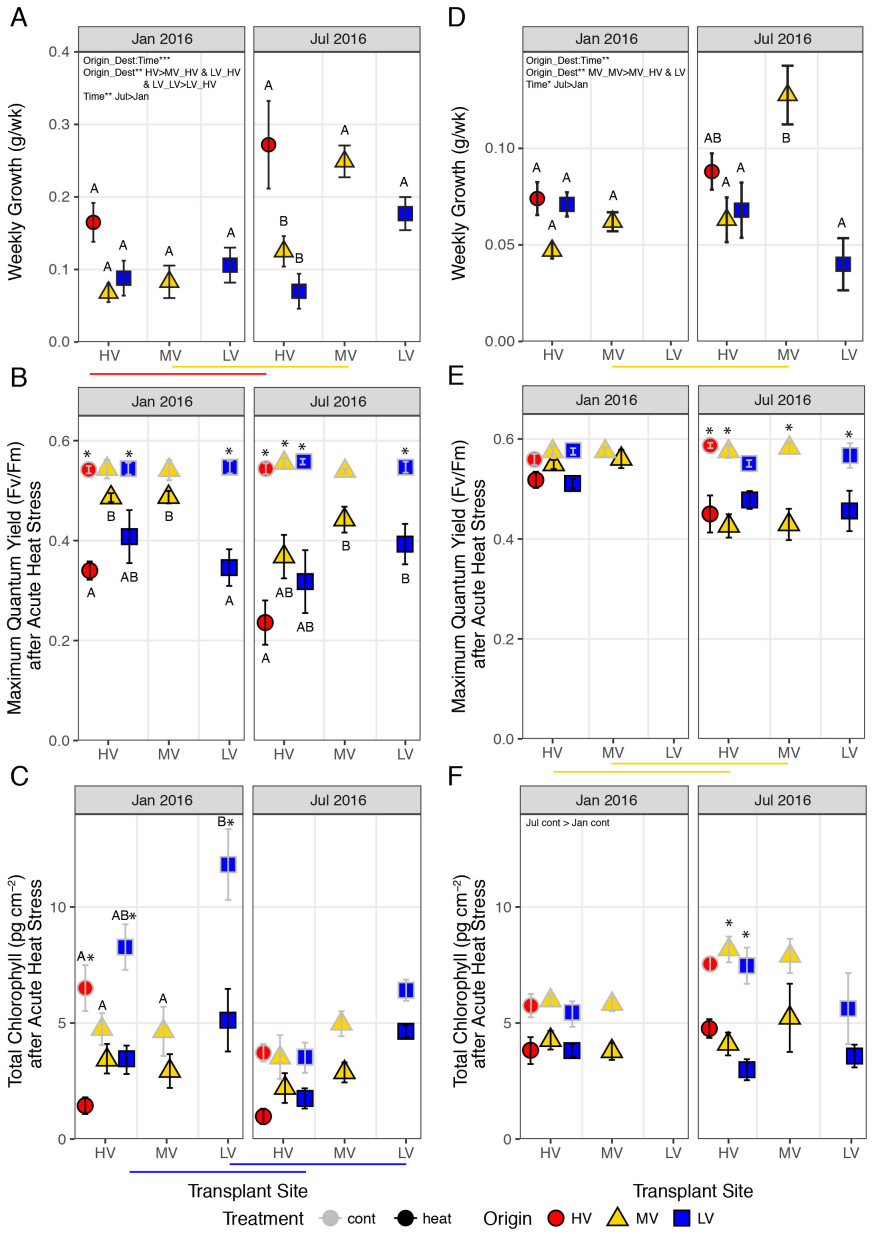

Figure 2.2. Weekly growth rate (g wk^{-1}; top panel), maximum quantum yield (F_v/F_m; middle panel), and total chlorophyll (pg cm^{-2}; bottom panel) of Symbiodiniaceae following acute heat stress (mean ± SE) in *P. lobata* (A-C) and *G. retiformis* (D-F) with respect to transplant destination and time. Only significant post-hoc comparisons of main effects are listed within the first panel, where comparisons among transplant groups within each time panel are represented by letters and an effect treatment are represented by asterisks. Colored horizontal lines represent significant differences within paired transplant groups over time.

Stable Symbiodiniaceae composition

Symbiodiniaceae internal transcribed spacer region 2 (ITS2) rDNA resulted in two distinct Amplicon Sequence Variants (ASVs) for *P. lobata* and 6 ASVs for *G. retiformis*. Dominant Symbiodiniaceae were all *Cladocopium spp.* (formerly Clade C; LaJeunesse et al. 2018) and species varied between *P. lobata* and *G. retiformis*. In *P. lobata*, *Cladocopium* ITS2 type C15 (NCBI accession #AY239369.1) was dominant at >99%, but a few coral individuals contained background proportions (<1%) of *Cladocopium* ITS2 type C40 (AY258485.1; Figure 2.3A; Table A4). For *P. lobata*, *Cladocopium* community composition did not change over time.

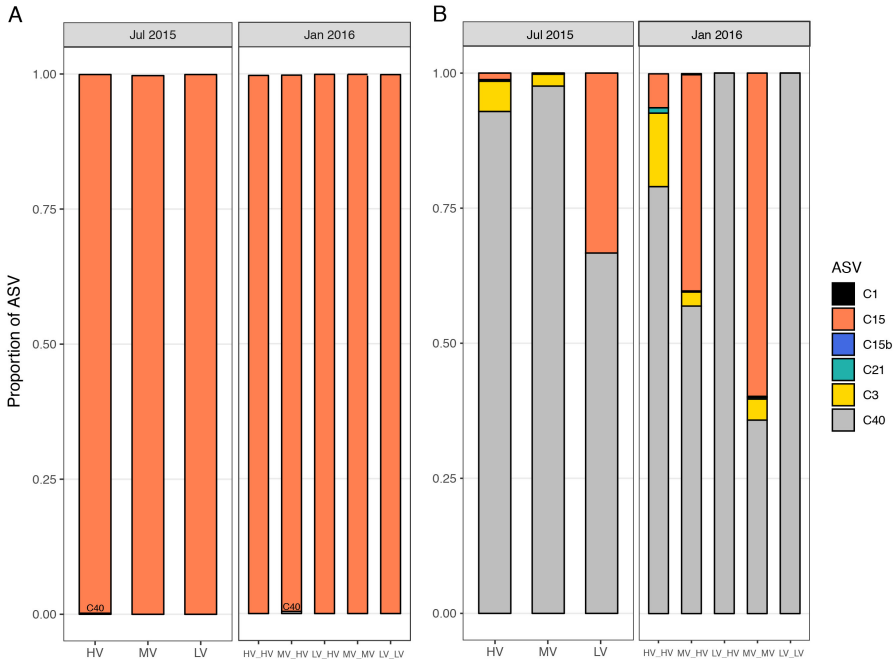

Figure 2.3. Relative proportion of Amplicon Sequence Variants (ASVs) belonging to Cladocopium spp. ITS2 types found in *P. lobata* (A) and *G. retiformis* (B). July 2015 panels represent community composition averaged over donor colonies in each backreef site, and January 2016 panels represent ASV proportions averaged for each transplant group.

Unlike *P. lobata, G. retiformis* corals contained mostly *Cladocopium* ITS2 type C40 at 50-73%, types C15 and C3 (AF499789.1) at 6-27% and 3-6%, respectively, and types C1

(AF333515.1), C15b (AY258491.1), and C21 (AY239372.1) were detected at background proportions (<1%; Figure 2.3B, Table A4). *G. retiformis* community composition varied by native backreef pool and time. ITS2 type C3 varied by origin, where it was present (5-10%) in *G. retiformis* from the HV and MV pool but absent from LV corals (PERMANOVA FDR <0.05 p = 0.0062). ITS2 type C15 was present (2-30%) in HV and LV *G. retiformis* but absent in MV corals (PERMANOVA FDR <0.05 p = 0.0014) until January 2016, when type C15 increased to 40-50% in MV corals and became absent from LV corals.

Discussion

I tested whether exposure to highly variable temperatures increased or decreased stress resistance in two massive coral species from distinct backreef environments. Corals transplanted for one year into the site with the Highest Variability (the HV pool common garden) did not increase growth or improve photophysiological responses following acute heat stress, as observed in previous studies (Palumbi et al. 2014). Instead, growth and stress tolerance responded differently to spatial and temporal variation in temperature regimes, and differently in *P. lobata* and *G. retiformis*. Unexpectedly, *P. lobata* native to the HV pool, the site with the highest thermal variability, were most sensitive to experimental bleaching. Previous work in Ofu found increased stress tolerance following acclimation to the greater thermal variability of the HV regime (Thomas et al. 2018), yet there was a negligible effect of this variability on thermal performance for corals transplanted into and a deleterious effect for corals from the HV pool. Our results suggest that not all coral species may respond positively (or similarly) to highly variable thermal habitats.

High magnitudes of temperature variation have recently been recognized as a significant promoter of reef-building coral thermal tolerance over small spatial scales (<10km) and could increase resilience to anticipated ocean warming (e.g., Palumbi et al. 2014; Kenkel et al. 2015; Barshis et al. 2018; Safaie et al. 2018). Coral populations from inshore/protected habitats with high diurnal fluctuations consistently exhibit greater growth and/or natural bleaching tolerance than conspecifics from offshore/exposed habitats, a paradigm congruent across the Caribbean (Castillo et al. 2011; Kenkel et al. 2013b; Kenkel et al. 2015), Red Sea (Pineda et al. 2013), Ofu Island in the South Pacific (Smith et al. 2007; Barshis et al. 2018), northwest Australia (Schoepf et al. 2015), and Great Barrier Reef (Howells et al. 2013). In contrast, coral growth in the present study was not different among the three backreef populations in their native environments (except lower growth in LV native *G. retiformis* in July 2016) despite differences in thermal regimes, although

MV and LV *P. lobata* transplants in the HV pool had lower growth than paired native ramets and HV native genets in July 2016. Moreover, HV native corals and corals transplanted into the HV pool were susceptible to acute bleaching stress during one or both time points. There was also no effect of acute heat stress on native and transplanted MV *P. lobata* corals (except for F_v/F_m values in MV transplants during July 2016). This contrasts with previous studies examining branching and massive coral species from or transplanted into the HV pool, which found higher: thermal tolerance limits (Oliver and Palumbi 2011; Palumbi et al. 2014; Barshis et al. 2018), prevalence of heat-tolerant *Durusdinium trenchii* (Oliver and Palumbi 2009), and transcription of heat responsive genes (Barshis et al. 2013) than MV pool corals. Despite persistent high magnitudes of thermal variability, the HV pool did not increase heat tolerance of massive coral species during our study, which complicates the notion that highly variable thermal habitats are universally beneficial for increasing the adaptive and acclimatory potential of all coral species.

The most obvious distinction between previous experiments and ours is that prior research has predominantly focused on corals in the genus *Acropora* (Middlebrook et al. 2008; Bellantuono et al. 2012b; Howells et al. 2013; Thomas et al. 2018). Biological traits such as colony morphology, growth rate, and reproductive mode separate branching corals such as *Acropora spp.* from massive coral species into "competitive" and "stress-tolerant" life-histories, respectively (Darling et al. 2012). Large, slow growing massive corals are thought to be more thermally tolerant to chronically variable and disturbed habitats than branching species in both the Caribbean (Alvarez-Filip et al. 2011) and Indo-Pacific (McClanahan et al. 2014) given life-history traits such as increased tissue thickness and energy surplus (Edmunds and Davies 1989; Loya et al. 2001; van Woesik et al. 2011). The HV population of *P. lobata* has previously exhibited higher growth (versus MV corals) and stress resistance (versus forereef corals; Barshis et al. 2018), but here, *P. lobata* in the HV pool demonstrate reduced stress tolerance compared to MV and LV populations. These massive coral species are naturally abundant within the HV pool (Craig et al. 2001), thus, their common occurrence, as well as the increased growth and stress resistance shown previously in HV *P. lobata* makes it unlikely that the taxonomic difference between the present and previous studies is the main explanation for contrasting results of minimal growth differences and reduced thermal tolerance of HV corals seen herein.

Although both *P. lobata* and *G. retiformis* are clustered into the stress-tolerant life-history strategy (Darling et al. 2012), species-specific responses are apparent under acute bleaching stress.

For both photochemical efficiency (Fv/Fm) and total chlorophyll, there was opposing effects of time, where heat stress affected *P. lobata* in January but *G. retiformis* corals were more affected in July 2016. In addition, stronger effects of pool of origin were evident for *P. lobata* bleaching responses and July 2016 growth versus *G. retiformis*. Ofu backreef *Acropora* populations harbor pool-specific Symbiodiniaceae communities, where *Acropora spp.* in the HV pool predominantly host *D. trenchii*, while MV corals host both *D. trenchii* and *Cladocopium* type C2 (Oliver and Palumbi 2010). In contrast, similar Symbiodiniaceae communities were observed within *P. lobata* (type C15) across the back-reef, site-specific assemblages within *G. retiformis* (type C40, C15, and C3), and distinct species-specific assemblages. While it is unclear whether different Symbiodiniaceae *Cladocopium* assemblages could be driving the observed species-specific seasonal variation in photophysiological responses to bleaching stress (Fitt et al. 2000), both intra- and inter-specific host and symbiont variation is known to shape growth and thermal tolerance limits in corals (e.g. Loya et al. 2001; Little et al. 2004; Parkinson and Baums 2014).

Additionally, it could be that corals in these backreef pools are locally adapted to their native thermal conditions. In the Florida Keys, mass gain, protein and lipid levels, and gene expression plasticity of *Porites astreoides* were greater for corals in their native environment in comparison to foreign transplants (Kenkel et al. 2015; Kenkel and Matz 2016). Similarly in Ofu, backreef (HV and/or MV) *P. lobata* had consistently higher growth, environmental tolerance, and cellular responses than corals from or reciprocally transplanted to a nearby forereef (Smith et al. 2007; Barshis et al. 2010; Barshis et al. 2018). In Barshis et al (2018), HV *P. lobata* grew more than forereef corals, and both HV and MV *P. lobata* exhibited increased tolerance under acute thermal stress compared to forereef corals regardless of acclimation to stable or fluctuating temperatures (though HV and MV did not differ; Barshis et al. 2018). Notably, this experiment utilized a 36d aquarium-based acclimation versus the 12mo field acclimatization performed herein and observed no differences between HV and MV populations. Also, the highest growth was found in HV natives versus MV and LV corals transplanted into the HV pool, but only for *P. lobata* during July 2016 and no differences among their native environments. However, differences in stress tolerance between paired native versus transplanted ramets exist for both species: a non-significant then significant reduction in both F_v/F_m for MV native vs. transplanted *P. lobata* and total chlorophyll for MV and LV native vs. transplanted *G. retiformis* from January to July 2016, suggesting a potentially higher stress level in transplanted ramets. For local adaptation to occur in

these backreef populations, individuals would need to perform better at home versus away (Kawecki and Ebert 2004), which is illustrated here for coral growth but not stress tolerance (excepting the instances mentioned above). In addition, HV corals have previously demonstrated increased tolerance due to the conditions of the HV pool (Oliver and Palumbi 2011; Palumbi et al. 2014), yet in this study, F_v/F_m values suggest HV native *P. lobata* were most susceptible to stress. Local adaptation could contribute to the complexity of the results, though it cannot be fully supported, as classic patterns of best performance at home versus away were not observed, nor was a full reciprocal transplant conducted by moving HV corals into the MV or LV pools.

For HV corals, increased growth but reduced stress tolerance could be evidence of tolerance trade-offs owing to specialization to highly variable habitats. Skeletal growth records of massive *Porites* colonies along the GBR illustrate progressive accretion rates associated with warming SST followed by precipitous declines following repeated mass bleaching events (De'ath et al. 2009; but see Barkley and Cohen 2016). I explored the relationship between HV *P. lobata* coral growth and response to acute thermal stress and found a negative, albeit non-significant, correlation between growth and total chlorophyll (Pearson's R = -0.41; Figure A5) and no correlation between growth and photochemical efficiency. Taken together, our results corroborate recent findings that coral growth is likely not a good predictor of bleaching responses under extreme temperatures (Edmunds 2017).

Compromised bleaching tolerance of HV native corals and a lack of enhanced performance for corals transplanted into the HV pool could also be attributed to the magnitude and duration of maximal summertime temperatures recorded during this study. From 2015-2016, a strong El Niño increased sea surface temperatures and triggered the third pan-tropical mass bleaching event (Eakin et al. 2016; Hughes et al. 2017b). This bleaching event was reported to be the most extensive and severe in recent human history; and reefs in American Samoa were predicted to experience intense bleaching conditions (Eakin et al. 2016). Our experiments were a few months prior to or post maximal bleaching stress on Ofu Island (2015: February-June, 2016: March-June; Figure 2.1C), however in January 2016, sparse paling in some HV pool branching corals was observed but not in our donor or transplanted corals (pers. obs.). Thus, the patterns observed herein could represent the initial stages of response to or accumulated after-effects of the thermal anomaly. The HV pool regularly experiences brief but frequent temperatures that reach over 35°C, which greatly exceed the regional bleaching threshold of 30.2 °C (Craig et al. 2001; Oliver and

Palumbi 2011), and our acute thermal stress assays serve as an experimental analogue to the strong thermal variation in this pool. Much of the thermal tolerance research previously conducted in Ofu utilized similar thermal stress assay profiles (Palumbi et al. 2014), yet these experiments occurred during milder years, where 2 DHW was rarely exceeded in comparison to 5-8 DHW during our study.

Summary

It is thus tempting to speculate whether the extreme temperatures in the HV pool during this study could have overwhelmed the physiological performance underlying temperature tolerance of this population of corals. However, this study would need to be repeated during non-bleaching years and during peak summer temperatures to effectively disentangle the effect of recent thermal history versus taxonomic, evolutionary, and population-specific drivers of massive coral species upper thermal limits. Indeed, the differences in thermal tolerance limits observed herein are complex, challenging our understanding of how naturally tolerant populations will fare under rapid climate change. Regardless of the complexity, it is clear that higher magnitudes of temperature variation were not a universal promoter of thermal tolerance limits and that species-specific mechanisms and regional thermal anomalies may be equally important in shaping coral responses to extreme temperatures.

CHAPTER 3

EXPLORING THE SCALE OF HIGH-RESOLUTION THERMAL VARIABILITY AND ITS RELATIONSHIP WITH BLEACHING SUSCEPTIBILITY

Introduction

As climate change intensifies, increases in mean temperatures and temperature variation result in an increased probability of summertime heat waves that are longer in duration and have warmer maximal and minimal temperatures (Pachauri et al. 2014; Stillman 2019). Marine heat waves are especially becoming more severe in tropical coral reef regions (Lough et al. 2018). Reef-building corals live within a relatively narrow temperature range close to their upper thermal limits (Jokiel and Coles 1990; Berkelmans and Willis 1999) and are particularly vulnerable to increased sea surface temperatures (SST) associated with anthropogenic climate change. As such, summertime heat waves are projected to cause annual mass coral bleaching (the symbiotic breakdown of coral animal and photosynthetic algae) on more than 90% of coral reefs worldwide by the end of the century (Frieler et al. 2013; Hughes et al. 2017b).

The link between coral bleaching events and increased SST forms the basis of a global thermal stress monitoring system by the National Oceanographic and Atmospheric Administration's Coral Reef Watch Program (NOAA CRW; Liu et al. 2003; Liu et al. 2014), where the magnitude and duration of remotely sensed SSTs above a fixed, locally defined average summer threshold temperature predicts the level of thermal stress on a coral reef region, called Degree Heating Weeks (DHW). This monitoring and predictive tool has been used to define the amount of DHWs associated with coral bleaching stress and mortality (Heron et al. 2016) and has guided targeted observations and management responses at reef locations worldwide. Despite these advances, the coarse spatiotemporal resolution of remotely sensed data (5km resolution) prevents realistic thermal stress quantification at small scales, as it misses the spatiotemporal heterogeneity within many reef regions and within individual reefs (Oliver and Palumbi 2011; Schoepf et al. 2015;

Safaie et al. 2018; Genevier et al. 2019). Differential bleaching responses at smaller spatial scales have been attributed to small-scale variation in the magnitude and duration of thermal stress and are poorly reflected by DHW predictions for a particular location (Langlais et al. 2017; Safaie et al. 2018; McClanahan et al. 2019).

Understanding and predicting the responses of corals to extreme heat waves is challenged by a myriad of climatic and local interactions of smaller-scale interannual and diurnal temperature variability (Donner 2011; Oliver and Palumbi 2011), stress exposure duration (Berkelmans 2002; Middlebrook et al. 2008), heating rate (Middlebrook et al. 2010), and water flow (McClanahan et al. 2005). Moreover, the individual response of the coral holobiont to thermal stress is influenced by life-history strategy (Darling et al. 2012), recent thermal history (Middlebrook et al. 2008), symbiont composition (Baker 2003; Ziegler et al. 2017), and feeding (Grottoli et al. 2006). A better understanding of thermal stress exposures and individual coral responses over various temporal and spatial scales will play a crucial role in determining coral thermal thresholds and ultimately reef-scale bleaching susceptibilities. The resilience and persistence of coral reefs under climate ultimately depends on whether corals can modify their stress response via acclimatization and/or local adaptation to keep pace with increasing climate variability. Another critical limitation of the NOAA CRW monitoring program assumes that coral reef thresholds remain constant over relatively short timescales (Van Hooidonk et al. 2013). Recently, many studies have demonstrated the capacity of coral communities to acclimatize to repeated heat stress exposures (Bellantuono et al. 2012b; Howells et al. 2013; Palumbi et al. 2014; Bay and Palumbi 2015), and that recent history of temperature variation beneficially influences coral's physiological tolerance (McClanahan et al. 2005; Oliver and Palumbi 2011; Barshis et al. 2013; Palumbi et al. 2014; Morikawa and Palumbi 2019). It is suggested that reef areas with large environmental fluctuations contain corals with higher heat tolerance in comparison to corals from stable environments (Oliver and Palumbi 2011; Kenkel et al. 2013b; Palumbi et al. 2014; Kenkel et al. 2015; Camp et al. 2017; Barshis et al. 2018; Safaie et al. 2018). These naturally variable environmental regimes across small-scale heterogeneous reef habitats provide opportunities for coral populations to modify and increase their thermal thresholds through mechanisms of acclimatization and adaptation (Boyd et al. 2016).

In Chapter 1, I sought out to test whether massive coral species from the naturally variable backreef pools of Ofu Island, American Samoa, could modify their stress tolerance via acclimatization to the highly variable (HV) pool. This well-studied pool is recognized to contain more thermally tolerant corals than nearby coral populations (Oliver and Palumbi 2011; Barshis et al. 2013; Palumbi et al. 2014; Morikawa and Palumbi 2019) and elicit increased thermal tolerance in corals transplanted into the HV pool (Palumbi et al. 2014). Unlike corals from the genus *Acropora*, I found that massive corals did not increase thermal tolerance following transplantation into the HV pool, and more importantly, native HV massive corals had a reduced tolerance under acute heat stress in Chapter 2. I did not observe enhanced physiological performance as the literature predicted despite greater environmental variation in the HV pool and hypothesize that at finer spatiotemporal scales, increased heat duration and magnitude coupled with recent bleaching stress could contribute to my contrasting results. Here, I compare different scales of *in situ* temperature data to the remotely sensed NOAA CRW DHW product to explore whether high resolution, *in situ* climatology can predict the physiological differences I observed previously in the massive coral *Porites lobata*. In addition, I sampled additional colonies and conducted a reciprocal transplant experiment between the HV and the moderately variable (MV) pool to elucidate: a) whether thermal tolerance changed (H_O: thermal tolerance unchanged) following transplantation in the HV pool, and b) whether HV corals exhibited reduced thermal tolerance regardless of transplant environment.

Materials and Methods

Coral collection & transplantation

Ten colonies (i.e., genets) of *P. lobata* were sampled from each of three backreef pools (LV, MV, and HV) between July 1-3, 2016 (n=30 genets total). Colonies were chosen based on visual appearance (non-bleached), size (1.5 – 3 m diameter), and at a distance of ~5m from other colonies to minimize chance for sampling clones (*sensu* Baums et al. 2006). From each colony, 24 cores (i.e., ramets) were collected and affixed to nylon bolts with marine epoxy and secured to an egg-crate light diffuser grid using nylon wingnuts. Ramets from each colony from each site were randomly assigned to a transplant grid based upon transplant site (Figure 3.1; 8 grids each at HV and MV, 4 grids at LV). Half of the

MV and LV samples (12 ramets per genet, n=120 total per site) were transplanted into the HV pool and the other half remained at the respective native reef site. In addition, half of the samples from the HV pool were transplanted into the MV site, and randomly mixed with MV ramets on grids. Transplantation of HV samples into the MV pool occurred on July 13, and MV and LV samples were transplanted into the HV pool July 15, 2016. This resulted in 6 unique transplant groups: HV_HV, HV_MV, MV_HV, MV_MV, LV_HV, and LV_LV (origin_destination).

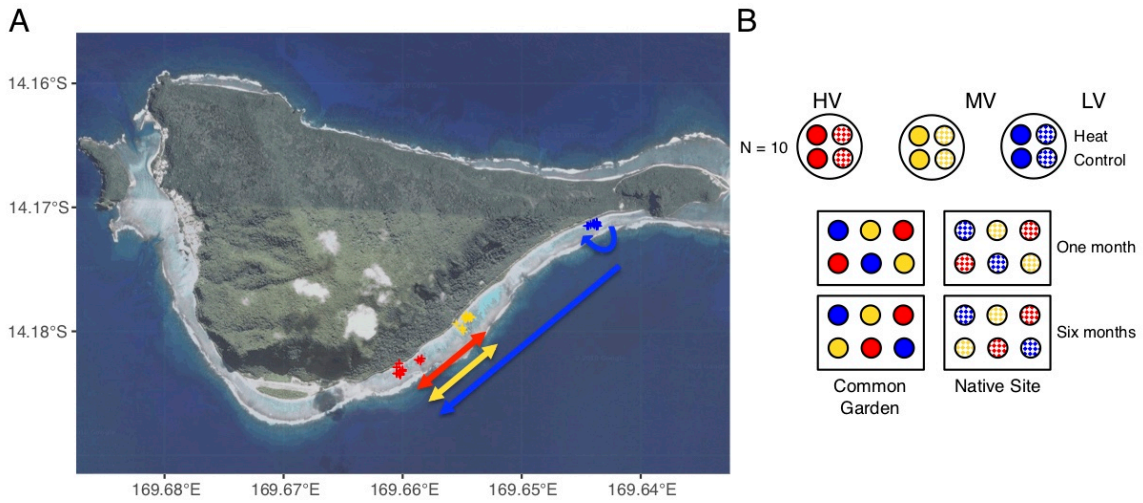

Figure 3.1. Second transplant experimental sites and design on Ofu Island, American Samoa. (A) Arrows show transplant design within three backreef pools – HV (red), MV (gold), LV (blue) – and crosses denote sampled *P. lobata* genets. (B) Twenty-four ramets from ten genets were sampled from each site (N=720), and half were transplanted into either the HV or MV (excluding LV ramets) common garden and the other half were returned to the native site. Two fragments per genet per site were collected after one (Aug 2016) and six months (Feb 2017).

Ofu backreef temperature profiling

HOBO® pendant temperature loggers (Onset Computer Corporation, Bourne, MA) were placed on each transplant grid and collected *in situ* temperature every 10 minutes for six months (July to January). For each pool, temperature data was averaged across three grids and subsequently binned into either winter (Apr. 16th – Oct. 15th) or summer (Oct. 16th – Apr. 15th) seasons for pool-specific comparisons of seasonal temperature metrics. In

addition, we obtained the National Park of American Samoa's (NPSA) Ofu Island temperature records spanning 2000-2017 (Barker 2018) to generate local climatologies and Degree Heating Weeks (DHW) for the three backreef pools. Three different Degree Heating metrics were calculated for each pool: NOAA CRW 5 km based Ofu DHW, *in situ* DHW, and *in situ* Degree Heating Minutes (DHM).

The NOAA CRW 5 km based Ofu time series data was obtained via a custom request to NOAA CRW staff that extracted the satellite grid 5 km NOAA CRW product containing Ofu Island's coordinates (-14.177949, -169.654364). For this dataset, the Maximum Monthly Mean (MMM) was 28.9 °C, previously calculated as the month with the highest maximum temperature after averaging daily temperature for a given month across years 1985-2012. This MMM was applied to the NPSA temperature time series dataset for each pool to then calculate NOAA CRW Hotspots and Degree Heating Weeks for Ofu. Following NOAA's Coral Reef Watch (CRW) Sea Surface Temperature (SST) climatology product methodology (Liu et al. 2006), daily hotspot values were recorded as the difference in daily mean minus MMM. The value was recorded if greater than or equal to one, otherwise the hotspot was given a value of 0. The number of Degree Heating Days (DHD) was calculated by summing daily hotspot values over a 12-week rolling window, and then divided by 7 to standardize units to Degree Heating Weeks (DHW). A separate MMM of 29.8 °C was calculated from the same range and non-bleaching years (2000-2001, 2004-2014) subset from the NOAA CRW Ofu specific time series dataset to be compared with the *in situ* calculations.

For *in situ* climatology calculations, we used the NPSA pool-specific *in situ* temperature time series data. Following the exact NOAA CRW Ofu methodology, Maximum Monthly Means (MMMs) for each pool were calculated as the average nightly temperature for a given month across years from the years 2000-2001 and 2004-2014, excluding the bleaching years 2002-03 and 2015-17. This resulted in similar - albeit slightly warmer (29.1-29.3 °C) - MMM's in comparison to the NOAA CRW MMM of 28.9 °C. Since *in situ* temperature records were measured continuously, daily (i.e., 24 hr) averaged values were also used to compute a more precise climatology for each backreef pool. For all three sites, April was the hottest month of the monthly mean temperatures and was used as the site-specific MMM to calculate hotspots. The MMM of the HV, MV, and

LV pool was 29.454 °C, 29.499 °C, and 29.498 °C, respectively. *in situ* DHW calculations followed the same methodology as the NOAA CRW Ofu DHW. Since the NPSA *in situ* temperature records were collected every 30 minutes, a finer-scale metric of heat loading was calculated by summing hotspot values over the number of rows totaling a 12-week rolling window (n = 4032), and then dividing by 336 to get "Degree Heating 30 min Intervals."

Coral growth and acute heat stress assays

At each timepoint - one month (August 5-8, 2016) and six months (February 9-11, 2017) – 2 ramets were collected per genet per transplant group (10 genets per transplant group, 6 transplant groups, n = 120 ramets total/timepoint) from the three Ofu backreef pools, scrubbed to remove algal and epiphyte growth, and buoyant weighed and photographed prior to controlled thermal stress experiments. Ramets were placed in a modified version of the Coral Bleaching Automated Stress System (CBASS; Voolstra et al. 2020), constructed from Coleman 24 L Party Stacker Coolers™ as head and sump tanks. A pump provided a flow of 88.9 mL sec^{1} to the head tank, which was also fitted with 6 LED bulbs (Phillips PAR38) with a light level of ~500 ± 20 µM quanta m^{-2} s^{-1} and a 12 hr light/dark photoperiod. A flow-through drip system provided 2.5 mL sec^{1} of local seawater throughout the duration of the experiment.

Controlled temperature ramp exposures occurred similar to Klepac & Barshis (2020). Briefly, samples were randomly assigned within two control and two heat tanks. In the heat tank, temperature increased over 3 hrs from 28 to 36.5 °C, followed by a 3 hr hold at 36.5 °C, then a ramp down to and hold at 28 °C for 16 hrs. The control tank was set to remain stable at 28 °C for 22 hrs (Figure A1). Samples were immediately wrapped in foil and stored at -20 °C until transportation back to Old Dominion University and subsequent storage at -20 °C.

A final timepoint – 24 months – occurred during June 2018 while breaking down the field research project. All remaining transplanted ramets (approximately 4 ramets per genet per transplant group) were removed from the pools, cleaned of encrusting growth, and buoyant weighed. Ramet growth rates were calculated as: ((final weight – initial weight) / initial weight) / number of weeks, then averaged for each transplant genet to avoid pseudoreplication.

Symbiodiniaceae physiology under heat stress

Dark-adapted maximum quantum yield (F_v/F_m) of photosystem II (PSII) was measured to quantify relative heat stress responses of *Symbiodiniaceae* during the acute assays (Warner et al. 1996). Following 30 min of dark-adaptation, ramets were repeatedly measured on top and in triplicate at 0 and 21 hrs during the experiment using a pulse amplitude modulation (PAM) fluorometer (Junior-PAM, Walz, Germany). Instrument settings were as follows: Measuring Light Intensity = 6; Saturation Intensity = 12; Saturation Pulse Width = 0.6 s; Gain = 2. Photochemical efficiency values (F_v/F_m) of coral samples measured at the end of each assay were normalized to measurements taken at the start of the experiment (ΔY = (0hr Y – 21hr Y)/0hr Y), giving the proportional change in maximum quantum yield.

At the end of the heat stress assays, coral tissue was airbrushed from the skeleton using 35 ppt unfiltered, artificial seawater. The resulting slurry was homogenized, centrifuged, and resuspended in 5 mL of unfiltered seawater before aliquoting out 3 mL for chlorophyll absorbance measurements (stored at -20 °C). For chlorophyll determination, 90% acetone was added to slurry samples, which was then homogenized using a glass tissue homogenizer and a 25 mm GF/F filter as a mechanical 'grit' for cellular disruption, and then stored at 4 °C for 24 hr. Absorbance spectra was measured using an Ocean Optics Spectrometer (Largo, FL), and cellular chlorophyll *a* and *c* values calculated using the Jeffrey and Humphrey (1975) equation. Total chlorophyll (*a* + c) absorbance was normalized to acetone volume and then scaled to the surface area of each ramet, measured using the paraffin wax method (Veal et al. 2010).

Natural bleaching of donor colonies

The Samoan archipelago had begun experiencing a mass bleaching event during the six-month timepoint (American Samoa Coral Reef Advisory Group (CRAG) 2017), where bleaching affected many corals in Ofu's backreef pools. We sampled small cores (2 cm^2) of both affected and healthy regions of donor colonies at all sites. In addition, we assigned each colony an overall bleaching score (0=healthy, 1=pale, 2=bleached) and recorded the percent area affected. Chlorophyll concentration and surface area was processed and measured as aforementioned. Healthy and affected chlorophyll values were averaged to get an average chlorophyll value for each colony.

Statistical analyses

All statistical analyses were performed using Rv3.6.3 (R Core Team 2020). The interactive effects between season and backreef pool on mean daily temperature range, min, max, and mean temperatures were tested using the aov function followed by lsmeans contrasts with season and backreef pool as fixed factors. *In situ* DHWs were compared across pools using a sliding window analysis followed by a Wilcox rank-sum test for two-week windows (sliding by one week) where DHWs were greater than 0 °C wk^{-1} (sensu Sale et al. 2019). Multiple tests were sequential Bonferroni adjusted.

Generalized linear mixed models (lmer) were used to examine the interactive effects of time (one- and six-month), transplant group (HV_HV, HV_MV, MV_HV, MV_MV, LV_HV, LV_LV), and treatment (control and heat) on weekly growth (sans treatment), photochemical efficiency (Fv/Fm), and total chlorophyll. Transplant group was created as a fixed variable since the nature of the transplantation effort was unbalanced (i.e. not all origins were transplanted into all destinations [no HV in LV, or LV in MV]). Models were run with coral colony/genet nested within tank as a random effect. Residual normality and homogeneity of variance was tested using Shapiro-Wilk (*stats* package) and Levene's HOV tests (*car* package), respectively. Multiple comparisons with multivariate adjustments were used to assess time * transplant group * treatment, time * transplant group, or time * treatment interactions using the *emmeans* package.

The natural bleaching event provided an opportunity to examine the relationship between donor colony and transplanted ramet bleaching. First, a linear mixed model incorporating fixed effects of site (HV, MV, LV) and sample (donor, heat, control), and colony as a random effect was tested against total chlorophyll values, with post-hoc comparisons of significant factors. Then, a Pearson's correlation was run against donor and control total chlorophyll, as well as a correlation matrix comparing days spent over the local bleaching threshold (30.2°C) and total chlorophyll of each sample type.

To investigate how coral holobiont physiological variables (weekly growth, control F_v/F_m, control total chlorophyll) related to seasonality and environmental metrics such as days spent over 31 and 32 °C, daily temperature range (DTR), maximum DTR, 90^{th} quartile daily range, monthly mean maximum, and monthly minimum and maximum temperatures, we conducted a Pearson's correlation matrix test between each physiological variable and

each temperature metric. In addition, a Principal Component Analysis was used to visualize log-transformed variables in a multivariate space. Log-transformed values were first centered and scaled prior to conducting the PCA and subsequent PERMANOVA using the *adonis* function with the dissimilarity index method set to 'Euclidian.'

Results

Ofu backreef temperature profiling

From July 2016-Jan 2017, the HV and MV pools had greater Daily Temperature Range (DTR), maximum, and minimum daily temperatures during summer (October – January) and winter months (July – October; DTR and minimum only) than the LV pool (aov site* season; DTR p = 3.49e-07, max p = 0.002207, min p = 0.01079; Figure A1A-C). Summer maximum temperatures were 33.4 ± 0.44 °C (mean ± SD) in the HV pool and 33.8 ± 0.58 °C in the MV pool in contrast to 32.1 ± 0.58 °C in the LV pool (Table 3.1, A5). Summer DTRs for HV and MV pools were 1.5-1.7-fold greater than summer DTR in the LV pool (Table 3.1, A5). All temperature metrics were greater in the summer compared to winter months. In addition, the HV, MV, and LV pools experienced 122, 128, and 106 days over the regional bleaching threshold of 30.2 °C, respectively, and of which, 75% of these days were during the summer months. Moreover, the HV pool had 69, 33, and 5 days over 31, 32, and 33 °C, whereas the MV pool had 72, 27, and 0 days, and the LV pool had only 38, 8, and 0 days over these temperatures respectively (Table 3.1).

Table 3.1 Ofu Pool Seasonal Temperature Summary. Average for all metrics except maxDTR (Daily Temperature Range). Winter spans April-October 2016, and Summer spans October 2016-April 2017.

		Water Temperature (°C)												
Site	**Season**	**Mean**	**SD**	**Max**	**SD**	**Min**	**SD**	**DTR**	**SD**	**max DTR**	**days > 30.2°C**	**days > 31°C**	**days > 32°C**	**days > 33°C**
HV	Winter	28.65	0.64	30.86	0.73	27.42	1.02	3.44	1.08	4.83	29	9	4	0
	Summer	29.89	0.49	33.82	0.58	28.11	0.58	5.71	0.64	6.61	93	60	29	5
	Annual	29.15	0.85	32.05	1.66	27.70	0.90	4.35	1.47		122	69	33	5
MV	Winter	28.63	0.60	31.09	0.60	27.28	0.81	3.80	0.51	4.14	35	14	3	0
	Summer	29.97	0.48	33.41	0.44	28.36	0.48	5.05	0.44	5.53	93	58	24	0
	Annual	29.17	0.87	32.01	1.30	27.71	0.87	4.30	0.79		128	72	27	0
LV	Winter	28.71	0.61	30.64	0.48	27.89	0.55	2.76	0.71	3.90	21	3	0	0
	Summer	29.94	0.48	32.09	0.58	28.90	0.41	3.18	0.52	3.56	85	35	8	0
	Annual	29.20	0.83	31.22	0.89	28.29	0.70	2.93	0.65		106	38	8	0

The NOAA CRW 5 km Ofu Island virtual station's Mean Monthly Maximum (MMM) of 28.9 °C was derived from 1985 – 2012 and used near-real-time satellite nighttime Sea Surface Temperatures (Liu et al. 2014). Before creating our own backreef-specific *in situ* climatologies from temperature data available from 2000-2017, we used the NOAA CRW MMM of 28.9 °C to calculate Ofu Degree Heating Weeks (DHW) for each pool (Figure 3.2A). From 2002-2007, NOAA CRW Ofu DHWs were 2- to 4-fold fewer than pool-specific DHW (derived from MMM of 28.9 °C; $p < 0.0001$; Figure 3.2A, Table A6), where sliding window analysis revealed pool-specific DHWs had approximately 20-30 windows (2wk increments) per year of significantly greater DHWs than the NOAA CRW time series. From 2009-2010, and 2013, pool-specific DHWs had 12 sliding windows that were 2-fold greater than NOAA CRW DHWs ($p < 0.0001$). However, from 2014-2016, this trend switched to NOAA CRW DHWs having significantly greater DHWs for 15-20 sliding windows in comparison to pool specific DHWs (Figure 3.2A, Table A6).

Daily *in situ* climatologies of each backreef pool resulted in MMM's of 29.4 °C for the HV pool, 29.5 °C for the MV pool, and 29.5 °C for the LV pool, much greater than the satellite derived MMM of 28.9 °C for the Ofu 5km product. Utilizing these *in situ* pool-specific MMMs instead of the satellite-derived NOAA CRW Ofu MMM (28.9 °C) resulted in a 7-fold reduction in DHWs (Figure 3.2A vs. 3.2B), as a higher MMM value results in fewer calculated DHWs. For the *in situ* DHW, the HV pool had a greater number of DHWs than both the MV and LV pool during the years 2001-2003, 2005-2007, 2015, and 2017 ($p < 0.001$, Figure 3.2B, Table A6). The MV pool had greater numbers of DHWs during 2002 and 2015 ($p < 0.001$). Since the NPSA long-term *in situ* temperature dataset measured temperatures every 30 min, a finer-scale approach to calculating degree heat loading could be examined. The resulting number of Degree Heating Minutes (Figure 3.2C) indicated that the HV pool had more DHM than the MV and LV pools across the entire time series, revealing a greater amount of overall heat loading regardless of bleaching years ($p < 0.001$). Moreover, the LV and MV pool did not differ in heat loading over time, except for during 2002.

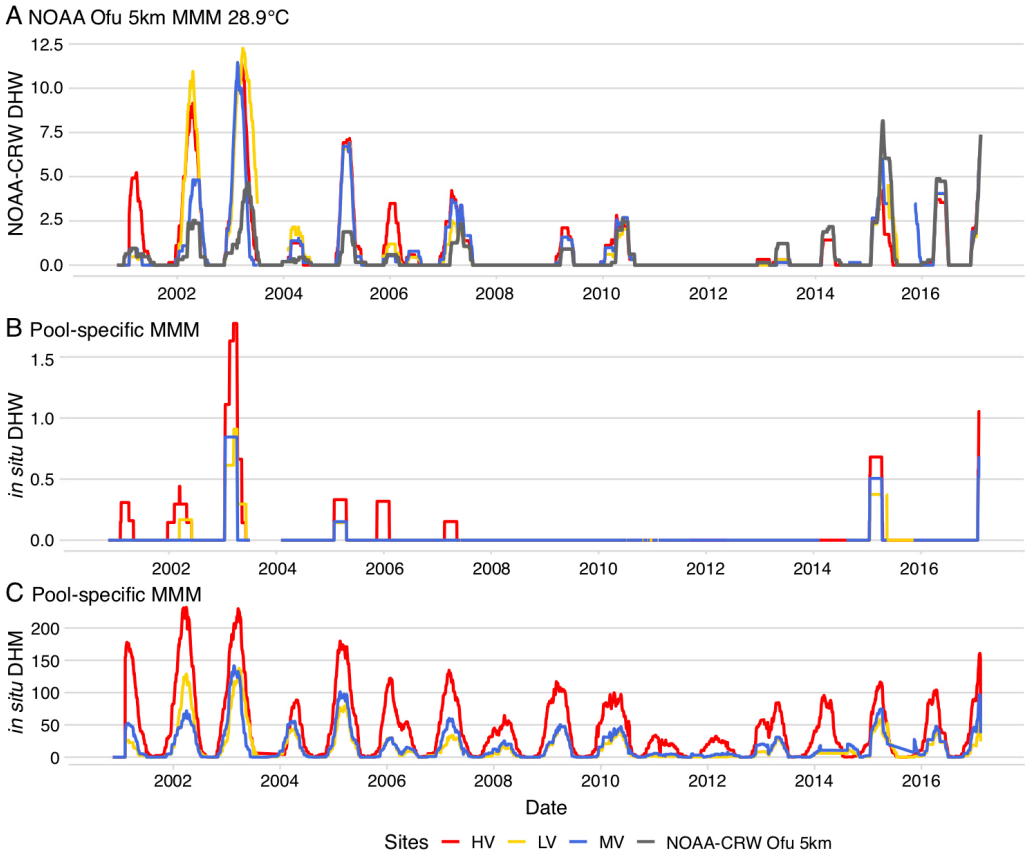

Figure 3.2. Comparison of Degree Heating Week (DHW) calculations for Ofu Island. (A) DHW derived from the NOAA CRW Ofu 5 km satellite product (gray line) using the Maximum Monthly Mean (MMM) of 28.9 °C. Pool DHW (HV [red], MV [gold], LV [blue]) were calculated using the same MMM. (B) *in situ* DHW using the National Park of American Samoa (NPSA) *in situ* temperature time series data to calculate pool specific MMMs. DHWs were derived from each pool's MMM value (HV = 29.4 °C, MV & LV = 29.5 °C). (C) *in situ* Degree Heating Minutes (30 min intervals) calculated from same pool specific MMMs. Gaps in lines signify missing temperature data.

Coral growth

Weekly growth rates for *Porites lobata* differed by the interaction between time and origin_destination. After one month of transplantation, HV corals transplanted into the MV pool had 7 times greater mean (± 1SD) weekly growth rates than MV native corals (HV_MV 0.138 ± 0.05 g wk^{-1} vs. MV_MV 0.019 ± 0.044; *emmeans* p = 0.0498; Figure 3.3). From one to six months and at six months, weekly growth rates did not change nor was it different among paired ramets (Table 3.2, A7). Ramets that were not used in acute bleaching assays remained in their transplant site for two years (June 2018), and coral weekly growth rates at the end of two years were 2-3

times higher than the six and one month samples, respectively (Figure 3.2, Table 3.2, A7) for HV_HV, MV_HV, LV_LV, and MV_MV transplant groups. In June 2018, there were no differences in weekly growth rates among paired native and transplant ramets (Table A7).

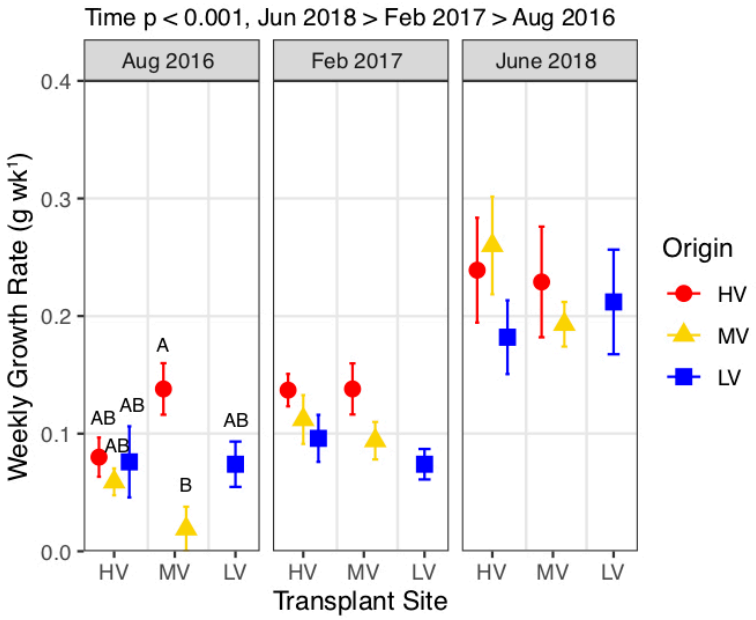

Figure 3.3. Mean weekly growth rates (g wk^{-1}) of *P. lobata* with respect to transplant destination and time. Only significant Tukey's post-hoc comparisons for overall effects are displayed above panels, within time point significant comparisons are denoted with letters, and error bars are 95% confidence intervals.

Symbiodiniaceae photophysiology under experimental and natural stress

Overall, there was a significant effect of transplant group (lmer origin_destination p = 0.0039), treatment (p < 0.001), and the interaction of the two (p = 0.0062) on F_v/F_m following 21hrs of heat stress. Heated MV_MV and MV_HV corals had ~1.5-2-fold higher F_v/F_m normalized values overall (i.e., not split by timepoint) in comparison to all other transplant groups (Figure 3.4A, Table 3.3, A7). Although there was an effect of treatment during the one-month timepoint (August), there were no differences in heat or control replicates among origin_destination transplant groups. By February, MV_MV corals were the only transplant group that did not have reduced F_v/F_m values as result of heat treatment. MV_MV corals had higher F_v/F_m values than both

HV_HV and HV_MV corals (MV_MV-HV_HV p = 0.0157, MV_MV-HV_MV p = 0.0029, Table A7), and MV_HV corals had greater F_v/F_m retention than HV_HV corals (MV_HV-HV_MV p = 0.0180).

In contrast to F_v/F_m values, there was an overall treatment by time interaction for total chlorophyll, where acute heat stress reduced total chlorophyll in August (except MV_HV) but not in February (Figure 3.4B, Table 3.3, A7). In addition, control total chlorophyll values decreased almost 2-fold by February, which coincidentally was at the beginning of the 2017 mass bleaching event.

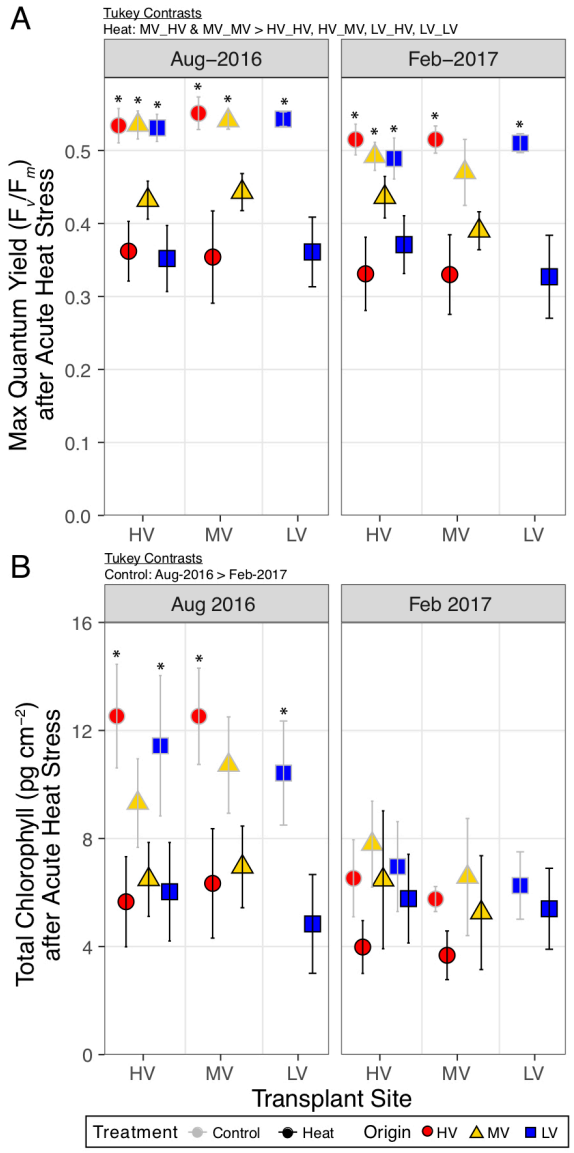

Figure 3.4. (A) Maximum quantum yield (F_v/F_m) and (B) total chlorophyll (pg cm^{-2}) of control (gray outline) and heated (black outline) Symbiodiniaceae following acute heat stress (mean ± 95% confidence intervals) with respect to transplant destination and time. Only significant Tukey's post-hoc comparisons for overall effects of time, origin_destination, treatment, and/or an interaction are displayed above panels and asterisks within each panel signify an effect of treatment for each timepoint.

During the onset of the local bleaching event in 2017, donor colony total chlorophyll values did not differ across backreef sites, where average percent bleaching was 21.5 ± 19.16%, 19.7 ± 13.82%, and 31.3 ± 27.04% for HV, MV, and LV corals respectively (Figure A6). Donor colony total chlorophyll values were not correlated with control sample total chlorophyll (Pearson's R =

-0.26, p = 0.210; Figure A7, Table A8) but were greater than both control and heated values (*emmeans* p = 0.0293, 0.0199, respectively; Figure A8, Table A8). Moreover, donor and control total chlorophyll values did not correlate with number of days spent over 31, 32, and 33° C (Table A8)

Coral physiology in relation to temperature metrics

Coral holobiont physiological variables (weekly growth, control F_v/F_m, control total chlorophyll) and their relationship to environmental metrics such as *in situ* DHW, days spent over 31 and 32 °C, daily temperature range (DTR), maximum DTR, 90^{th} quartile daily range, monthly mean maximum, and monthly minimum and maximum temperatures were examined using a Pearson's correlation matrix (Figure 3.5). Weekly growth was positively correlated with all temperature metrics except 90^{th} quartile daily range. Control F_v/F_m and total chlorophyll were negatively associated with metrics such as: *in situ* DHW, days over 31° and 32 °C, daily temperature range (DTR), maximum DTR, monthly mean maximum, and monthly minimum and maximum temperatures (Table A9); with a stronger correlation for total chlorophyll values compared to F_v/F_m. A Principal Component Analyses (PCA) combining all log-transformed variables further demonstrated the relationship among coral physiology and environment (Figure 3.6, Table A9), where PC1 (Season: DTR, mean, min, and max monthly temperatures) explains 54.8% of the variance, and PC2 (Treatment: weekly growth, Fv/Fm, and total chlorophyll) explains 21.1% of the variance. Individual points cluster by time, where temperature metrics in February (PC1>0) are greater than in August (PC1<0; *adonis* p = 0.001). Values cluster slightly by backreef pool during August, and during February, values do not differ between the HV and MV pool but there is clustering of the LV environment (*adonis* p = 0.001; Table A9). Values cross PC2 based on treatment, where points above '0' represent control samples, and those below '0' are heated samples.

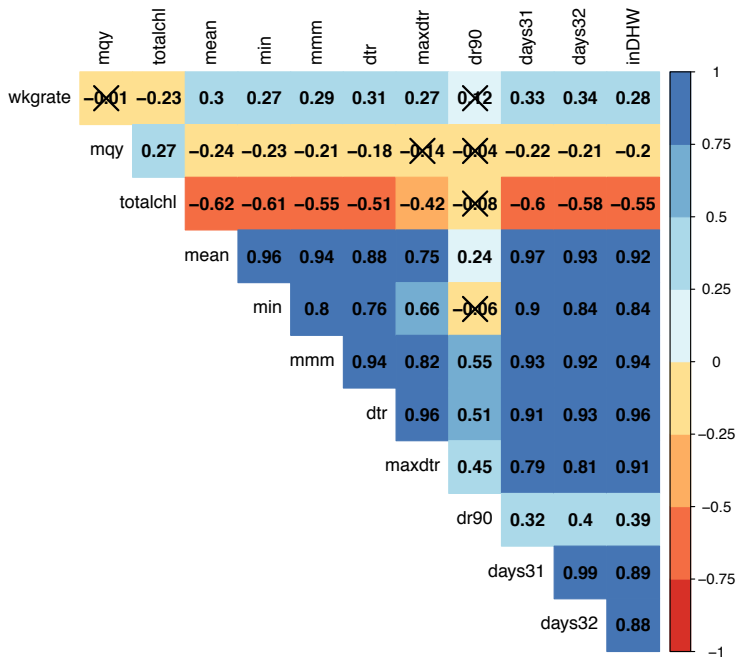

Figure 3.5. Pearson correlation heatmap based on scaled average for 120 ramets (all sites, both timepoints) of control *P. lobata* physiology (weekly growth, F_v/F_m, and total chlorophyll) and Ofu temperature metrics (mean and minimum daily temperatures, maximum mean monthly temperatures, daily temperature range, maximum daily temperature range, 90th quartile daily temperatures, days over 31 and 32 °C, and *in situ* DHW). Colors and values within the squares represent the magnitude and direction of the Pearson correlation according to the key. Non-significant ($p > 0.05$) Pearson pairwise correlations are indicated with an "X."

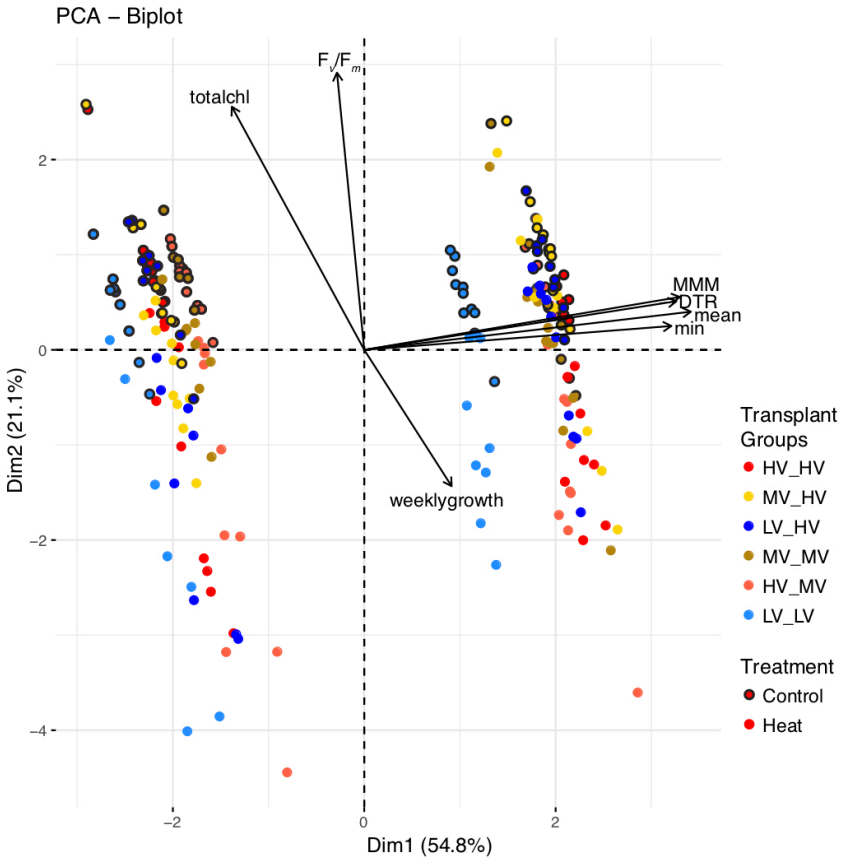

Figure 3.6. Principal Component Analysis Biplot of log-transformed physiological trait data for 240 ramets of P. *lobata* (10 per treatment per transplant site per timepoint) and pool-specific temperature metrics. Data points are colored by transplant group and outlined by treatment. Arrows are the loadings for trait and temperature metrics along the first two principal component axes.

Discussion

Scale-dependent disparities in temperature metrics

Degree Heating Weeks (DHW) have long been recognized as an effective predictor and monitor for global coral bleaching stress (SST; Liu et al. 2006). This study, however, highlights that DHW (or more broadly Degree Heating 'Time'), are quite sensitive to different sources and scales of temperature measurements. The magnitude of thermal anomalies at a reef locale depends on whether accumulated heat stress is modeled using NOAA's CRW or *in situ* temperature, and which data are used to establish the historical climatology/baseline. NOAA's CRW products are all calculated from nighttime satellite 5 km sea surface temperature data (Liu et al. 2003), and can

over- or under-estimate *in situ* temperature regimes at smaller reef-scales (Liu et al. 2013). When we applied the NOAA CRW 5 km Mean Monthly Maximum (MMM) of 28.9 °C for Ofu Island to our own *in situ* temperatures, the number of pool-specific DHWs are much greater than DHWs from the NOAA CRW remotely-sensed data from 2002-2007, but then are roughly similar from 2008-2017 (Figure 3.2A). However, the NOAA CRW derived pool specific DHWs are 2-3 times greater than the *in situ* DHWs derived using MMMs calculated from each pool's daily temperatures (Figure 3.2A vs. B). The first discrepancy between the two climatologies in Figure 3.2 is using nighttime (NOAA CRW) versus 24 hr (*in situ*) temperature data, where nighttime temperature based climatologies result in lower daily and monthly temperature means and a subsequently lower MMM calculated for the NOAA CRW backreef climatology. Second, NOAA CRW products are based on a 5 km scale compared to our *in situ* temperature loggers (~1km between pools), which result in averaged SST that also contributes to lower MMMs and greater number of DHWs. One additional consideration is the different range of years used to calculate the historical climatologies – *in situ* temperature records only date back to 2000 and NOAA CRW utilized the years 1985-1993. When the same years as the *in situ* dataset were applied to the NOAA CRW dataset, a MMM increase of 1 °C resulted for the NOAA CRW time series dataset (not plotted). Given the steady increase in sea surface temperatures over the past decades (Lough et al 2018), it is very likely a location's MMM would be greater if calculated from recent years. In combination with the temporal and spatial scales used to calculate *in situ* backreef climatologies, it is highly likely that the actual MMMs calculated for each pool are greater than what is reported for the 5 km region.

Then which temperature metrics are best for predicting or understanding coral bleaching events? Metrics of thermal stress accumulation – daily variability, acute and cumulative thermal stress, heating rate, thermal trajectory – implies a different amount of stress exposure (Safaie et al. 2018) that could explain bleaching prevalence. McClanahan et al. (2019) demonstrated that the combination of multiple sea surface temperature metrics (i.e. peak hot, duration of cool, and temperature bimodality) explained ~50% of the variance in coral bleaching prevalence during the global 2016 coral bleaching event as opposed to only 9% explained by DHW. The intensity, frequency, and rate of heat loading also influences coral bleaching outcomes in mass bleaching events (Skirving et al. 2019). Additionally, high-frequency temperature variability can have a mitigating effect, reducing the odds of severe bleaching outcomes (Safaie et al. 2018). Therefore,

quantification of *in situ* temperature metrics and cumulative heat loading may improve our predictions and understanding of thermal stress induced coral bleaching. This also highlights the need for a better modeling tool to understand coral bleaching by integrating environmental and biological processes of the stress and bleaching process.

The complex relationship between thermal variability and bleaching sensitivity

Increased thermal variability has positive effects on coral growth and bleaching resistance at exposures up to the local thermal optimum (Buddemeier et al. 2008; Lough 2008; Safaie et al. 2018), especially in the Ofu backreef (Oliver and Palumbi 2011; Thomas et al. 2018). Here, backreef coral growth was positively correlated with multiple temperature metrics, in particular daily temperature range (DTR) and maximum DTR. Other *P. lobata* research on Ofu Island has also demonstrated greater coral growth in the backreef compared to forereef environments attributed to differences in thermal variability between the two habitats (Smith et al. 2007; Barshis et al. 2018). Although increased backreef thermal variability was positively correlated to coral growth, it appears growth is decoupled from thermal tolerance (see Edmunds 2017), as HV_MV corals grew the most initially but did not exhibit increased thermal tolerance. In contrast to growth, thermal variability metrics had a strong negative relationship with *P. lobata* chlorophyll levels in native pool control ramets (Figure 3.5). Seasonality is recognized as a driver of coral pigment cycles (Fitt et al. 2000), with greater pigment concentrations in the winter, and here, coral ramets also had reduced pigment concentrations during the austral summer, which could be attributed to natural seasonal patterns and/or initial bleaching stress.

Coral bleaching in the Ofu backreef typically begins around March-April, and bleaching severity has been shown to vary across species and pool of origin (Morikawa and Palumbi 2019; Thomas et al. 2019). During the bleaching events of 2015 and 2017, greater bleaching was observed in corals originating from the MV pool compared with the HV pool (Morikawa and Palumbi 2019). Here, the natural bleaching stress observed in February 2017 did not result in site-specific differences in bleaching – percent bleaching and total chlorophyll – among our *P. lobata* donor populations. Bleaching responses of donor corals was measured at the early onset of the 2017 bleaching event; therefore, corals may not have accrued enough heat stress in their own environment to demonstrate site-specific differences. Also in contrast to the findings of Morikawa and Palumbi (2019), reduced chlorophyll in native ramets did not significantly correlate with considerable (>25-50%) site-specific bleaching responses of donor colonies at the onset of the

2017 bleaching event. In this instance, it appears unlikely that the bleaching responses of experimental ramets could serve as a proxy for bleaching susceptibility in natural coral populations, but could instead represent size-specific bleaching responses (Hughes and Jackson 1985; but see Edmunds 2017) between the massive donor colonies and small ramets.

Contrary to the donor colony thermal tolerance observations during the hottest time of this study (February), experimentally heated ramets revealed site-specific variation in bleaching responses. Previous studies examining thermal tolerances of Ofu backreef *P. lobata* demonstrated a strong effect of origin, where backreef HV and MV corals had elevated tolerance limits in comparison to nearby forereef corals (Barshis et al. 2018). Similar to Barshis et al. (2018), there was an effect of native reef environment on chlorophyll fluorescence under acute heat stress, however it was the MV native corals that had greater F_m/F_m values than HV native and transplanted ramets. In addition, MV native coral F_m/F_m values were not significantly affected by acute heat stress in February, and total chlorophyll of MV ramets transplanted into the HV pool did not respond to acute heat stress in August, suggesting that MV corals had greater tolerance limits than other backreef *P. lobata* in the present study. While most thermal tolerance studies of branching corals on Ofu have shown greater heat tolerance in HV native coral populations or corals transplanted into the HV pool (Thomas et al. 2018), MV pool *P. lobata* corals have consistently displayed increased tolerance limits over two bleaching years (Klepac & Barshis 2020; this study) and there was no effect of the HV common garden on increasing bleaching tolerance. Thus, this is the first reported instance of reduced bleaching susceptibility in corals from the moderately variable backreef environment of Ofu Island.

Here and in Chapter 2, *P. lobata* corals from the HV pool did not have increased thermal tolerance as has been found in other coral species from the HV pool (Oliver and Palumbi 2010; Oliver and Palumbi 2011; Palumbi et al. 2014; Morikawa and Palumbi 2019). A recent study examining thermal tolerance retention of four coral species from the MV and HV pool found two to three times less bleaching in corals from the HV versus MV pool after the 2015 and 2017 bleaching events (Morikawa and Palumbi 2019). Corals in this study were transplanted into a nearby less variable reef site, where accumulated thermal stress was not as severe as in the native pools. Species-specific bleaching susceptibility could also explain the disparities between studies, where the most severe bleaching was observed in *Acropora spp.*, followed by *Pocillopora spp.* and then *Porites cylindrica*, all branching growth forms. Different life history strategies (Darling

et al. 2012) between weedy (*Pocillopora spp.*), competitive (*Acropora spp.*), and tolerant (*Porites spp.*) corals respond to heat variability and accumulated stress differently, so it is possible weedy and competitive coral species from the HV pool may show greater variation in bleaching susceptibility than the more tolerant massive *P. lobata*.

Summary

Even though the *in situ* pool-specific climatologies of DHW and DHM revealed fine-scale spatial variability and a greater cumulative thermal stress in the HV pool, they did not necessarily predict physiological bleaching outcomes of donor colonies observed herein. Moreover, similar summer maximal and daily temperature ranges of the HV and MV pool did not reveal a strong effect of environment on the differential responses to acute thermal stress. Relatively low bleaching responses despite high variability and Degree Heating metrics could be a result of timing or other non-thermal factors, such as differences in sunlight, turbidity, water flow and quality among the backreef pools. Yet, origin-specific responses to heat stress again indicated that the MV_MV transplants (from the moderately variable transplanted to their native pool) had subtle, but distinctly higher tolerance of our short-term stress exposure that corals from or transplanted into the highly variable (HV) site. Sustained growth and bleaching resistance demonstrated by MV corals during this study and in Chapter 2 suggests that moderately variable environments with conditions just below an organisms thermal optimum could maximize fitness (Trmax; Martin and Huey 2008) as climate warms. These results also indicate *P. lobata* in this system behaves differently that previously examined species in the backreef pools of Ofu. Acute spikes in thermal variation have been recognized as beneficial for coral stress responses, but the combination of thermal spikes with chronic heat loading, as experienced in the HV pool over two consecutive bleaching years (2015 & 2016), may overwhelm coral thermal performance and native HV_HV corals could be in a chronic state of thermal stress susceptibility.

CHAPTER 4

POPULATION-SPECIFIC GENE EXPRESSION PATTERNS IN RESPONSE TO ACUTE HEAT STRESS AND NOVEL REEF ENVIRONMENTS

Introduction

Although corals are predicted to be susceptible to rapidly warming oceans (Hughes et al. 2017a), variation in bleaching and heat stress responses have been documented across many coral populations, species, regions, and even within individual reefs (Loya et al. 2001; Hughes et al. 2003; McClanahan et al. 2005; Ulstrup et al. 2006; Brandt 2009; van Woesik et al. 2011; Kenkel et al. 2013b; Hughes et al. 2018; Genevier et al. 2019; Thomas et al. 2019). Coral populations adapted to naturally high temperatures or environmental variability have been identified as more thermally tolerant than nearby conspecifics from more stable reef environments (Jokiel and Coles 1990; Coles 1997; Craig et al. 2001; Oliver and Palumbi 2010; Oliver and Palumbi 2011; Fine et al. 2013; Palumbi et al. 2014; Kenkel et al. 2015; Schoepf et al. 2015; Howells et al. 2016), and coral populations transplanted into these more extreme environments demonstrate increases in bleaching resistance (Palumbi et al. 2014). Thus, coral populations from these variable environments may best be able to cope with rapid climate change and are an invaluable source of information on the mechanisms underlying the coral stress response and differential bleaching susceptibilities.

Physiological differences in coral bleaching resilience have been characterized in a plethora of coral populations, contributing to our understanding of acclimatory and adaptive responses to environmental stress, yet molecular stress responses are only recently being described (Seneca et al. 2010; Davy et al. 2012; Kenkel et al. 2014; Palumbi et al. 2014; Dixon et al. 2015; Rose et al. 2016). Gene expression analyses provide the mechanistic link between genotype and phenotype and offers insight into coral responses, resistance, and/or resilience to environmental stress (López-Maury et al. 2008). Moreover, common garden and reciprocal transplant experiments in conjunction with physiological and genetic investigations improve our understanding of the mechanisms of thermal tolerance. In the backreef pools of Ofu Island,

American Samoa, *Acropora hyacinthus* corals from the highly variable (HV) pool reveal gene expression profiles indicative of increased heat tolerance (Barshis et al. 2013; Palumbi et al. 2014), and corals from a nearby moderately variable (MV) pool transplanted into the HV pool show both physiological and genetic evidence of acclimatization gains in thermal tolerance (Palumbi et al. 2014). Distinct transcriptomic responses correlated with increased heat tolerance following a natural bleaching event have also been identified in the massive coral *Porites astreoides* from inshore reef habitats in the Florida Keys (Kenkel et al. 2013a; Kenkel and Matz 2016). As such, detailed transcriptional profiling of the coral response to transplantation and heat stress can provide insight into potential molecular mechanisms that could enable corals to respond to environmental change.

A variety of gene expression patterns have recently been discovered as potential mechanisms for enhanced stress tolerance in corals from or exposed to environmental extremes (Barshis et al. 2013; Bay and Palumbi 2015; Seneca and Palumbi 2015; Kenkel and Matz 2016). The ability of coral gene expression to respond rapidly and resist experimental bleaching stress was first observed by Seneca and Palumbi (2015), where coral expression values returned to pre-stress levels following 15 hr of experimental bleaching stress, defined as transcriptome resilience (Franssen et al. 2011). Corals have also shown rapid acclimatization abilities in heat resilience, where the magnitude of expression changes before and after experimental heat stress was lower in corals acclimated to elevated and variable temperatures (Bellantuono et al. 2012b; Bay and Palumbi 2015). Long-term acclimatization and/or local adaptation to environmental variability has been linked to baseline changes in gene expression, called constitutive upregulation or 'frontloading' (Barshis et al. 2013), where resilient corals have a suite of stress response genes that are already upregulated before heat stress. An alternative mechanism for coral adaptation to temperature variation was revealed by Kenkel and Matz (2016), where gene expression plasticity was defined as the magnitude of a shift in gene expression to match or be similar to that of the transplantation site. Elevated gene expression plasticity was suggested to be adaptive as it was significantly correlated with increased tolerance to a natural bleaching event (Kenkel and Matz 2016). These studies were conducted using previously recognized tolerant coral populations from variable reef environments, and collectively, the diversity of molecular responses to stress indicates that different strategies could allow some coral populations and species to adapt to future warming oceans.

Accompanying Chapter 3, here, I examined transcriptomic responses to acute heat stress and transplantation in adult populations of the massive coral *Porites lobata* from the distinct backreef pools of Ofu Island. Physiological responses to acute heat stress and transplantation during the austral winter (August 2016) and following summer (February 2017) indicated that HV native and transplanted corals (HV_HV and HV_MV) did not have increased bleaching tolerance, as seen in previous research of branching coral populations from this highly variable reef environment (Thomas et al. 2018). Moreover, MV and LV corals transplanted into the HV pool (MV_HV and LV_HV) did not increase their thermal tolerance, corroborating Chapter 2 results and evidence of origin-specific differences in thermal tolerance. Corals from the MV pool maintained elevated symbiont photosynthetic efficiency under acute heat stress which could indicate a broader stress tolerance for this population. The present study explores the hypothesis that origin-specific differences in thermal tolerance may be due to specialization of the coral-algal holobiont in each of their respective environments. I analyzed global gene expression profiles from host and algal symbiont transcripts to assess molecular responses to acute heat stress and transplantation in the corals from the same reciprocal transplant experiment (between HV and MV pools) as Chapter 3 following the one-month heat stress experiment.

Materials and Methods

Coral collection & transplantation

Ten colonies (i.e., genets) of *P. lobata* from each of two backreef pools (MV and HV) were sampled between July 1-3, 2016. Colonies were chosen based on visual appearance (non-bleached) and size (1.5 – 3 m diameter), and at a distance of ~5 m to other colonies to minimize chance for sampling clones (*sensu* Baums et al. 2006). From each colony, 24 cores (i.e., ramets) were sampled and affixed to nylon bolts with marine epoxy and secured to an egg-crate light diffuser grid using nylon wingnuts. Ramets from each colony from each site were randomly assigned to a transplant grid based upon transplant site (Figure 1; 8 grids at HV and MV, 4 grids at LV). Half of the MV and LV samples (12 ramets per genet, n = 120 total per site) were transplanted into the HV pool and the other half remained at the respective native reef site. In addition, half of the samples from the HV pool were transplanted into the MV site, and randomly mixed with MV nubbins on grids. Transplantation of HV samples into the MV pool occurred on July 13, and MV and LV samples

were transplanted into the HV pool July 15, 2016. This resulted in 4 unique transplant groups: HV_HV, HV_MV, MV_HV, and MV_MV (origin_destination).

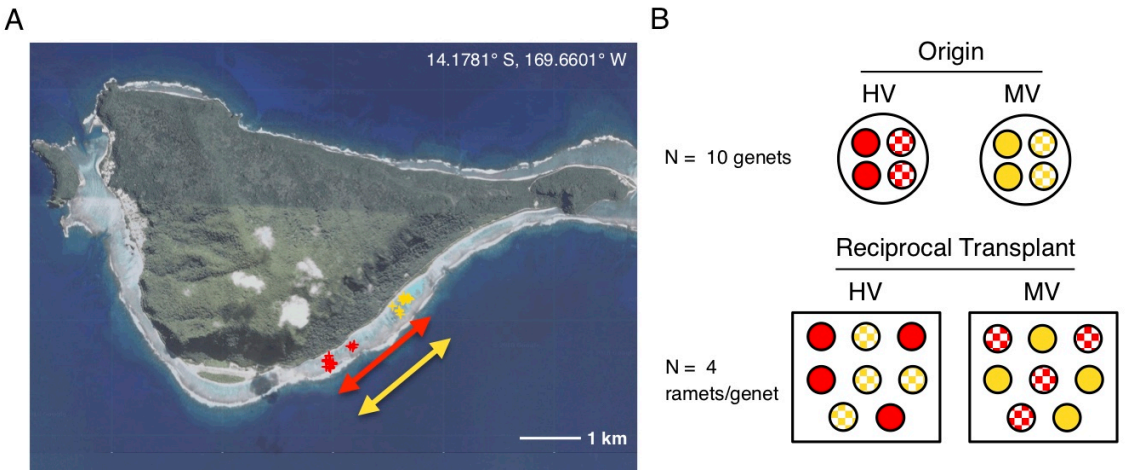

Figure 4.1. Reciprocal transplant experiment between HV and MV pools on Ofu Island, American Samoa. (A) Arrows show transplant design within three backreef pools – HV (red), MV (gold) – and crosses denote sampled *P. lobata* genets. (B) Twenty-four ramets per ten genets were sampled from each site (N = 720), and half were transplanted into either the HV or MV common garden and the other half were returned to the native site. Four ramets per genet per site were collected after one month (Aug 2016).

Acute heat stress exposure

One month post-transplantation (August 5-8, 2016), 120 coral ramets were collected from the three Ofu backreef pools (2 per genet per species per site) and placed in the Coral Bleaching Automated Stress System (CBASS; Voolstra et al. 2020) constructed from Coleman 24 L Party Stacker Coolers™ as head and sump tanks. A pump provided a flow of 88.9 mL sec^{1} to the head tank, which was also fitted with 6 LED bulbs (Phillips PAR38 LED) with a light level of ~500 ± 20 µM photons/m/s and 12 hr light/dark photoperiod. A flow-through drip system provided 2.5 mL sec^{1} of local seawater throughout the duration of the experiment.

Controlled temperature ramp exposures occurred similar to Klepac & Barshis (2020). Briefly, samples were randomly assigned within two control and two heat tanks. In the heat tank, temperature increased over 3 hrs from 28 to 36.5 °C, followed by a 3 hr hold at 36.5 °C, then a ramp down to and hold at 28 °C for 16 hrs. The control tank was set to remain stable at 28 °C for

22 hrs. Small (~1.5 cm) biopsies from the side of each nubbin were scraped using a sterile razor blade 1 hr after reaching the maximum temperature hold set point (4 hrs into the experiment). We adopted this approach *sensu* Seneca and Palumbi (2015), who demonstrated that expression-level changes at the onset of heat shock were approximately two-fold higher than at the end of each experiment. Samples were immediately placed into an RNALater buffer, stored at -20 °C until transportation back to Old Dominion University and at -80 °C until processing.

Coral host genotyping

Mitochondrial molecular markers were used to identify coral host genetic differentiation across the three backreef sites. A small (1 cm^2) fragment was sampled from 10 individuals per site, totaling 30 for *P. lobata*. Samples were incubated for 1-1.5 hr at 65 °C in a 1% SDS in DNABuffer (protocols.io dx.doi.org/10.17504/protocols.io.dyq7vv; Baker and Cunning 2016b) and then transported to Old Dominion University. Genomic DNA was extracted from the archived coral samples using a guanidinium-based extraction protocol (Baker and Cunning 2016b) and quantified spectrophotometrically. DNA extracts were used for both coral host and Symbiodiniaceae sequencing.

To identify genets at the species level, corals were genotyped using three mitochondrial markers (Table S1). Three sets of forward and reverse mitochondrial DNA markers were amplified under thermal cycling conditions outlined previously (Forsman et al. 2009, 2015; Huang et al. 2011, 2014) corresponding to: (1) NAD5 intron; (2) putative control region (PCr); (3) cytochrome c oxidase subunit I gene (COI). All PCR amplifications (20 µL) contained 2 µL of DNA template, 10 µL of Premix ExTaq HS (Takara Biotech USA, Inc., Mountain View, CA), 0.2 µL of 10 µM primer, and nuclease-free water to volume (20 µL). PCR products were treated with ExoSAP-IT™ (Affymetrix Inc., Santa Clara, CA) for 15 min at 37 °C, followed by 80 °C for 15 min. Cleaned products were directly sequenced in-house on an ABI 3130XL Genetic Analyzer (Applied Biosystems, Foster City, CA).

Resulting sequences were inspected and aligned for each mtDNA region using default parameters in Geneious R9 (Biomatters Inc., Newark, NJ). Alignments were trimmed to the same length and resulting contigs were collapsed (FaBox; Villesen 2007) to generate a NEXUS file of haplotype sequences. Molecular phylogenetic networks by reef site and amplicon were constructed using the median-joining algorithm in PopART (Leigh and Bryant 2015). In addition to computing

phylogenetic networks, PopART was also used to calculated population specific F_{ST} values, Analysis of Molecular Variance (AMoVA), and nucleotide diversity indices (X and Z).

RNA isolation and mRNA sequencing

Total RNA was extracted using a modified RNAqueous 4-PCR kit (Ambion, Life Technologies; sensu Kenkel and Matz 2016). Samples were crushed with a sterile razor blade in lysis buffer and kept on ice for 1 hr with intermittent vortexing to increase RNA yields. Following centrifugation for 2 min at 16,000**g*, 700 uL of supernatant was used for RNA purification following the manufacturers protocol. At the final elution step, the same 50 uL of elute was twice passed through a spin column to maximize the concentration of RNA. Samples were DNAse treated (sensu Kenkel et al. 2011) and then cleaned with Kapa Pure Beads and two 80% ethanol washes to remove DNAse reaction buffers. Isolated and cleaned RNA was quantified using a Qubit RNA High Sensitivity assay (ThermoFisher Scientific, Waltham, MA) and a Fragment Analyzer High Sensitivity RNA Kit (DNF-472; Agilent, Santa Clara, CA). Input total RNA (0.05-1.0 ug/uL) from 84 samples were used to construct double-stranded complementary DNA (dscDNA) libraries with a KAPA mRNA HyperPrep kit and KAPA Unique Dual-Indexed adapters (KAPA Biosystems, Roche Sequencing and Life Sciences Wilmington, MA). After preparation, library concentrations were quantified via qPCR via KAPA's library quantification kit. Adapter-ligated ds-cDNA libraries were sent to UC Berkeley's Vincent J. Coates Genomics Sequencing Laboratory and sequenced on a single lane of Illumina NovaSeq 6000 (100 bases, paired-end reads, S4 lane chemistry). Each coral genotype had 4 corresponding RNA samples (native, transplant, heat and control), where 6 individuals from HV and 5 (due to technical errors) individuals from MV were used for library preparation (11 individuals*4 samples per individual = 44 samples).

Gene expression analysis

Data analysis followed an updated version of the Simple Fool's Guide to Populations Genomics via RNA-Seq (De Wit et al. 2012). Adaptor sequences and poor-quality segments from raw sequences were trimmed and reads <20 bp were discarded using the fastx_clipper and fastx_trimmer functions of the fastx toolbox (Gordon and Hannon 2010). Unfiltered reads were mapped to a combined coral (*Porites lutea* genome, reefgenomics.org/sitemap.html; Robbins et al. 2019) and Symbiodiniaceae (*Symbiodinium goreaui* [type C1] genome, reefgenomics.org/sitemap.html; Liew et al. 2016) reference assembly via Bowtie2 v2.4.1 [local -

x -k n/5] (Langmead and Salzberg 2012). A Sequence Alignment Map (SAM) file was created for each sample, containing unique and singly mapped read counts for each contig. In total, there were 6,546,588-132,397,504 mapped reads (median = 22,344,424). On average, each sample library had an average alignment score of 48.63% ± 6.36% (1SD), and contained 31,811,229 ± 25,108,043 total aligned reads, 16,205,794 ± 12,631,477 zero aligned reads (51.37% ± 6.36%), 10,221,882 ± 8,368,508 reads that aligned exactly one time (32.24% ± 5.03%), and 5,383,552 ± 4,630,452 reads that aligned greater than one time (16.39% ± 2.23%; Figure A9).

Read counts were analyzed using the DESeq2 (Anders and Huber 2010) package in Rv3.6.3 (R Core Team 2020) to identify differentially expressed genes. The count dataset was then subdivided by coral host and symbiont contiguous sequences (contigs, representative of and herein referred to as "genes"), resulting in 31,126 and 35,913 genes, for host and symbiont respectively. Genes with less than 10 counts in 90% of samples were filtered out, which resulted in 8,069 genes for the coral host and 15,241 for symbiont. A total of four pairwise comparisons were performed on each dataset to examine gene expression pattern differences in response to temperature treatment based on transplant (origin_destination) site: (i) HV_HV heat (h) vs. control (c); (ii) HV_MV h vs. c; (iii) MV_HV h vs. c; and (iv) MV_MV h vs. c.

Filtered DESeq counts for each host and symbiont dataset were further normalized using the regularized log (rlog) transformation in DESeq2 prior to conducting a principal component analysis (PCA) to examine broad scale variation in gene expression patterns explained by the interaction of transplant group and treatment, and the effect of origin_destination within each treatment. A PERMANOVA (*adonis* function) using the Euclidean distance matrix function tested the effects of origin_destination*treatment, origin_destination, and treatment.

Similar to Barshis et al. (2013), the genes that had a greater response to heat stress in one transplant group but not the another were used to further examine differences in baseline expression prior to the acute heat stress response. Log2-fold changes in expression, i.e., the magnitude of response, was compared between coral transplant groups in the HV pool (HV_HV and MV_HV), MV pool (HV_MV and MV_MV), and native versus transplants (HV_HV and HV_MV, MV_HV and MV_MV). Symbiont comparisons included native versus transplants (HV_HV and HV_MV). The significantly unique genes were subset from each transplant group, and to assess whether a lack of significant change in one group was a result of lower fold-change and not higher variance in comparison to the other group, a chi-square test was performed on both

up- and down-regulated genes against an expected 50/50 distribution. Then, genes with significantly reduced upregulation (X^2 p-value <0.05) were subset from both transplant groups to compute a linear regression comparing the log2-fold change difference between heat and control expression on the x-axis and the ratio of base-mean control expression (i.e., the fold change in control expression) on the y-axis between the two groups. Each gene's difference in fold change is associated with reduced upregulation if $x < 0$ and higher constitutive expression if $y > 1$.

To characterize the variation in gene expression among the RTE corals from the HV and MV pools, a discriminant analysis of principal components (DAPC; Jombart et al. 2010) was conducted. DAPC determines the axis in multivariate space where the difference in variation between specified groups is maximized (contrary to an ANOVA and PCA which describes global variance between and within groups). Filtered DESeq counts were regularized log (rlog) transformed to differentiate between gene expression profiles of native HV and MV corals. Sample group sizes were: MV to MV (n=5), MV to HV (n=5), HV to HV (n=6), and HV to MV (n=6). Using the native population (MV to MV, and HV to HV) as groups, the discriminant function defined these groups as the measuring scale axis. Ramets transplanted across habitats were then scored along this axis to quantify whether corals shifted expression upon transplantation. To compare the magnitude of this shift, i.e., a measure of gene expression plasticity, the MCMCglmm package modeled DAPC scores as a function of origin plus the origin-specific effect of being transplanted away (with 2,800 sets of parameter estimates). P-values were calculated as the difference between absolute values of origin-specific effects of being transplanted away (Kenkel and Matz 2016).

Of the original 31,126 coding sequences (CDS), 21,004 (67%) contigs from the assembled *P. lutea* genome were identified through protein similarity (BLASTp) against the SwisProt protein database (Robbins et al. 2019). Gene identification codes in the resulting table were then annotated to include gene name, description, and Gene Ontology (GO). Gene ontology enrichment analysis using the R package GO-MWU (https://github.com/z0on/GO_MWU) was performed on the coral host, where a Mann-Whitney U test measured whether genes belonging to GO categories were significantly clustered based on ranking of signed log p-values (Wright et al. 2015).

Symbiodiniaceae genotyping

Relative Symbiodiniaceae clade representation was conducted by mapping quality-control unfiltered reads to a concatenated Symbiodiniaceae genome (clades A, B, C, D) provided by

Mikhail Matz, University of Texas. Mapping to the reference assembly followed the same alignment parameters specified for gene expression analyses. Resulting SAM files containing the number of reads mapped to each clade (represented as a single chromosome) were then calculated for relative clade abundance based on the number of high-quality mappings using the perl script zooxtype.pl (https://github.com/z0on/2bRAD_denovo/blob/master/zooxType.pl). Differences in Symbiodiniaceae proportions between origin_transplant, treatment, clade type, and the interaction were analyzed using PERMANOVA *adonis*, with 999 permutations of residuals based on Euclidean distances.

Results

Shared coral host haplotypes and Symbiodiniaceae composition

Three mitochondrial DNA (mtDNA) sequence datasets, cytochrome C oxidase subunit I gene (COI), NAD5 intron region (NAD5), and putative control region (PCr), were produced from seven to ten colonies of *P. lobata* per backreef pool, yielding a total of 23, 28, and 26 samples for each locus, respectively. For the three populations of *P. lobata*, each mtDNA locus produced roughly similar haplotype networks (Figure A10). For all three mtDNA loci, F_{ST} values ranged from 0.02-0.04 and were non-significant ($p > 0.05$; Table A10), and AMOVA results attribute 96-98% of variation to within populations (Table A10).

Symbiodiniaceae genotyping indicated significant differences in clade proportion (*adonis* $p = 0.001$), where Clade B and C were dominant, or greater than 50%, (18-61% [low in MV_MV control] and 30-90%, respectively) and relatively low proportions of Clade A (2-7%; absent in HV_MV control and MV_MV heat) and D (2-3%) in all transplant groups (Figure A11; Table A11). During bleaching stress, proportions varied by treatment (*adonis* $p = 0.018$), where Clade B increased, and Clade C decreased in all groups but HV_MV (Figure A11). In addition, proportions of Clade D increased by ~0.5% in HV corals under heat stress but increased from 2% to 3% in MV corals.

Coral host gene expression differences in response to acute heat stress and transplantation

During peak bleaching stress (1hr after maximum temperature hold), 3,116 differentially expressed genes (DEGs; out of 8,069 post-filtered contigs at FDR 5%) were upregulated (39%) in response to heat stress and 2,716 DEGs were downregulated (34%; Table A12). Principal component analysis revealed that 66% of the variance in expression differences of the regularized

log transformed DEGs were a result of the interaction of origin_destination and heat treatment (*adonis* p = 0.001; Figure 4.2, Table A13). Pairwise comparisons among transplant group*treatment resulted in significant differences between MV_MV and MV_HV heated corals (p = 0.01). At the individual factor level, origin_destination did not have an effect on gene expression (*adonis* p = 0.939), neither within heat nor control treatment (*adonis* p = 0.969 & 0.905, respectively), although there was a post-hoc pairwise difference in expression between MV_MV and HV_HV corals (*adonis* p = 0.031, Table A13). Overall, corals from the HV pool had the greatest number of DEGs in response to treatment (HV_HV = 3,948, HV_MV = 4,086), followed by MV corals with the lowest number of DEGs (MV_MV = 3,486, MV_HV = 3,497; Figure 4.3A, Table A12).

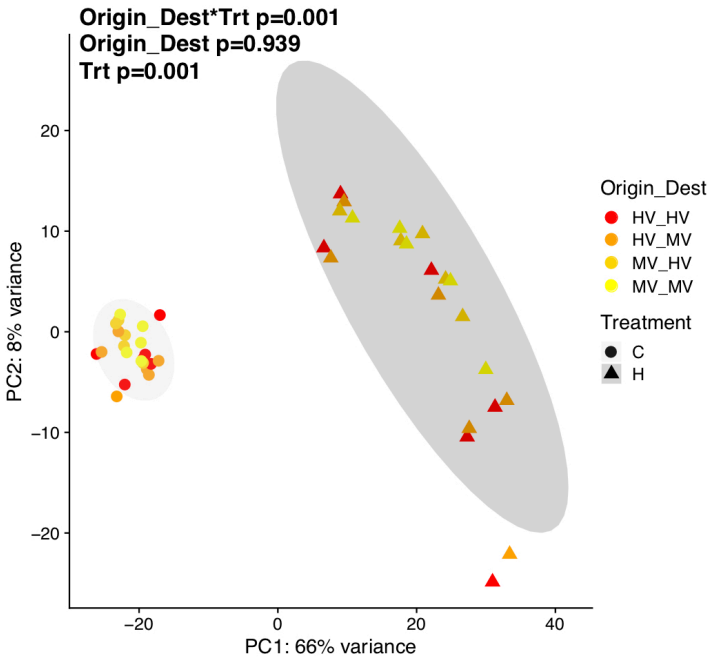

Figure 4.2. Principal Component Analysis (PCA) of normalized expression values for 8,069 contigs of *P. lobata* comparisons for transplant group (origin_destination) and treatment (heat and control). Axes labels show proportion of variance explained by each principal component. Symbols in the upper panel represent treatment (triangles: heat, circles: control), and color represents transplant group. Ellipses indicate 95% confidence intervals for each group (or treatment). PERMANOVA *adonis* results of significance are denoted for p-values.

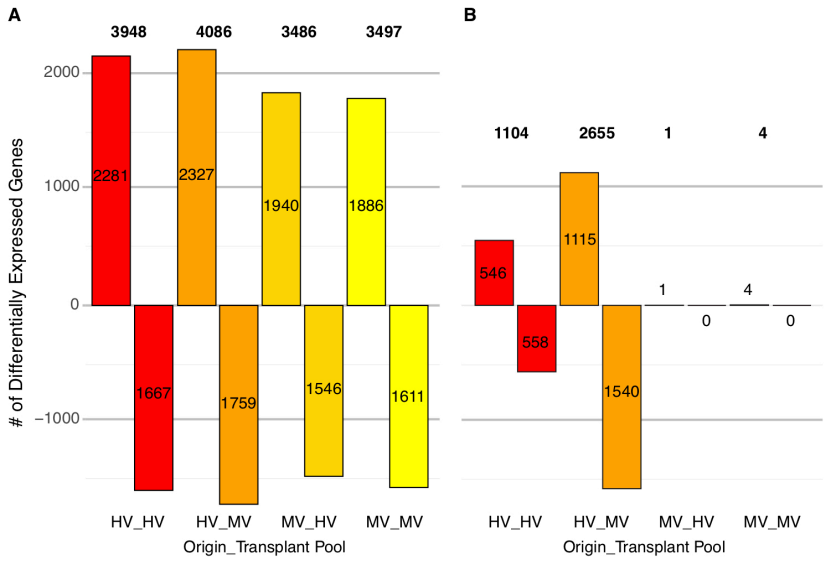

Figure 4.3. Differentially expressed genes (DEGs) for each transplant group in (A) *P. lobata* and (B) Symbiodiniaceae. Numbers above 0 represent significant up-regulated DEGs and below 0 indicates down-regulated DEGs. Bolded numbers above bars signify total number of significant DEGs and colors represent each transplant group.

Of the filtered 8,069 coral host contigs, functional enrichment analysis between heated and control samples produced 23 significant (10% FDR) gene ontology (GO) molecular function, 32 GO cellular component, and 102 GO biological process categories (Figure A12, Table A14). Activation, regulation, and transduction of signaling cascades and ubiquitin pathways were upregulated in response to heat stress, whereas cytoskeletal motor complexes, metabolic, and meiotic processes were downregulated.

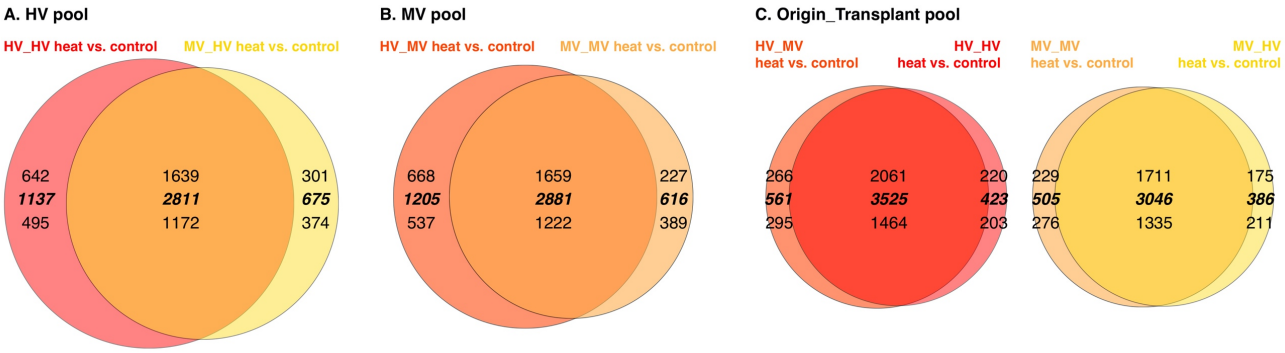

Figure 4.4. Venn diagram showing the number of differentially expressed genes (DEGs) detected in *P. lobata* based on change in expression (bold: total DEGs, above bold: up-regulated DEGs, below bold: down-regulated DEGs) in response to acute heat stress with regards to transplant destination: (A) HV pool, (B) MV pool, (C) origin vs. transplant pool.

Corals transplanted into the HV and/or MV pool

In corals transplanted into the HV pool common garden, transplant groups had a large concerted overlap in differential gene expression, where 2,811 DEGs were shared among HV_HV (71% of total DEG) and MV_HV (81%; Figure 4.4A). Of the shared DEGs, the most significantly expressed were zinc finger proteins, heat shock protein 70, adenylate cyclase, cytochrome P450, and kinase-activated protein kinase. HV_HV corals had 1,137 (29%) unique DEGs in comparison to the 675 (19%) unique DEGs in MV_HV corals (Figure 4.4A). Gene expression comparisons between HV and MV corals transplanted into the MV pool resulted in 2,881 (61% of total DEGs) genes that were shared between the populations, yet again HV_MV corals had more uniquely expressed genes (1,205, 26%) that did not change significantly in MV_MV corals (616 genes, 13%; Figure 4.4B).

To characterize the variation in gene expression among the RTE between the HV and MV pools, a discriminant analysis of principal components (DAPC; Jombart et al. 2010) was conducted on filtered gene datasets subset by treatment. For heat and control corals, MV native coral gene expression was not differentiated from HV native corals (MCMC p = 1, 0.98, respectively; Figure 4.5A&C, Table A15). In addition, neither heated nor control MV and HV ramets shifted their gene expression in response to transplantation into the HV or MV pool, respectively (MCMC p = 0.47, 0.73; Table A15).

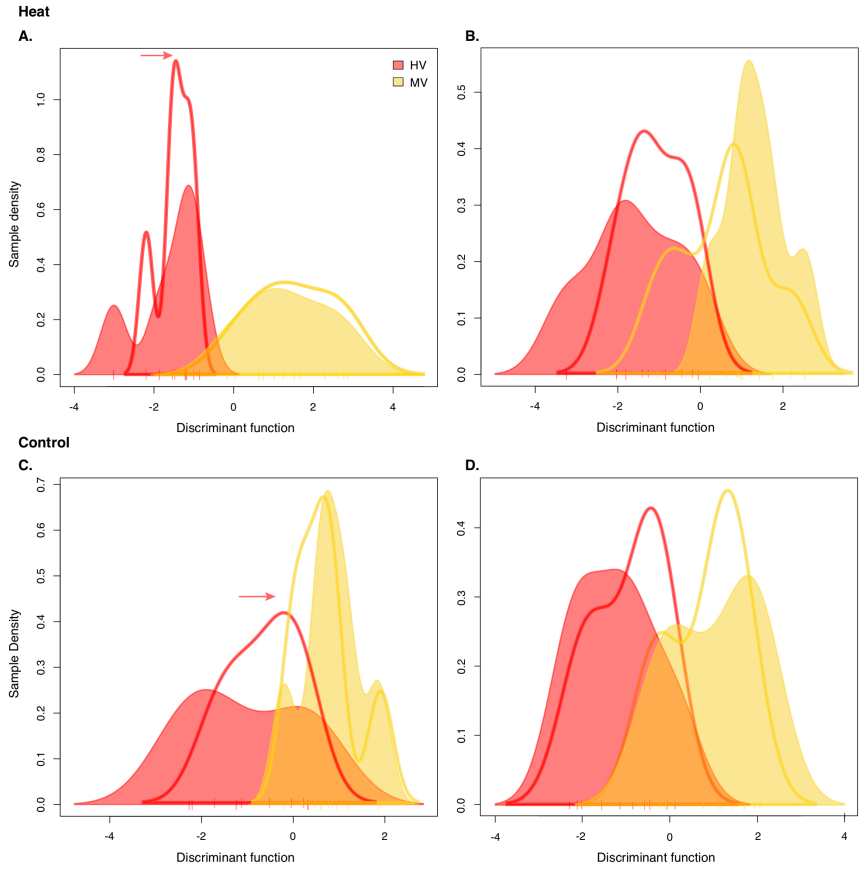

Figure 4.5. Population-level variation in gene expression plasticity with regards to treatment (heat: A&B, control: C&D) in *P. lobata* (8,069; A&C) and Symbiodiniaceae (15,241; B&D) genes. The x-axis is the direction in multivariate space along which the difference between pool of origin (solid density plots) and transplant destination (open density plots) is maximized. Density plots correspond to transplant groups, where red indicates corals or symbionts from the HV pool, and gold represents corals or symbionts from the MV pool. The tick marks are predictive shifts in individual samples as a function of the discriminant analysis. Arrows indicate mean changes in gene expression as a result of transplantation.

Native versus transplanted corals

To investigate whether transplantation had any effect on gene expression in response to heat stress, paired native and transplant ramets were compared. Comparisons revealed a large overlap in shared differentially expressed genes between natives and transplants in response to heat stress: 3,525 (78%) DEGs were shared between HV_HV and HV_MV corals, and 3,046 (77%) genes were shared between MV_HV and MV_MV corals (Figure 4.4C), with many fewer

uniquely expressed genes among paired origin_transplant groups. Differential gene expression was greater in the MV pool for both HV_MV transplants and MV_MV natives than in the HV pool.

Reduced expression changes in corals from or acclimated to highly variable conditions has recently been attributed to 'frontloading', or constitutive upregulation, where genes that had a lower magnitude of expression change under heat stress also had higher baseline expression, presumably conferring a proactive benefit during subsequent heat stress (Barshis et al. 2013). There were 561 genes that reacted to heat stress in HV_MV corals but not in HV_HV corals. A lower fold change (lower magnitude of response) was detected in up-regulated (249 of 250; X^2 test $p < 2.2e^{-16}$; Figure A13A, Table A16) and down-regulated genes in HV_HV corals (0 of 287; X^2 test $p < 2.2e^{-16}$). Across the 247 genes with significantly reduced up-regulation (bordered box in Figure A13A), 212 of them showed higher control (i.e. baseline) expression than in HV_MV controls (85%, $p < 2.2e^{16}$; Figure A13B, y-axis). Similar to Barshis et al. (2013), reduced up-regulation in HV_HV corals (each gene's difference between HV_HV and HV_MV fold change upon heat stress) and higher constitutive expression in HV_HV controls relative to HV_MV controls (each gene's ratio of HV to HV control expression) could be associated with 'frontloading' of control genes as a resilience mechanism. However, the same pattern was detected in the opposite direction: 164/195 significantly up-regulated genes (84%, $p < 2.2e^{16}$; Figure A13D, Table A16) fell into the frontloading category for HV_MV control expression filtered from the 423 uniquely expressed genes in HV_HV corals not in HV_MV corals (Figure A13C-D).

Similarly, there was a lower magnitude of response under heat stress in 505 DEGs from MV_HV corals in comparison to MV_MV corals (up-regulated genes: 160 of 160, down-regulated genes: 0 of 270, X^2 test $p < 2.2e^{-16}$; Figure A14A, Table A16). Of the 160 upregulated genes with a lower reaction to heat stress in MV_HV corals, 137 (85%) had greater control expression than MV_MV ($p = 2.82e^{12}$; Figure A14B). When the opposite comparison between 386 unique genes significantly expressed in MV_HV corals but not significant in MV_MV corals was examined, a lowered response and greater baseline expression was detected in 175/205 (85%) significantly up-regulated genes from control MV_MV corals in comparison to MV_HV corals (Figure A14C-D, Table A16).

Symbiodiniaceae gene expression differences in response to acute heat stress and transplantation

Symbiodiniaceae gene expression patterns in response to heat stress – albeit lower in number of DEGs than the coral host despite a greater number of contigs (35,913 symbiont vs. 31,126 host) – resulted in 2,659 upregulated DEGs (17%, out of 15,241 filtered total contigs) and 3,349 (22%) downregulated DEGs (Table A17). Gene expression was significantly affected by the interaction of transplant group and acute heat stress (*adonis* p = 0.02; Figure 4.6, Table A18). Similar to the coral host, symbionts from the HV pool had the greatest amount of differential gene expression in response to heat stress (*adonis* HV_MV heat vs. control p = 0.019; HV_HV = 1,104 DEGs, HV_MV = 2,655, Figure 4.3B), followed by a nearly zero response in MV symbionts (MV_MV = 4, MV_HV = 1 DEGs). Within treatment, there were no differences in gene expression among transplant groups (heat p = 0.819, control p = 0.839, respectively; Table A18).

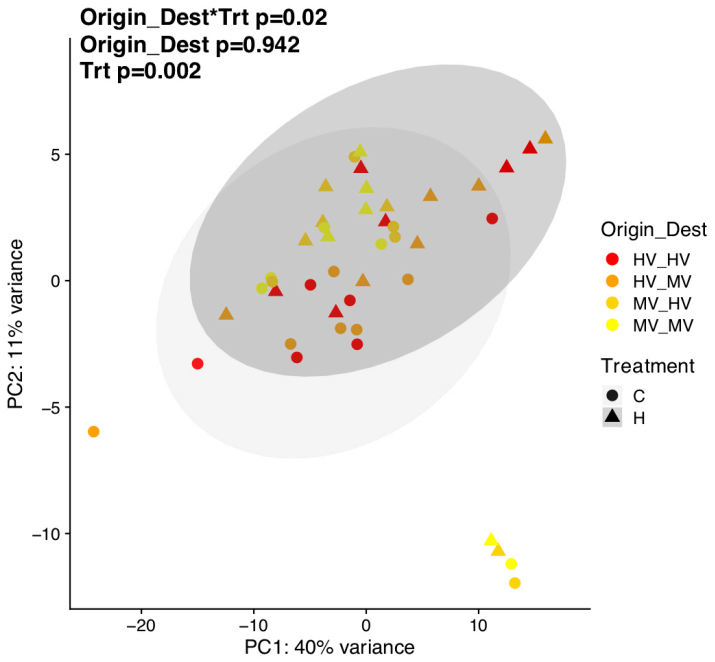

Figure 4.6. Principal Component Analysis (PCA) of normalized expression values for 15,241 contigs of Symbiodiniaceae comparisons for transplant group and treatment. Axes labels show proportion of variance explained by each principal component. Symbols in the upper panel represent treatment (triangles: heat, circles: control), and color represents transplant group. Ellipses indicate 95% confidence intervals for each group (or treatment). PERMANOVA *adonis* results of significance are denoted for p-values.

Functional enrichment analysis between heated and control samples from the filtered 15,241 symbiont contigs produced 22 significant (10% FDR) gene ontology (GO) molecular function, 15 GO cellular component, and 28 GO biological process categories (Figure A12B, Table A19). Metabolic and signaling pathways were upregulated in response to heat stress, whereas photosynthesis and ribosomal processes were largely downregulated.

Symbionts transplanted into the HV and MV pools

In contrast to the coral host, there was little to no shared symbiont gene expression patterns among transplant groups. In the HV pool, HV_HV symbionts mounted the largest response to heat stress with 1,090 (98.7% of total DEGs) uniquely expressed genes, as opposed to no unique DEGs in MV_HV transplants (Figure 4.7A, Table A17). Within the MV pool, HV_MV transplants had the greatest number of DEGs, where 2,651 (99.8%, out of 2,655) were unique to the HV_MV symbiont stress response (Figure 4.7B). Again, there were no unique DEGs expressed by MV_MV native symbionts, but four significantly expressed DEGs were shared between HV_MV and MV_MV. Three of the four contigs were for a mitochondrial glutaryl-CoA dehydrogenase, dynamin-related protein, and metal tolerance protein (the fourth was not annotated nor had meaningful BLASTn hits).

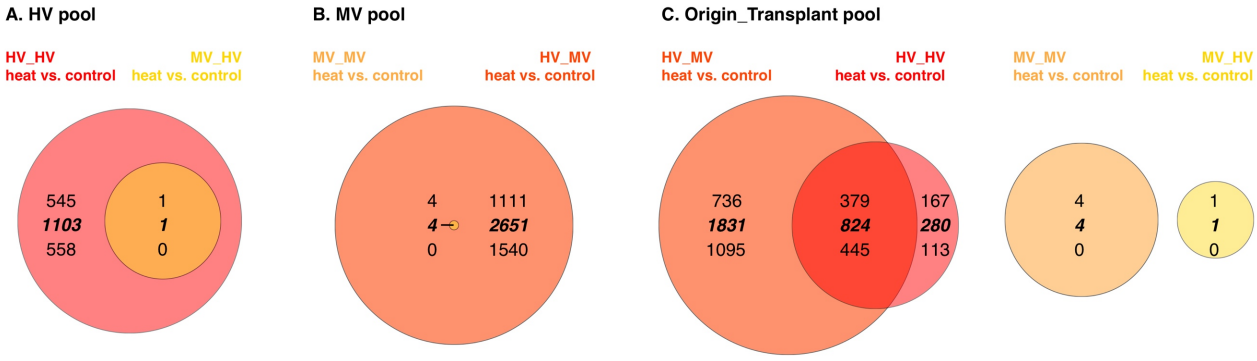

Figure 4.7. Venn diagram showing the number of differentially expressed genes (DEGs) detected in *P. lobata* based on change in expression (bold: total DEGs, above bold: up-regulated DEGs, below bold: down-regulated DEGs) in response to acute heat stress with regards to transplant destination: (A) HV pool, (B) MV pool, (C) native vs. transplant pool.

DAPC was also conducted to elucidate any shifts in symbiont expression in response to transplantation, and similar to the coral host, heat and control symbiont gene expression did not differ by origin (HV vs. MV p = 1, 0.99, respectively; Figure 4.5B, Table A20) or shift as a result of transplantation (HV_HV to HV_MV vs. MV_MV to MV_HV p = 0.32, 0.55).

Symbionts between native and transplanted pools

Comparing the effect of transplantation on gene expression responses in Symbiodiniaceae showed a much lower overlap in shared DEGs in contrast to the coral host. There were only 824 shared DEGs between HV_HV and HV_MV symbionts (28% of total DEGS, Figure 4.7C), and HV_MV symbionts had a greater number of unique DEGs (1,831, 68.9% of total HV_MV DEGs) in response to acute heat stress as opposed to the HV_HV symbionts (280 DEGs, 25.3%). Of the 1,831 unique genes expressed by HV_MV symbionts, there was a lower fold change in upregulated (715 of 736; X^2 test p <2.2e^{-16}; Figure A15A, Table A21) and down-regulated (27 of 1095; X^2 test p <2.2e^{-16}) in gene expression of the HV_HV symbionts. Across the 731 genes that showed reduced up-regulation in HV_HV symbionts, 660 genes (90%) had higher expression in HV_MV transplants relative to HV_HV controls (Figure A15B). Examining the opposite – the 280 DEGs unique in HV_HV that were not significant in HV_MV - revealed 165 of the upregulated DEGs had a lower magnitude of response, and of those, 124 genes (75%) also had higher control expression in HV_MV symbionts in comparison to HV_HV native symbionts (Figure A15C-D, Table A21).

There was no shared response between MV symbionts in the MV and HV pool, and MV natives had 4 differentially expressed genes in comparison to the 1 gene in MV symbionts transplanted into the HV pool (Figure 4.7A); a predicted RNA cytidine acetyltransferase 2.

Discussion

Following one month of transplantation, gene expression profiles in both the coral host *P. lobata* and *in hospite* Symbiodiniaceae revealed significant changes under elevated temperatures and in response to transplantation. The main pattern of gene expression in *Porites lobata* was a large, shared response to acute heat stress, followed by subtle differences across pool of origin and in response to transplantation. In contrast, *in hospite* Symbiodiniaceae demonstrated considerable variation in gene expression across pool of origin and transplant site. Overall, corals and symbionts from the HV pool mounted the largest number of differentially expressed genes (DEGs) in

response to heat stress compared to MV corals and symbionts (i.e. MV symbionts had few to no DEGs) regardless of where they were transplanted. Previous studies of transcriptomic responses in corals from the backreef pools of Ofu Island have indicated transcriptomic resistance or frontloading (gene expression constitutively upregulated before stress and no change during stress; Barshis et al. 2013), transcriptional dampening (a lower reaction of gene expression in response to stress; Bay and Palumbi 2015), and/or resilience (rate of gene expression levels recovering to pre-stress baselines; Seneca and Palumbi 2015; Thomas et al. 2019) as mechanisms of increased bleaching tolerance. The shared expression patterns in response to heat stress, yet uniquely subtle responses to transplantation and population-level differences in symbiont gene expression observed here contrasts previous research, highlighting substantial intergeneric variation (*Acropora* vs. *Porites*) in Ofu coral responses to transplantation and heat stress. In addition, previously characterized transcriptomic patterns – frontloading, dampening, resilience – in corals from the HV and MV pool may not be mutually exclusive to mechanism of thermal tolerance based on the results found herein.

Conserved gene expression responses to acute heat stress

Under acute heat stress, *P. lobata* from both the HV and MV backreef pools had similar gene expression responses when transplanted to either common garden (i.e., HV_HV vs. MV_HV or HV_MV vs. MV_MV). Here, 61% of the response to heat stress was shared among populations of *P. lobata* in the HV pool as well as in the MV pool. Similar heat stress reactions among populations contradict previous findings from HV and MV pool corals from the genus *Acropora*, which found fixed differences in response to heat stress between HV and MV corals and greater differential expression in MV corals (Barshis et al. 2013; Palumbi et al. 2014). Population-level differences in gene expression have also been demonstrated for *Porites astreoides* from contrasting environments within the Florida Keys (Kenkel and Matz 2016). In these studies, corals originating from the more variable reef habitat had a lower reaction to heat stress in comparison to corals from nearby, less variable environments. Moreover, spatial variation in thermal tolerance has been correlated with genetic divergence in these distinct environments (Kenkel et al. 2013a; Bay and Palumbi 2014), yet there was no genetic differentiation among populations of *P. lobata* in this study at the mtDNA level.

A lack of origin-specific differences in gene expression patterns could result from similar thermal regimes in the two common garden pools during the austral winter. Typically, daily

variability, maximum, and minimum temperatures are higher in the HV versus the MV pool (Craig et al. 2001; Oliver and Palumbi 2011), and this thermal variation contributes to pool-specific differences in bleaching susceptibility and gene expression patterns (Barshis et al. 2013; Palumbi et al. 2014; Morikawa and Palumbi 2019). However, temperature regimes during the 2016 austral winter did not differ between the two backreef pools (see Chapter 3), and as a result, transplanted corals were exposed to similar conditions. Alternatively, 2016 was another particularly warm year, due to rapid global warming and a prolonged El Niño (Eakin et al. 2016), and coral recovery following summer temperature extremes could take up to six to twelve months (Thomas and Palumbi 2017). It is then possible that the transcriptomes from each coral population were still perturbed and responded similarly under acute heat stress despite normal thermal conditions in the winter.

Within the symbionts, origin-specific differences were more apparent and could indicate recovery at the transcriptomic level, which has been observed to occur four months post-bleaching (Thomas and Palumbi 2017). The return of symbiont densities, pigment, and transcription levels found in Thomas and Palumbi (2017) are consistent with other studies of bleaching recovery (Fitt et al. 2000), further corroborating that the photophysiological results from Chapter 3 could be normal or recovered values in Symbiodiniaceae. Moreover, the photophysiological variation observed across pool of origin is similar to gene expression profiles despite shared coral host responses, suggesting a symbiont role in coral holobiont thermal tolerance (Oliver and Palumbi 2009; van Oppen et al. 2009; Leggat et al. 2011; LaJeunesse et al. 2014). Largely, differences in bleaching susceptibility have been attributed to symbiont type (Abrego et al. 2008; Jones et al. 2008; Sampayo et al. 2008; DeSalvo et al. 2010; Oliver and Palumbi 2010; Bellantuono et al. 2012a; Cunning and Baker 2014; Thomas et al. 2019), where modifications in symbiont composition, defined as ‘shuffling’ (modifying proportions of *in hospite* assemblages) or ‘switching’ (changing dominant assemblage entirely; Baker 2003; Berkelmans and Van Oppen 2006), increases bleaching resistance and/or recovery. Here, signatures of shuffling were detected in all transplant groups under maximum heat stress, indicated by an increase in proportion of Clade B (and 1% increase in Clade D in MV_HV and MV_MV). These proportional changes are only speculative as the surrounding water was not sampled to determine preferential loss of certain Clades, nor do they explain origin-specific differences to acute heat stress.

Subtle/strong pool of origin differences for host/symbionts

Despite the largely shared response to heat stress, there were subtle differences in gene expression across pool of origin for *P. lobata* and distinct response differences in Symbiodiniaceae. Coral hosts and symbionts from the HV pool had the greatest number of differentially expressed genes for both the HV_HV and HV_MV groups. This pattern also contradicts previous transcriptomic stress responses in Ofu corals from the genus *Acropora*, which revealed reduced gene expression in native HV corals or corals acclimated to the variable conditions of the HV pool and greater responses to heat stress in MV corals (Barshis et al. 2013; Palumbi et al. 2014; Bay and Palumbi 2015). The reduced gene expression response in HV *Acropora* mirrored greater thermal tolerance capacity in these corals, thus was posited as a transcriptomic signature of increased tolerance.

Large changes in gene expression could indicate greater levels of stress (5/8 reviewed studies; DeBiasse and Kelly 2016), or alternatively, could suggest adaptive responses to stress (3/8 of reviewed studies). In conjunction with physiological responses to heat stress, it has been acknowledged that corals from the HV pool have greater thermal tolerance and bleaching resistance than corals from the nearby MV pool (Oliver and Palumbi 2011; Morikawa and Palumbi 2019). However, bleaching responses from *P. lobata* corals from the MV and HV pool herein indicated a greater maintenance of photosynthetic efficiency (F_v/F_m) and a greater retention of total chlorophyll following heat stress in corals from the MV pool, not HV pool. The absence of significant gene expression in MV symbionts under acute heat stress corroborates the notion of increased tolerance for this population, contrary to previous Ofu research.

Subtle responses in tuning gene expression to a new environment

Reduced expression changes in corals from or acclimated to highly variable conditions has recently been attributed to frontloading, or constitutive upregulation, where genes that had a lower magnitude of expression change under heat stress also had higher baseline expression, presumably conferring a proactive benefit during subsequent heat stress (Barshis et al. 2013). This muted stress response could confer a greater resilience under heat stress through priming of the protein pool in pathways important in the heat stress response (sensu Berry and Gasch 2008). Moreover, transcriptional dampening (Bay and Palumbi 2015) is another rapid acclimatory mechanism resulting from a lower reaction of a suite of genes to acute heat stress, and has also been demonstrated in individuals exposed to higher temperatures. In the comparisons between *P. lobata*

and symbiont transplant groups that showed fewer uniquely expressed genes in response to heat stress relative to the other group (*e.g.* MV_HV 675 DEGs vs. HV_HV 1,137 DEGs), a subset of 322 genes were found to express higher baseline expression and have a lower magnitude of expression under heat stress. However, some of these comparisons were weak and when the analyses were applied in the opposite direction (*e.g.* HV_HV 1,137 DEGs vs MV_HV 675 DEGs), a different subset of 193 genes was also found to meet this frontloading criterion. Thus, it appears in this context that frontloading could be decoupled from tolerance, where increased baseline expression is not mutually exclusive of heat tolerance but could also be a result of genes acclimating in response to a new environment.

With respect to acclimation to a new environment, HV *P. lobata* and symbionts had greater gene expression in response to transplantation in comparison to their native reef environment. To elucidate whether gene expression patterns shifted in response to transplantation, a discriminant analysis of principal components (DAPC) was performed on both reciprocally transplanted corals and symbionts between the HV and MV pools. For both, there was no significant shift in gene expression to match that of the new environment, or expression plasticity (Kenkel and Matz 2016). Kenkel and Matz (2016) correlated elevated plasticity of the environmental stress response with lower susceptibility to natural bleaching, where increased plasticity of inshore corals was an adaptive mechanism of tolerance, not frontloading. In their study, corals were transplanted in new environments for one year; therefore, the absence of expression plasticity despite a slight shift towards the new/transplant environment observed here could indicate temporally driven mechanisms of expression plasticity that are not detectable at one month following transplantation.

The lack of expression plasticity and decoupled frontloading revealed among native and transplant groups despite subtle differences in gene expression in each group could indicate fine-tuning mechanisms to cope with a new environment. In the frontloading comparative analyses aforementioned, each transplant group mounted a unique subset of genes that were: not significantly expressed in the opposite group, had dampened responses to heat stress, and had higher baseline expression. Moreover, these comparisons did not explain a mechanistic basis for reduced/enhanced tolerance and could instead signify a fine-tuning of the expression response when placed in a different environment. Bay and Palumbi (2015) found a dampened stress response to short-term acclimation of *Acropora nana* corals under elevated and variable temperatures (i.e., transcriptomic dampening), but here, short-term acclimation in the transplant

HV and MV common gardens did not contribute to increased heat tolerance. Patterns of frontloading and/or gene expression which corroborate enhanced heat tolerance were also detected in *Acropora hyacinthus* corals from their pool of origin under natural conditions (Barshis et al. 2013) or following one year of reciprocal transplantation between the HV and MV pools (Palumbi et al. 2014). In contrast to these prior studies the backreef environments weren't different with respect to temperature during our study period, but it is possible that other aspects of the thermal regime that weren't examined and/or other environmental conditions (flow, light, nutrients, salinity, etc.) might be important for determining expression patterns. The findings presented here represent a nuanced perspective of initial transcriptomic adjustments to a new environment that may be associated with long-term acclimation in novel reef environments.

Summary

Taken together, these findings show that populations of *P. lobata* mount a large shared gene expression response to acute heat stress with subtle genetic patterns of initial acclimatization to transplantation. Their symbionts, however, had distinct variation in reacting to heat stress, both at the physiological and transcriptomic level. In contrast to previous Ofu research with *Acropora* corals, HV corals and symbionts had the greatest amount of gene expression under heat stress whereas MV corals and symbionts had much smaller reactions to stress. LV corals were neither more tolerant than HV corals nor more susceptible than MV corals physiologically, and therefore fall in between the two populations on a 'stress response continuum' (Weis 2010). It is tempting to speculate that the corals from the MV pool have a broader tolerance to transplantation and acute heat stress, or that the HV environment has recently become chronic and native corals have not had sufficient recovery. Future studies incorporating a longer transplant period and/or during non-bleaching years could disentangle whether long-term acclimatization could induce transcriptomic plasticity in massive corals (sensu Kenkel and Matz 2016) or whether these populations are broadly adapted to the entire Ofu backreef environment.

CHAPTER 5

CONCLUSIONS

This dissertation aims to characterize massive coral thermal tolerance abilities and/or limits through an integrative assessment of physiological and genetic responses to acute heat stress following transplantation to distinct backreef pools of Ofu Island, American Samoa. Acclimatory and/or adaptive mechanisms that contribute to increased tolerance have been previously demonstrated in other coral species from these pools and in other massive corals from variable environments, yet this study is the first to demonstrate reduced, not increased, thermal tolerance in corals from the most variable habitat. Instead, fixed population-level differences in stress responses reveal the possibility that the thermal conditions of the most variable pool may have recently become chronic, no longer promoting enhanced coral thermal tolerance but reaching or even exceeding upper thermal limits in these massive coral species. These findings illustrate novel implications for corals living in variable habitats and their survival under future climate change.

In chapter 1, I present novel results of reduced thermal tolerance in massive coral species from a well-studied highly variable (HV) backreef pool in Ofu Island, American Samoa, previously claimed to contain bleaching resistant corals and promote increased heat tolerance via acclimatory mechanisms (Palumbi et al. 2014). Instead, coral ramets transplanted into the HV pool had similar physiological responses under experimental heat stress as their native counterparts, contributing to origin-specific differences as a potential driver of thermal tolerance as opposed to acclimatization in high variability environments. These findings also highlight differences in coral life history strategies (Darling et al. 2012), as previous thermal tolerance research in Ofu focused on branching coral species from the genus *Acropora* which demonstrated acclimatization and increased thermal tolerance in corals transplanted into the HV pool. My contrasting results may be attributed to the timing and capacity for acclimatization associated with different life history strategies, advocating caution against using one genera and/or coral growth form to characterize a reef as tolerant or susceptible. An additional hypothesis for the observed thermal tolerance differences is that 2015-2016 was a mass global bleaching year and Ofu's backreef temperatures exceeded historical records. Since the HV pool's temperature regime was more extreme and

variable than the MV and LV pool during this study and hotter in comparison to past years, it is possible the corals in HV thermal environment are experiencing chronic thermal stress exposures. To corroborate my speculations, additional studies examining massive coral thermal tolerance during non-bleaching years should be conducted.

As a continuation of chapter 1's findings, chapter 2 evaluated the scale of various temperature metrics used to predict coral bleaching and relate these spatial scales to natural and experimental bleaching stress in order to address how temperature variability in Ofu's backreef contributes to different bleaching susceptibility. Alternative to using nighttime satellite sea surface temperature data for predicting coral bleaching stress (Liu et al. 2014), *in situ* site specific temperatures indicated fewer numbers of Degree Heating Weeks (DHW) within each backreef pool. Historically, the cumulative number of *in situ* DHW and Degree Heating Minutes (DHM) were greater in the HV pool relative to the MV and LV pools, although other thermal metrics such as daily temperature range and maximum daily temperatures did not differ between HV and MV pools. Similar to recent studies, a variety of temperature metrics in addition to the standard predictive remote monitoring have shown more informative for predicting bleaching responses. These metrics were positively correlated with backreef coral growth and negatively correlated with symbiont photophysiology. I also found similar physiological responses to acute heat stress as in chapter 1, despite increasing the number of sampled *P. lobata* colonies and conducting a reciprocal transplant experiment between the HV and MV pool. Although 2016-2017 was another anomalously warm year for the region, HV corals still had reduced thermal tolerance in comparison to MV and LV native *P. lobata*, and there was yet again no effect of heat treatment on MV native coral photophysiology. The final aim of this chapter was to determine whether experimental acute heat stress could be an effective predictor of natural bleaching responses, yet my inconclusive findings either indicate a mismatch in the timing of the experiment (early onset of bleaching) or size-specific differences in bleaching (Hughes and Jackson 1985).

Chapter 3 used gene expression profiling of *P. lobata* and *in hospite* Symbiodiniaceae used in Chapter 2's one-month reciprocal transplant experiment to characterize molecular responses underlying population level variation in response to transplantation and acute heat stress and understand patterns of acclimatization/adaptation. I did not find genetic differentiation in *P. lobata* across the three populations using common mitochondrial markers, and this population-level genetic similarity was reflected in shared gene expression responses to acute heat stress. Despite a

largely shared response to heat stress, each transplant group had subtle unique gene sets that were differentially expressed in response to transplantation, demonstrating fine scale adjustments to a novel environment decoupled from thermal tolerance. In contrast, *in hospite* Symbiodiniaceae revealed strong population-level gene expression differences in reaction to heat stress as well as fine-tuned expression level changes in response to transplantation. In Ofu, *Acropora hyacinthus* corals from the HV pool demonstrated gene expression patterns consistent with increased heat tolerance (reduced magnitude of response and constituitive frontloading; Barshis et al. 2013; Palumbi et al. 2014), yet I found a greater amount of gene expression (number of genes and magnitude of expression change) in transplanted and native HV corals/symbionts. Native and transplanted MV corals/symbionts had fewer differentially expressed genes in response to heat, and symbiont gene expression patterns matched photophysiological results, where there was no significant response to experimental heat stress. These parsimonious transcriptomic results further suggest reduced tolerance in the HV population and a broad thermal tolerance within the MV *P. lobata* population.

Although this body of research found subtle patterns of physiological and transcriptomic acclimatization following exposure (experimental or natural) to more thermally variable conditions, it was not in the beneficial direction previously described in coral tolerance research (Edmunds 2014; Palumbi et al. 2014; Bay and Palumbi 2015). Instead of acclimatization gains in increased thermal tolerance, these results did not show significant shifts (increased/decreased) in coral growth or response to acute heat stress as a result of environment, with the only exception being HV_MV rapid initial growth in the MV pool. Provided consistent results across two separate studies, the second incorporating a larger sample size of one species, spanning one year and six months, respectively, possible explanations for the different results herein could be attributed to the life history strategy of coral species and/or the timing of acclimatization. Branching species have demonstrated acclimatization gains in thermal tolerance in as little as two weeks (Bellantuono et al. 2012b; Bay and Palumbi 2015) to up to two years (Palumbi et al. 2014) when exposed to more variable temperature regimes. However, massive corals *Porites astreoides* in the Florida Keys (Kenkel et al. 2015) and *Porites lobata* from Ofu (Barshis et al. 2018) displayed minimal to no effects of acclimation despite one month to one year of exposure to novel environmental conditions. Taken together it appears that massive corals from the genus *Porites* are broadly tolerant to small-scale differences in environmental variation. Future studies incorporating longer

exposure periods (>one year) and/or between sites with larger differences (i.e. forereef versus backreef) in environmental conditions could confirm whether acclimatization is possible in massive species.

Alternative to acclimatization, the three coral populations appeared to demonstrate fixed responses attributed to adaptation to their local environment. Ecological specialization is a result of phenotypic and genetic differentiation along an environmental gradient, contributing to a higher fitness in an organisms native environment (Kawecki and Ebert 2004; Savolainen et al. 2013). Local adaptation theory states that a native population has increased fitness in comparison to foreign transplants, and that natives perform better at home than away (Kawecki and Ebert 2004). Origin-specific differences in thermal tolerance is a likely explanation for the results observed herein since local adaptation has also been documented in the massive corals from the genus *Porites* from the Ofu reef system and in the wider Caribbean (Kenkel et al. 2015; Kenkel and Matz 2016; Barshis et al. 2018). However, I did not find explicit signatures of local adaptation as native and transplanted ramets from the same genet had similar physiological and transcriptomic responses. Instead, it is possible that *Porites lobata* in Ofu's backreef is broadly specialized to the entire Ofu backreef system – not each pool – due to: 1) lack of coral genetic (at the mitochondrial level) and transcriptomic differentiation among the three populations and, 2) environmental similarity at the small spatial scale investigated may not be a strong enough driver of environmental selection for massive coral species. The studies that found signatures of local adaptation compared populations from more contrasting environments (inshore/backreef vs. offshore/forereef), so it is likely the greater differences in thermal variability contributed to adaptive differentiation in growth and stress resistance. Adaptation to the entire Ofu backreef suggests that these corals could be viable candidates for ecosystem restoration in nearby reefs with relatively similar environmental conditions (Morikawa and Palumbi 2019).

Despite subtle patterns of acclimatization to new reef environments and broad tolerance to the entire Ofu reef system were discovered under small-scale differences in thermal variability, the recent thermal environment within each backreef pool, namely the HV environment, is likely contributing to the differences in thermal tolerance. The most notable and potentially alarming result is reduced tolerance of HV corals relative to MV and LV corals. The HV pool is touted to contain 'super corals', thriving in extreme reef environments (Palumbi et al. 2014; Camp et al. 2018), yet this body of work is the first to demonstrate massive corals from this environment are

not the most thermally tolerant but more susceptible than nearby populations. Although speculative without confirmation from studies conducted during normal non-bleaching years, it is possible that the corals investigated here could be approaching or at a tipping point in thermal tolerance. It is well understood that the HV pool has greater daily variability and cumulative heat stress (Craig et al. 2001; Oliver and Palumbi 2011), however, in the past few years, previously acute thermal conditions may have likely become chronic, contributing to a weakened state of stress recovery. Given that HV corals never demonstrated improved thermal tolerances over multiple seasons and had greater gene expression even during the austral winter, lasting effects of chronic thermal stress on coral physiology could pre-empt resilience for this population (Thomas and Palumbi 2017).

In contrast to previous studies between HV and MV pool corals, massive corals from the MV pool demonstrated thermal resistance to acute heat stress and represent the more tolerant population examined herein. Anecdotally, the MV environment is wider and deeper, so the microenvironments within the pool are more moderate and potentially more conducive to the greater size and abundance of *Porites lobata* colonies observed (pers. obs.). As a result, there could be a greater amount of standing variation in the MV pool, which may contribute to higher thermal tolerance regardless of similar thermal conditions to the HV pool in recent years. The LV pool massive corals were neither more susceptible than MV corals nor more tolerant than HV corals. Species living in environments below their thermal maxima, such as in the MV and LV pool, may have a greater ability to increase their upper thermal limits and could be less impacted by future climate change (Stillman 2003).

Anthropogenic climate change is rapidly altering environmental conditions and threatens species survival globally by disrupting adaptation to the local environment and causing degraded ecosystems. In this context, researchers are searching to identify resilient populations and characterize the ability of rapid acclimatization and/or evolutionary rescue (Hofmann and Todgham 2010; Hoffmann and Sgro 2011). By assessing various scales of environmental, temporal thermal variability across various levels of biological organization, the results of this dissertation challenge the extent of thermal variability that promotes coral bleaching tolerance as well as characterization of resilient coral populations based on single-genus assessments. Variation in bleaching tolerances within reef habitats have been documented globally, and this work highlights that multiple coral-algal and environmental characteristics contribute to differences in stress responses within small spatial scales of < 5km. Reef ecosystems likely contain multiple

individuals and coral species that fall along a stress response continuum (Weis 2010), where certain individuals/species/populations are more susceptible – HV pool, more resilient – MV pool, or somewhere in the middle – LV pool. In a rapidly changing climate, it is crucial to incorporate multiple species across a multiple times scales to validate tolerance limits and abilities to not only predict future reef ecosystem assemblages but also effectively utilize stress tolerant populations for proactive management and restoration strategies.

Future Directives

Given ample time and funding to continue this research, I can envision several interesting research ideas to further our understanding of the tolerance limits and abilities of Ofu backreef corals and the potential outcomes of coral populations representative of future reef assemblages. The first study would be to incorporate similar analyses using one or two coral species from each life history strategy – weedy, competitive, and tolerant – in each of the three backreef locations. Incorporating different coral growth forms over a longer study period (2 yrs, with 6 mo timepoints) could reveal not only the timing of potential acclimatization gains in thermal tolerance for each life history strategy, but also encompass multiple seasons with or without natural bleaching stress to determine realized physiological differences in thermal tolerances. In addition to the field transplant experiment and subsequent acute heat stress assays, conducting a large global gene expression analysis across the three life history strategies could also reveal the differences and similarities underlying cellular responses to acute heat stress and transplantation, portraying a holistic overview of how different coral species within small spatial scales react. This information would be critically important in predicting future coral reef assemblage responses to increased temperatures and disentangle how thermal variability influences coral bleaching resistance or susceptibility.

Another research idea that would contribute to the Ofu coral tolerance story would be to incorporate other environmental parameters, as low tide conditions in the backreef system impacts more than just temperature but was outside the scope of my dissertation. Observations of and factorial experimental designs using modifications in flow, pH, and dissolved oxygen could fill knowledge gaps of how variable reef environmental conditions promote or reduce thermal tolerance of coral species. Another critical aspect to understanding the reduced tolerance in HV massive coral species would be to conduct multiple physiological and genetic assessments over shorter timescales surrounding a bleaching year. As some of my results from winter timepoints

could be indicative of coral recovery following summer bleaching stress, tracking recovery before, during, and after a bleaching event could reveal how recent thermal history plays into the ability and speed of massive coral recovery. Therefore, we could gauge the impacts of increasing and/or recurrent bleaching events on coral recovery, mortality, and future reef community assemblages.

Not included in this dissertation, but intended for peer-reviewed publication, is the analysis of single nucleotide polymorphism (SNPs) outlier detection for potential loci under environmental selection. Previous research on Ofu *Acropora* species found few, small effect loci that explained thermal tolerance differences between the two pools despite high gene flow. The aim of this study will be to determine whether candidate loci for tolerance differences exist at higher allele frequencies and/or higher alternative allele frequencies in the MV *Porites lobata* population not in HV corals, an additional line of evidence for higher tolerance in the MV population. If there are no candidate loci under environmental selection, then it can be suggested that recent environmental conditions (i.e. recurrent bleaching years surpassing the HV thermal threshold) are the strongest drivers in the bleaching tolerance differences observed.

REFERENCES

(CRAG) ASCRAG (2017) American Samoa bleaching monitoring report 2015–2017. Unpublished draft

Abrego D, Ulstrup KE, Willis BL, van Oppen MJ (2008) Species-specific interactions between algal endosymbionts and coral hosts define their bleaching response to heat and light stress. Proceedings Biological Sciences / The Royal Society 275:2273-2282

Alvarez-Filip L, Dulvy NK, Côté IM, Watkinson AR, Gill JA (2011) Coral identity underpins architectural complexity on Caribbean reefs. Ecological Applications 21:2223-2231

Anders S, Huber W (2010) Differential expression analysis for sequence count data. Genome Biology 11:1

Baird A, Marshall P (2002) Mortality, growth and reproduction in scleractinian corals following bleaching on the Great Barrier Reef. Marine Ecology Progress Series 237:133-141

Baker A, Cunning R (2016) Bulk gDNA extraction from coral samples. Protocols io Available at: https://www.protocols io/view/Bulk-gDNA-extraction-from-coral-samples-dyq7vv[Google Scholar]

Baker AC (2003) Flexibility and specificity in coral-algal symbiosis: diversity, ecology, and biogeography of *Symbiodinium*. Annual Review of Ecology, Evolution, and Systematics 34:661-689

Baker AC, Glynn PW, Riegl B (2008) Climate change and coral reef bleaching: an ecological assessment of long-term impacts, recovery trends and future outlook. Estuarine, Coastal and Shelf Science 80:435-471

Barker V (2018) Exceptional thermal tolerance of coral reefs in American Samoa: a review. Current Climate Change Reports 4:417-427

Barkley HC, Cohen AL (2016) Skeletal records of community-level bleaching in *Porites* corals from Palau. Coral Reefs 35:1407-1417

Barott KL, Venn AA, Perez SO, Tambutté S, Tresguerres M (2015) Coral host cells acidify symbiotic algal microenvironment to promote photosynthesis. Proceedings of the National Academy of Sciences 112:607-612

Barshis D, Stillman J, Gates R, Toonen R, Smith L, Birkeland C (2010) Protein expression and genetic structure of the coral *Porites lobata* in an environmentally extreme Samoan back reef: does host genotype limit phenotypic plasticity? Molecular Ecology 19:1705-1720

Barshis DJ, Birkeland C, Toonen RJ, Gates RD, Stillman JH (2018) High-frequency temperature variability mirrors fixed differences in thermal limits of the massive coral *Porites lobata*. Journal of Experimental Biology 221

Barshis DJ, Ladner JT, Oliver TA, Seneca FO, Traylor-Knowles N, Palumbi SR (2013) Genomic basis for coral resilience to climate change. Proceedings of the National Academy of Sciences 110:1387-1392

Bates D, Sarkar D, Bates MD, Matrix L (2007) The lme4 package. R package version 2:74

Baums IB, Miller MW, Hellberg ME (2006) Geographic variation in clonal structure in a reef‐building Caribbean coral, *Acropora palmata*. Ecological Monographs 76:503-519

Bay LK, Doyle J, Logan M, Berkelmans R (2016) Recovery from bleaching is mediated by threshold densities of background thermo-tolerant symbiont types in a reef-building coral. Open Science 3:160322

Bay RA, Palumbi SR (2014) Multilocus adaptation associated with heat resistance in reef-building corals. Current Biology 24:2952-2956

Bay RA, Palumbi SR (2015) Rapid acclimation ability mediated by transcriptome changes in reef-building corals. Genome Biology and Evolution 7:1602-1612

Bellantuono AJ, Hoegh-Guldberg O, Rodriguez-Lanetty M (2012a) Resistance to thermal stress in corals without changes in symbiont composition. Proceedings Biological Sciences / The Royal Society 279:1100-1107

Bellantuono AJ, Granados-Cifuentes C, Miller DJ, Hoegh-Guldberg O, Rodriguez-Lanetty M (2012b) Coral thermal tolerance: tuning gene expression to resist thermal stress. PloS One 7:e50685

Berkelmans R (2002) Time-integrated thermal bleaching thresholds of reefs and their variation on the Great Barrier Reef. Marine Ecology Progress Series 229:73-82

Berkelmans R, Willis B (1999) Seasonal and local spatial patterns in the upper thermal limits of corals on the inshore Central Great Barrier Reef. Coral Reefs 18:219-228

Berkelmans R, Van Oppen MJ (2006) The role of zooxanthellae in the thermal tolerance of corals: a 'nugget of hope'for coral reefs in an era of climate change. Proceedings of the Royal Society of London B: Biological Sciences 273:2305-2312

Berry DB, Gasch AP (2008) Stress-activated genomic expression changes serve a preparative role for impending stress in yeast. Molecular Biology of the Cell 19:4580-4587

Boyd PW, Cornwall CE, Davison A, Doney SC, Fourquez M, Hurd CL, Lima ID, McMinn A (2016) Biological responses to environmental heterogeneity under future ocean conditions. Global Change Biology 22:2633-2650

Brandt ME (2009) The effect of species and colony size on the bleaching response of reef-building corals in the Florida Keys during the 2005 mass bleaching event. Coral Reefs 28:911-924

Brown B (1997) Coral bleaching: causes and consequences. Coral Reefs 16:S129-S138

Brown BE, Dunne RP, Edwards AJ, Sweet MJ, Phongsuwan N (2015) Decadal environmental 'memory'in a reef coral? Marine Biology 162:479-483

Buddemeier RW, Fautin DG (1993) Coral bleaching as an adaptive mechanism. Bioscience 43:320-326

Buddemeier RW, Jokiel PL, Zimmerman KM, Lane DR, Carey JM, Bohling GC, Martinich JA (2008) A modeling tool to evaluate regional coral reef responses to changes in climate and ocean chemistry. Limnology and Oceanography: Methods 6:395-411

Burgess SC, Marshall DJ (2011) Temperature-induced maternal effects and environmental predictability. Journal of Experimental Biology 214:2329-2336

Callahan BJ, McMurdie PJ, Rosen MJ, Han AW, Johnson AJA, Holmes SP (2016) DADA2: high-resolution sample inference from Illumina amplicon data. Nature Methods 13:581

Calosi P, Bilton DT, Spicer JI (2008) Thermal tolerance, acclimatory capacity and vulnerability to global climate change. Biology Letters 4:99-102

Calosi P, Rastrick SP, Lombardi C, de Guzman HJ, Davidson L, Jahnke M, Giangrande A, Hardege JD, Schulze A, Spicer JI (2013) Adaptation and acclimatization to ocean acidification in marine ectotherms: an *in situ* transplant experiment with polychaetes at a shallow CO_2 vent system. Philosophical Transactions of the Royal Society B: Biological Sciences 368:20120444

Camp EF, Schoepf V, Mumby PJ, Hardtke LA, Rodolfo-Metalpa R, Smith DJ, Suggett DJ (2018) The future of coral reefs subject to rapid climate change: lessons from natural extreme environments. Frontiers in Marine Science 5:4

Camp EF, Nitschke MR, Rodolfo-Metalpa R, Houlbreque F, Gardner SG, Smith DJ, Zampighi M, Suggett DJ (2017) Reef-building corals thrive within hot-acidified and deoxygenated waters. Scientific Reports 7:2434

Castillo KD, Ries JB, Weiss JM (2011) Declining coral skeletal extension for forereef colonies of *Siderastrea siderea* on the Mesoamerican Barrier Reef System, Southern Belize. PloS One 6:e14615

Coles S (1997) Reef corals occurring in a highly fluctuating temperature environment at Fahal Island, Gulf of Oman (Indian Ocean). Coral Reefs 16:269-272

Coles S, Brown BE (2003) Coral bleaching—capacity for acclimatization and adaptation. Advances in Marine Biology 46:183-223

Coles SL (1975) A comparison of effects of elevated temperature versus temperature fluctuations on reef corals at Kahe Point, Oahu. Pacific Sciences 29:15-18

Coles SL, Jokiel PL, Lewis CR (1976) Thermal tolerance in tropical versus subtropical Pacific reef corals. Pacific Sciences 30:159-166

Craig P, Birkeland C, Belliveau S (2001) High temperatures tolerated by a diverse assemblage of shallow-water corals in American Samoa. Coral Reefs 20:185-189

Cunning R, Baker AC (2014) Not just who, but how many: the importance of partner abundance in reef coral symbioses. Frontiers in Microbiology 5:400

Cunning R, Gillette P, Capo T, Galvez K, Baker AC (2014) Growth tradeoffs associated with thermotolerant symbionts in the coral *Pocillopora damicornis* are lost in warmer oceans. Coral Reefs 34:155-160

Darling ES, Alvarez‐Filip L, Oliver TA, McClanahan TR, Côté IM (2012) Evaluating life‐history strategies of reef corals from species traits. Ecology Letters 15:1378-1386

Davison IR, Pearson GA (1996) Stress tolerance in intertidal seaweeds. Journal of Phycology 32:197-211

Davy SK, Allemand D, Weis VM (2012) Cell biology of cnidarian-dinoflagellate symbiosis. Microbiology and Molecular Biology Reviews : MMBR 76:229-261

De Wit P, Pespeni MH, Ladner JT, Barshis DJ, Seneca F, Jaris H, Therkildsen NO, Morikawa M, Palumbi SR (2012) The simple fool's guide to population genomics via RNA‐Seq: an introduction to high‐throughput sequencing data analysis. Molecular Ecology Resources 12:1058-1067

De'ath G, Lough JM, Fabricius KE (2009) Declining coral calcification on the Great Barrier Reef. Science 323:116-119

DeBiasse MB, Kelly MW (2016) Plastic and evolved responses to global change: what can we learn from comparative transcriptomics? Journal of Heredity 107:71-81

DeSalvo MK, Sunagawa S, Fisher PL, Voolstra CR, Iglesias-Prieto R, Medina M (2010) Coral host transcriptomic states are correlated with *Symbiodinium* genotypes. Molecular Ecology 19:1174-1186

Dixon GB, Davies SW, Aglyamova GV, Meyer E, Bay LK, Matz MV (2015) Genomic determinants of coral heat tolerance across latitudes. Science 348:1460-1462

Donner SD (2011) An evaluation of the effect of recent temperature variability on the prediction of coral bleaching events. Ecological Applications 21:1718-1730

Donner SD, Skirving WJ, Little CM, Oppenheimer M, Hoegh‐Guldberg O (2005) Global assessment of coral bleaching and required rates of adaptation under climate change. Global Change Biology 11:2251-2265

Douglas A (2003) Coral bleaching—how and why? Marine Pollution Bulletin 46:385-392

Eakin C, Liu G, Gomez A, De La Cour J, Heron S, Skirving W, Geiger E, Tirak K, Strong A (2016) Global coral bleaching 2014–2017: status and an appeal for observations. Reef Encounter 31:20-26

Edmunds P, Davies PS (1989) An energy budget for *Porites porites* (Scleractinia), growing in a stressed environment. Coral Reefs 8:37-43

Edmunds PJ (2014) Is acclimation beneficial to scleractinian corals, *Porites spp.*? Marine Biology 161:1531-1542

Edmunds PJ (2017) Intraspecific variation in growth rate is a poor predictor of fitness for reef corals. Ecology 98:2191-2200

Edmunds PJ, Adjeroud M, Baskett ML, Baums IB, Budd AF, Carpenter RC, Fabina NS, Fan TY, Franklin EC, Gross K, Han X, Jacobson L, Klaus JS, McClanahan TR, O'Leary JK, van Oppen MJ, Pochon X, Putnam HM, Smith TB, Stat M, Sweatman H, van Woesik R, Gates RD (2014) Persistence and change in community composition of reef corals through present, past, and future climates. PloS One 9:e107525

Fine M, Gildor H, Genin A (2013) A coral reef refuge in the Red Sea. Global Change Biology 19:3640-3647

Fitt WK, McFarland F, Warner ME, Chilcoat GC (2000) Seasonal patterns of tissue biomass and densities of symbiotic dinoflagellates in reef corals and relation to coral bleaching. Limnology and Oceanography 45:677-685

Fitt WK, Brown BE, Warner ME, Dunne RP (2001) Coral bleaching: interpretation of thermal tolerance limits and thermal thresholds in tropical corals. Coral Reefs 20:51-65

Forsman Z, Wellington GM, Fox GE, Toonen RJ (2015) Clues to unraveling the coral species problem: distinguishing species from geographic variation in *Porites* across the Pacific with molecular markers and microskeletal traits. PeerJ 3:e751

Forsman ZH, Barshis DJ, Hunter CL, Toonen RJ (2009) Shape-shifting corals: molecular markers show morphology is evolutionarily plastic in *Porites*. BMC Evolutionary Biology 9:1

Franssen SU, Gu J, Bergmann N, Winters G, Klostermeier UC, Rosenstiel P, Bornberg-Bauer E, Reusch TB (2011) Transcriptomic resilience to global warming in the seagrass *Zostera marina*, a marine foundation species. Proceedings of the National Academy of Sciences 108:19276-19281

Frieler K, Meinshausen M, Golly A, Mengel M, Lebek K, Donner S, Hoegh-Guldberg O (2013) Limiting global warming to 2 °C is unlikely to save most coral reefs. Nature Climate Change 3:165-170

Gates RD, Edmunds PJ (1999) The physiological mechanisms of acclimatization in tropical reef corals. American Zoologist 39:30-43

Genevier LG, Jamil T, Raitsos DE, Krokos G, Hoteit I (2019) Marine heatwaves reveal coral reef zones susceptible to bleaching in the Red Sea. Global Change Biology 25:2338-2351

Gilchrist GW (1995) Specialists and generalists in changing environments. I. Fitness landscapes of thermal sensitivity. The American Naturalist 146:252-270

Gleason DF, Wellington GM (1993) Ultraviolet radiation and coral bleaching. Nature 365:836-838

Gordon A, Hannon G (2010) Fastx-toolkit. FASTQ/A short-reads preprocessing tools (unpublished) http://hannonlab. cshl. edu/fastx_toolkit, 5

Goreau TF (1964) Mass expulsion of zooxanthellae from Jamaican reef communities after Hurricane Flora. Science 145:383-386

Goreau TJ, Hayes RL (1994) Coral bleaching and ocean" hot spots". Ambio-Journal of Human Environment Research and Management 23:176-180

Green EA, Davies SW, Matz MV, Medina M (2014) Quantifying cryptic *Symbiodinium* diversity within *Orbicella faveolata* and *Orbicella franksi* at the Flower Garden Banks, Gulf of Mexico. PeerJ 2:e386

Grottoli AG, Rodrigues LJ, Palardy JE (2006) Heterotrophic plasticity and resilience in bleached corals. Nature 440:1186-1189

Heron SF, Maynard JA, Van Hooidonk R, Eakin CM (2016) Warming trends and bleaching stress of the world's coral reefs 1985–2012. Scientific Reports 6:38402

Hoegh-Guldberg O (1999) Climate change, coral bleaching and the future of the world's coral reefs. Marine and Freshwater Research 50:839-866

Hoegh-Guldberg O, Jones RJ (1999) Photoinhibition and photoprotection in symbiotic dinoflagellates from reef-building corals. Marine Ecology Progress Series 183:73-86

Hoffmann AA, Sgro CM (2011) Climate change and evolutionary adaptation. Nature 470:479-485

Hoffmann AA, Sørensen JG, Loeschcke V (2003) Adaptation of *Drosophila* to temperature extremes: bringing together quantitative and molecular approaches. Journal of Thermal Biology 28:175-216

Hofmann GE, Todgham AE (2010) Living in the now: physiological mechanisms to tolerate a rapidly changing environment. Annual Review of Physiology 72:127-145

Hothorn T, Bretz F, Westfall P, Heiberger RM, Schuetzenmeister A, Scheibe S, Hothorn MT (2016) Package 'multcomp'. Simultaneous inference in general parametric models. R Package Version 1.2–13

Howells E, Abrego D, Meyer E, Kirk N, Burt J (2016) Host adaptation and unexpected symbiont partners enable reef‐building corals to tolerate extreme temperatures. Global Change Biology 22(8): 2702-2714

Howells EJ, Berkelmans R, van Oppen MJ, Willis BL, Bay LK (2013) Historical thermal regimes define limits to coral acclimatization. Ecology 94:1078-1088

Huang D, Licuanan WY, Baird AH, Fukami H (2011) Cleaning up the 'Bigmessidae': Molecular phylogeny of scleractinian corals from Faviidae, Merulinidae, Pectiniidae and Trachyphylliidae. BMC Evolutionary Biology 11:1

Huang D, Benzoni F, Fukami H, Knowlton N, Smith ND, Budd AF (2014) Taxonomic classification of the reef coral families Merulinidae, Montastraeidae, and Diploastraeidae (Cnidaria: Anthozoa: Scleractinia). Zoological Journal of the Linnean Society 171:277-355

Huey RB, Berrigan D, Gilchrist GW, Herron JC (1999) Testing the adaptive significance of acclimation: a strong inference approach. American Zoologist 39:323-336

Hughes T, Jackson J (1985) Population dynamics and life histories of foliaceous corals. Ecological Monographs 55:141-166

Hughes TP, Baird AH, Bellwood DR, Card M, Connolly SR, Folke C, Grosberg R, Hoegh-Guldberg O, Jackson J, Kleypas J (2003) Climate change, human impacts, and the resilience of coral reefs. Science 301:929-933

Hughes TP, Barnes ML, Bellwood DR, Cinner JE, Cumming GS, Jackson JB, Kleypas J, Van De Leemput IA, Lough JM, Morrison TH (2017a) Coral reefs in the Anthropocene. Nature 546:82

Hughes TP, Kerry JT, Álvarez-Noriega M, Álvarez-Romero JG, Anderson KD, Baird AH, Babcock RC, Beger M, Bellwood DR, Berkelmans R (2017b) Global warming and recurrent mass bleaching of corals. Nature 543:373

Hughes TP, Anderson KD, Connolly SR, Heron SF, Kerry JT, Lough JM, Baird AH, Baum JK, Berumen ML, Bridge TC (2018) Spatial and temporal patterns of mass bleaching of corals in the Anthropocene. Science 359:80-83

Jeffrey S, Humphrey G (1975) New spectrophotometric equations for determining chlorophylls a, b, c1 and c2 in higher plants, algae and natural phytoplankton. Biochem Physiol Pflanz BPP

Jokiel P, Coles S (1990) Response of Hawaiian and other Indo-Pacific reef corals to elevated temperature. Coral Reefs 8:155-162

Jokiel PL (2004) Temperature stress and coral bleaching. In *Coral health and disease*: 401-425. Springer, Berlin, Heidelberg.

Jombart T, Devillard S, Balloux F (2010) Discriminant analysis of principal components: a new method for the analysis of genetically structured populations. BMC Genetics 11:94

Jones AM, Berkelmans R (2011) Tradeoffs to thermal acclimation: energetics and reproduction of a reef coral with heat tolerant *Symbiodinium* type-D. Journal of Marine Biology doi.org/10.1155/2011/185890

Jones AM, Berkelmans R, van Oppen MJ, Mieog JC, Sinclair W (2008) A community change in the algal endosymbionts of a scleractinian coral following a natural bleaching event: field evidence of acclimatization. Proceedings of the Royal Society of London B: Biological Sciences 275:1359-1365

Jones RJ, Yellowlees D (1997) Regulation and control of intracellular algae (= zooxanthellae) in hard corals. Philosophical Transactions of the Royal Society of London B: Biological Sciences 352:457-468

Kawecki TJ, Ebert D (2004) Conceptual issues in local adaptation. Ecology letters 7:1225-1241

Kenkel C, Meyer E, Matz M (2013a) Gene expression under chronic heat stress in populations of the mustard hill coral (*Porites astreoides*) from different thermal environments. Molecular Ecology 22:4322-4334

Kenkel C, Sheridan C, Leal MC, Bhagooli R, Castillo KD, Kurata N, McGinty E, Goulet T, Matz M (2014) Diagnostic gene expression biomarkers of coral thermal stress. Molecular Ecology Resources 14:667-678

Kenkel CD, Matz MV (2016) Gene expression plasticity as a mechanism of coral adaptation to a variable environment. Nature Ecology & Evolution 1:0014

Kenkel CD, Almanza AT, Matz MV (2015) Fine‐scale environmental specialization of reef‐building corals might be limiting reef recovery in the Florida Keys. Ecology 96:3197-3212

Kenkel CD, Goodbody-Gringley G, Caillaud D, Davies SW, Bartels E, Matz MV (2013b) Evidence for a host role in thermotolerance divergence between populations of the mustard hill coral (*Porites astreoides*) from different reef environments. Molecular Ecology 22:4335-4348

Kenkel CD, Aglyamova G, Alamaru A, Bhagooli R, Capper R, Cunning R, Haslun JA, Hédouin L, Keshavmurthy S, Kuehl KA (2011) Development of gene expression markers of acute heat-light stress in reef-building corals of the genus *Porites*. PloS One 6:e26914

Klepac C, Barshis D (2020a) Reduced thermal tolerance of massive coral species in a highly variable environment. Proceedings of the Royal Society B 287:20201379

Klepac C, Barshis D (2020b) Data from: Reduced thermal tolerance of massive coral species in a highly variable environment. GitHub https://github.com/courtneyklepac/project_reducedtolerance_massivecorals_variablehabitats

LaJeunesse TC, Wham DC, Pettay DT, Parkinson JE, Keshavmurthy S, Chen CA (2014) Ecologically differentiated stress-tolerant endosymbionts in the dinoflagellate genus *Symbiodinium* (Dinophyceae) Clade D are different species. Phycologia 53:305-319

LaJeunesse TC, Parkinson JE, Gabrielson PW, Jeong HJ, Reimer JD, Voolstra CR, Santos SR (2018) Systematic revision of *Symbiodiniaceae* highlights the antiquity and diversity of coral endosymbionts. Current Biology 28:2570-2580. e2576

LaJeunesse TC, Pettay DT, Sampayo EM, Phongsuwan N, Brown B, Obura DO, Hoegh-Guldberg O, Fitt WK (2010) Long-standing environmental conditions, geographic isolation and host-symbiont specificity influence the relative ecological dominance and genetic diversification of coral endosymbionts in the genus *Symbiodinium*. Journal of Biogeography 37:785-800

Langlais C, Lenton A, Evenhuis C, Gupta AS, Brown J, Kuchinke M (2017) Coral bleaching pathways under the control of regional temperature variability. Nature Climate Change 7(11): 839-844

Langmead B, Salzberg SL (2012) Fast gapped-read alignment with Bowtie 2. Nature Methods 9:357

Leggat W, Seneca F, Wasmund K, Ukani L, Yellowlees D, Ainsworth TD (2011) Differential responses of the coral host and their algal symbiont to thermal stress. PloS One 6:e26687

Leigh JW, Bryant D (2015) popart: full‐feature software for haplotype network construction. Methods in Ecology and Evolution 6:1110-1116

Lenth R, Lenth MR (2018) Package 'lsmeans'. The American Statistician 34:216-221

Leroi AM, Bennett AF, Lenski RE (1994) Temperature acclimation and competitive fitness: An experimental test of the beneficial acclimation assumption. Proceedings of the Nationall Academy of Science 91:1917-1921

Lesser MP (1996) Elevated temperatures and ultraviolet radiation cause oxidative stress and inhibit photosynthesis in symbiotic dinoflagellates. Limnology and Oceanography 41:271-283

Levin SA, Paine RT (1974) Disturbance, patch formation, and community structure. Proceedings of the National Academy of Sciences 71:2744-2747

Li H, Handsaker B, Wysoker A, Fennell T, Ruan J, Homer N, Marth G, Abecasis G, Durbin R (2009) The sequence alignment/map format and SAMtools. Bioinformatics 25:2078-2079

Liew YJ, Aranda M, Voolstra CR (2016) Reefgenomics. Org-a repository for marine genomics data. Database 2016

Little AF, Van Oppen MJ, Willis BL (2004) Flexibility in algal endosymbioses shapes growth in reef corals. Science 304:1492-1494

Liu G, Strong AE, Skirving W (2003) Remote sensing of sea surface temperatures during 2002 Barrier Reef coral bleaching. Transactions American Geophysical Union 84:137-141

Liu G, Strong AE, Skirving W, Arzayus LF (2006) Overview of NOAA coral reef watch program's near-real time satellite global coral bleaching monitoring activities. Proceedings of the 10th International Coral Reef Symposium: Okinawa:1783-1793

Liu G, Rauenzahn JL, Heron SF, Eakin CM, Skirving WJ, Christensen T, Strong AE, Li J (2013) NOAA coral reef watch 50 km satellite sea surface temperature-based decision support system for coral bleaching management. NOAA Technical Report NESDIS 143. NOAA/NESDIS. College Park, MD. 33pp

Liu G, Heron SF, Eakin CM, Muller-Karger FE, Vega-Rodriguez M, Guild LS, De La Cour JL, Geiger EF, Skirving WJ, Burgess TF (2014) Reef-scale thermal stress monitoring of coral ecosystems: new 5-km global products from NOAA Coral Reef Watch. Remote Sensing 6:11579-11606

López-Maury L, Marguerat S, Bähler J (2008) Tuning gene expression to changing environments: from rapid responses to evolutionary adaptation. Nature Reviews Genetics 9:583-593

Lough J, Anderson K, Hughes T (2018) Increasing thermal stress for tropical coral reefs: 1871–2017. Scientific Reports 8:1-8

Lough JM (2008) Coral calcification from skeletal records revisited. Marine Ecology Progress Series 373:257-264

Loya Y, Sakai K, Yamazato K, Nakano Y, Sambali H, Van Woesik R (2001) Coral bleaching: the winners and the losers. Ecology Letters 4:122-131

Martin TL, Huey RB (2008) Why "suboptimal" is optimal: Jensen's inequality and ectotherm thermal preferences. The American Naturalist 171:E102-E118

McClanahan T, Maina J, Moothien-Pillay R, Baker AC (2005) Effects of geography, taxa, water flow, and temperature variation on coral bleaching intensity in Mauritius. Marine Ecology Progress series 298:131-142

McClanahan TR, Starger CJ, Baker AC (2014) Decadal changes in common reef coral populations and their associations with algal symbionts (*Symbiodinium* spp.). Marine Ecology 36(4): 1215-1229

McClanahan TR, Darling ES, Maina JM, Muthiga NA, D'agata S, Jupiter SD, Arthur R, Wilson SK, Mangubhai S, Nand Y (2019) Temperature patterns and mechanisms influencing coral bleaching during the 2016 El Niño. Nature Climate Change 9:845-851

Middlebrook R, Hoegh-Guldberg O, Leggat W (2008) The effect of thermal history on the susceptibility of reef-building corals to thermal stress. Journal of Experimental Biology 211:1050-1056

Middlebrook R, Anthony KR, Hoegh-Guldberg O, Dove S (2010) Heating rate and symbiont productivity are key factors determining thermal stress in the reef-building coral *Acropora formosa*. Journal of Experimental Biology 213:1026-1034

Moberg F, Folke C (1999) Ecological goods and services of coral reef ecosystems. Ecological Economics 29:215-233

Morikawa MK, Palumbi SR (2019) Using naturally occurring climate resilient corals to construct bleaching-resistant nurseries. Proceedings of the National Academy of Sciences 116:10586-10591

Muller-Landau HC (2010) The tolerance–fecundity trade-off and the maintenance of diversity in seed size. Proceedings of the National Academy of Sciences 107:4242-4247

Muscatine L, Porter JW (1977) Reef corals: mutualistic symbioses adapted to nutrient-poor environments. Bioscience 27:454-460

NOAA-CRW (2017) NOAA Coral Reef Watch Version 3.0 Daily Global 5-km Satellite Virtual Station Time Series Data for Ofu Island, American Samoa, Jan. 1, 2010-Dec. 31, 2017. NOAA Coral Reef Watch, College Park, Maryland, USA.

Oksanen J, Blanchet FG, Kindt R, Legendre P, Minchin PR, O'hara R, Simpson GL, Solymos P, Stevens MHH, Wagner H (2011) vegan: Community ecology package. R package version:117-118

Oliver TA, Palumbi SR (2009) Distributions of stress-resistant coral symbionts match environmental patterns at local but not regional scales. Marine Ecology Progress Series 378:93-103

Oliver TA, Palumbi SR (2010) Many corals host thermally resistant symbionts in high-temperature habitat. Coral Reefs 30:241-250

Oliver T, Palumbi S (2011) Do fluctuating temperature environments elevate coral thermal tolerance? Coral Reefs 30:429-440

Pachauri RK, Allen MR, Barros VR, Broome J, Cramer W, Christ R, Church JA, Clarke L, Dahe Q, Dasgupta P (2014) Climate change 2014: synthesis report. Contribution of Working Groups I, II and III to the fifth assessment report of the Intergovernmental Panel on Climate Change. IPCC

Palumbi SR, Barshis DJ, Traylor-Knowles N, Bay RA (2014) Mechanisms of reef coral resistance to future climate change. Science 344:895-898

Parkinson JE, Baums IB (2014) The extended phenotypes of marine symbioses: ecological and evolutionary consequences of intraspecific genetic diversity in coral–algal associations. Frontiers in Microbiology 5:445

Parmesan C (2006) Ecological and evolutionary responses to recent climate change. Annual Review of Ecology, Evolution, and Systematics:637-669

Pineda J, Starczak V, Tarrant A, Blythe J, Davis K, Farrar T, Berumen M, da Silva JC (2013) Two spatial scales in a bleaching event: Corals from the mildest and the most extreme thermal environments escape mortality. Limnology and Oceanography 58:1531-1545

Pochon X, LaJeunesse T, Pawlowski J (2004) Biogeographic partitioning and host specialization among foraminiferan dinoflagellate symbionts (*Symbiodinium*; Dinophyta). Marine Biology 146:17-27

Pochon X, Pawlowski J, Zaninetti L, Rowan R (2001) High genetic diversity and relative specificity among *Symbiodinium*-like endosymbiotic dinoflagellates in soritid foraminiferans. Marine Biology 139:1069-1078

Putnam HM, Gates RD (2015) Preconditioning in the reef-building coral *Pocillopora damicornis* and the potential for trans-generational acclimatization in coral larvae under future climate change conditions. Journal of Experimental Biology 218:2365-2372

Quigley KM, Davies SW, Kenkel CD, Willis BL, Matz MV, Bay LK (2014) Deep-sequencing method for quantifying background abundances of *Symbiodinium* types: exploring the rare *Symbiodinium* biosphere in reef-building corals. PloS One 9:e94297

Riegl BM, Purkis SJ, Al-Cibahy AS, Abdel-Moati MA, Hoegh-Guldberg O (2011) Present limits to heat-adaptability in corals and population-level responses to climate extremes. PloS One 6:e24802

Robbins SJ, Singleton CM, Chan CX, Messer LF, Geers AU, Ying H, Baker A, Bell SC, Morrow KM, Ragan MA (2019) A genomic view of the reef-building coral *Porites lutea* and its microbial symbionts. Nature Microbiology 4:2090-2100

Rose NH, Seneca FO, Palumbi SR (2016) Gene networks in the wild: identifying transcriptional modules that mediate coral resistance to experimental heat stress. Genome Biology and Evolution 8:243-252

Rowan R, Knowlton N (1995) Intraspecific diversity and ecological zonation in coral-algal symbiosis. Proceedings of the National Academy of Sciences 92:2850-2853

Safaie A, Silbiger NJ, McClanahan TR, Pawlak G, Barshis DJ, Hench JL, Rogers JS, Williams GJ, Davis KA (2018) High frequency temperature variability reduces the risk of coral bleaching. Nature Communications 9:1-12

Sale TL, Marko PB, Oliver TA, Hunter CL (2019) Assessment of acclimatization and subsequent survival of corals during repeated natural thermal stress events in Hawai‘i. Marine Ecology Progress Series 624:65-76

Sampayo E, Ridgway T, Bongaerts P, Hoegh-Guldberg O (2008) Bleaching susceptibility and mortality of corals are determined by fine-scale differences in symbiont type. Proceedings of the National Academy of Sciences 105:10444-10449

Savolainen O, Lascoux M, Merilä J (2013) Ecological genomics of local adaptation. Nature Reviews Genetics 14:807-820

Schlichter D, Fricke H (1990) Coral host improves photosynthesis of endosymbiotic algae. Naturwissenschaften 77:447-450

Schoepf V, Stat M, Falter JL, McCulloch MT (2015) Limits to the thermal tolerance of corals adapted to a highly fluctuating, naturally extreme temperature environment. Scientific Reports 5:1-14

Seneca FO, Palumbi SR (2015) The role of transcriptome resilience in resistance of corals to bleaching. Molecular Ecology 24:1467-1484

Seneca FO, Foret S, Ball EE, Smith-Keune C, Miller DJ, van Oppen MJ (2010) Patterns of gene expression in a scleractinian coral undergoing natural bleaching. Marine Biotechnology 12:594-604

Sgro CM, Overgaard J, Kristensen TN, Mitchell KA, Cockerell FE, Hoffmann AA (2010) A comprehensive assessment of geographic variation in heat tolerance and hardening capacity in populations of *Drosophila melanogaster* from eastern Australia. Journal of Evolutionary Biology 23:2484-2493

Skirving W, Heron S, Marsh B, Liu G, De La Cour J, Geiger E, Eakin C (2019) The relentless march of mass coral bleaching: a global perspective of changing heat stress. Coral Reefs 38:547-557

Smith E, D'Angelo C, Salih A, Wiedenmann J (2013) Screening by coral green fluorescent protein (GFP)-like chromoproteins supports a role in photoprotection of zooxanthellae. Coral Reefs 32:463-474

Smith L, Barshis D, Birkeland C (2007) Phenotypic plasticity for skeletal growth, density and calcification of *Porites lobata* in response to habitat type. Coral Reefs 26:559-567

Smith LW, Wirshing H, Baker AC, Birkeland C (2008) Environmental versus genetic influences on growth rates of the corals *Pocillopora eydouxi* and *Porites lobata* (Anthozoa: Scleractinia) 1. Pacific Science 62:57-69

Somero G (2010) The physiology of climate change: how potentials for acclimatization and genetic adaptation will determine 'winners' and 'losers'. Journal of Experimental Biology 213:912-920

Stat M, Carter D, Hoegh-Guldberg O (2006) The evolutionary history of *Symbiodinium* and scleractinian hosts—symbiosis, diversity, and the effect of climate change. Perspectives in Plant Ecology, Evolution and Systematics 8:23-43

Stat M, Pochon X, Cowie RO, Gates RD (2009) Specificity in communities of *Symbiodinium* in corals from Johnston Atoll. Marine Ecology Progress Series 386:83-96

Stillman JH (2003) Acclimation capacity underlies susceptibility to climate change. Science 301:65-65

Stillman JH (2019) Heat waves, the new normal: summertime temperature extremes will impact animals, ecosystems, and human communities. Physiology 34:86-100

Stillman JH, Somero GN (2000) A comparative analysis of the upper thermal tolerance limits of eastern Pacific porcelain crabs, genus *Petrolisthes*: influences of latitude, vertical zonation, acclimation, and phylogeny. Physiological and Biochemical Zoology 73:200-208

Team RC (2020) R: A language and environment for statistical computing.

Thomas L, Palumbi SR (2017) The genomics of recovery from coral bleaching. Proceedings of the Royal Society B: Biological Sciences 284:20171790

Thomas L, López EH, Morikawa MK, Palumbi SR (2019) Transcriptomic resilience, symbiont shuffling, and vulnerability to recurrent bleaching in reef‐building corals. Molecular Ecology 28:3371-3382

Thomas L, Rose NH, Bay RA, López EH, Morikawa MK, Ruiz-Jones L, Palumbi SR (2018) Mechanisms of thermal tolerance in reef-building corals across a fine-grained environmental mosaic: lessons from Ofu, American Samoa. Frontiers in Marine Science 4:434

Tomanek L, Somero GN (1999) Evolutionary and acclimation-induced variation in the heat-shock responses of congeneric marine snails (genus *Tegula*) from different thermal habitats: implications for limits of thermotolerance and biogeography. Journal of Experimental Biology 202:2925-2936

Trench R (1993) Microalgal-invertebrate symbioses-a review. Endocytobiosis and Cell Research 9:135-175

Tresguerres M, Barott KL, Barron ME, Deheyn DD, Kline DI, Linsmayer LB (2017) Cell biology of reef-building corals: ion transport, acid/base regulation, and energy metabolism: 193-218. In *Acid-Base Balance and Nitrogen Excretion in Invertebrates*. Springer, Cham

Ulstrup KE, Berkelmans R, Ralph PJ, Van Oppen MJ (2006) Variation in bleaching sensitivity of two coral species across a latitudinal gradient on the Great Barrier Reef: the role of zooxanthellae. Marine Ecology Progress Series 314:135-148

Van Hooidonk R, Maynard J, Planes S (2013) Temporary refugia for coral reefs in a warming world. Nature Climate Change 3:508-511

van Oppen MJ, Baker AC, Coffroth MA, Willis BL (2009) Bleaching resistance and the role of algal endosymbionts. In *Coral Bleaching*: 83-102. Springer, Berlin, Heidelberg

Van Woesik R, De Vantier L, Glazebrook J (1995) Effects of Cyclone Joy on nearshore coral communities of the Great Barrier Reef. Marine Ecology Progress Series 128:261-270

van Woesik R, Sakai K, Ganase A, Loya Y (2011) Revisiting the winners and the losers a decade after coral bleaching. Marine Ecology Progress Series 434:67-76

Veal C, Carmi M, Fine M, Hoegh-Guldberg O (2010) Increasing the accuracy of surface area estimation using single wax dipping of coral fragments. Coral Reefs 29:893-897

Villesen, P (2007) FaBox: an online toolbox for fasta sequences. Molecular Ecology Notes **7**(6): 965-968.

Voolstra CR, Buitrago‐López C, Perna G, Cárdenas A, Hume BC, Rädecker N, Barshis DJ (2020) Standardized short‐term acute heat stress assays resolve historical differences in coral thermotolerance across microhabitat reef sites. Global Change Biology, 26(8): 4328-4343

Warner M, Fitt W, Schmidt G (1996) The effects of elevated temperature on the photosynthetic efficiency of zooxanthellae in hospite from four different species of reef coral: a novel approach. Plant, Cell & Environment 19:291-299

Weis VM (2010) The susceptibility and resilience of corals to thermal stress: adaptation, acclimatization or both? Molecular Ecology 19:1515-1517

Wilkinson C (2000) Global Coral Reef Monitoring Network - Status of coral reefs of the world: 2000. Status of Coral Reefs of the World, Australian Institute of Marine Science:349-358

Wilkinson C (2006) Status of coral reefs of the world: summary of threats and remedial action. Coral Reef Conservation:3-39

Wright RM, Aglyamova GV, Meyer E, Matz MV (2015) Gene expression associated with white syndromes in a reef building coral, *Acropora hyacinthus*. BMC Genomics 16:371

Yellowlees D, Rees TAV, Leggat W (2008) Metabolic interactions between algal symbionts and invertebrate hosts. Plant Cell Environment 31:679-694

Ziegler M, Seneca FO, Yum LK, Palumbi SR, Voolstra CR (2017) Bacterial community dynamics are linked to patterns of coral heat tolerance. Nature Communications 8:1-8

APPENDICES

FIGURES

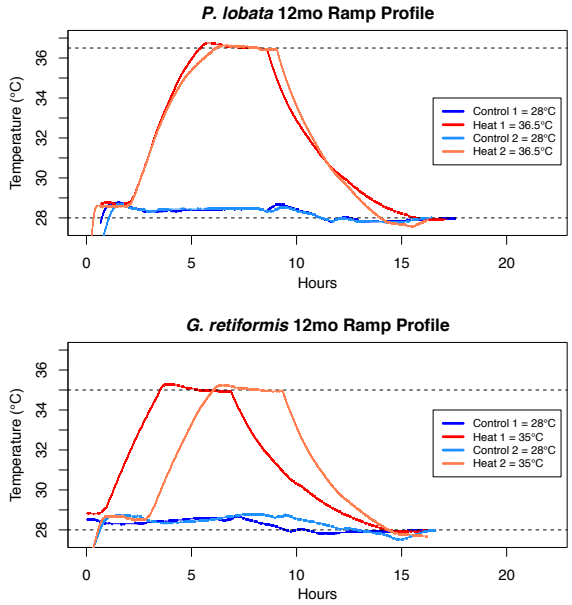

Figure A1. Thermal profile of replicate temperature controlled acute heat stress assays for *Porites lobata* (upper panel) and *Goniastrea retiformis* (lower panel). Dotted lines represent set temperature for control and heated tanks.

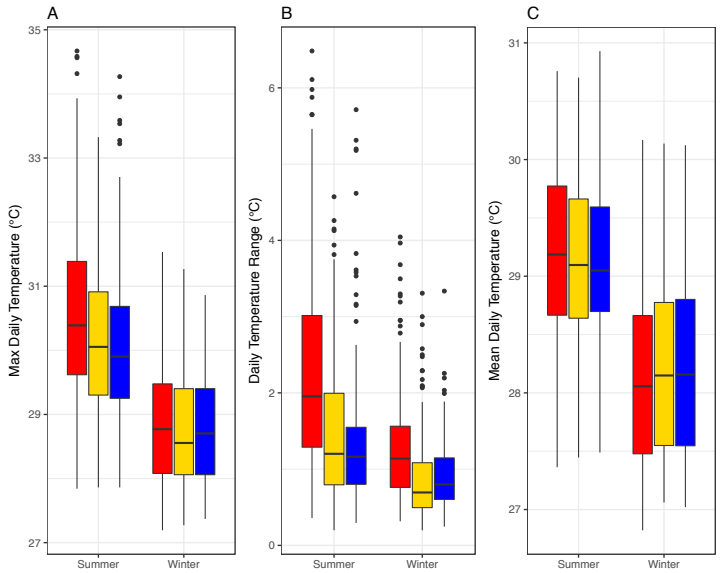

Figure A2. Seasonal distribution of Ofu's three backreef pools *in situ* thermal regimes. A. Daily max temperatures, B. daily temperature range, and C. daily mean temperatures of the HV (red), MV (gold), and LV (blue) pools collected during July 2015 – June 2016. Winter includes the months April-October, and

summer includes October-April. Boxplots constructed using ggplot2's geom_boxplot display the median, hinges (first and third quartile), and whiskers (largest/smallest value no further than 1.5*IQR).

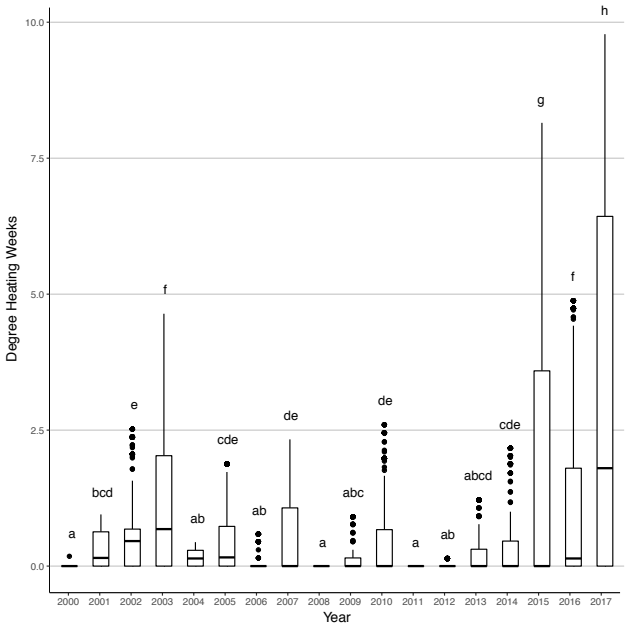

Figure A3. Distribution of the Degree Heating Weeks (DHW) of Ofu Island spanning 2000-2017. Letters indicate Tukey's post-hoc pairwise comparisons.

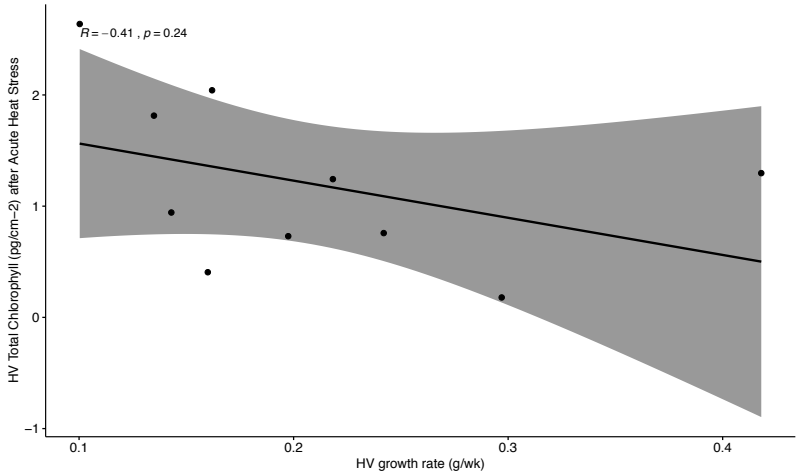

Figure A4. Pearson's correlation between HV pool *P. lobata* weekly growth rate and total chlorophyll after acute heat stress.

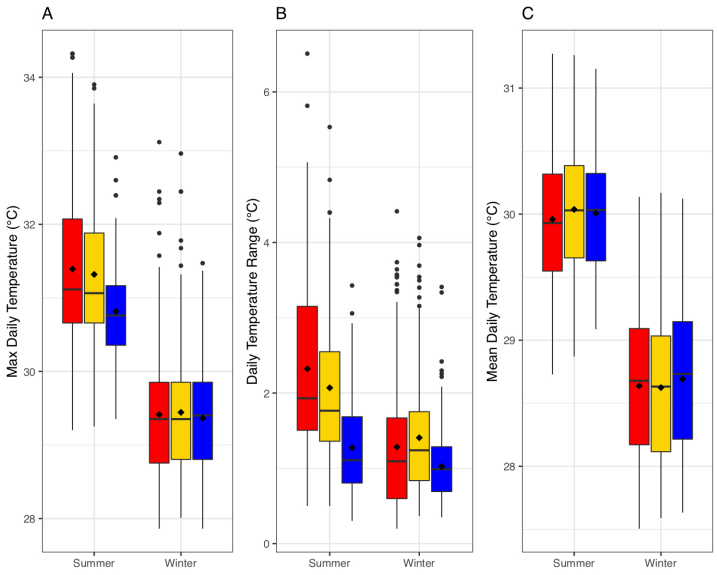

Figure A5. Seasonal distribution of Ofu's three backreef pools *in situ* thermal regimes during July 2016 – February 2017. A. Daily max temperatures, B. daily temperature range, and C. daily mean temperatures of the HV (red), MV (gold), and LV (blue) pools. Winter includes the months July-October, and summer includes October-February. Boxplots display the mean (diamonds), median (horizontal line), first and third quartile (hinges), and largest/smallest value no further than 1.5*IQR (whiskers).

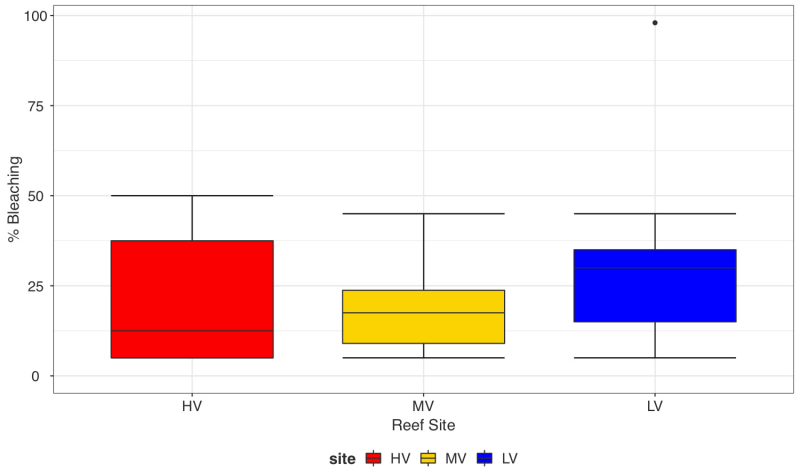

Figure A6. Percent bleaching boxplots of donor *P. lobata* colonies at the early onset (February) of the 2017 natural bleaching event. Boxplots display median, first and third quartile (hinges), and largest/smallest value no further than 1.5*IQR (whiskers).

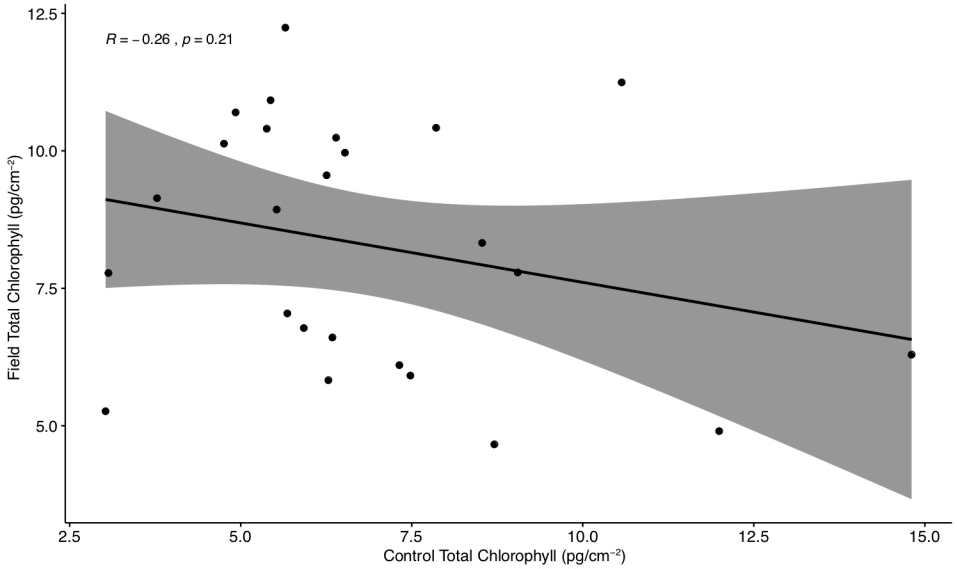

Figure A7. Correlation of donor *P. lobata* colony (y-axis) with control native ramet (x-axis) total chlorophyll from combined Ofu backreef pools.

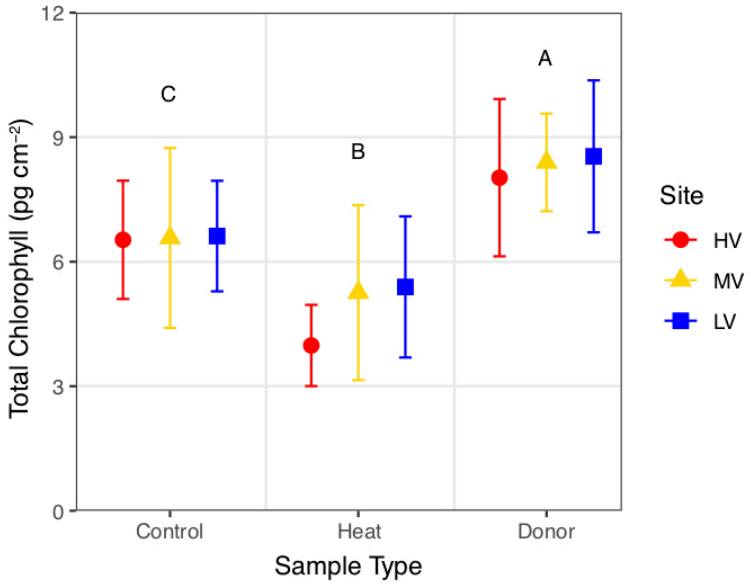

Figure A8. Mean (95% CI) total chlorophyll (pg cm^{-2}) of control native ramets, heated native ramets, and donor *P. lobata* colonies collected during the early onset of natural bleaching stress. Letters represent *post hoc* pairwise comparisons of significance.

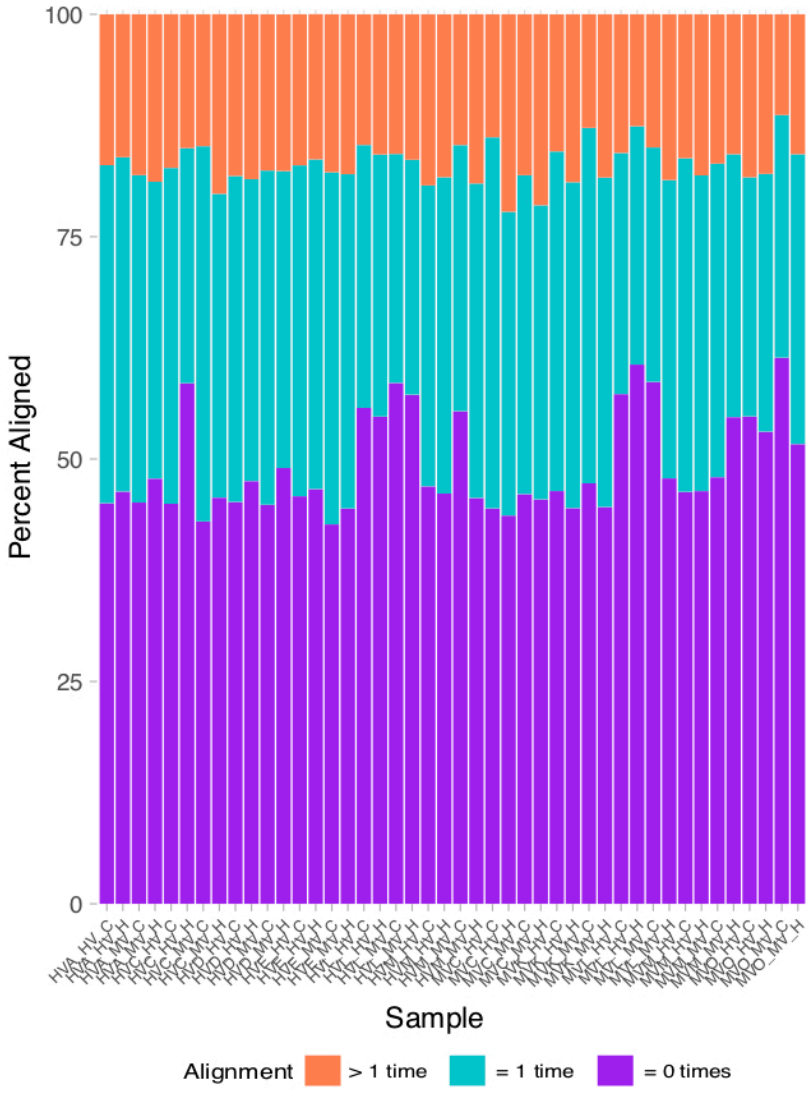

Figure A9. Percent alignment summary for 44 samples mapped to a concatenated *Porites lutea* and Symbiodiniaceae *Cladocopium* type C1 genomes.

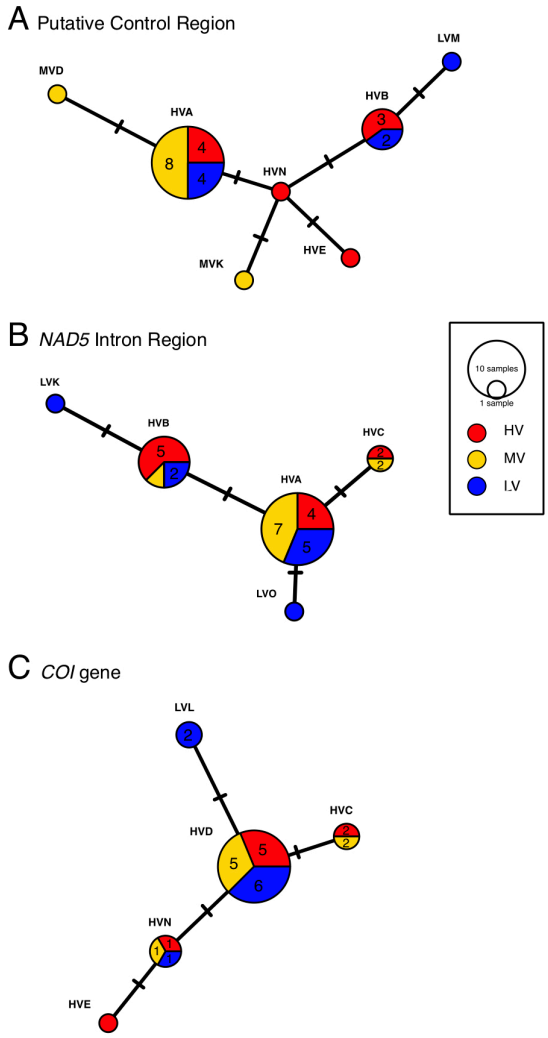

Figure A10. Median-joining haplotype networks of three mtDNA loci ([A] PCr, [B] NAD5, [C] COI) from three populations of *P. lobata*. Number of cross-hatched lines between nodes represent the number of single substitutions, gaps, and/or indels. Diameter of haplotype circles is proportional to the number of colonies with identical sequences. Nodes with >1 colony per haplotype have the corresponding number of sequences specified in each trait group. Trait groups are colored by backreef site (HV=red, MV=gold, LV=blue), and individual sequence names correspond to the specific backreef site followed by colony letter.

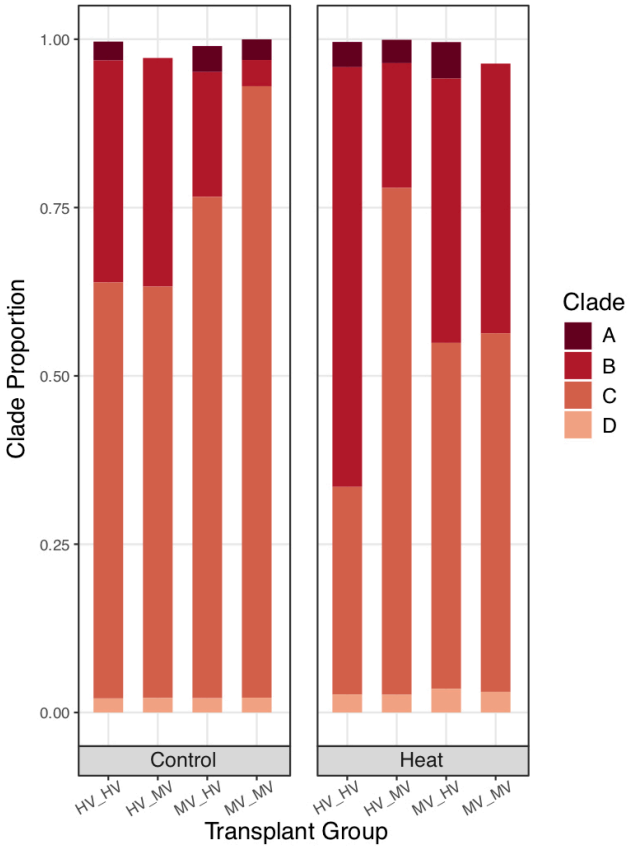

Figure A11. Mean relative proportion of Symbiodiniaceae clades within each transplant group by treatment. Proportions were determined from mRNA sequence reads mapped to a concatenated symbiont clade genome.


Porites lobata
Symbiodiniaceae
A. Molecular Functions
39/39 S−adenosylmethionine−dependent methyltransferase
56/57 transferase, transferring one−carbon groups
202/218 DNA−binding transcription factor
62/65 DNA−binding transcription activator, RNA polymerase II−specific
334/361 transcription regulator
51/52 ubiquitin−like protein binding
121/133 ubiquitin−like protein ligase binding
103/111 ubiquitin−like protein ligase
211/227 ubiquitin−like protein transferase
22/23 ubiquitin−like protein conjugating enzyme binding
12/12 phosphatidylinositol 3−kinase binding
238/256 kinase binding
227/243 protein domain specific binding
139/159 endopeptidase
65/74 actin filament binding
75/85 motor
62/69 isomerase
25/27 aminoacyl−tRNA ligase
8/8 aminoacyl−tRNA editing
17/17 oxidoreductase, acting on the aldehyde or oxo group of donors
17/19 solute:sodium symporter
9/9 neurotransmitter:sodium symporter
10/10 organic acid:sodium symporter
p < 0.001
p < 0.01
p < 0.05
85/109 tetrapyrrole binding
32/42 chlorophyll binding
263/350 cofactor binding
24/33 sulfur compound binding
111/134 structural molecule
79/92 structural constituent of ribosome
25/29 rRNA binding
63/82 voltage−gated cation channel
176/247 channel
114/150 metal ion transmembrane transporter
10/12 phosphotransferase, phosphate group as acceptor
139/175 protein serine/threonine kinase
258/328 phosphotransferase, alcohol group as acceptor
17/19 calcium−dependent protein serine/threonine kinase
297/385 kinase
167/207 ATPase
B. Biological Processes
195/215 enzyme linked receptor protein signaling pathway
492/536 intracellular signal transduction
517/555 cellular response to stress
24/24 intrinsic apoptotic signaling pathway in response to DNA damage
431/479 regulation of cell death
199/223 regulation of MAPK cascade
327/364 positive regulation of protein modification process
256/283 regulation of protein modification process
280/310 positive regulation of phosphate metabolic process
476/529 positive regulation of protein metabolic process
413/453 positive regulation of molecular function
56/58 positive regulation of stress−activated protein kinase signaling cascade
80/85 regulation of stress−activated protein kinase signaling cascade
362/388 regulation of response to stress
470/524 regulation of intracellular signal transduction
127/139 regulation of cytokine production
901/924 proteolysis involved in cellular protein catabolic process
424/471 proteolysis
185/214 protein catabolic process
381/423 macromolecule catabolic process
369/397 protein modification by small protein conjugation or removal
143/150 protein polyubiquitination
270/295 microtubule−based process
258/324 organonitrogen compound biosynthetic process
168/203 cellular amide metabolic process
55/72 polysaccharide metabolic process
42/53 glucan metabolic process
79/98 proteolysis involved in cellular protein catabolic process
151/188 intracellular signal transduction
234/294 protein phosphorylation
32/40 RNA splicing, via transesterification reactions
41/52 protein−chromophore linkage
52/67 photosynthesis
C. Cellular Components
32/35 PML body
247/267 nuclear body
155/167 ubiquitin ligase complex
7/7 small nucleolar ribonucleoprotein complex
15/15 phagophore assembly site
41/45 methyltransferase complex
86/99 receptor complex
10/11 CD40 receptor complex
37/39 plasma membrane signaling receptor complex
82/87 side of membrane
79/86 cell cortex
157/174 cell body
8/8 chaperonin−containing T−complex
8/9 retromer complex
59/67 motile cilium
176/195 cilium
35/38 dynein complex
77/85 microtubule associated complex
73/78 ciliary basal body
46/48 centriole
31/34 vesicle tethering complex
254/278 Golgi membrane
6/7 Arp2/3 protein complex
14/14 multivesicular body
6/6 ESCRT III complex
83/102 mitochondrial protein complex
18/23 respiratory chain complex I
44/54 oxidoreductase complex
11/11 proteasome regulatory particle
37/37 proteasome complex
8/8 proteasome regulatory particle, base subcomplex
14/14 proteasome accessory complex
6/6 cytosolic ribosome
86/103 ribosome
17/18 small ribosomal subunit
12/13 cytosolic large ribosomal subunit
21/23 large ribosomal subunit
38/41 ribosomal subunit
5/5 U2 snRNP
30/37 spliceosomal complex
87/106 ribonucleoprotein complex
17/18 catalytic step 2 spliceosome
8/8 precatalytic spliceosome
18/24 light−harvesting complex
173/218 plastid
75/96 thylakoid
34/42 photosystem
134/176 cell projection
68/82 cilium
72/103 transporter complex
72/101 intrinsic component of plasma membrane
20/23 cullin−RING ubiquitin ligase complex
11/11 SCF ubiquitin ligase complex
13/16 peptidase complex

Figure A12. Functional enrichment of Gene Ontology (GO) categories ([A] Molecular Functions, [B] Biological Processes, [C] Cellular Components) in heated versus control samples of *P. lobata* and *in hopsite* Symbiodiniaceae. The significance of up-regulated (red) and down-regulated (blue) terms are indicated by text shape and size (see inset p-value key). Fractions preceding GO terms indicate the number of genes annotated with the term that pass an unadjusted p-value threshold of 0.05. The trees indicate sharing of genes among GO categories (categories with no branch length between them are subsets of each other).

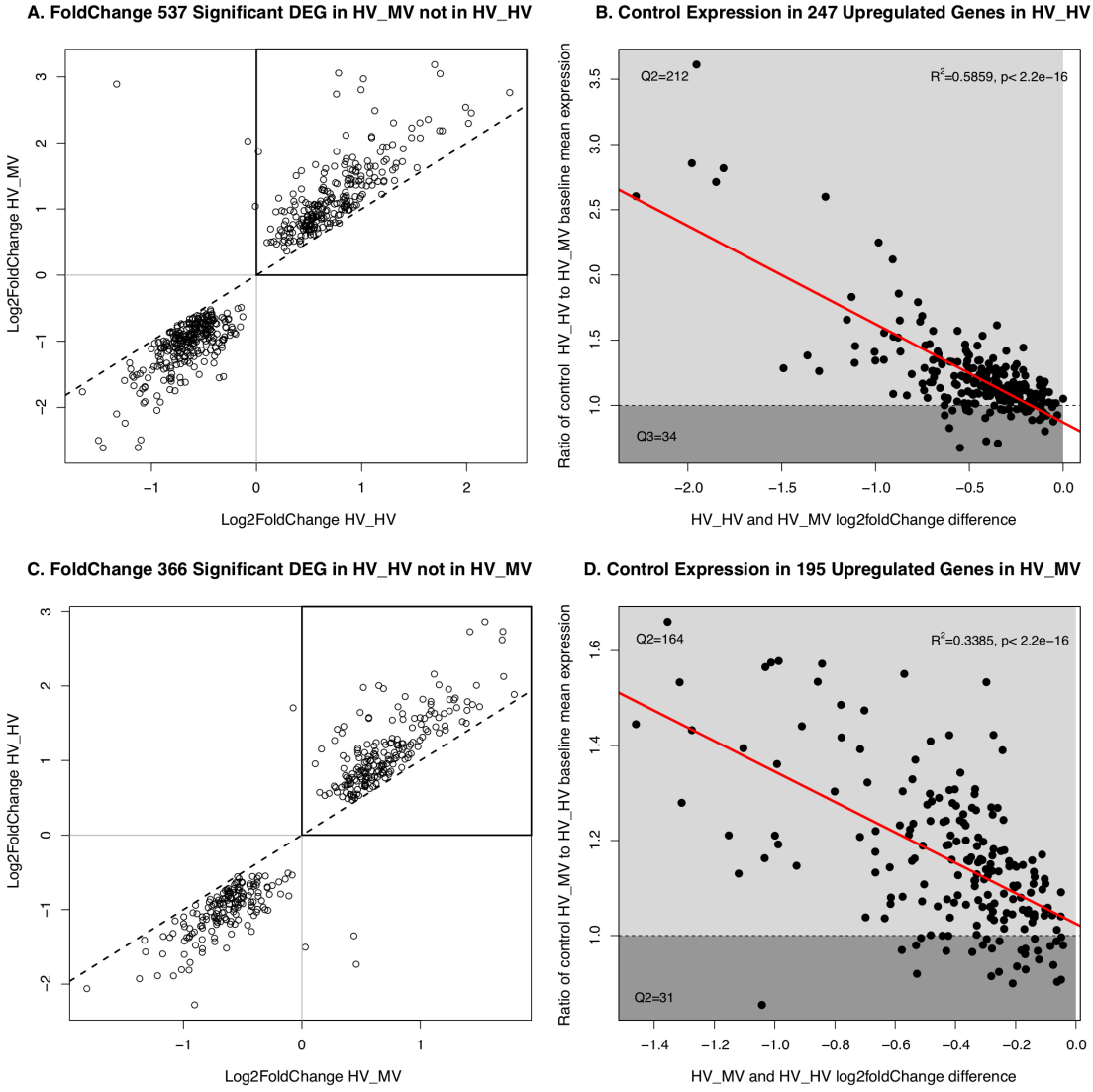

Figure A13. Scatterplots comparing changes in gene expression between (A-B) 537 genes that were not significantly unique to HV_HV *P. lobata* corals and (C-D) 366 genes that were not unique to HV_MV corals. (A&B) Log_2fold change (i.e. magnitude of response) in gene expression in response to heat stress for subset number of genes that are unique to each transplant group comparison. Each open circle represents an individual gene, and the dashed line is a 1:1 line. Quadrat 1 and 3 represents up-regulated and down-regulated genes for both transplant groups, respectively. (C&D) Scatterplot comparing the log_2fold change difference in expression (x axis) to the ratio of control mean expression (y axis) between transplant groups across the upregulated genes from Quadrat 1 in A/C (bordered box). A higher constitutive expression and

reduced response to heat stress for control samples from one transplant group relative to the other transplant group's control samples are those gene points that are > 1 on the y axis and < 0 on the x axis (Quadrat 2). The lighter (Q2) and darker (Q3) quadrats represent the number of genes that are potentially frontloaded or stress indicators in expression, respectively. A linear regression and associated R^2 were calculated to visualize the relationship of these genes.

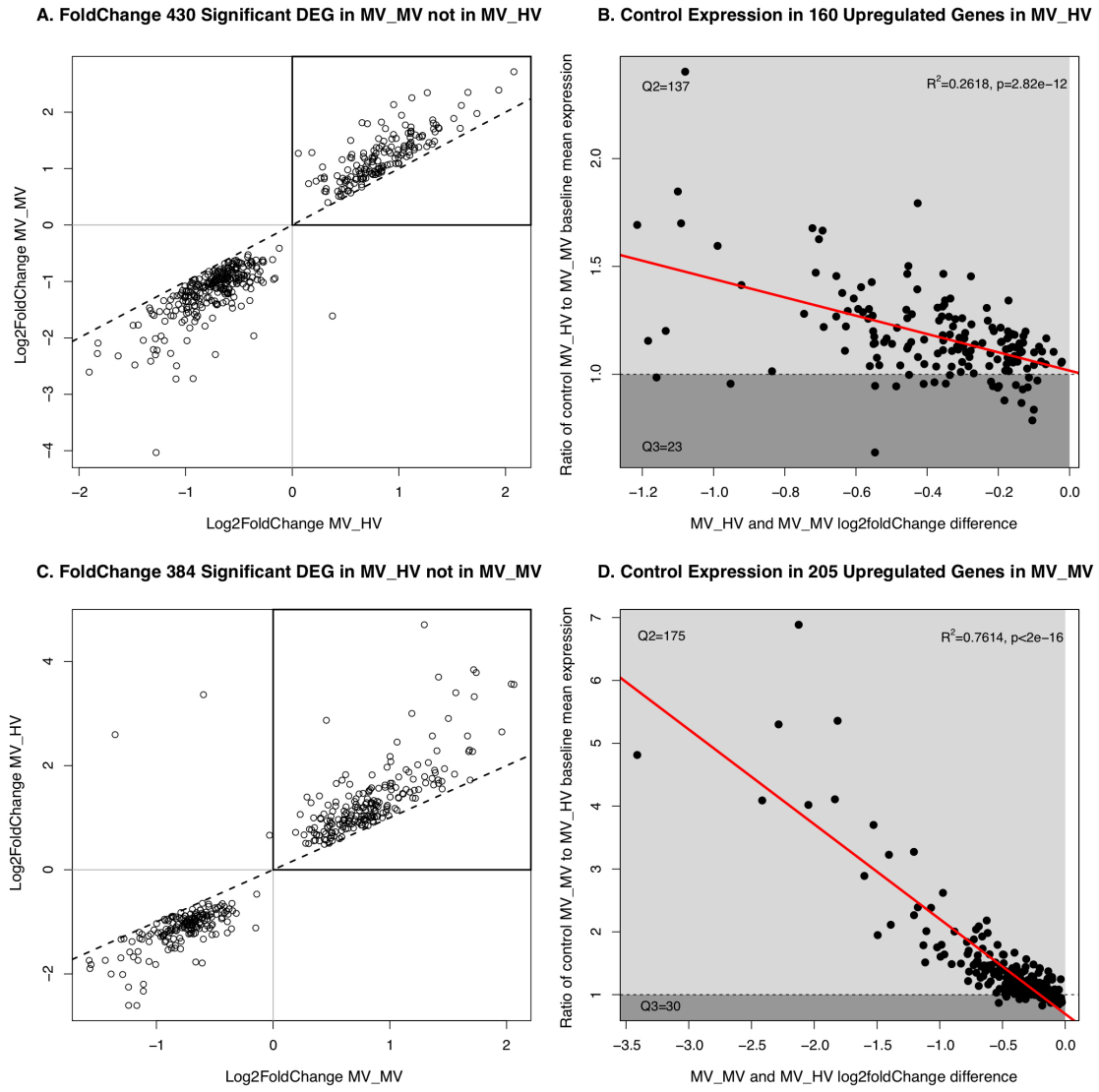

Figure A14. Scatterplots comparing changes in gene expression between (A-B) 430 genes that were not significantly unique to MV_HV *P. lobata* corals and (C-D) 384 genes that were not unique to MV_MV corals. (A&B) Log_2fold change (i.e. magnitude of response) in gene expression in response to heat stress for subset number of genes that are unique to each transplant group comparison. Each open circle represents an individual gene, and the dashed line is a 1:1 line. Quadrat 1 and 3 represents up-regulated and down-regulated genes for both transplant groups, respectively. (C&D) Scatterplot comparing the log_2fold change difference in expression (x axis) to the ratio of control mean expression (y axis) between transplant groups across the upregulated genes from Quadrat 1 in A/C (bordered box). A higher constitutive expression and reduced response to heat stress for control samples from one transplant group relative to the other transplant group's control samples are those gene points that are > 1 on the y axis and < 0 on the x axis (Quadrat 2).

The lighter (Q2) and darker (Q3) quadrats represent the number of genes that are potentially frontloaded or stress indicators in expression, respectively. A linear regression and associated R^2 were calculated to visualize the relationship of these genes.

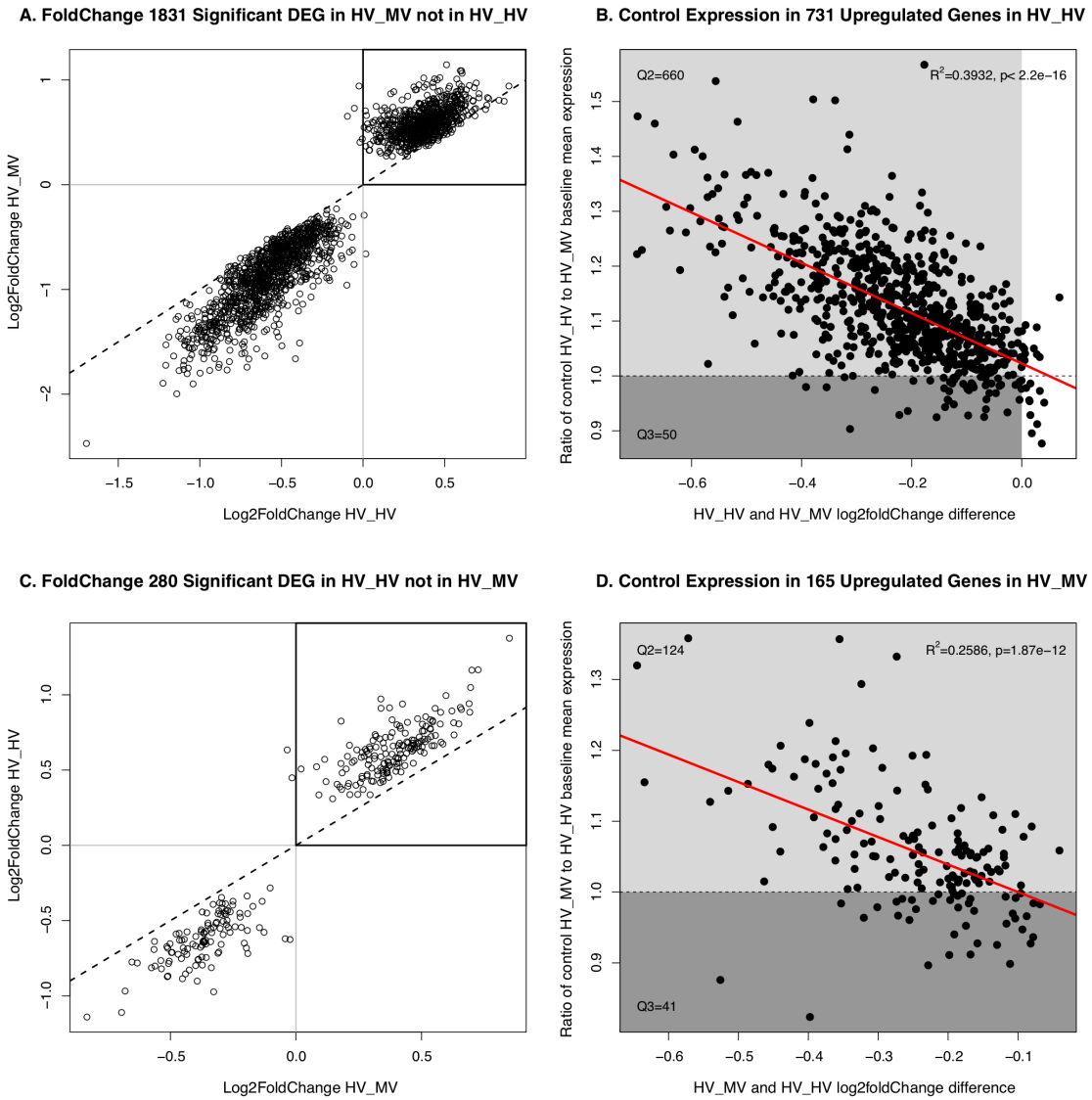

Figure A15. Scatterplots comparing changes in gene expression between (A-B) 1831 genes that were not significantly unique to HV_HV *in hospite* Symbiodiniaceae and (C-D) 280 genes that were not unique to HV_MV symbionts. (A&B) Log_2fold change (i.e. magnitude of response) in gene expression in response to heat stress for subset number of genes that are unique to each transplant group comparison. Each open circle represents an individual gene, and the dashed line is a 1:1 line. Quadrat 1 and 3 represents up-regulated and down-regulated genes for both transplant groups, respectively. (C&D) Scatterplot comparing the log_2fold change difference in expression (x axis) to the ratio of control mean expression (y axis) between transplant groups across the upregulated genes from Quadrat 1 in A/C (bordered box). A higher constitutive expression and reduced response to heat stress for control samples from one transplant group relative to the other transplant group's control samples are those gene points that are > 1 on the y axis and < 0 on the x axis (Quadrat 2). The lighter (Q2) and darker (Q3) quadrats represent the number of genes that are

potentially frontloaded or stress indicators in expression, respectively. A linear regression and associated R^2 were calculated to visualize the relationship of these genes.

TABLES

Table A1 Ofu Temperature

A. Ofu Pools Max Daily Temperatures

ANOVA

Model: max ~ site*seaon	Factor	Df	Sum Sq	Mean Sq	F value	Pr(>F)
	site	2	20.8600	10.4300	9.1371	**0.0001157**
	season	1	634.2100	634.2100	555.5856	**<.0001**
	site:season	2	17.5700	8.7800	7.6950	**0.0004792**
	Residuals	1139	1300.1900	1.1400		

Tukey's Test

	Contrast	Estimate	SE	Df	t-ratio	p-value
site	**HV - LV**	0.3039	0.0772	1139.0000	3.9350	**0.0003000**
	HV - MV	0.2950	0.0775	1139.0000	3.8080	**0.0004000**
	LV - MV	-0.0090	0.0776	1139.0000	-0.1160	0.9926
season	**Summer-Winter**	1.4890	0.0632	1139.0000	23.5510	**<.0001**
site*season	**HV_Summer-LV_Summer**	0.5930	0.1117	1139.0000	5.3090	**<.0001**
	HV_Summer-MV_Summer	0.5182	0.1123	1139.0000	4.6130	**0.0001000**
	LV_Summer-MV_Summer	-0.0748	0.1123	1139.0000	-0.6660	0.9856
	HV_Winter-LV_Winter	0.0149	0.1067	1139.0000	0.1400	1.000
	HV_Winter-MV_Winter	0.0718	0.1067	1139.0000	0.6730	0.9849
	LV_Winter-MV_Winter	0.0569	0.1071	1139.0000	0.5310	0.9949
	HV_Summer-HV_Winter	1.8305	0.1090	1139.0000	16.7880	**<.0001**
	LV_Summer-LV_Winter	1.2524	0.1094	1139.0000	11.4450	**<.0001**
	MV_Summer-MV_Winter	1.3841	0.1101	1139.0000	12.5760	**<.0001**

B. Ofu Pools Min Daily Temperatures

ANOVA

Model: min ~ site*season	Factor	Df	Sum Sq	Mean Sq	F value	Pr(>F)
	site	2	28.2500	14.1240	22.3507	**<.0001**
	season	1	174.6300	174.6260	276.3347	**<.0001**
	site:season	2	0.3700	0.1860	0.2938	0.7455
	Residuals	1139	719.7700	0.6320		

	Contrast	Estimate	SE	Df	t-ratio	p-value
site	**HV - LV**	-0.3446	0.0575	1139.0000	-5.9960	**<.0001**
	HV - MV	-0.3133	0.0576	1139.0000	-5.4370	**<.0001**
	LV - MV	0.0312	0.0577	1139.0000	0.5410	0.8510
season	**Summer-Winter**	0.7817	0.0470	1139.0000	16.6170	**<.0001**
site*season	**HV_Summer-LV_Summer**	-0.3346	0.0831	1139.0000	-4.0260	**0.0009000**
	HV_Summer-MV_Summer	-0.2710	0.0836	1139.0000	-3.2430	**0.01540**
	LV_Summer-MV_Summer	0.0636	0.0836	1139.0000	0.7610	0.9739
	HV_Winter-LV_Winter	-0.3546	0.0794	1139.0000	-4.4660	**0.0001000**
	HV_Winter-MV_Winter	-0.3557	0.0794	1139.0000	-4.4800	**0.0001000**
	LV_Winter-MV_Winter	-0.0011	0.0797	1139.0000	-0.0140	1.000
	HV_Summer-HV_Winter	0.8166	0.0811	1139.0000	10.0650	**<.0001**

	LV_Summer-LV_Winter	0.7966	0.0814	1139.0000	9.7840	**<.0001**
	MV_Summer-MV_Winter	0.7319	0.0819	1139.0000	8.9380	**<.0001**

C. Ofu Pools Mean Daily Temperatures

ANOVA

Model: mean ~ site*seasc	Factor	Df	Sum Sq	Mean Sq	F value	Pr(>F)
	site	2	0.3200	0.1580	0.2640	0.7681
	season	1	275.5600	275.5630	460.7104	**<.0001**
	site:season	2	1.0400	0.5210	0.8704	0.4191
	Residuals	1139	681.2700	0.5980		

	Contrast	Estimate	SE	Df	t-ratio	p-value
season	**Summer-Winter**	0.9820	0.04577	1139	21.4560	**<.0001**

Table A1 Ofu Temperature

D. NOAACRW DHW of Ofu Island from 2010-12 & 2015-16

ANOVA

Model: DHW ~ year	Factor	Df	Sum Sq	Mean Sq	F value	Pr(>F)
	year	17	4159.4000	244.6720	157.7300	**<0.0001**

Tukey's Test

	Contrast	Estimate	SE	Df	t-ratio	p-value
year	**2010 - 2011**	0.5982	0.0922	6557	6.4890	**<.0001**
	2010 - 2012	0.5852	0.0921	6557	6.3520	**<.0001**
	2010 - 2015	-1.3454	0.0922	6557	-14.5930	**<.0001**
	2010 - 2016	-0.6612	0.0921	6557	-7.1770	**<.0001**
	2011 - 2012	-0.0130	0.0921	6557	-0.1410	1
	2011 - 2015	-1.9436	0.0922	6557	-21.0820	**<.0001**
	2011 - 2016	-1.2594	0.0921	6557	-13.6700	**<.0001**
	2012 - 2015	-1.9306	0.0921	6557	-20.9550	**<.0001**
	2012 - 2016	-1.2464	0.0921	6557	-13.5380	**<.0001**
	2015 - 2016	0.6842	0.0921	6557	7.4270	**<.0001**

E. NOAACRW SST of Ofu Island from 2010-12 & 2015-16

ANOVA

Model: SST ~ year

	Factor	Df	Sum Sq	Mean Sq	F value	Pr(>F)
	year	17	209.6000	12.3280	25.4690	**<0.0001**

Tukey's Test

	Contrast	Estimate	SE	Df	t-ratio	p-value
year	**2010 - 2011**	0.5198	0.0515	6557	10.0940	**<.0001**
	2010 - 2012	0.3170	0.0515	6557	6.1590	**<.0001**
	2010 - 2015	0.2721	0.0515	6557	5.2840	**<.0001**
	2010 - 2016	0.0099	0.0515	6557	0.1930	1.000
	2011 - 2012	-0.2029	0.0515	6557	-3.9420	**0.01010**
	2011 - 2015	-0.2477	0.0515	6557	-4.8100	**0.000200**
	2011 - 2016	-0.5099	0.0515	6557	-9.9080	**<.0001**
	2012 - 2015	-0.0448	0.0515	6557	-0.8710	1.000
	2012 - 2016	-0.3070	0.0514	6557	-5.9700	**<.0001**
	2015 - 2016	-0.2622	0.0515	6557	-5.0950	**0.0001**

F. NOAACRW SSTAnomalies of Ofu Island from 2010-12 & 2015-16

ANOVA

Model: SSTA ~ year

	Factor	Df	Sum Sq	Mean Sq	F value	Pr(>F)
	year	17	210.1600	12.3623	94.5920	**<.0001**

Tukey's Test

	Contrast	Estimate	SE	t-ratio	p-value
year	**2010 - 2011**	0.5199	0.0268	19.4280	**<.0001**
	2010 - 2012	0.3188	0.0267	11.9200	**<.0001**
	2010 - 2015	0.2722	0.0268	10.1700	**<.0001**
	2010 - 2016	0.0118	0.0267	0.4400	1.000
	2011 - 2012	-0.2011	0.0267	-7.5210	**<.0001**
	2011 - 2015	-0.2477	0.0268	-9.2570	**<.0001**
	2011 - 2016	-0.5081	0.0267	-19.0010	**<.0001**
	2012 - 2015	-0.0466	0.0267	-1.7420	0.9584
	2012 - 2016	-0.3070	0.0267	-11.4880	**<.0001**
	2015 - 2016	-0.2604	0.0267	-9.7380	**<.0001**

Table A2 *Porites lobata* physiology

WEEKLY GROWTH RATE

A. Growth (g) over Time ((final-initial) / weeks)

Shapiro-wilk

growth ~ time+origin+dest	time	origin	dest	p-value
	Jan-16	HV	HV	0.05005
		MV	HV	0.05031
		LV	HV	0.3070
		MV	MV	0.1381
		LV	LV	0.8672
	Jul-16	HV	HV	0.4296
		MV	**HV**	**0.01741**
		LV	HV	0.3606
		MV	MV	0.8815
		LV	LV	0.5801

Bartlett HOV

growth ~ time+origin_dest	time	K-squared	df	p-value
	Jan-16	1.8024	4	0.7720
	Jul-16	6.6295	4	0.1568

ANOVA

Model: grate ~ time*origin_dest + Error(colony)

	Factor	Df	Sum Sq	Mean Sq	F value	Pr(>F)
Error: Between	time	1	0.0234	0.0234	2.217	0.1670
	origin_dest	3	0.0733	0.0244	2.31	0.1380
	residuals	10	0.1057	0.0106		
Error: Within	**time**	1	0.0604	0.0604	33.75	**< 0.0001**
	origin_dest	2	0.0359	0.0180	10.04	**0.0006780**
	time:origin_dest	4	0.0356	0.0089	4.97	**0.004596**
	residuals	24	0.0430	0.0018		

Tukey's Test

	Contrast	Estimate	Std. Error	z value	Pr(>|z|)
origin_dest	**MV_HV - HV_HV**	-0.1291	0.0422	-3.0580	**0.02230**
	LV_HV - HV_HV	-0.1415	0.0435	-3.2500	**0.01150**
	MV_MV - HV_HV	-0.0658	0.0422	-1.5580	1.000
	LV_LV - HV_HV	-0.0770	0.0414	-1.8580	0.6314
	LV_HV - MV_HV	-0.0123	0.0443	-0.2780	1.000
	MV_MV - MV_HV	0.0633	0.0334	1.8960	0.5801
	LV_LV - MV_HV	0.0521	0.0422	1.2350	1.000
	MV_MV - LV_HV	0.0757	0.0443	1.7090	0.8748
	LV_LV - LV_HV	0.0645	0.0344	1.8750	0.6083
	LV_LV - MV_MV	-0.0112	0.0422	-0.2650	1.000
time*origin_dest					
Jan-16	Jan-16.MV_HV - Jan-16.HV_HV	-0.0970	0.0438	-2.2170	1.000

	Jan-16.LV_HV - Jan-16.HV_HV	-0.0807	0.0452	-1.7850	1.000
	Jan-16.MV_MV - Jan-16.HV_HV	-0.0820	0.0438	-1.8740	1.000
	Jan-16.LV_LV - Jan-16.HV_HV	-0.0590	0.0438	-1.3480	1.000
	Jan-16.LV_HV-Jan-16.MV_HV	0.0163	0.0452	0.3620	1.000
	Jan-16.MV_MV-Jan-16.MV_HV	0.0150	0.0270	0.5550	1.000
	Jan-16.LV_LV-Jan-16.MV_HV	0.0380	0.0438	0.8680	1.000
	Jan-16.MV_MV-Jan-16.LV_HV	-0.0013	0.0452	-0.0300	1.000
	Jan-16.LV_LV-Jan-16.LV_HV	0.0217	0.0293	0.7400	1.000
	Jan-16.LV_LV-Jan-16.MV_MV	0.0230	0.0438	0.5260	1.000
Jul-16	**Jul-16.MV_HV-Jul-16.HV_HV**	-0.1547	0.0452	-3.4250	**0.02769**
	Jul-16.LV_HV-Jul-16.HV_HV	-0.2052	0.0452	-4.5410	**0.0002520**
	Jul-16.MV_MV-Jul-16.HV_HV	-0.0310	0.0452	-0.6860	1.000
	Jul-16.LV_LV-Jul-16.HV_HV	-0.0950	0.0438	-2.1710	1.000
	Jul-16.LV_HV-Jul-16.MV_HV	-0.0504	0.0466	-1.0830	1.000
	Jul-16.MV_MV-Jul-16.MV_HV	0.1238	0.0302	4.0950	**0.001904**
	Jul-16.MV_MV-Jul-16.LV_HV	0.1742	0.0466	3.7410	**0.008253**
	Jul-16.LV_LV-Jul-16.LV_HV	0.1102	0.0293	3.7630	**0.007564**
	Jul-16.LV_LV-Jul-16.MV_MV	-0.0640	0.0452	-1.4170	1.000
Jan-16 vs. Jul-16	**Jul-16.HV_HV-Jan-16.HV_HV**	0.1070	0.0270	3.9580	**0.003399**
	Jul-16.MV_HV-Jan-16.MV_HV	0.0493	0.0293	1.6830	1.000
	Jul-16.LV_HV-Jan-16.LV_HV	-0.0175	0.0302	-0.5790	1.000
	Jul-16.MV_MV-Jan-16.MV_MV	0.1580	0.0293	5.3980	**< 0.0001**
	Jul-16.LV_LV-Jan-16.LV_LV	0.0710	0.0270	2.6260	0.3883

Table A2 *Porites lobata* physiology

Fv/Fm

B. Normalized Fv/Fm following heat stress ((0hr-21hr)/0hr)

Shapiro-wilk

Model: Fvfm ~ time+orig	time	origin	dest	trt	p-value
	Jan-16	HV	HV	heat	0.4211
		HV	HV	cont	0.1014
		MV	HV	heat	0.3078
		MV	HV	cont	0.5283
		MV	MV	heat	0.9036
		MV	MV	cont	0.4504
		LV	HV	heat	0.4676
		LV	HV	cont	0.5751
		LV	LV	heat	0.7559
		LV	LV	cont	0.0651
	Jul-16	HV	HV	heat	0.2175
		HV	HV	cont	0.4771
		MV	**HV**	**heat**	**0.01827**
		MV	HV	cont	0.9470
		MV	MV	heat	0.4734
		MV	MV	cont	0.1270
		LV	HV	heat	0.6272
		LV	HV	cont	0.3074
		LV	LV	heat	0.7562
		LV	LV	cont	0.7022

Bartlett HOV

Model: Fvfm ~ time+orig	time	K-squared	df	p-value
	Jan-16	14.8220	4	**0.005085**
	Jul-16	8.4805	4	0.07548

ANOVA

Model: Fvfmnorm ~ time*origin_dest*trt + Error(colony)

	Factor	Df	Sum Sq	Mean Sq	F value	Pr(>F)
Between Subjects	time	1	0.0271	0.0271	1.7770	0.2193
	origin_dest	4	0.3094	0.0774	5.0660	**0.02480**
	time:origin_dest	1	0.0103	0.0103	0.6740	0.4355
	Residuals	8	0.1222	0.0153		
Within Subjects	time	1	0.0001	0.0001	0.0140	0.9053
	origin_dest	2	0.0205	0.0102	1.5330	0.2245
	trt	1	1.5442	1.5442	231.0940	**< 0.0001**
	time:origin_dest	4	0.0329	0.0082	1.2290	0.3085
	time:trt	1	0.0869	0.0869	13.0100	**0.0006460**
	origin_dest:trt	4	0.2591	0.0648	9.6950	**< 0.0001**
	time:origin_dest:trt	4	0.0560	0.0140	2.0960	0.09293
	Residuals	58	0.3876	0.0067		

Tukey's Test (Bonferroni corrected)

	Contrast	Estimate	Std. Error	z value	Pr(>|z|)
origin_dest	MV_HV - HV_HV	-0.1121	0.0568	-1.9750	0.4820
	LV_HV - HV_HV	-0.0449	0.0609	-0.7380	1.000
	LV_HV - MV_HV	0.0672	0.0623	1.0790	1.000
	MV_MV - HV_HV	-0.1435	0.0553	-2.5970	0.09400
	LV_LV - HV_HV	-0.0416	0.0568	-0.7330	1.000
	MV_MV - MV_HV	-0.0314	0.0568	-0.5530	1.000
	LV_LV - LV_HV	0.0033	0.0623	0.0530	1.000
	LV_LV - MV_HV	0.0705	0.0582	1.2100	1.000
	MV_MV - LV_HV	-0.0986	0.0609	-1.6190	1.000
	LV_LV - MV_MV	0.1019	0.0568	1.7940	0.7270
origin_dest*trt	**HV_HV.heat - HV_HV.cont**	0.4266	0.0410	10.4160	**< 0.0001**
	MV_HV.heat - MV_HV.cont	0.1847	0.0432	4.2780	**0.0008500**
	LV_HV.heat - LV_HV.cont	0.2846	0.0490	5.8140	**< 0.0001**
	MV_MV.heat - MV_MV.cont	0.1258	0.0410	3.0720	0.09578
	LV_LV.heat - LV_LV.cont	0.2901	0.0432	6.7200	**< 0.0001**
	MV_HV.heat - HV_HV.heat	-0.2327	0.0502	-4.6330	**0.0001620**
	MV_HV.cont - HV_HV.cont	0.0092	0.0502	0.1840	1.000
	LV_HV.heat - HV_HV.heat	-0.1265	0.0533	-2.3730	0.7950
	LV_HV.cont - HV_HV.cont	0.0155	0.0533	0.2910	1.000
	LV_HV.heat - MV_HV.heat	0.1062	0.0543	1.9560	1.000
	LV_HV.cont - MV_HV.cont	0.0063	0.0543	0.1160	1.000
	MV_MV.heat - HV_HV.heat	-0.2939	0.0492	-5.9720	**< 0.0001**
	MV_MV.cont - HV_HV.cont	0.0069	0.0492	0.1400	1.000
	LV_LV.heat - HV_HV.heat	-0.1029	0.0502	-2.0480	1.000
	LV_LV.cont - HV_HV.cont	0.0336	0.0502	0.6690	1.000
	MV_MV.heat - MV_HV.heat	-0.0612	0.0422	-1.4510	1.000
	MV_MV.cont - MV_HV.cont	-0.0023	0.0422	-0.0550	1.000
	LV_LV.heat - LV_HV.heat	0.0237	0.0471	0.5020	1.000
	LV_LV.cont - LV_HV.cont	0.0181	0.0471	0.3850	1.000
	LV_LV.heat - MV_HV.heat	0.1299	0.0512	2.5350	0.5062
	LV_LV.cont - MV_HV.cont	0.0244	0.0512	0.4760	1.000
	MV_MV.heat - LV_HV.heat	-0.1674	0.0533	-3.1380	0.07650
	MV_MV.cont - LV_HV.cont	-0.0086	0.0533	-0.1610	1.000
	LV_LV.heat - MV_MV.heat	0.1910	0.0502	3.8030	**0.006428**
	LV_LV.cont - MV_MV.cont	0.0267	0.0502	0.5320	1.000
time*trt	**Jan-16.heat - Jan-16.cont**	0.2038	0.0296	6.8800	**< 0.0001**
	Jul-16.heat - Jul-16.cont	0.3284	0.0317	10.3690	**< 0.0001**
	Jan-16.heat - Jul-16.heat	-0.0591	0.0308	-1.9220	0.3280
	Jan-16.cont - Jul-16.cont	0.0655	0.0308	2.1280	0.2000

time*origin_dest*trt

Jan-16	**Jan-16.HV_HV.heat - Jan-16.HV_HV.cont**	0.3172	0.0521	6.0860	**< 0.0001**
	Jan-16.MV_HV.heat - Jan-16.MV_HV.cont	0.0994	0.0521	1.9070	1.000
	Jan-16.LV_HV.heat - Jan-16.LV_HV.cont	0.2068	0.0583	3.5480	**0.07367**
	Jan-16.MV_MV.heat - Jan-16.MV_MV.cont	0.0824	0.0521	1.5810	1.000
	Jan-16.LV_LV.heat - Jan-16.LV_LV.cont	0.3140	0.0521	6.0250	**< 0.0001**
	Jan-16.MV_HV.heat - Jan-16.HV_HV.heat	-0.2248	0.0590	-3.8130	**0.02612**
	Jan-16.LV_HV.heat - Jan-16.HV_HV.heat	-0.1106	0.0621	-1.7800	1.000
	Jan-16.MV_MV.heat - Jan-16.HV_HV.heat	-0.2482	0.0590	-4.2100	**0.004862**
	Jan-16.LV_LV.heat - Jan-16.HV_HV.heat	0.0122	0.0590	0.2070	1.000
	Jan-16.MV_MV.heat - Jan-16.MV_HV.heat	-0.0234	0.0521	-0.4490	1.000
	Jan-16.LV_HV.heat - Jan-16.MV_HV.heat	0.1142	0.0621	1.8380	1.000
	Jan-16.LV_LV.heat - Jan-16.MV_HV.heat	0.2370	0.0590	4.0200	**0.01108**
	Jan-16.LV_LV.heat - Jan-16.LV_HV.heat	0.1228	0.0557	2.2050	1.000
	Jan-16.MV_MV.heat - Jan-16.LV_HV.heat	-0.1376	0.0621	-2.2140	1.000
	Jan-16.LV_LV.heat - Jan-16.MV_MV.heat	0.2604	0.0590	4.4160	**0.001906**
	Jan-16.MV_HV.cont - Jan-16.HV_HV.cont	-0.0070	0.0590	-0.1190	1.000
	Jan-16.LV_HV.cont - Jan-16.HV_HV.cont	-0.0002	0.0621	-0.0020	1.000
	Jan-16.MV_MV.cont - Jan-16.HV_HV.cont	-0.0134	0.0590	-0.2270	1.000
	Jan-16.LV_LV.cont - Jan-16.HV_HV.cont	0.0154	0.0590	0.2610	1.000
	Jan-16.MV_MV.cont - Jan-16.MV_HV.cont	-0.0064	0.0521	-0.1230	1.000
	Jan-16.LV_HV.cont - Jan-16.MV_HV.cont	0.0068	0.0621	0.1100	1.000
	Jan-16.LV_LV.cont - Jan-16.MV_HV.cont	0.0224	0.0590	0.3800	1.000
	Jan-16.MV_MV.cont - Jan-16.LV_HV.cont	-0.0132	0.0621	-0.2130	1.000
	Jan-16.LV_LV.cont - Jan-16.LV_HV.cont	0.0156	0.0557	0.2790	1.000
	Jan-16.LV_LV.cont - Jan-16.MV_MV.cont	0.0288	0.0590	0.4880	1.000
Jul-16	**Jul-16.HV_HV.heat - Jul-16.HV_HV.cont**	0.5360	0.0521	10.2850	**< 0.0001**
	Jul-16.MV_HV.heat - Jul-16.MV_HV.cont	0.2913	0.0583	4.9980	**0.0001100**
	Jul-16.LV_HV.heat - Jul-16.LV_HV.cont	0.3883	0.0673	5.7720	**< 0.0001**
	Jul-16.MV_MV.heat - Jul-16.MV_MV.cont	0.1692	0.0521	3.2470	0.2219
	Jul-16.LV_LV.heat - Jul-16.LV_LV.cont	0.2603	0.0583	4.4660	**0.001511**
	Jul-16.MV_HV.heat - Jul-16.HV_HV.heat	-0.2255	0.0621	-3.6330	0.05317
	Jul-16.LV_HV.heat - Jul-16.HV_HV.heat	-0.1259	0.0670	-1.8790	1.000
	Jul-16.MV_MV.heat - Jul-16.HV_HV.heat	-0.3396	0.0590	-5.7600	**< 0.0001**
	Jul-16.LV_LV.heat - Jul-16.HV_HV.heat	-0.2310	0.0621	-3.7220	**0.03759**
	Jul-16.MV_MV.heat - Jul-16.MV_HV.heat	-0.1141	0.0556	-2.0530	1.000
	Jul-16.LV_HV.heat - Jul-16.MV_HV.heat	0.0996	0.0698	1.4270	1.000
	Jul-16.LV_LV.heat - Jul-16.MV_HV.heat	-0.0056	0.0650	-0.0860	1.000
	Jul-16.LV_LV.heat - Jul-16.LV_HV.heat	-0.1051	0.0646	-1.6280	1.000
	Jul-16.MV_MV.heat - Jul-16.LV_HV.heat	-0.2137	0.0670	-3.1890	0.2715
	Jul-16.LV_LV.heat - Jul-16.MV_MV.heat	0.1086	0.0621	1.7490	1.000
	Jul-16.MV_HV.cont - Jul-16.HV_HV.cont	0.0193	0.0621	0.3100	1.000
	Jul-16.LV_HV.cont - Jul-16.HV_HV.cont	0.0218	0.0670	0.3250	1.000
	Jul-16.MV_MV.cont - Jul-16.HV_HV.cont	0.0272	0.0590	0.4610	1.000
	Jul-16.LV_LV.cont - Jul-16.HV_HV.cont	0.0447	0.0621	0.7200	1.000

	Jul-16.MV_MV.cont - Jul-16.MV_HV.cont	0.0079	0.0556	0.1430	1.000
	Jul-16.LV_HV.cont - Jul-16.MV_HV.cont	0.0025	0.0698	0.0360	1.000
	Jul-16.LV_LV.cont - Jul-16.MV_HV.cont	0.0254	0.0650	0.3910	1.000
	Jul-16.MV_MV.cont - Jul-16.LV_HV.cont	0.0054	0.0670	0.0810	1.000
	Jul-16.LV_LV.cont - Jul-16.LV_HV.cont	0.0230	0.0646	0.3550	1.000
	Jul-16.LV_LV.cont - Jul-16.MV_MV.cont	0.0175	0.0621	0.2820	1.000
Jan-16 vs. Jul-16	Jan-16.HV_HV.cont - Jul-16.HV_HV.cont	0.0886	0.0521	1.7000	1.000
	Jan-16.HV_HV.heat - Jul-16.HV_HV.heat	-0.1302	0.0521	-2.4980	1.000
	Jan-16.LV_HV.cont - Jul-16.LV_HV.cont	0.0667	0.0634	1.0520	1.000
	Jan-16.LV_HV.heat - Jul-16.LV_HV.heat	-0.1149	0.0634	-1.8120	1.000
	Jan-16.LV_LV.cont - Jul-16.LV_LV.cont	0.0593	0.0556	1.0660	1.000
	Jan-16.LV_LV.heat - Jul-16.LV_LV.heat	0.1130	0.0556	2.0320	1.000
	Jan-16.MV_HV.cont - Jul-16.MV_HV.cont	0.0623	0.0556	1.1210	1.000
	Jan-16.MV_HV.heat - Jul-16.MV_HV.heat	-0.1295	0.0556	-2.3300	1.000
	Jan-16.MV_MV.cont - Jul-16.MV_MV.cont	0.0480	0.0521	0.9210	1.000
	Jan-16.MV_MV.heat - Jul-16.MV_MV.heat	-0.0388	0.0521	-0.7440	1.000

Table A2 *Porites lobata* physiology

CHL

C. Total Chlorophyll Retention (1-(control-heat)/control)

Shapiro-wilk

Model: chlratio ~ time+ori	time	origin	dest	p-value
	Jan-16	**HV**	**HV**	**0.02362**
		MV	HV	0.3643
		MV	MV	0.8767
		LV	HV	0.1460
		LV	LV	0.3353
	Jul-16	HV	HV	0.3350
		MV	HV	0.8908
		MV	MV	0.4590
		LV	HV	0.7497
		LV	LV	0.3829

Bartlett HOV

Model: chlratio ~ time+ori	time	K-squared	df	p-value
	Jan-16	2.5123	4	0.6424
	Jul-16	10.4210	4	**0.03391**

ANOVA

Model: chlratio ~ time*origin*dest + Error(colony)

	Factor	Df	Sum Sq	Mean Sq	F value	Pr(>F)
Error: Between	time	1	0.0014	0.0014	0.0100	0.9232
	origin	2	0.9778	0.4889	3.4930	0.08120
	dest	2	0.1895	0.0947	0.6770	0.5351
	time:dest	1	0.2877	0.2877	2.0550	0.1896
	Residuals	8	1.1199	0.1400		
Error: Within	time	1	0.0335	0.0335	0.8540	0.3650
	dest	2	0.0464	0.0232	0.5920	0.5610
	time:origin	2	0.2499	0.1250	3.1860	0.06000
	time:dest	2	0.0318	0.0159	0.4050	0.6720
	Residuals	23	0.9020	0.0392		

Tukey's Test (Bonferroni corrected)

	Contrast	Estimate	Std. Error	z value	Pr(>|z|)
origin	MV - HV	1.7321	0.8984	1.9280	0.1616
	LV - HV	2.9576	0.9072	3.2600	**0.003340**
	LV - MV	1.2254	0.8737	1.4030	0.4822
time*origin	**Jan-16.MV - Jan-16.HV**	0.4609	0.1562	2.9510	**0.04760**
	Jan-16.LV - Jan-16.HV	0.2171	0.1578	1.3750	1.000
	Jan-16.LV - Jan-16.MV	-0.2438	0.1459	-1.6710	1.000
	Jul-16.MV - Jul-16.HV	0.2732	0.1577	1.7320	1.000
	Jul-16.LV - Jul-16.HV	0.3772	0.1617	2.3330	0.2948
	Jul-16.LV - Jul-16.MV	0.1040	0.1517	0.6850	1.000
	Jul-16.HV - Jan-16.HV	0.0809	0.1202	0.6730	1.000

	Jul-16.MV - Jan-16.MV	-0.1068	0.0878	-1.2160	1.000
	Jul-16.LV - Jan-16.LV	0.2410	0.0967	2.4920	0.1905

ANOVA

Model: chlratio ~ time*origin_dest + Error(colony)

	Factor	Df	Sum Sq	Mean Sq	F value	Pr(>F)
Error: Between	time	1	0.0014	0.0014	0.0100	0.9230
	origin_dest	4	1.1673	0.2918	2.0850	0.1750
	time:origin_dest	1	0.2877	0.2877	2.0550	0.1900
	Residuals	8	1.1199	0.1400		
Error: Within	time	1	0.0335	0.0335	0.8540	0.3650
	origin_dest	2	0.0464	0.0232	0.5920	0.5610
	time:origin_dest	4	0.2817	0.0704	1.7960	0.1640
	Residuals	23	0.9020	0.0392		

Tukey's Test (Bonferroni corrected)

	Contrast	Estimate	Std. Error	z value	Pr(>|z|)
origin_dest	MV_HV - HV_HV	0.4011	0.1502	2.6700	0.07580
	LV_HV - HV_HV	0.3134	0.1571	1.9950	0.4608
	MV_MV - HV_HV	0.3436	0.1483	2.3180	0.2046
	LV_LV - HV_HV	0.2582	0.1502	1.7180	0.8571
	MV_MV - MV_HV	-0.0575	0.0965	-0.5950	1.000
	LV_HV - MV_HV	-0.0877	0.1590	-0.5520	1.000
	LV_LV - MV_HV	-0.1430	0.1522	-0.9400	1.000
	LV_LV - LV_HV	-0.0553	0.1109	-0.4980	1.000
	MV_MV - LV_HV	0.0302	0.1571	0.1920	1.000
	LV_LV - MV_MV	-0.0855	0.1502	-0.5690	1.000
time*origin_dest	Jan-16.MV_HV - Jan-16.HV_HV	0.5204	0.1721	3.0250	0.1120
	Jan-16.LV_HV - Jan-16.HV_HV	0.2491	0.1795	1.3880	1.000
	Jan-16.MV_MV - Jan-16.HV_HV	0.4013	0.1721	2.3320	0.8860
	Jan-16.LV_LV - Jan-16.HV_HV	0.1945	0.1721	1.1300	1.000
	Jan-16.MV_MV - Jan-16.MV_HV	-0.1191	0.1255	-0.9490	1.000
	Jan-16.LV_HV - Jan-16.MV_HV	-0.2713	0.1795	-1.5120	1.000
	Jan-16.LV_LV - Jan-16.MV_HV	-0.3259	0.1721	-1.8940	1.000
	Jan-16.LV_LV - Jan-16.LV_HV	-0.0546	0.1356	-0.4030	1.000
	Jan-16.LV_HV - Jan-16.MV_MV	-0.1523	0.1795	-0.8480	1.000
	Jan-16.LV_LV - Jan-16.MV_MV	-0.2068	0.1721	-1.2020	1.000
	Jul-16.MV_HV - Jul-16.HV_HV	0.2569	0.1790	1.4350	1.000
	Jul-16.LV_HV - Jul-16.HV_HV	0.4179	0.1907	2.1910	1.000
	Jul-16.MV_MV - Jul-16.HV_HV	0.2859	0.1721	1.6620	1.000
	Jul-16.LV_LV - Jul-16.HV_HV	0.3490	0.1791	1.9480	1.000
	Jul-16.MV_MV - Jul-16.MV_HV	0.0291	0.1349	0.2150	1.000
	Jul-16.LV_HV - Jul-16.MV_HV	0.1610	0.1970	0.8170	1.000
	Jul-16.LV_LV - Jul-16.MV_HV	0.0921	0.1858	0.4950	1.000
	Jul-16.LV_LV - Jul-16.LV_HV	-0.0689	0.1609	-0.4280	1.000
	Jul-16.LV_HV - Jul-16.MV_MV	0.1319	0.1907	0.6920	1.000

Jul-16.LV_LV - Jul-16.MV_MV	0.0630	0.1791	0.3520	1.000
Jan-16.HV_HV - Jul-16.HV_HV	-0.0809	0.1255	-0.6440	1.000
Jan-16.MV_HV - Jul-16.MV_HV	0.1827	0.1349	1.3540	1.000
Jan-16.LV_HV - Jul-16.LV_HV	-0.2497	0.1543	-1.6180	1.000
Jan-16.MV_MV - Jul-16.MV_MV	0.0345	0.1255	0.2750	1.000
Jan-16.LV_LV - Jul-16.LV_LV	-0.2353	0.1351	-1.7420	1.000

Table A2 *Porites lobata* physiology

CHL

D. Total Chlorophyll (control and heat)

Shapiro-wilk

Model: totalchl ~ time+o	time	origin	dest	trt	p-value
Jan-16	**Jan-16**	**HV**	**HV**	**cont**	**0.02567**
	Jan-16	MV	HV	cont	0.3534
	Jan-16	LV	HV	cont	0.1598
	Jan-16	**MV**	**MV**	**cont**	**0.00527**
	Jan-16	LV	LV	cont	0.8198
	Jan-16	HV	HV	heat	0.3989
	Jan-16	MV	HV	heat	0.1726
	Jan-16	LV	HV	heat	0.9793
	Jan-16	MV	MV	heat	0.7432
	Jan-16	LV	LV	heat	0.1124
Jul-16	Jul-16	HV	HV	cont	0.8330
	Jul-16	MV	HV	cont	0.1121
	Jul-16	LV	HV	cont	0.6726
	Jul-16	MV	MV	cont	0.1662
	Jul-16	LV	LV	cont	0.5304
	Jul-16	HV	HV	heat	0.8063
	Jul-16	MV	HV	heat	0.3501
	Jul-16	LV	HV	heat	0.1002
	Jul-16	MV	MV	heat	0.1215
	Jul-16	LV	LV	heat	0.4485

Bartlett HOV

Model: chlratio ~ time+o	time	K-squared	df	p-value
	Jan-16	10.7390	9	0.2940
	Jul-16	4.8643	9	0.8460

ANOVA

Model: totalchl ~ time*origin_dest*trt + Error(colony)

	Factor	Df	Sum Sq	Mean Sq	F value	Pr(>F)
Error: Between	**time**	1	32.89	32.89	13.849	**0.007442**
	origin_dest	4	184.25	46.06	19.398	**0.000686**
	trt	1	0.21	0.21	0.09	0.7725
	time:origin_dest	1	8.46	8.46	3.561	0.1011
	Residuals	7	16.62	2.37		
Error: Within	**time**	1	58.33	58.33	28.488	**< 0.0001**
	origin_dest	2	28.79	14.4	7.031	**0.001850**
	trt	1	204.34	204.34	99.797	**< 0.0001**
	time:origin_dest	4	39.44	9.86	4.815	**0.002010**
	time:trt	1	19.49	19.49	9.518	**0.003120**
	origin_dest:trt	4	34.88	8.72	4.258	**0.004330**
	time:origin_dest:trt	4	21	5.25	2.564	**0.04767**
	Residuals	58	118.76	2.05		

Tukey's Test (Bonferroni corrected)

	Contrast	Estimate	Std. Error	z value	Pr(>|z|)
time	**Jul-16 - Jan-16**	-1.744	0.5956	-2.928	0.003410
origin_dest	MV_HV - HV_HV	0.3739	0.8481	0.441	1.000
	LV_HV - HV_HV	1.3267	0.9096	1.459	1.000
	MV_MV - HV_HV	0.6939	0.8255	0.841	1.000
	LV_LV - HV_HV	4.0084	0.8481	4.73E+00	**< 0.0001**
	LV_HV - MV_HV	0.9528	0.9302	1.024	1.000
	MV_MV - MV_HV	0.32	0.8481	0.377	1.000
	LV_LV - MV_HV	3.6346	0.8701	4.177	**0.0002950**
	MV_MV - LV_HV	-0.6328	0.9096	-0.696	1.000
time*origin_dest*trt					
16-Jan	**Jan-16.HV_HV.heat - Jan-16.HV_HV.cont**	-5.0682	0.90949	-5.573	**< 0.0001**
	Jan-16.MV_HV.heat - Jan-16.MV_HV.cont	-1.322	0.90949	-1.454	1.000
	Jan-16.LV_HV.heat - Jan-16.LV_HV.cont	-4.8135	1.01684	-4.734	**0.0004190**
	Jan-16.MV_MV.heat - Jan-16.MV_MV.cont	-1.709	0.90949	-1.879	1.000
	Jan-16.LV_LV.heat - Jan-16.LV_LV.cont	-6.7094	0.90949	-7.377	**< 0.0001**
	Jan-16.MV_HV.heat - Jan-16.HV_HV.heat	1.9786	1.10737	1.787	1.000
	Jan-16.LV_HV.heat - Jan-16.HV_HV.heat	2.49669	1.16064	2.151	1.000
	Jan-16.MV_MV.heat - Jan-16.HV_HV.heat	1.493	1.10737	1.348	1.000
	Jan-16.LV_LV.heat - Jan-16.HV_HV.heat	3.685	1.10737	3.328	0.1664
	Jan-16.MV_MV.heat - Jan-16.MV_HV.heat	-0.4856	0.90949	-0.534	1.000
	Jan-16.LV_HV.heat - Jan-16.MV_HV.heat	0.51809	1.16064	0.446	1.000
	Jan-16.LV_LV.heat - Jan-16.MV_HV.heat	1.7064	1.10737	1.541	1.000
	Jan-16.LV_LV.heat - Jan-16.LV_HV.heat	1.18831	0.97364	1.22	1.000
	Jan-16.LV_HV.heat - Jan-16.MV_MV.heat	1.00369	1.16064	0.865	1.000
	Jan-16.LV_LV.heat - Jan-16.MV_MV.heat	2.192	1.10737	1.979	1.000
	Jan-16.MV_HV.cont - Jan-16.HV_HV.cont	-1.7676	1.10737	-1.596	1.000
	Jan-16.LV_HV.cont - Jan-16.HV_HV.cont	2.24199	1.16064	1.932	1.000
	Jan-16.MV_MV.cont - Jan-16.HV_HV.cont	-1.8662	1.10737	-1.685	1.000
	Jan-16.LV_LV.cont - Jan-16.HV_HV.cont	5.3262	1.10737	4.81	**0.0002870**
	Jan-16.MV_MV.cont - Jan-16.MV_HV.cont	-0.0986	0.90949	-0.108	1.000
	Jan-16.LV_HV.cont - Jan-16.MV_HV.cont	4.00959	1.16064	3.455	0.1047
	Jan-16.LV_LV.cont - Jan-16.MV_HV.cont	7.0938	1.10737	6.406	**< 0.0001**
	Jan-16.LV_LV.cont - Jan-16.LV_HV.cont	3.08421	0.97364	3.168	0.2919
	Jan-16.LV_HV.cont - Jan-16.MV_MV.cont	4.10819	1.16064	3.54	0.07614
	Jan-16.LV_LV.cont - Jan-16.MV_MV.cont	7.1924	1.10737	6.495	**< 0.0001**
16-Jul	Jul-16.HV_HV.heat - Jul-16.HV_HV.cont	-2.7412	0.90949	-3.014	0.4899
	Jul-16.MV_HV.heat - Jul-16.MV_HV.cont	-1.305	1.01684	-1.283	1.000
	Jul-16.LV_HV.heat - Jul-16.LV_HV.cont	-1.78367	1.17414	-1.519	1.000
	Jul-16.MV_MV.heat - Jul-16.MV_MV.cont	-2.0976	0.90949	-2.306	1.000
	Jul-16.LV_LV.heat - Jul-16.LV_LV.cont	-1.87106	1.03114	-1.815	1.000
	Jul-16.MV_HV.heat - Jul-16.HV_HV.heat	1.54053	1.15866	1.33	1.000
	Jul-16.LV_HV.heat - Jul-16.HV_HV.heat	1.02966	1.2419	0.829	1.000

	Jul-16.MV_MV.heat - Jul-16.HV_HV.heat	1.8962	1.10737	1.712	1.000
	Jul-16.LV_LV.heat - Jul-16.HV_HV.heat	3.55196	1.15844	3.066	0.4120
	Jul-16.MV_MV.heat - Jul-16.MV_HV.heat	0.35567	0.97127	0.366	1.000
	Jul-16.LV_HV.heat - Jul-16.MV_HV.heat	-0.51087	1.28784	-0.397	1.000
	Jul-16.LV_LV.heat - Jul-16.MV_HV.heat	2.01143	1.20755	1.666	1.000
	Jul-16.LV_LV.heat - Jul-16.LV_HV.heat	2.5223	1.13135	2.229	1.000
	Jul-16.LV_HV.heat - Jul-16.MV_MV.heat	-0.86654	1.2419	-0.698	1.000
	Jul-16.LV_LV.heat - Jul-16.MV_MV.heat	1.65576	1.15844	1.429	1.000
	Jul-16.MV_HV.cont - Jul-16.HV_HV.cont	0.10433	1.15866	0.09	1.000
	Jul-16.LV_HV.cont - Jul-16.HV_HV.cont	0.07213	1.2419	0.058	1.000
	Jul-16.MV_MV.cont - Jul-16.HV_HV.cont	1.2526	1.10737	1.131	1.000
	Jul-16.LV_LV.cont - Jul-16.HV_HV.cont	2.68182	1.15844	2.315	1.000
	Jul-16.MV_MV.cont - Jul-16.MV_HV.cont	1.14827	0.97127	1.182	1.000
	Jul-16.LV_HV.cont - Jul-16.MV_HV.cont	-0.0322	1.28784	-0.025	1.000
	Jul-16.LV_LV.cont - Jul-16.MV_HV.cont	2.57749	1.20755	2.134	1.000
	Jul-16.LV_LV.cont - Jul-16.LV_HV.cont	2.60969	1.13135	2.307	1.000
	Jul-16.LV_HV.cont - Jul-16.MV_MV.cont	-1.18047	1.2419	-0.951	1.000
	Jul-16.LV_LV.cont - Jul-16.MV_MV.cont	1.42922	1.15844	1.234	1.000
Jan-16 vs. Jul-16	Jul-16.HV_HV.heat - Jan-16.HV_HV.heat	-0.4632	0.90949	-0.509	1.000
	Jul-16.HV_HV.cont - Jan-16.HV_HV.cont	-2.7902	0.90949	-3.068	0.4096
	Jul-16.MV_HV.heat - Jan-16.MV_HV.heat	-0.90127	0.97127	-0.928	1.000
	Jul-16.MV_HV.cont - Jan-16.MV_HV.cont	-0.91827	0.97127	-0.945	1.000
	Jul-16.LV_HV.heat - Jan-16.LV_HV.heat	-1.93023	1.10826	-1.742	1.000
	Jul-16.LV_HV.cont - Jan-16.LV_HV.cont	-4.96006	1.10826	-4.476	**0.001448**
	Jul-16.MV_MV.heat - Jan-16.MV_MV.heat	-0.06	0.90949	-0.066	1.000
	Jul-16.MV_MV.cont - Jan-16.MV_MV.cont	0.3286	0.90949	0.361	1.000
	Jul-16.LV_LV.heat - Jan-16.LV_LV.heat	-0.59624	0.97101	-0.614	1.000
	Jul-16.LV_LV.cont - Jan-16.LV_LV.cont	-5.43458	0.97101	-5.597	**< 0.0001**

Table A3 *Goniastrea retiformis* physiology

WEEKLY GROWTH RATE

A. Growth (g) over Time ((final-initial) / weeks)

Shapiro-wilk

Model: grate ~ time+orig	time	origin	dest	p-value
Jan-16	Jan-16	HV	HV	0.7828
	Jan-16	MV	HV	0.8258
	Jan-16	LV	HV	0.8234
	Jan-16	MV	MV	0.6071
Jul-16	Jul-16	HV	HV	0.05427
	Jul-16	MV	HV	0.9189
	Jul-16	LV	HV	0.3550
	Jul-16	MV	MV	0.8627
	Jul-16	LV	LV	0.9511

Bartlett HOV

Model: grate ~ time+orig	time	K-squared	df	p-value
	Jan-16	2.1946	3	0.5330
	Jul-16	0.8560	4	0.9308

ANOVA

Model: grate ~ time*origin_dest + Error(colony)

	Factor	Df	Sum Sq	Mean Sq	F value	Pr(>F)
Error: Between	**time**	1	0.0053	0.0053	8.1820	**0.01550**
	origin_dest	2	0.0014	0.0007	1.1040	0.3655
	residuals	11	0.0071	0.0006		
Error: Within	**time**	1	0.0040	0.0040	10.7760	**0.003260**
	origin_dest	2	0.0109	0.0055	14.6980	**<0.0001**
	time:origin_dest	3	0.0069	0.0023	6.1470	**0.003170**
	residuals	23	0.0085	0.0004		

Tukey's Test

	Contrast	Estimate	Std. Error	z value	Pr(>|z|)
origin_dest	MV_HV-HV_HV	-0.0260	0.0126	-2.0710	0.2289
	LV_HV-HV_HV	-0.0115	0.0126	-0.9160	0.8890
	MV_MV-HV_HV	0.0145	0.0126	1.1550	0.7737
	LV_LV-HV_HV	-0.0410	0.0166	-2.4690	0.09562
	LV_HV-MV_HV	0.0145	0.0126	1.1550	0.7737
	MV_MV-MV_HV	0.0405	0.0126	3.2260	**0.01060**
	LV_LV-MV_HV	-0.0150	0.0166	-0.9030	0.8940
	MV_MV-LV_HV	0.0260	0.0126	2.0710	0.2289
	LV_LV-LV_HV	-0.0295	0.0166	-1.7760	0.3827
	LV_LV-MV_MV	-0.0555	0.0166	-3.3420	**0.007330**
time*origin_dest					
Jan-16	Jan-16.MV_HV-Jan-16.HV_HV	-0.0270	0.0146	-1.8460	0.6420

	Jan-16.LV_HV-Jan-16.HV_HV	-0.0030	0.0146	-0.2050	1.000	
	Jan-16.MV_MV-Jan-16.HV_HV	-0.0120	0.0146	-0.8210	0.9961	
	Jan-16.LV_HV-Jan-16.MV_HV	0.0240	0.0146	1.6410	0.7747	
	Jan-16.MV_MV-Jan-16.MV_HV	0.0150	0.0124	1.2100	0.9523	
	Jan-16.MV_MV-Jan-16.LV_HV	-0.0090	0.0146	-0.6150	0.9995	
Jul-16	Jul-16.MV_HV-Jul-16.HV_HV	-0.0250	0.0146	-1.7100	0.7330	
	Jul-16.LV_HV-Jul-16.HV_HV	-0.0200	0.0146	-1.3680	0.9060	
	Jul-16.MV_MV-Jul-16.HV_HV	0.0410	0.0146	2.8040	0.1107	
	Jul-16.LV_LV-Jul-16.HV_HV	-0.0444	0.0154	-2.8810	0.09085	.
	Jul-16.LV_HV-Jul-16.MV_HV	0.0050	0.0146	0.3420	1.000	
	Jul-16.MV_MV-Jul-16.MV_HV	0.0660	0.0124	5.3230	**<0.001**	
	Jul-16.LV_LV-Jul-16.MV_HV	-0.0194	0.0154	-1.2580	0.9403	
	Jul-16.MV_MV-Jul-16.LV_HV	0.0610	0.0146	4.1720	**<0.001**	
	Jul-16.LV_LV-Jul-16.LV_HV	-0.0244	0.0133	-1.8320	0.6523	
	Jul-16.LV_LV-Jul-16.MV_MV	-0.0854	0.0154	-5.5430	**<0.001**	
Jan-16 vs. Jul-16	Jul-16.HV_HV-Jan-16.HV_HV	0.0140	0.0124	1.1290	0.9683	
	Jul-16.MV_HV-Jan-16.MV_HV	0.0160	0.0124	1.2900	0.9314	
	Jul-16.LV_HV-Jan-16.LV_HV	-0.0030	0.0124	-0.2420	1.000	
	Jul-16.MV_MV-Jan-16.MV_MV	0.0670	0.0124	5.4030	**<0.001**	

Table A3 *Goniastrea retiformis* physiology

Fv/Fm

B. Normalized Fv/Fm following heat stress ((0hr-21hr)/0hr)

Shapiro-wilk

Model: Fvfm ~ time+orig	time	origin	dest	trt	p-value
Jan-16	Jan-16	HV	HV	heat	0.3392
	Jan-16	HV	HV	cont	0.6714
	Jan-16	MV	HV	heat	0.2319
	Jan-16	MV	HV	cont	0.6557
	Jan-16	**MV**	**MV**	**heat**	**0.002411**
	Jan-16	MV	MV	cont	0.7516
	Jan-16	LV	HV	heat	0.1755
	Jan-16	LV	HV	cont	0.8139
Jul-16	Jul-16	HV	HV	heat	0.4215
	Jul-16	HV	HV	cont	0.8722
	Jul-16	MV	HV	heat	0.1138
	Jul-16	**MV**	**HV**	**cont**	**0.001938**
	Jul-16	MV	MV	heat	0.7234
	Jul-16	MV	MV	cont	0.4404
	Jul-16	**LV**	**HV**	**heat**	**0.03077**
	Jul-16	LV	HV	cont	0.2898
	Jul-16	LV	LV	heat	0.6048
	Jul-16	LV	LV	cont	0.4351

Bartlett HOV

Model: Fvfm ~ time+orig	time	K-squared	df	p-value
	Jan-16	3.2157	3	0.3595
	Jul-16	4.6762	4	0.3222

ANOVA

Model: Fvfm ~ time*origin*dest*trt + Error(colony)

	Factor	Df	Sum Sq	Mean Sq	F value	Pr(>F)
Error: Between	time	1	0.0040	0.0040	0.5770	0.4650
	origin	2	0.0034	0.0017	0.2420	0.7890
	dest	1	0.0001	0.0001	0.0130	0.9130
Error: Within	**time**	1	0.0688	0.0688	17.9780	**0.0001**
	dest	2	0.0062	0.0031	0.8070	0.4516
	trt	1	0.3484	0.3484	91.0520	**<0.0001**
	time:origin	2	0.0031	0.0015	0.4000	0.6726
	time:dest	1	0.0026	0.0026	0.6690	0.4170
	time:trt	1	0.0967	0.0967	25.2640	**<0.0001**
	origin:trt	2	0.0026	0.0013	0.3450	0.7099
	dest:trt	2	0.0001	0.0001	0.0150	0.9853
	time:origin:trt	2	0.0287	0.0144	3.7540	**0.02970**
	time:dest:trt	1	0.0001	0.0001	0.0320	0.8587

Tukey's Test (Bonferroni corrected)

	Contrast	Estimate	Std. Error	z value	Pr(>|z|)
time	**Jul-16 - Jan-16**	0.0536	0.0214	2.5060	**0.01220**
time*trt	**Jan-16.heat - Jan-16.cont**	0.0542	0.0200	2.7070	**0.04068**
	Jul-16.heat - Jul-16.cont	0.1905	0.0182	10.4770	**<0.0001**
	Jul-16.heat - Jan-16.heat	0.1230	0.0192	6.4160	**<0.0001**
	Jul-16.cont - Jan-16.cont	-0.0133	0.0192	-0.6960	1.000
time*origin*trt					
Jan-16	Jan-16.HV.heat - Jan-16.HV.cont	0.0575	0.0428	1.3420	1.000
	Jan-16.MV.heat - Jan-16.MV.cont	0.0293	0.0271	1.0810	1.000
	Jan-16.LV.heat - Jan-16.LV.cont	0.1012	0.0383	2.6410	0.5455
	Jan-16.MV.heat - Jan-16.HV.heat	-0.0257	0.0392	-0.6560	1.000
	Jan-16.MV.cont - Jan-16.HV.cont	0.0025	0.0392	0.0630	1.000
	Jan-16.LV.heat - Jan-16.HV.heat	0.0269	0.0436	0.6160	1.000
	Jan-16.LV.cont - Jan-16.HV.cont	-0.0168	0.0436	-0.3850	1.000
	Jan-16.MV.heat - Jan-16.LV.heat	-0.0526	0.0365	-1.4420	1.000
	Jan-16.MV.cont - Jan-16.LV.cont	0.0193	0.0365	0.5290	1.000
Jul-16	**Jul-16.HV.heat - Jul-16.HV.cont**	0.2162	0.0383	5.6420	**<0.0001**
	Jul-16.MV.heat - Jul-16.MV.cont	0.2205	0.0271	8.1380	**<0.0001**
	Jul-16.LV.heat - Jul-16.LV.cont	0.1369	0.0303	4.5180	**0.0004**
	Jul-16.MV.heat - Jul-16.HV.heat	0.0259	0.0365	0.7100	1.000
	Jul-16.MV.cont - Jul-16.HV.cont	0.0216	0.0365	0.5920	1.000
	Jul-16.LV.heat - Jul-16.HV.heat	-0.0312	0.0378	-0.8260	1.000
	Jul-16.LV.cont - Jul-16.HV.cont	0.0481	0.0378	1.2720	1.000
	Jul-16.MV.heat - Jul-16.LV.heat	0.0571	0.0326	1.7540	1.000
	Jul-16.MV.cont - Jul-16.LV.cont	-0.0265	0.0326	-0.8130	1.000
Jan-16 vs. Jul-16	Jul-16.HV.heat - Jan-16.HV.heat	0.1163	0.0409	2.8420	0.2954
	Jul-16.HV.cont - Jan-16.HV.cont	-0.0424	0.0409	-1.0370	1.000
	Jul-16.MV.heat - Jan-16.MV.heat	0.1679	0.0271	6.1970	**<0.0001**
	Jul-16.MV.cont - Jan-16.MV.cont	-0.0233	0.0271	-0.8600	1.000
	Jul-16.LV.heat - Jan-16.LV.heat	0.0582	0.0346	1.6800	1.000
	Jul-16.LV.cont - Jan-16.LV.cont	0.0225	0.0346	0.6490	1.000

ANOVA

Model: Ylossnorm ~ time*origin_dest*trt + Error(colony)

	Factor	Df	Sum Sq	Mean Sq	F value	Pr(>F)
Error: Between	time	1	0.0040	0.0040	0.5770	0.4650
	origin_dest	3	0.0035	0.0012	0.1660	0.9170
	Residuals	10	0.0700	0.0070		
Error: Within	**time**	1	0.0688	0.0688	17.9780	**< 0.0001**
	origin_dest	2	0.0062	0.0031	0.8070	0.4516
	trt	1	0.3484	0.3484	91.0520	**< 0.0001**
	time:origin_dest	3	0.0056	0.0019	0.4890	0.6911
	time:trt	1	0.0967	0.0967	25.2640	**< 0.0001**
	origin_dest:trt	4	0.0028	0.0007	0.1800	0.9479

	time:origin_dest:trt	3	0.0289	0.0096	2.5130	0.06810
	Residuals	54	0.2066	0.0038		

Tukey's Test

time*origin_dest*trt	Contrast	Estimate	Std. Error	z value	Pr(>|z|)
Jan-16 heat vs. control	Jan-16.HV_HV.heat - Jan-16.HV_HV.cont	0.0575	0.0437	1.3150	0.9979
	Jan-16.MV_HV.heat - Jan-16.MV_HV.cont	0.0336	0.0391	0.8590	1.0000
	Jan-16.LV_HV.heat - Jan-16.LV_HV.cont	0.1012	0.0391	2.5870	0.4589
	Jan-16.MV_MV.heat - Jan-16.MV_MV.cont	0.0250	0.0391	0.6390	1.0000
Jan-16 heat	Jan-16.MV_HV.heat - Jan-16.HV_HV.heat	-0.0432	0.0442	-0.9770	1.0000
	Jan-16.LV_HV.heat - Jan-16.HV_HV.heat	0.0266	0.0442	0.6010	1.0000
	Jan-16.MV_MV.heat - Jan-16.HV_HV.heat	-0.0088	0.0442	-0.1990	1.0000
	Jan-16.LV_HV.heat - Jan-16.MV_HV.heat	0.0698	0.0418	1.6710	0.9709
	Jan-16.MV_MV.heat - Jan-16.MV_HV.heat	0.0344	0.0391	0.8790	1.0000
	Jan-16.MV_MV.heat - Jan-16.LV_HV.heat	-0.0354	0.0418	-0.8470	1.0000
Jan-16 control	Jan-16.MV_HV.cont - Jan-16.HV_HV.cont	-0.0193	0.0442	-0.4360	1.0000
	Jan-16.LV_HV.cont - Jan-16.HV_HV.cont	-0.0171	0.0442	-0.3870	1.0000
	Jan-16.MV_MV.cont - Jan-16.HV_HV.cont	0.0237	0.0442	0.5360	1.0000
	Jan-16.LV_HV.cont - Jan-16.MV_HV.cont	0.0022	0.0418	0.0530	1.0000
	Jan-16.MV_MV.cont - Jan-16.MV_HV.cont	0.0430	0.0391	1.0990	0.9998
	Jan-16.MV_MV.cont - Jan-16.LV_HV.cont	0.0408	0.0418	0.9770	1.0000
Jul-16 heat vs. control	**Jul-16.HV_HV.heat - Jul-16.HV_HV.cont**	0.2162	0.0391	5.5270	**<0.0001**
	Jul-16.MV_HV.heat - Jul-16.MV_HV.cont	0.2178	0.0391	5.5670	**<0.0001**
	Jul-16.LV_HV.heat - Jul-16.LV_HV.cont	0.1090	0.0391	2.7860	0.3181
	Jul-16.MV_MV.heat - Jul-16.MV_MV.cont	0.2232	0.0391	5.7050	**<0.0001**
	Jul-16.LV_LV.heat - Jul-16.LV_LV.cont	0.1833	0.0505	3.6300	**0.03030**
Jul-16 heat	Jul-16.MV_HV.heat - Jul-16.HV_HV.heat	0.0212	0.0418	0.5080	1.0000
	Jul-16.LV_HV.heat - Jul-16.HV_HV.heat	-0.0396	0.0418	-0.9480	1.0000
	Jul-16.MV_MV.heat - Jul-16.HV_HV.heat	0.0306	0.0418	0.7330	1.0000
	Jul-16.LV_LV.heat - Jul-16.HV_HV.heat	-0.0183	0.0480	-0.3810	1.0000
	Jul-16.MV_MV.heat - Jul-16.MV_HV.heat	0.0094	0.0391	0.2400	1.0000
	Jul-16.LV_HV.heat - Jul-16.MV_HV.heat	-0.0608	0.0418	-1.4560	0.9931
	Jul-16.LV_LV.heat - Jul-16.MV_HV.heat	-0.0395	0.0480	-0.8230	1.0000
	Jul-16.MV_MV.heat - Jul-16.LV_HV.heat	0.0702	0.0418	1.6810	0.9691
	Jul-16.LV_LV.heat - Jul-16.MV_MV.heat	-0.0489	0.0480	-1.0190	0.9999
	Jul-16.LV_LV.heat - Jul-16.LV_HV.heat	0.0213	0.0457	0.4670	1.0000
Jul-16 control	Jul-16.MV_HV.cont - Jul-16.HV_HV.cont	0.0196	0.0418	0.4690	1.0000
	Jul-16.LV_HV.cont - Jul-16.HV_HV.cont	0.0676	0.0418	1.6180	0.9787
	Jul-16.MV_MV.cont - Jul-16.HV_HV.cont	0.0236	0.0418	0.5650	1.0000
	Jul-16.LV_LV.cont - Jul-16.HV_HV.cont	0.0146	0.0480	0.3040	1.0000
	Jul-16.MV_MV.cont - Jul-16.MV_HV.cont	0.0040	0.0391	0.1020	1.0000
	Jul-16.LV_HV.cont - Jul-16.MV_HV.cont	0.0480	0.0418	1.1490	0.9996
	Jul-16.LV_LV.cont - Jul-16.MV_HV.cont	-0.0050	0.0480	-0.1040	1.0000
	Jul-16.MV_MV.cont - Jul-16.LV_HV.cont	-0.0440	0.0418	-1.0530	0.9999
	Jul-16.LV_LV.cont - Jul-16.LV_HV.cont	-0.0530	0.0457	-1.1610	0.9996
	Jul-16.LV_LV.cont - Jul-16.MV_MV.cont	-0.0090	0.0480	-0.1880	1.0000

Jan-16 vs. Jul-16	Jul-16.HV_HV.heat - Jan-16.HV_HV.heat	0.1160	0.0417	2.7790	0.3211
	Jul-16.MV_HV.heat - Jan-16.MV_HV.heat	0.1804	0.0391	4.6110	**<0.0100**
	Jul-16.LV_HV.heat - Jan-16.LV_HV.heat	0.0498	0.0391	1.2730	0.9986
	Jul-16.MV_MV.heat - Jan-16.MV_MV.heat	0.1554	0.0391	3.9720	**< 0.0001**
	Jul-16.HV_HV.cont - Jan-16.HV_HV.cont	-0.0427	0.0417	-1.0230	0.9999
	Jul-16.MV_HV.cont - Jan-16.MV_HV.cont	-0.0038	0.0391	-0.0970	1.0000
	Jul-16.LV_HV.cont - Jan-16.LV_HV.cont	0.0420	0.0391	1.0740	0.9998
	Jul-16.MV_MV.cont - Jan-16.MV_MV.cont	-0.0428	0.0391	-1.0940	0.9998

Table A3 *Goniastrea retiformis* physiology

CHL

C. Total Chlorophyll Ratio (1-(control-heat)/control)

Shapiro-wilk

Model: chlratio ~ time+origin+dest	time	origin	dest	p-value
Jan-16	Jan-16	HV	HV	0.6371
	Jan-16	MV	HV	0.2933
	Jan-16	MV	MV	0.9573
	Jan-16	LV	HV	0.8825
Jul-16	Jul-16	HV	HV	0.3222
	Jul-16	MV	HV	0.5389
	Jul-16	MV	MV	0.5554
	Jul-16	LV	HV	0.1717
	Jul-16	LV	LV	0.5228

Bartlett HOV

Model: chlratio ~ time+origin_dest	time	K-squared	df	p-value
	Jan-16	1.5667	3	0.6670
	Jul-16	10.0580	4	**0.03947**

ANOVA

Model: chlrat ~ time*origin_dest + Error(colony)

	Factor	Df	Sum Sq	Mean Sq	F value	Pr(>F)
Error: Between	time	1	0.1651	0.1651	3.0590	0.1110
	origin_dest	3	0.2141	0.0714	1.3220	0.3210
	Residuals	10	0.5398	0.0540		
Error: Within	**time**	1	0.2094	0.2094	5.4710	**0.02980**
	origin_dest	2	0.0450	0.0225	0.5890	0.5645
	time:origin_dest	3	0.2539	0.0846	2.2120	0.1183
	Residuals	20	0.7654	0.0383		

Tukey's Test (Bonferroni corrected)

	Contrast	Estimate	Std. Error	z value	Pr(>|z|)
time	Jan-16 - Jul-16	0.11334	0.06758	1.6770	0.09350

Table A3 *Goniastrea retiformis* physiology

CHL

D. Total Chlorophyll (control and heat)

Shapiro-wilk

Model: totalchl ~ origin+time+dest	time	origin	dest	totalchl	p-value
Jan-16	Jan-16	HV	HV	cont	0.8659
	Jan-16	HV	HV	heat	0.8399
	Jan-16	MV	HV	cont	0.7286
	Jan-16	MV	MV	cont	0.6472
	Jan-16	MV	HV	heat	0.2830
	Jan-16	MV	MV	heat	0.1244
	Jan-16	LV	HV	cont	0.7202
	Jan-16	LV	HV	heat	0.5631
Jul-16	Jul-16	HV	HV	cont	0.5288
	Jul-16	HV	HV	heat	0.1293
	Jul-16	MV	HV	cont	0.4584
	Jul-16	MV	MV	cont	0.5670
	Jul-16	MV	HV	heat	0.8153
	Jul-16	MV	MV	heat	0.3280
	Jul-16	LV	HV	cont	0.2118
	Jul-16	LV	LV	cont	0.5669
	Jul-16	LV	HV	heat	0.9143
	Jul-16	LV	LV	heat	0.1170

Bartlett HOV

Model: totalchl~origin_dest+trt	time	K-squared	df	p-value
	Jan-16	3.2255	7	0.8634
	Jul-16	15.6320	9	0.07498

ANOVA

Model: totalchl ~ time*origin_dest*trt + Error(colony)

	Factor	Df	Sum Sq	Mean Sq	F value	Pr(>F)
Error: Between	time	1	6.8300	6.8300	2.6890	0.1320
	origin_dest	3	2.7390	0.9130	0.3590	0.7840
	Residuals	10	25.4010	2.5400		
Error: Within	**time**	1	29.7000	29.7000	16.4070	**0.0001710**
	origin_dest	2	0.6700	0.3400	0.1860	0.8309
	trt	1	146.0500	146.0500	80.6790	**<0.0001**
	time:origin	3	2.1300	0.7100	0.3930	0.7588
	time:trt	1	10.8100	10.8100	5.9730	**0.01796**
	origin_dest	4	5.2300	1.3100	0.7220	0.5806
	time:origin	3	4.0400	1.3500	0.7440	0.5309
	Residuals	52	94.1300	1.8100		

Tukey's Test (Bonferroni corrected)

	Contrast	Estimate	Std. Error	z value	Pr(>|z|)
time	**Jan-16 - Jul**	-0.9789	0.4369	-2.2410	**0.02510**

trt	**heat - cont**	-2.6691	0.3242	-8.2330	**<0.0001**
time*trt	**Jan-16.hea**	-1.8482	0.4277	-4.3210	**<0.0001**
	Jul-16.heat	-3.3116	0.3784	-8.7520	**<0.0001**
	Jan-16.con	-1.8360	0.4080	-4.5000	**<0.0001**
	Jan-16.heat	-0.3727	0.4080	-0.9130	1.000
time*origin_dest*trt					
Jan-16 heat vs. control	HV_HV.hea	-1.9210	0.8362	-2.2970	1.000
	MV_MV.he	-1.7070	0.8362	-2.0410	1.000
	MV_MV.he	-1.6453	1.0795	-1.5240	1.000
	LV_HV.heat	-2.0384	0.8362	-2.4380	1.000
Jan-16 heat	MV_HV.hea	0.4342	0.8682	0.5000	1.000
	LV_HV.heat	-0.0558	1.0008	-0.0560	1.000
	MV_MV.he	-0.0494	0.8682	-0.0570	1.000
	LV_HV.heat	0.4900	1.0008	0.4900	1.000
	MV_MV.he	-0.4836	0.8362	-0.5780	1.000
	MV_MV.he	0.0064	1.0008	0.0060	1.000
Jan-16 control	MV_HV.cor	0.2202	0.8682	0.2540	1.000
	LV_HV.cont	-0.3314	1.0008	-0.3310	1.000
	MV_MV.co	0.0680	0.8682	0.0780	1.000
	LV_HV.cont	0.5516	1.0008	0.5510	1.000
	MV_MV.co	-0.1522	0.8362	-0.1820	1.000
	MV_MV.co	0.3994	1.0008	0.3990	1.000
Jul-16 heat vs. control	HV_HV.hea	-2.7818	0.8362	-3.3270	0.1345
	MV_HV.hea	**-4.0754**	**0.8362**	**-4.8740**	**0.0001680**
	LV_HV.hea	**-4.4840**	**0.8362**	**-5.3620**	**<0.0001**
	MV_MV.he	-2.6672	0.8362	-3.1900	0.2179
	LV_LV.heat	-2.0417	1.0795	-1.8910	1.000
Jul-16 heat	MV_HV.hea	-0.6658	0.8682	-0.7670	1.000
	LV_HV.heat	-1.7750	0.8682	-2.0440	1.000
	MV_MV.he	0.4612	0.8682	0.5310	1.000
	LV_LV.heat	-1.1352	1.0008	-1.1340	1.000
	LV_HV.heat	1.1092	0.8682	1.2780	1.000
	MV_MV.he	1.1270	0.8362	1.3480	1.000
	LV_LV.heat	0.4694	1.0008	0.4690	1.000
	MV_MV.he	2.2362	0.8682	2.5760	1.000
	LV_LV.heat	0.6398	0.9731	0.6580	1.000
	LV_LV.heat	1.5964	1.0008	1.5950	1.000
Jul-16 control	MV_HV.cor	0.6278	0.8682	0.7230	1.000
	LV_HV.cont	-0.0728	0.8682	-0.0840	1.000
	MV_MV.co	0.3466	0.8682	0.3990	1.000
	LV_LV.cont	-1.8753	1.0008	-1.8740	1.000
	LV_HV.cont	0.7006	0.8682	0.8070	1.000
	MV_MV.co	-0.2812	0.8362	-0.3360	1.000
	LV_LV.cont	2.5031	1.0008	2.5010	1.000

	MV_MV.co	0.4194	0.8682	0.4830	1.000
	LV_LV.cont	-1.8025	0.9731	-1.8520	1.000
	LV_LV.cont	2.2219	1.0008	2.2200	1.000
Jan-16 vs. Jul-16	HV_HV.hea	0.9366	0.8362	1.1200	1.000
	MV_HV.hea	-0.1634	0.8362	-0.1950	1.000
	LV_HV.heat	-0.7826	0.9731	-0.8040	1.000
	MV_MV.he	1.4472	0.8362	1.7310	1.000
	HV_HV.con	1.7974	0.8362	2.1490	1.000
	MV_HV.cor	2.2050	0.8362	2.6370	1.000
	LV_HV.cont	2.0560	0.9731	2.1130	1.000
	MV_MV.co	2.0760	0.8362	2.4830	1.000

Table A4 Symbiodiniaceae genotyping

A. Symbiodiniaceae ITS-2 Amplicon Sequencing and DADA2 Summary

		N	Input	Filtered	Denoised	Merged
P. lobata		79	367307	289420	289420	2086
HV		25	111735	98299	98299	470
MV	HV	5	47020	32042	32042	319
	MV	23	80810	50210	50210	430
LV	HV	6	27959	22591	22591	160
	LV	20	99783	86278	86278	707
G. retiformis		58	121221	84153	84153	621
HV		19	71172	41050	41050	352
MV	HV	5	15526	13158	13158	55
	MV	14	33540	29263	29263	214
LV	HV	4	184	182	182	0
	LV	16	799	500	500	0

B. PERMANOVA of *Cladocopium* ITS types representing >1% in *P. lobata* samples

Model: scores ~ origin_dest * time, Euclidean method

	Df	SumsOfSqs	MeanSqs	F.Model	R2	Pr(>F)
origin_dest	4	1.5090	0.3773	0.5809	0.0237	0.7460
time	3	1.1790	0.3929	0.6049	0.0185	0.6690
origin_dest:t	8	3.8680	0.4835	0.7444	0.0607	0.6790
Residuals	88	57.1580	0.6495	0.8971		
Total	103	63.7140	1.0000			

C. PERMANOVA of *Cladocopium* ITS types representing >1% in *G. retiformis* colonies

Model: scores ~ origin_dest * time, Euclidean method

	Df	SumsOfSqs	MeanSqs	F.Model	R2	Pr(>F)
origin_dest	4	269.21	67.3020	1.5783	0.1732	0.1580
time	1	44.28	44.2810	1.0384	0.0285	0.3440
origin_dest:t	2	175.13	87.5630	2.0534	0.1126	0.0980
Residuals	25	1066.08	42.6430	0.6857		
Total	32	1554.69	1.0000			

D. Average ITS2 type proportion in samples

Species	Time	Site	Location	C15	C3	C40	A4a	C60	B2	C2	C21	C3k	Total
P. lobata	Jul-15	HV	side	33273	18	62	0	0	0	0	0	0	33353
			top	21896	10	0	0	0	0	0	0	0	21906
		MV	side	20240	32	0	0	0	0	0	0	0	20272
			top	15069	0	264	0	0	102	0	0	0	15435
		LV	side	22260	11	79	14	0	0	65	0	0	22429
			top	30751	0	0	0	0	0	0	0	0	30751
	Average Relative Proportion			0.994	0.001	0.004	0.000	0.000	0.001	0.000	0.000	0.000	
	Jan-16	HV	HV	39877	60	0	0	0	0	0	0	0	39937
		MV	HV	31121	15	110	0	16	0	0	0	0	31262
			MV	13125	26	0	0	0	0	51	0	0	13202
		LV	HV	22203	6	0	0	0	0	0	0	0	22209
			LV	30951	58	0	0	0	0	0	0	0	31009
	Average Relative Proportion			0.997	0.001	0.001	0.000	0.000	0.000	0.001	0.000	0.000	
	Jul-16	HV	HV	90	0	0	0	0	0	0	0	0	90
		MV	MV	230	0	0	0	0	0	0	0	0	230
		LV	LV	114	0	0	0	0	0	0	0	0	114
	Average Relative Proportion			1.000	0.000	0.000	0.000	0.000	0.000	0.000	0.000	0.000	
G. retiformis	Jul-15	HV	side	139	351	1860	0	0	0	0	32	0	2382
			top	43	1368	11582	0	0	0	0	31	0	13024
		MV	side	0	607	4942	0	0	0	0	57	0	5606
			top	43	0	180	0	0	0	0	0	0	223
		LV	side	0	0	73	0	0	0	0	0	0	73
			top	14	0	64	0	0	0	0	0	0	78
	Average Relative Proportion			0.072	0.060	0.863	0.000	0.000	0.000	0.000	0.004	0.000	
	Jan-16	HV	HV	640	2722	21297	0	0	0	0	219	0	24878
		MV	HV	9208	480	3215	0	0	0	0	45	0	12948
			MV	14439	828	7697	0	0	0	0	59	0	23023
		LV	HV	0	0	63	0	0	0	0	0	0	63
			LV	0	0	123	0	0	0	0	0	13	136
	Average Relative Proportion			0.27	0.036	0.669	0.000	0.000	0.000	0.000	0.003	0.019	

Table A4 Symbiodiniaceae genotyping

E. Adjusted p-values between Multiple Comparisons of *Cladocopium* ITS type C40 in *P. lobata* colonies

	HV_HV:Jul-15	HV_HV:Jan-16	HV_HV:Jul-16	LV_LV:Jul-15	LV_LV:Jan-16	LV_LV:Jul-16	LV_HV:Jul-15	LV_HV:Jan-16	LV_HV:Jul-16	MV_HV:Jul-15	MV_HV:Jan-16
HV_HV:Jul-15	NA	-33.053	-38.690	-67.691	93.763	-112.305	56.592	-29.818	-1607.520	609.216	131.867
HV_HV:Jan-16	1.000	NA	-5.637	-34.638	126.816	-79.251	89.645	3.235	-1574.466	642.269	164.920
HV_HV:Jul-16	1.000	1.000	NA	-29.001	132.453	-73.615	95.282	8.872	-1568.830	647.906	170.557
LV_LV:Jul-15	1.000	1.000	1.000	NA	161.454	-44.614	124.283	37.873	-1539.828	676.907	199.558
LV_LV:Jan-16	1.000	1.000	1.000	1.000	NA	-206.067	-37.171	-123.581	-1701.282	515.454	38.104
LV_LV:Jul-16	1.000	1.000	1.000	1.000	0.2214	NA	168.897	82.486	-1495.215	721.521	244.172
LV_HV:Jul-15	1.000	1.000	1.000	1.000	1.000	1.000	NA	-86.410	-1664.112	552.624	75.275
LV_HV:Jan-16	1.000	1.000	1.000	1.000	0.8879	1.000	1.000	NA	-1577.701	639.035	161.685
LV_HV:Jul-16	1.000	1.000	1.000	1.000	1.000	1.000	1.000	1.000	NA	2216.736	1739.386
MV_HV:Jul-15	1.000	1.000	1.000	1.000	1.000	1.000	1.000	1.000	1.000	NA	-477.349
MV_HV:Jan-16	1.000	1.000	0.2455	1.000	1.000	0.1604	1.000	0.1604	1.000	1.000	NA
MV_HV:Jul-16	1.000	1.000	1.000	1.000	1.000	1.000	1.000	1.000	1.000	1.000	1.000
MV_MV:Jul-15	1.000	1.000	1.000	1.000	1.000	0.8199	1.000	1.000	1.000	1.000	1.000
MV_MV:Jan-16	1.000	1.000	1.000	1.000	0.1604	1.000	1.000	1.000	1.000	1.000	**0.003706**
MV_MV:Jul-16	1.000	1.000	1.000	1.000	1.000	1.000	1.000	1.000	1.000	1.000	1.000

F. Adjusted p-values between Multiple Comparisons of *Cladocopium* ITS types in G. *retiformis* colonies

	HV_HV:Jul-15	HV_HV:Jan-16	LV_HV:Jul-15	LV_HV:Jan-16	LV_LV:Jul-15	LV_LV:Jan-16	MV_HV:Jul-15	MV_HV:Jan-16	MV_MV:Jul-15	MV_MV:Jan-16
C1										
HV_HV:Jul-15	NA	24.1244	-1168.9859	-7.5019	-75.1456	-60.2601	-423.0424	24.6817	-113.0263	-5.8451
HV_HV:Jan-16	0.5466	NA	-1193.1103	-31.6263	-99.2700	-84.3845	-447.1668	0.5572	-137.1507	-29.9695
LV_HV:Jul-15	0.9997	0.9997	NA	1161.4840	1093.8403	1108.7257	745.9434	1193.6680	1055.9596	1163.1408
LV_HV:Jan-16	0.9997	0.4883	0.9997	NA	-67.6437	-52.7583	-415.5405	32.1835	-105.5244	1.6568
LV_LV:Jul-15	0.7368	0.6106	0.9997	0.8874	NA	14.8854	-347.8968	99.8272	-37.8807	69.3005
LV_LV:Jan-16	0.7132	0.3554	0.9997	0.7132	0.9997	NA	-362.7823	84.9418	-52.7661	54.4151
MV_HV:Jul-15	0.9997	0.9997	0.9997	0.9997	0.9997	0.9997	NA	447.7241	310.0161	417.1974
MV_HV:Jan-16	0.5320	0.9997	0.9997	0.4820	0.6106	0.3523	0.9997	NA	-137.7079	-30.5267
MV_MV:Jul-15	0.1105	**0.001400**	0.9997	0.1208	0.9997	0.6106	0.9997	**0.001437**	NA	107.1812
MV_MV:Jan-16	0.9997	0.3655	0.9997	0.9997	0.8874	0.7323	0.9997	0.3655	0.05363	NA
C15										

HV_HV:Jul-15	NA	0.7538	744.6356	-49.2301	1.6292	-46.5213	828.5051	2.1524	-218.4267	3.0256
HV_HV:Jan-16	0.9997	NA	743.8818	-49.9839	0.8754	-47.2751	827.7513	1.3987	-219.1805	2.2718
LV_HV:Jul-15	0.9997	0.9997	NA	-793.8658	-743.0064	-791.1569	83.8694	-742.4832	-963.0623	-741.6101
LV_HV:Jan-16	0.5064	0.5064	0.9997	NA	50.8593	2.7088	877.7352	51.3826	-169.1966	52.2557
LV_LV:Jul-15	0.9997	0.9997	0.9997	0.4993	NA	-48.1505	826.8758	0.5232	-220.0559	1.3963
LV_LV:Jan-16	0.3655	0.3655	0.9997	0.9997	0.3647	NA	875.0263	48.6737	-171.9054	49.5468
MV_HV:Jul-15	0.9997	0.9997	0.9997	0.9997	0.9997	0.9997	NA	-826.3526	-1046.9320	-825.4795
MV_HV:Jan-16	0.9997	0.9997	0.9997	0.4904	0.9997	0.3554	0.9997	NA	-220.5791	0.8731
MV_MV:Jul-15	**0.001437**	**0.001437**	0.9997	0.1110	**0.001437**	0.1082	0.9997	**0.001437**	NA	221.4522
MV_MV:Jan-16	0.7323	0.8874	0.9997	0.4866	0.9997	0.3523	0.9997	0.9997	**0.001437**	NA
					C15b					
HV_HV:Jul-15	NA	-46.6837	-1652.3083	9.5933	-49.4357	-69.9185	1166.9340	35.5739	-29.5635	35.0848
HV_HV:Jan-16	0.5064	NA	-1605.6246	56.2770	-2.7521	-23.2348	1213.6177	82.2575	17.1202	81.7685
LV_HV:Jul-15	0.9997	0.9997	NA	1661.9016	1602.8725	1582.3898	2819.2423	1687.8821	1622.7448	1687.3931
LV_HV:Jan-16	0.9997	0.7568	0.9997	NA	-59.0290	-79.5118	1157.3407	25.9806	-39.1568	25.4915
LV_LV:Jul-15	0.4255	0.9997	0.9997	0.6228	NA	-20.4827	1216.3697	85.0096	19.8723	84.5205
LV_LV:Jan-16	0.3655	0.9997	0.9997	0.4896	0.9997	NA	1236.8525	105.4924	40.3550	105.0033
MV_HV:Jul-15	0.9997	0.9997	0.9997	0.9997	0.9997	0.9997	NA	-1131.3601	-1196.4975	-1131.8492
MV_HV:Jan-16	0.3655	0.3655	0.9997	0.6106	0.3254	0.1082	0.9997	NA	-65.1373	-0.4891
MV_MV:Jul-15	0.9997	0.9997	0.9997	0.5064	0.9997	0.9997	0.9997	0.1491	NA	64.6483
MV_MV:Jan-16	0.3655	0.3655	0.9997	0.6106	0.3274	0.1082	0.9997	0.9997	0.1534	NA
					C21					
HV_HV:Jul-15	NA	1.5364	137.5845	-70.9126	-47.0547	-34.3445	-117.3467	-0.5148	0.3103	-0.3785
HV_HV:Jan-16	0.7220	NA	136.0481	-72.4490	-48.5911	-35.8809	-118.8831	-2.0512	-1.2261	-1.9149
LV_HV:Jul-15	0.9997	0.9997	NA	-208.4972	-184.6393	-171.9291	-254.9312	-138.0993	-137.2743	-137.9631
LV_HV:Jan-16	0.3655	0.3655	0.9997	NA	23.8579	36.5681	-46.4340	70.3979	71.2229	70.5341
LV_LV:Jul-15	0.3655	0.3655	0.9997	0.9997	NA	12.7102	-70.2920	46.5400	47.3650	46.6762
LV_LV:Jan-16	0.3720	0.3655	0.9997	0.9754	0.9997	NA	-83.0022	33.8298	34.6548	33.9660
MV_HV:Jul-15	0.9997	0.9997	0.9997	0.9997	0.9997	0.9997	NA	116.8319	117.6569	116.9682
MV_HV:Jan-16	0.9997	0.5064	0.9997	0.3655	0.3655	0.3746	0.9997	NA	0.8250	0.1362
MV_MV:Jul-15	0.9997	0.9004	0.9997	0.3655	0.3655	0.3655	0.9997	0.9997	NA	-0.6888
MV_MV:Jan-16	0.9997	0.4330	0.9997	0.3655	0.3655	0.3746	0.9997	0.9997	0.9997	NA
					C3					
HV_HV:Jul-15	NA	1.6633	1299.7742	-38.5247	-140.0756	-22.8138	568.0491	-2.1865	-1.3394	-1.4546
HV_HV:Jan-16	0.9004	NA	1298.1109	-40.1881	-141.7389	-24.4771	566.3857	-3.8499	-3.0027	-3.1180

LV_HV:Jul-15	0.9997	0.9997	NA	-1338.2990	-1439.8500	-1322.5880	-731.7252	-1301.9608	-1301.1136	-1301.2289
LV_HV:Jan-16	0.6087	0.5606	0.9997	NA	-101.5509	15.7110	606.5738	36.3382	37.1854	37.0701
LV_LV:Jul-15	**0.006248**	**0.006248**	0.9997	0.3655	NA	117.2619	708.1247	137.8891	138.7362	138.6210
LV_LV:Jan-16	0.5064	0.4778	0.9997	0.9997	0.0965	NA	590.8628	20.6272	21.4744	21.3591
MV_HV:Jul-15	0.9997	0.9997	0.9997	0.9997	0.9997	0.9997	NA	-570.2356	-569.3884	-569.5037
MV_HV:Jan-16	0.7587	0.3655	0.9997	0.6251	**0.006468**	0.5821	0.9997	NA	0.8472	0.7319
MV_MV:Jul-15	0.9997	0.5466	0.9997	0.6106	**0.006248**	0.5466	0.9997	0.9997	NA	-0.1153
MV_MV:Jan-16	0.9997	0.4247	0.9997	0.6106	**0.006248**	0.5466	0.9997	0.9997	0.9997	NA
C40										
HV_HV:Jul-15	NA	-0.0485	-793.5264	**0.0216**	-0.7061	**0.0273**	217.2640	-1.7745	**0.0278**	-2.7056
HV_HV:Jan-16	0.9997	NA	-793.4779	0.0701	-0.6576	0.0758	217.3125	-1.7260	0.0762	-2.6572
LV_HV:Jul-15	0.9997	0.9997	NA	793.5480	792.8203	793.5537	1010.7904	791.7519	793.5542	790.8208
LV_HV:Jan-16	0.9997	0.9997	0.9997	NA	-0.7277	**0.0057**	217.2424	-1.7961	**0.0062**	-2.7272
LV_LV:Jul-15	0.9997	0.9997	0.9997	0.9997	NA	0.7334	217.9701	-1.0684	0.7339	-1.9995
LV_LV:Jan-16	0.9997	0.9997	0.9997	0.9997	0.9997	NA	217.2367	-1.8018	**0.0005**	-2.7330
MV_HV:Jul-15	0.9997	0.9997	0.9997	0.9997	0.9997	0.9997	NA	-219.0385	-217.2363	-219.9697
MV_HV:Jan-16	0.3655	0.3746	0.9997	0.5466	0.8874	0.4255	0.9997	NA	1.8023	-0.9311
MV_MV:Jul-15	0.9997	0.9997	0.9997	0.9997	0.9997	0.9997	0.9997	0.3655	NA	-2.7334
MV_MV:Jan-16	0.1311	0.1308	0.9997	0.3554	0.4159	0.2170	0.9997	0.8874	0.1082	NA

Table A5 Ofu Pool Temperature Summary

A. Max Daily Temperatures

ANOVA

Model:max~site*season	Factor	Df	Sum Sq	Mean Sq	F value	Pr(>F)
	site	2	10.88	5.44	6.4574	**1.65E-03**
	season	1	630.28	630.28	748.3302	**< 2.2e-16**
	site:season	2	10.38	5.19	6.1597	**0.002207**
	Residuals	861	725.18	0.84		

Tukey's Test

	Contrast	Estimate	SE	Df	t-ratio	p-value
emmeans of site	HV - MV	0.0078	0.0763	861	0.102	1
	HV - LV	0.2414	0.0763	861	3.162	**0.0049**
	MV - LV	0.2336	0.0763	861	3.06	**0.0068**
lsmeans of season	**Summer-Winter**	1.57413	0.0589593	861	26.699	**<.0001**
lsmeans of site:season	HV_Summer-MV_Summer	0.0728	0.1261	861	0.578	1
	HV_Summer-LV_Summer	0.5736	0.1261	861	4.55	**<.0001**
	MV_Summer-LV_Summer	0.5008	0.1261	861	3.973	**0.0005**
	HV_Winter-MV_Winter	-0.0298	0.0959	861	-0.311	1
	HV_Winter-LV_Winter	0.049	0.0959	861	0.511	1
	MV_Winter-LV_Winter	0.0789	0.0959	861	0.822	1
	HV_Summer-HV_Winter	1.98	0.112	861	17.66	**<.0001**
	MV_Summer-MV_Winter	1.88	0.112	861	16.744	**<.0001**
	LV_Summer-LV_Winter	1.45	0.112	861	12.977	**<.0001**

B. Min Daily Temperatures

ANOVA

Model: min ~ site*season	Factor	Df	Sum Sq	Mean Sq	F value	Pr(>F)
	site	2	17.714	8.857	24.9246	**3.00E-11**
	season	1	251.998	251.998	709.1545	**< 2e-16**
	site:season	2	3.236	1.618	4.5531	**0.01079**
	Residuals	861	305.957	0.355		

	Contrast	Estimate	SE	Df	t-ratio	p-value
lsmeans of site	HV - MV	-0.00666	0.0496	861	-0.134	1
	HV - LV	-0.30649	0.0496	861	-6.181	**<.0001**
	MV - LV	-0.29983	0.0496	861	-6.046	**<.0001**
lsmeans of season	**Summer-Winter**	0.955116	0.0374408	861	25.51	**<.0001**
lsmeans of site:season	HV_Summer-MV_Summer	-0.1796	0.0819	861	-2.194	0.1711
	HV_Summer-LV_Summer	-0.4739	0.0819	861	-5.788	**<.0001**
	MV_Summer-LV_Summer	-0.2943	0.0819	861	-3.594	**0.0021**
	HV_Winter-MV_Winter	0.0935	0.0623	861	1.501	0.8025
	HV_Winter-LV_Winter	-0.2095	0.0623	861	-3.362	**0.0049**
	MV_Winter-LV_Winter	-0.303	0.0623	861	-4.863	**<.0001**
	HV_Summer-HV_Winter	0.939	0.0728	861	12.912	**<.0001**
	MV_Summer-MV_Winter	1.213	0.0728	861	16.666	**<.0001**
	LV_Summer-LV_Winter	1.204	0.0728	861	16.546	**<.0001**

C. Mean Daily Temperatures

ANOVA

Model: mean ~ site*season	Factor	Df	Sum Sq	Mean Sq	F value	Pr(>F)

	site	2	0.39	0.2	0.6228	5.37E-01
	season	1	366.97	366.97	1165.3522	**<2e-16**
	site:season	2	0.4	0.2	0.6396	0.5278
	Residuals	861	271.13	0.31		

	Contrast	Estimate	SE	Df	t-ratio	p-value
lsmeans of season	**Summer - Winter**	1.151777	0.0348301	861	33.068	**<.0001**
lsmeans of site:season	HV_Summer-MV_Summer	-0.0784	0.0771	861	-1.017	1
	HV_Summer-LV_Summer	-0.0477	0.0771	861	-0.619	1
	MV_Summer-LV_Summer	0.0307	0.0771	861	0.398	1
	HV_Winter-MV_Winter	0.0131	0.0587	861	0.224	1
	HV_Winter-LV_Winter	-0.054	0.0587	861	-0.921	1
	MV_Winter-LV_Winter	-0.0672	0.0587	861	-1.145	1
	HV_Summer-HV_Winter	1.32	0.0685	861	19.294	**<.0001**
	MV_Summer-MV_Winter	1.41	0.0685	861	20.631	**<.0001**
	LV_Summer-LV_Winter	1.32	0.0685	861	19.202	**<.0001**

D. Daily Temperature Range

ANOVA

Model: dtr ~ site*season	Factor	Df	Sum Sq	Mean Sq	F value	Pr(>F)
	site	2	56.35	28.176	40.772	**< 2.2e-16**
	season	1	85.21	85.21	123.303	**< 2.2e-16**
	site:season	2	20.91	10.455	15.129	**3.49E-07**
	Residuals	861	595.01	0.691		

	Contrast	Estimate	SE	Df	t-ratio	p-value
lsmeans of site	HV - MV	0.0145	0.0692	861	0.209	1
	HV - LV	0.5479	0.0692	861	7.923	**<.0001**
	MV - LV	0.5334	0.0692	861	7.714	**<.0001**
lsmeans of season	**Summer-Winter**	0.6190139	0.0572482	861	10.813	**<.0001**
lsmeans of site:season	HV_Summer-MV_Summer	0.252	0.1142	861	2.211	0.1639
	HV_Summer-LV_Summer	1.048	0.1142	861	9.174	**<.0001**
	MV_Summer-LV_Summer	0.795	0.1142	861	6.963	**<.0001**
	HV_Winter-MV_Winter	-0.123	0.0869	861	-1.42	0.9362
	HV_Winter-LV_Winter	0.259	0.0869	861	2.974	**0.0181**
	MV_Winter-LV_Winter	0.382	0.0869	861	4.394	**0.0001**
	HV_Summer-HV_Winter	1.039	0.101	861	10.238	**<.0001**
	MV_Summer-MV_Winter	0.663	0.101	861	6.534	**<.0001**
	LV_Summer-LV_Winter	0.25	0.101	861	2.462	**0.0421**

Table A6 Ofu Pool Specific and NOAA CRW 5km DHW Summary

A. *in situ* derived pool-specific DHWs

ANOVA

Model:inDHW~site*year	Factor	Df	Sum Sq	Mean Sq	F value	Pr(>F)
	Site	2	4.443	2.2214	161.706	**< 2.2e-16**
	year	17	170.232	10.0136	728.937	**< 2.2e-16**
	Site:year	34	23.879	0.7023	51.126	**< 2.2e-16**
	Residuals	16243	223.135	0.0137		

Tukey's Test

year	contrast	estimate	SE	df	t-ratio	p-value
2000	HV - LV	0	0.02392	16243	0	1
	HV - MV	0	0.02392	16243	0	1
	LV - MV	0	0.02392	16243	0	1
2001	**HV - LV**	0.06393	0.00868	16243	7.368	**<.0001**
	HV - MV	0.06393	0.00868	16243	7.368	**<.0001**
	LV - MV	0	0.00868	16243	0	1
2002	**HV - LV**	0.05936	0.00869	16243	6.833	**<.0001**
	HV - MV	0.0981	0.00869	16243	11.292	**<.0001**
	LV - MV	0.03873	0.00869	16243	4.458	**0.0004**
2003	**HV - LV**	0.39054	0.01215	16243	32.133	**<.0001**
	HV - MV	0.41964	0.01215	16243	34.527	**<.0001**
	LV - MV	0.0291	0.01215	16243	2.394	0.9004
2004	HV - LV	0	0.00907	16243	0	1
	HV - MV	0	0.00907	16243	0	1
	LV - MV	0	0.00907	16243	0	1
2005	**HV - LV**	0.08393	0.00868	16243	9.674	**<.0001**
	HV - MV	0.08208	0.00868	16243	9.46	**<.0001**
	LV - MV	-0.00185	0.00868	16243	-0.213	1
2006	**HV - LV**	0.03267	0.00868	16243	3.766	**0.009**
	HV - MV	0.03267	0.00868	16243	3.766	**0.009**
	LV - MV	0	0.00868	16243	0	1
2007	**HV - LV**	0.03512	0.00868	16243	4.048	**0.0028**
	HV - MV	0.03512	0.00868	16243	4.045	**0.0028**
	LV - MV	0	0.00868	16243	0	1
2008	HV - LV	0	0.00866	16243	0	1
	HV - MV	0	0.00866	16243	0	1
	LV - MV	0	0.00866	16243	0	1
2009	HV - LV	0	0.00868	16243	0	1
	HV - MV	0	0.00868	16243	0	1
	LV - MV	0	0.00868	16243	0	1
2010	HV - LV	0	0.00868	16243	0	1
	HV - MV	0	0.00884	16243	0	1
	LV - MV	0	0.00884	16243	0	1
2011	HV - LV	0	0.00957	16243	0	1
	HV - MV	0	0.00875	16243	0	1
	LV - MV	0	0.00957	16243	0	1
2012	HV - LV	0	0.00985	16243	0	1
	HV - MV	0	0.00866	16243	0	1
	LV - MV	0	0.00985	16243	0	1
2013	HV - LV	0	0.00868	16243	0	1

	HV - MV	0	0.00868	16243	0	1
	LV - MV	0	0.00868	16243	0	1
2014	HV - LV	0	0.01062	16243	0	1
	HV - MV	0	0.01062	16243	0	1
	LV - MV	0	0.01225	16243	0	1
2015	**HV - LV**	0.062	0.00889	16243	6.975	**<.0001**
	HV - MV	-0.07536	0.01062	16243	-7.099	**<.0001**
	LV - MV	-0.13737	0.01079	16243	-12.73	**<.0001**
2016	HV - LV	0	0.00866	16243	0	1
	HV - MV	0	0.00866	16243	0	1
	LV - MV	0	0.00866	16243	0	1
2017	**HV - LV**	0.18238	0.02654	16243	6.871	**<.0001**
	HV - MV	0.12823	0.02654	16243	4.831	**0.0001**
	LV - MV	-0.05415	0.02654	16243	-2.04	1

Table A6 Ofu Pool Specific and NOAA CRW 5km DHW Summary

B. NOAA CRW MMM 28.9°C derived DHWs

ANOVA

Model:inDHW~site*year	Factor	Df	Sum Sq	Mean Sq	F value	Pr(>F)
	Site	3	827	275.63	157.21	**< 2.2e-16**
	year	17	23558	1385.74	790.39	**< 2.2e-16**
	Site:year	51	9275	181.86	103.73	**< 2.2e-16**
	Residuals	22155	38843	1.75		

Tukey's Test

year	contrast	estimate	SE	df	t-ratio	p-value
2000	HV - LV	0	0.2703	22155	0	1.000
	HV - MV	0	0.2703	22155	0	1.000
	HV - Ofu 5km	-0.00375	0.2703	22155	-0.014	1.000
	LV - MV	0	0.2703	22155	0	1.000
	LV - Ofu 5km	-0.00375	0.2703	22155	-0.014	1.000
	MV - Ofu 5km	-0.00375	0.2703	22155	-0.014	1.000
2001	**HV - LV**	1.09645	0.098	22155	11.187	**<.0001**
	HV - MV	1.00551	0.098	22155	10.259	**<.0001**
	HV - Ofu 5km	0.87552	0.098	22155	8.933	**<.0001**
	LV - MV	-0.09094	0.098	22155	-0.928	1.000
	LV - Ofu 5km	-0.22093	0.098	22155	-2.254	1.000
	MV - Ofu 5km	-0.12999	0.098	22155	-1.326	1.000
2002	HV - LV	-0.17817	0.0981	22155	-1.815	1.000
	HV - MV	1.29566	0.0981	22155	13.201	**<.0001**
	HV - Ofu 5km	2.11505	0.0981	22155	21.549	**<.0001**
	LV - MV	1.47383	0.0981	22155	15.016	**<.0001**
	LV - Ofu 5km	2.29322	0.0981	22155	23.365	**<.0001**
	MV - Ofu 5km	0.81939	0.0981	22155	8.348	**<.0001**
2003	**HV - LV**	-2.1627	0.1373	22155	-15.751	**<.0001**
	HV - MV	1.1594	0.1373	22155	8.444	**<.0001**
	HV - Ofu 5km	5.07032	0.1193	22155	42.505	**<.0001**
	LV - MV	3.3221	0.1373	22155	24.196	**<.0001**
	LV - Ofu 5km	7.23303	0.1193	22155	60.636	**<.0001**
	MV - Ofu 5km	3.91092	0.1193	22155	32.786	**<.0001**
2004	HV - LV	-0.26275	0.1025	22155	-2.564	1.000
	HV - MV	-0.04466	0.1025	22155	-0.436	1.000
	HV - Ofu 5km	0.19622	0.1002	22155	1.958	1.000
	LV - MV	0.21809	0.1025	22155	2.128	1.000
	LV - Ofu 5km	0.45897	0.1002	22155	4.581	**0.001**
	MV - Ofu 5km	0.24088	0.1002	22155	2.404	1.000
2005	**HV - LV**	0.34381	0.098	22155	3.508	**0.049**
	HV - MV	0.36175	0.098	22155	3.691	**0.024**
	HV - Ofu 5km	1.55513	0.098	22155	15.866	**<.0001**
	LV - MV	0.01794	0.098	22155	0.183	1.000
	LV - Ofu 5km	1.21131	0.098	22155	12.359	**<.0001**
	MV - Ofu 5km	1.19338	0.098	22155	12.176	**<.0001**
2006	**HV - LV**	0.45125	0.098	22155	4.604	**0.001**
	HV - MV	0.46837	0.098	22155	4.779	**0.000**
	HV - Ofu 5km	0.64407	0.098	22155	6.571	**<.0001**
	LV - MV	0.01712	0.098	22155	0.175	1.000

	LV - Ofu 5km	0.19282	0.098	22155	1.967	1.000
	MV - Ofu 5km	0.1757	0.098	22155	1.793	1.000
2007	**HV - LV**	0.48169	0.098	22155	4.915	**0.000**
	HV - MV	0.02948	0.0981	22155	0.301	1.000
	HV - Ofu 5km	0.75211	0.098	22155	7.674	**<.0001**
	LV - MV	-0.45222	0.0981	22155	-4.611	**0.000**
	LV - Ofu 5km	0.27042	0.098	22155	2.759	0.627
	MV - Ofu 5km	0.72263	0.0981	22155	7.368	**<.0001**
2008	HV - LV	0	0.0979	22155	0	1.000
	HV - MV	0	0.0979	22155	0	1.000
	HV - Ofu 5km	0	0.0979	22155	0	1.000
	LV - MV	0	0.0979	22155	0	1.000
	LV - Ofu 5km	0	0.0979	22155	0	1.000
	MV - Ofu 5km	0	0.0979	22155	0	1.000
2009	HV - LV	0.12335	0.098	22155	1.258	1.000
	HV - MV	0.12184	0.098	22155	1.243	1.000
	HV - Ofu 5km	0.28386	0.098	22155	2.896	0.409
	LV - MV	-0.00151	0.098	22155	-0.015	1.000
	LV - Ofu 5km	0.16051	0.098	22155	1.638	1.000
	MV - Ofu 5km	0.16202	0.098	22155	1.653	1.000
2010	HV - LV	2.27E-01	9.80E-02	2.22E+04	2.31E+00	1.000
	HV - MV	-0.07532	0.0999	22155	-0.754	1.000
	HV - Ofu 5km	2.30E-01	9.80E-02	2.22E+04	2.34E+00	1.000
	LV - MV	-0.30208	0.0999	22155	-3.025	0.269
	LV - Ofu 5km	0.00286	0.098	22155	0.029	1.000
	MV - Ofu 5km	0.30494	0.0999	22155	3.053	0.245
2011	HV - LV	0	0.1081	22155	0	1.000
	HV - MV	0	0.0988	22155	0	1.000
	HV - Ofu 5km	0	0.0984	22155	0	1.000
	LV - MV	0	0.1081	22155	0	1.000
	LV - Ofu 5km	0	0.1077	22155	0	1.000
	MV - Ofu 5km	0	0.0984	22155	0	1.000
2012	HV - LV	0.03123	0.1113	22155	0.281	1.000
	HV - MV	0.01571	0.0979	22155	0.16	1.000
	HV - Ofu 5km	0.01822	0.0979	22155	0.186	1.000
	LV - MV	-0.01552	0.1113	22155	-0.14	1.000
	LV - Ofu 5km	-0.013	0.1113	22155	-0.117	1.000
	MV - Ofu 5km	0.00252	0.0979	22155	0.026	1.000
2013	HV - LV	0.04258	0.098	22155	0.434	1.000
	HV - MV	0.05757	0.098	22155	0.587	1.000
	HV - Ofu 5km	-0.18702	0.098	22155	-1.908	1.000
	LV - MV	0.01499	0.098	22155	0.153	1.000
	LV - Ofu 5km	-0.2296	0.098	22155	-2.343	1.000
	MV - Ofu 5km	-0.24459	0.098	22155	-2.495	1.000
2014	HV - LV	0.32727	0.1199	22155	2.729	0.687
	HV - MV	0.25849	0.1199	22155	2.155	1.000
	HV - Ofu 5km	-0.17212	0.098	22155	-1.756	1.000
	LV - MV	-0.06878	0.1384	22155	-0.497	1.000
	LV - Ofu 5km	-0.4994	0.1199	22155	-4.164	**0.003**
	MV - Ofu 5km	-0.43062	0.1199	22155	-3.59	**0.036**
2015	HV - LV	-0.28913	0.1004	22155	-2.879	0.431

	HV - MV	-1.8419	0.1199	22155	-15.358	**<.0001**
	HV - Ofu 5km	-0.9712	0.098	22155	-9.909	**<.0001**
	LV - MV	-1.55277	0.1219	22155	-12.737	**<.0001**
	LV - Ofu 5km	-0.68207	0.1004	22155	-6.792	**<.0001**
	MV - Ofu 5km	0.87069	0.1199	22155	7.26	**<.0001**
2016	HV - LV	-0.04131	0.0979	22155	-0.422	1.000
	HV - MV	-0.06436	0.0979	22155	-0.658	1.000
	HV - Ofu 5km	-0.2585	0.0979	22155	-2.641	0.894
	LV - MV	-0.02305	0.0979	22155	-0.236	1.000
	LV - Ofu 5km	-0.21719	0.0979	22155	-2.219	1.000
	MV - Ofu 5km	-0.19413	0.0979	22155	-1.983	1.000
2017	HV - LV	0.4018	0.2998	22155	1.34	1.000
	HV - MV	0.05475	0.2998	22155	0.183	1.000
	HV - Ofu 5km	0.12534	0.2998	22155	0.418	1.000
	LV - MV	-0.34705	0.2998	22155	-1.157	1.000
	LV - Ofu 5km	-0.27645	0.2998	22155	-0.922	1.000
	MV - Ofu 5km	0.07059	0.2998	22155	0.235	1.000

Table A7 *Porites lobata* physiology

GROWTH

A. Growth over Time (final-initial / weeks)

Shapiro-wilk

Model: resid(grate ~ origin* dest * time + (1|colony))

W = 0.90413 p-value = 2.595e-09

ANOVA

Model: lmer(grate ~ origin_dest * time + (1|colony)

	Sum Sq	Mean Sq	NumDF	DenDF	F value	Pr(>F)
origin_dest	0.0474	0.00948	5	60.356	2.0781	0.08049
time	0.67399	0.33699	2	132.546	73.8695	**< 2e-16**
origin_dest:time	0.05473	0.00547	10	132.514	1.1997	0.297

Tukey's Test

	contrast	estimate	SE	df	t.ratio	p.value
origin_dest	HV_HV - MV_HV	0.0094	0.0257	45.1	0.366	1
	HV_HV - LV_HV	0.03369	0.0256	44.4	1.317	1
	HV_HV - MV_MV	0.05088	0.0257	45.2	1.979	0.8087
	HV_HV - HV_MV	-0.01658	0.0174	132	-0.951	1
	HV_HV - LV_LV	0.0301	0.0257	45.2	1.171	1
	MV_HV - LV_HV	0.0243	0.0257	45.1	0.945	1
	MV_HV - MV_MV	0.04148	0.0178	132.6	2.33	0.3195
	MV_HV - HV_MV	-0.02598	0.0257	45.1	-1.011	1
	MV_HV - LV_LV	0.0207	0.0258	45.9	0.802	1
	LV_HV - MV_MV	0.01719	0.0257	45.2	0.669	1
	LV_HV - HV_MV	-0.05027	0.0256	44.4	-1.965	0.8349
	LV_HV - LV_LV	-0.00359	0.0176	132.3	-0.204	1
	MV_MV - HV_MV	-0.06746	0.0257	45.2	-2.624	0.1771
	MV_MV - LV_LV	-0.02078	0.0258	45.9	-0.805	1
	HV_MV - LV_LV	0.04668	0.0257	45.2	1.816	1
time	**1mo - 6mo**	-0.0341	0.0125	132	-2.741	**0.0209**
	1mo - 24mo	-0.1443	0.0124	132	-11.631	**<.0001**
	6mo - 24mo	-0.1102	0.0125	133	-8.78	**<.0001**
time*origin_dest						
1mo	HV_HV - MV_HV	0.0215	0.0355	115	0.605	1
	HV_HV - LV_HV	0.0047	0.0355	115	0.132	1
	HV_HV - MV_MV	0.0613	0.0355	115	1.725	1
	HV_HV - HV_MV	-0.0576	0.0302	132	-1.907	1
	HV_HV - LV_LV	0.0062	0.0355	115	0.174	1
	MV_HV - LV_HV	-0.0168	0.0355	115	-0.473	1
	MV_HV - MV_MV	0.0398	0.0302	132	1.318	1
	MV_HV - HV_MV	-0.0791	0.0355	115	-2.226	1
	MV_HV - LV_LV	-0.0153	0.0355	115	-0.431	1
	LV_HV - MV_MV	0.0566	0.0355	115	1.593	1
	LV_HV - HV_MV	-0.0623	0.0355	115	-1.753	1
	LV_HV - LV_LV	0.0015	0.0302	132	0.05	1
	MV_MV - HV_MV	-0.1189	0.0355	115	-3.346	**0.0498**
	MV_MV - LV_LV	-0.0551	0.0355	115	-1.551	1
	HV_MV - LV_LV	0.0638	0.0355	115	1.795	1
6mo	HV_HV - MV_HV	0.02898	0.0363	120	0.798	1

	HV_HV - LV_HV	0.04066	0.0355	115	1.144	1
	HV_HV - MV_MV	0.0432	0.0355	115	1.216	1
	HV_HV - HV_MV	-0.0008	0.0302	132	-0.026	1
	HV_HV - LV_LV	0.05794	0.0363	120	1.594	1
	MV_HV - LV_HV	0.01168	0.0363	120	0.321	1
	MV_HV - MV_MV	0.01422	0.0311	133	0.457	1
	MV_HV - HV_MV	-0.02978	0.0363	120	-0.82	1
	MV_HV - LV_LV	0.02897	0.0371	123	0.78	1
	LV_HV - MV_MV	0.00254	0.0355	115	0.072	1
	LV_HV - HV_MV	-0.04146	0.0355	115	-1.167	1
	LV_HV - LV_LV	0.01729	0.0311	133	0.555	1
	MV_MV - HV_MV	-0.044	0.0355	115	-1.238	1
	MV_MV - LV_LV	0.01474	0.0363	120	0.406	1
	HV_MV - LV_LV	0.05874	0.0363	120	1.617	1
24mo	HV_HV - MV_HV	-0.02216	0.0357	115	-0.621	1
	HV_HV - LV_HV	0.05633	0.0355	115	1.585	1
	HV_HV - MV_MV	0.04783	0.0363	120	1.316	1
	HV_HV - HV_MV	0.00962	0.0302	132	0.318	1
	HV_HV - LV_LV	0.02703	0.0355	115	0.761	1
	MV_HV - LV_HV	0.07849	0.0357	115	2.198	1
	MV_HV - MV_MV	0.06999	0.0314	134	2.232	1
	MV_HV - HV_MV	0.03178	0.0357	115	0.89	1
	MV_HV - LV_LV	0.04919	0.0357	115	1.377	1
	LV_HV - MV_MV	-0.0085	0.0363	120	-0.234	1
	LV_HV - HV_MV	-0.04671	0.0355	115	-1.315	1
	LV_HV - LV_LV	-0.0293	0.0302	132	-0.97	1
	MV_MV - HV_MV	-0.03821	0.0363	120	-1.051	1
	MV_MV - LV_LV	-0.0208	0.0363	120	-0.572	1
	HV_MV - LV_LV	0.01741	0.0355	115	0.49	1
1mo vs. 6mo	HV_HV	-0.0566	0.0302	132	-1.874	1
	MV_HV	-0.04912	0.0311	133	-1.578	1
	LV_HV	-0.02064	0.0302	132	-0.683	1
	MV_MV	-0.0747	0.0302	132	-2.473	0.264
	HV_MV	0.0002	0.0302	132	0.007	1
	LV_LV	-0.00486	0.0311	133	-0.156	1
1mo vs. 24mo	**HV_HV**	-0.15853	0.0302	132	-5.248	**<.0001**
	MV_HV	-0.20219	0.0304	134	-6.648	**<.0001**
	LV_HV	-0.1069	0.0302	132	-3.539	**0.01**
	MV_MV	-0.172	0.0312	133	-5.522	**<.0001**
	HV_MV	-0.09131	0.0302	132	-3.023	0.0542
	LV_LV	-0.1377	0.0302	132	-4.559	**0.0002**
6mo vs. 24mo	**HV_HV**	-0.10193	0.0302	132	-3.374	**0.0175**
	MV_HV	-0.15307	0.0316	136	-4.851	**0.0001**
	LV_HV	-0.08626	0.0302	132	-2.856	0.0898
	MV_MV	-0.0973	0.0312	133	-3.124	**0.0395**
	HV_MV	-0.09151	0.0302	132	-3.03	0.0531
	LV_LV	-0.13284	0.0311	133	-4.265	**0.0007**

Table A7 *Porites lobata* physiology

PAM

B. Fv/Fm normalized ((0hr-21hr)/0hr)

Shapiro-wilk

Model: residuals(lmer(ylossnorm~origin_dest*time*trt+(1|tank/colony)

W = 0.96389, p-value = 9.746e-06

Levene's HOV

	Df	F value	Pr(>F)
group	232	4.21E+29	**< 2.2e-16**

LMER

Model: ylossnorm ~ origin_dest * time * trt + (1 | colony)

Random effects:

Groups	Name	Variance	Std.Dev.
colony:tank	(Intercept)	6.65E-03	0.0816
tank	(Intercept)	6.44E-12	0.0000
Residual		4.91E-03	7.00E-02

ANOVA-like table for random-effects: Single term deletions

	npar	logLik	AIC	LRT	Df	Pr(>Chisq)
<none>	27	168.65	-283.29			
(1 | colony:tank)	26	148.49	-244.97	40	1.00E+00	**2.16E-10**
(1 | tank)	26	168.65	-285.29	0	1	1

Type III Analysis of Variance Table with Satterthwaite's method

	Sum Sq	Mean Sq	NumDF	DenDF	F value	Pr(>F)
origin_dest	**0.08983**	**0.01797**	**5**	**125**	**3.662**	**0.003989**
time	0.00504	0.00504	1	107	1.0264	0.313301
trt	**1.03215**	**1.03215**	**1**	**107**	**210.3789**	**< 2.2e-16**
origin_dest:time	0.0042	0.00084	5	125	0.1712	0.972812
origin_dest:trt	**0.08398**	**0.0168**	**5**	**125**	**3.4234**	**0.00622**
time:trt	0.00034	0.00034	1	107	0.069	0.79328
origin_dest:time:trt	0.01458	0.00292	5	125	0.5943	0.704345

Tukey's Test (Bonferroni corrected)

	contrast	estimate	SE	df	t.ratio	p.value
cont-heat	**1mo**	-0.257	0.0248	7	-10.379	**<.0001**
	6mo	-0.248	0.0249	12	-9.974	**<.0001**
1mo - 6mo	cont	-0.0223	0.0248	9	-0.9	0.7843
	heat	-0.0129	0.0249	9	-0.518	1
1mo*cont - heat	**HV_HV**	-0.276	0.0482	79	-5.729	**<.0001**
	MV_HV	-0.174	0.0482	79	-3.613	**0.0064**
	LV_HV	-0.311	0.0482	79	-6.462	**<.0001**
	HV_MV	-0.315	0.0482	79	-6.543	**<.0001**
	MV_MV	-0.164	0.0482	79	-3.403	**0.0126**
	LV_LV	-0.304	0.0482	79	-6.323	**<.0001**
6mo* cont - heat	**HV_HV**	-0.321	0.049	114	-6.55	**<.0001**
	MV_HV	-0.185	0.0489	106	-3.795	**0.003**
	LV_HV	-0.224	0.0491	110	-4.567	**0.0002**
	HV_MV	-0.342	0.0482	107	-7.108	**<.0001**
	MV_MV	-0.126	0.0478	106	-2.634	0.1164
	LV_LV	-0.29	0.0491	113	-5.916	**<.0001**

cont*1mo-6mo	HV_HV	-0.0144	0.0482	92	-0.299	1
	MV_HV	0.003	0.0484	89	0.062	1
	LV_HV	-0.04641	0.0489	97	-0.948	1
	HV_MV	-0.0191	0.0482	92	-0.397	1
	MV_MV	-0.0292	0.0478	91	-0.61	1
	LV_LV	-0.02734	0.0483	93	-0.566	1
heat*1mo-6mo	HV_HV	-0.05973	0.049	98	-1.218	1
	MV_HV	-0.00849	0.0486	94	-0.175	1
	LV_HV	0.04043	0.0483	90	0.836	1
	HV_MV	-0.0463	0.0482	92	-0.961	1
	MV_MV	0.0087	0.0482	92	0.181	1
	LV_LV	-0.01309	0.0489	98	-0.268	1
cont	HV_HV - MV_HV	0.017063	0.0341	152	0.501	1.00000
	HV_HV - LV_HV	-0.019437	0.0343	151	-0.567	1.00000
	HV_HV - HV_MV	0.00526	0.0222	106	0.237	1.00000
	HV_HV - MV_MV	-0.004769	0.0339	150	-0.141	1.00000
	HV_HV - LV_LV	-0.000542	0.034	147	-0.016	1.00000
	MV_HV - LV_HV	-0.036501	0.0343	155	-1.063	1.00000
	MV_HV - HV_MV	-0.011803	0.0341	152	-0.347	1.00000
	MV_HV - MV_MV	-0.021832	0.0228	113	-0.958	1.00000
	MV_HV - LV_LV	-0.017605	0.0341	151	-0.516	1.00000
	LV_HV - HV_MV	0.024697	0.0343	151	0.721	1.00000
	LV_HV - MV_MV	0.014669	0.0342	153	0.429	1.00000
	LV_HV - LV_LV	0.018895	0.0229	112	0.826	1.00000
	HV_MV - MV_MV	-0.010029	0.0339	150	-0.296	1.00000
	HV_MV - LV_LV	-0.005802	0.034	147	-0.17	1.00000
	MV_MV - LV_LV	0.004227	0.0339	149	0.125	1.00000
heat	**HV_HV - MV_HV**	0.135813	0.0345	152	3.939	**0.00370**
	HV_HV - LV_HV	0.011069	0.0344	150	0.322	1.00000
	HV_HV - HV_MV	-0.024912	0.0226	108	-1.101	1.00000
	HV_HV - MV_MV	0.148673	0.0343	151	4.333	**0.00080**
	HV_HV - LV_LV	0.000523	0.0346	154	0.015	1.00000
	MV_HV - LV_HV	-0.124744	0.0342	148	-3.646	**0.01100**
	MV_HV - HV_MV	-0.160725	0.0342	149	-4.705	**0.00020**
	MV_HV - MV_MV	0.01286	0.0224	109	0.574	1.00000
	MV_HV - LV_LV	-0.135291	0.0344	152	-3.928	**0.00390**
	LV_HV - HV_MV	-0.035981	0.034	147	-1.057	1.00000
	LV_HV - MV_MV	0.137604	0.034	147	4.041	**0.00260**
	LV_HV - LV_LV	-0.010547	0.0229	112	-0.461	1.00000
	HV_MV - MV_MV	0.173585	0.034	148	5.106	**<.0001**
	HV_MV - LV_LV	0.025435	0.0343	151	0.742	1.00000
	MV_MV - LV_LV	-0.14815	0.0343	151	-4.322	**0.00080**
1mo*control	HV_HV - MV_HV	0.0084	0.0481	148	0.175	1.0000
	HV_HV - LV_HV	-0.0035	0.0481	148	-0.073	1.0000
	HV_HV - HV_MV	0.0076	0.0313	106	0.243	1.0000
	HV_HV - MV_MV	0.0026	0.0481	148	0.054	1.0000
	HV_HV - LV_LV	0.0059	0.0481	148	0.123	1.0000
	MV_HV - LV_HV	-0.0119	0.0481	148	-0.248	1.0000
	MV_HV - HV_MV	-0.0008	0.0481	148	-0.017	1.0000
	MV_HV - MV_MV	-0.0058	0.0313	106	-0.185	1.0000

	MV_HV - LV_LV	-0.0025	0.0481	148	-0.052	1.0000
	LV_HV - HV_MV	0.0111	0.0481	148	0.231	1.0000
	LV_HV - MV_MV	0.0061	0.0481	148	0.127	1.0000
	LV_HV - LV_LV	0.0094	0.0313	106	0.3	1.0000
	HV_MV - MV_MV	-0.005	0.0481	148	-0.104	1.0000
	HV_MV - LV_LV	-0.0017	0.0481	148	-0.035	1.0000
	MV_MV - LV_LV	0.0033	0.0481	148	0.069	1.0000
1mo*heat	HV_HV - MV_HV	0.0258	0.0483	156	0.535	1.0000
	HV_HV - LV_HV	-0.03551	0.0489	154	-0.727	1.0000
	HV_HV - HV_MV	0.0029	0.0313	106	0.093	1.0000
	HV_HV - MV_MV	-0.0122	0.0477	153	-0.256	1.0000
	HV_HV - LV_LV	-0.00704	0.0482	146	-0.146	1.0000
	MV_HV - LV_HV	-0.06131	0.0491	162	-1.25	1.0000
	MV_HV - HV_MV	-0.0229	0.0483	156	-0.475	1.0000
	MV_HV - MV_MV	-0.038	0.0331	120	-1.148	1.0000
	MV_HV - LV_LV	-0.03284	0.0484	154	-0.678	1.0000
	LV_HV - HV_MV	0.03841	0.0489	154	0.786	1.0000
	LV_HV - MV_MV	0.02331	0.0485	159	0.48	1.0000
	LV_HV - LV_LV	0.02847	0.0334	118	0.853	1.0000
	HV_MV - MV_MV	-0.0151	0.0477	153	-0.316	1.0000
	HV_MV - LV_LV	-0.00994	0.0482	146	-0.206	1.0000
	MV_MV - LV_LV	0.00516	0.0479	151	0.108	1.0000
6mo*control	HV_HV - MV_HV	0.1103	0.0481	148	2.294	1.0000
	HV_HV - LV_HV	-0.0388	0.0481	148	-0.807	1.0000
	HV_HV - HV_MV	-0.0316	0.0313	106	-1.009	1.0000
	HV_HV - MV_MV	0.1146	0.0481	148	2.384	1.0000
	HV_HV - LV_LV	-0.0227	0.0481	148	-0.472	1.0000
	MV_HV - LV_HV	-0.1491	0.0481	148	-3.101	0.1385
	MV_HV - HV_MV	-0.1419	0.0481	148	-2.951	0.2207
	MV_HV - MV_MV	0.0043	0.0313	106	0.137	1.0000
	MV_HV - LV_LV	-0.133	0.0481	148	-2.766	0.3836
	LV_HV - HV_MV	0.0072	0.0481	148	0.15	1.0000
	LV_HV - MV_MV	0.1534	0.0481	148	3.191	0.1040
	LV_HV - LV_LV	0.0161	0.0313	106	0.514	1.0000
	HV_MV - MV_MV	0.1462	0.0481	148	3.041	0.1675
	HV_MV - LV_LV	0.0089	0.0481	148	0.185	1.0000
	MV_MV - LV_LV	-0.1373	0.0481	148	-2.856	0.2947
6mo*heat	HV_HV - MV_HV	0.16154	0.0494	155	3.267	0.0802
	HV_HV - LV_HV	0.06136	0.0491	152	1.249	1.0000
	HV_HV - HV_MV	-0.01817	0.0327	110	-0.556	1.0000
	HV_HV - MV_MV	0.18303	0.049	154	3.737	**0.0157**
	HV_HV - LV_LV	0.02394	0.0498	159	0.481	1.0000
	MV_HV - LV_HV	-0.10018	0.0487	147	-2.058	1.0000
	MV_HV - HV_MV	-0.17971	0.0485	149	-3.702	**0.0180**
	MV_HV - MV_MV	0.02149	0.032	111	0.671	1.0000
	MV_HV - LV_LV	-0.1376	0.0493	155	-2.789	0.3569
	LV_HV - HV_MV	-0.07953	0.0482	146	-1.649	1.0000
	LV_HV - MV_MV	0.12167	0.0482	146	2.523	0.7625
	LV_HV - LV_LV	-0.03742	0.0334	118	-1.12	1.0000
	HV_MV - MV_MV	0.2012	0.0481	148	4.185	**0.0029**
	HV_MV - LV_LV	0.04211	0.0489	154	0.862	1.0000
	MV_MV - LV_LV	-0.15909	0.0489	154	-3.255	0.0836

Table A7 *Porites lobata* physiology

CHL

D. Total Chlorophyll Retention (1-(control-heat)/control)

Shapiro-wilk

Model:resid(chlratio ~ time+origin_dest+(1 | colony:tank))

W = 0.94596, p-value = 0.0001359

Levene's HOV

	Df	F value	Pr(>F)
group	112	4.66E+29	**< 2.2e-16**

LMER

Model:lmer(chlrat ~ origin_dest * time + (1|tank/colony)

Random effects:

Groups	Name	Variance	Std.Dev.
colony:tank	(Intercept)	0.06794	0.2606
tank	(Intercept)	0	0
	Residual	0.04563	0.2136

ANOVA-like table for random-effects: Single term deletions

	npar	logLik	AIC	LRT	Df	Pr(>Chisq)
<none>	15	-36.564	103.13			
(1 | colony:tank)	14	-47.315	122.63	21.501	1	**3.54E-06**
(1 | tank)	14	-36.564	101.13	0	1	0.9997

Type III Analysis of Variance Table with Satterthwaite's method

	Sum Sq	Mean Sq	NumDF	DenDF	F value	Pr(>F)
origin_dest	0.1355	0.0271	5	60.212	0.5939	0.704615
time	0.3419	0.3419	1	51.5	7.4932	**0.008481**
origin_dest:time	0.20597	0.04119	5	60.212	0.9028	0.48529

Tukey's Test (Bonferroni corrected)

	contrast	estimate	SE	df	t.ratio	p.value
time	**1mo - 6mo**	-0.218	0.0799	4.54	-2.727	**0.0459**
1mo - 6mo	HV_HV	-0.166	0.157	48.2	-1.055	1
	MV_HV	-0.046	0.156	46.3	-0.295	1
	LV_HV	-0.363	0.152	42.5	-2.388	0.1287
	HV_MV	-0.112	0.155	46.3	-0.721	1
	MV_MV	-0.136	0.151	43.5	-0.896	1
	LV_LV	-0.474	0.154	45.9	-3.085	**0.0207**
1mo	HV_HV - MV_HV	-0.19843	0.1507	70.3	-1.317	1
	HV_HV - LV_HV	-0.07378	0.1507	70.3	-0.49	1
	HV_HV - HV_MV	-0.05723	0.0955	52.2	-0.599	1
	HV_HV - MV_MV	-0.16214	0.1507	70.3	-1.076	1
	HV_HV - LV_LV	0.00606	0.1507	70.3	0.04	1
	MV_HV - LV_HV	0.12465	0.1507	70.3	0.827	1
	MV_HV - HV_MV	0.1412	0.1507	70.3	0.937	1
	MV_HV - MV_MV	0.03629	0.0955	52.2	0.38	1
	MV_HV - LV_LV	0.20449	0.1507	70.3	1.357	1
	LV_HV - HV_MV	0.01655	0.1507	70.3	0.11	1
	LV_HV - MV_MV	-0.08836	0.1507	70.3	-0.586	1
	LV_HV - LV_LV	0.07984	0.0955	52.2	0.836	1
	HV_MV - MV_MV	-0.10491	0.1507	70.3	-0.696	1
	HV_MV - LV_LV	0.06329	0.1507	70.3	0.42	1

	MV_MV - LV_LV	0.1682	0.1507	70.3	1.116	1
6mo	HV_HV - MV_HV	-0.07879	0.1612	75.3	-0.489	1
	HV_HV - LV_HV	-0.27121	0.1575	71.4	-1.722	1
	HV_HV - HV_MV	-0.00356	0.1035	54.6	-0.034	1
	HV_HV - MV_MV	-0.13204	0.1567	71.5	-0.842	1
	HV_HV - LV_LV	-0.30208	0.159	73.9	-1.9	1
	MV_HV - LV_HV	-0.19242	0.1558	73.2	-1.235	1
	MV_HV - HV_MV	0.07523	0.1596	74.7	0.471	1
	MV_HV - MV_MV	-0.05325	0.1026	56.4	-0.519	1
	MV_HV - LV_LV	-0.22329	0.1576	76.7	-1.416	1
	LV_HV - HV_MV	0.26765	0.1559	70.9	1.717	1
	LV_HV - MV_MV	0.13917	0.1513	69.7	0.92	1
	LV_HV - LV_LV	-0.03087	0.1024	57.6	-0.302	1
	HV_MV - MV_MV	-0.12848	0.1551	70.9	-0.828	1
	HV_MV - LV_LV	-0.29852	0.1573	73.2	-1.898	1
	MV_MV - LV_LV	-0.17004	0.1531	73.1	-1.111	1
origin_dest	HV_HV - MV_HV	-0.14014	0.1102	72.8	-1.272	1
	HV_HV - LV_HV	-0.16996	0.1089	70.8	-1.561	1
	HV_HV - HV_MV	-0.03109	0.0703	53.4	-0.442	1
	HV_HV - MV_MV	-0.14748	0.1086	70.9	-1.357	1
	HV_HV - LV_LV	-0.14406	0.1094	72.1	-1.317	1
	MV_HV - LV_HV	-0.02982	0.1083	71.7	-0.275	1
	MV_HV - HV_MV	0.10906	0.1096	72.5	0.995	1
	MV_HV - MV_MV	-0.00734	0.07	54.3	-0.105	1
	MV_HV - LV_LV	-0.00392	0.109	73.5	-0.036	1
	LV_HV - HV_MV	0.13888	0.1084	70.6	1.282	1
	LV_HV - MV_MV	0.02249	0.1068	70	0.211	1
	LV_HV - LV_LV	0.0259	0.0699	54.9	0.371	1
	HV_MV - MV_MV	-0.11639	0.1081	70.6	-1.077	1
	HV_MV - LV_LV	-0.11297	0.1088	71.7	-1.038	1
	MV_MV - LV_LV	0.00342	0.1074	71.6	0.032	1

Table A7 *Porites lobata* physiology

E. Total Chlorophyll (control and heat)

Shapiro-wilk

Model:resid(totalchl ~ time+origin_dest+trt +(1 | colony:tank))

W = 0.97481, p-value = 0.0003173

Levene's HOV

	Df	F value	Pr(>F)
group	118	11.709	< 2.2e-16

LMER

Model:lmer(totalchl ~ origin_dest * time * trt + (1|tank/colony)

Random effects

Groups	Name	Variance	Std.Dev.
colony:tank	(Intercept)	4.54863	2.1328
tank	(Intercept)	0.07751	0.2784
	Residual	3.11907	1.7661

ANOVA-like table for random-effects: Single term deletions

	npar	logLik	AIC	LRT	Df	Pr(>Chisq)
<none>	27	-523.77	1101.5			
(1 | colony:tank)	26	-548.17	1148.3	48.797	1	**2.84E-12**
(1 | tank)	26	-523.8	1099.6	0.06	1	0.8068

Type III Analysis of Variance Table with Satterthwaite's method

	Sum Sq	Mean Sq	NumDF	DenDF	F value	Pr(>F)
origin_dest	9.981	1.996	5	122.924	0.64	0.6695898
time	109.616	109.616	1	10.895	35.1439	**0.0001029**
trt	152.861	152.861	1	10.895	49.0087	**2.38E-05**
origin_dest:time	32.358	6.472	5	122.924	2.0748	0.0730061
origin_dest:trt	12.853	2.571	5	122.924	0.8242	0.5347708
time:trt	41.012	41.012	1	10.895	13.1487	**4.04E-03**
origin_dest:time:trt	7.09	1.418	5	122.924	0.4546	0.8092409

Tukey's Test (Bonferroni corrected)

	contrast	estimate	SE	df	t.ratio	p.value
time	**1mo - 6mo**	2.86	0.481	9.09	5.932	**0.0002**
treatment	**cont - heat**	3.37	0.481	9.04	6.996	**0.0001**
cont-heat	**1mo**	5.09	0.681	7.13	7.463	**0.0003**
	6mo	1.61	0.68	12.01	2.367	0.0712
1mo - 6mo	**cont**	4.57	0.676	8.8	6.759	**0.0002**
	heat	1.09	0.685	9.42	1.597	0.2866
1mo*cont - heat	**HV_HV**	6.853	1.26	69.5	5.434	**<.0001**
	MV_HV	2.806	1.26	69.5	2.225	0.3519
	LV_HV	5.384	1.26	69.5	4.269	**0.0007**
	HV_MV	6.168	1.26	69.5	4.89	**0.0001**
	MV_MV	3.75	1.26	69.5	2.974	**0.0485**
	LV_LV	5.566	1.26	69.5	4.413	**0.0004**
6mo* cont - heat	HV_HV	2.562	1.3	105.4	1.966	0.6235
	MV_HV	1.548	1.3	99.2	1.191	1
	LV_HV	1.281	1.28	99	1	1
	HV_MV	2.09	1.29	101.7	1.62	1
	MV_MV	1.356	1.25	94.8	1.087	1
	LV_LV	0.857	1.28	101.7	0.67	1

1mo*control	HV_HV - MV_HV	3.2201	1.238	144	2.600	0.6172
	HV_HV - LV_HV	1.0979	1.238	144	0.887	1
	HV_HV - HV_MV	0.0062	0.79	105	0.008	1
	HV_HV - MV_MV	1.8121	1.238	144	1.463	1
	HV_HV - LV_LV	2.1074	1.238	144	1.702	1
	MV_HV - LV_HV	-2.1222	1.238	144	-1.714	1
	MV_HV - HV_MV	-3.2139	1.238	144	-2.595	0.6259
	MV_HV - MV_MV	-1.408	0.79	105	-1.783	1
	MV_HV - LV_LV	-1.1127	1.238	144	-0.899	1
	LV_HV - HV_MV	-1.0917	1.238	144	-0.882	1
	LV_HV - MV_MV	0.7142	1.238	144	0.577	1
	LV_HV - LV_LV	1.0095	0.79	105	1.278	1
	HV_MV - MV_MV	1.8059	1.238	144	1.458	1
	HV_MV - LV_LV	2.1012	1.238	144	1.697	1
	MV_MV - LV_LV	0.2953	1.238	144	0.238	1
1mo*heat	HV_HV - MV_HV	-0.8265	1.238	144	-0.667	1
	HV_HV - LV_HV	-0.3708	1.238	144	-0.299	1
	HV_HV - HV_MV	-0.6788	0.79	105	-0.859	1
	HV_HV - MV_MV	-1.2904	1.238	144	-1.042	1
	HV_HV - LV_LV	0.8205	1.238	144	0.663	1
	MV_HV - LV_HV	0.4557	1.238	144	0.368	1
	MV_HV - HV_MV	0.1477	1.238	144	0.119	1
	MV_HV - MV_MV	-0.4639	0.79	105	-0.587	1
	MV_HV - LV_LV	1.647	1.238	144	1.33	1
	LV_HV - HV_MV	-0.308	1.238	144	-0.249	1
	LV_HV - MV_MV	-0.9196	1.238	144	-0.743	1
	LV_HV - LV_LV	1.1913	0.79	105	1.508	1
	HV_MV - MV_MV	-0.6116	1.238	144	-0.494	1
	HV_MV - LV_LV	1.4993	1.238	144	1.211	1
	MV_MV - LV_LV	2.1109	1.238	144	1.705	1
6mo*control	HV_HV - MV_HV	-0.7215	1.242	152	-0.581	1
	HV_HV - LV_HV	-0.3115	1.258	149	-0.248	1
	HV_HV - HV_MV	0.7674	0.79	105	0.972	1
	HV_HV - MV_MV	-0.0815	1.229	149	-0.066	1
	HV_HV - LV_LV	0.1633	1.242	142	0.131	1
	MV_HV - LV_HV	0.41	1.263	158	0.325	1
	MV_HV - HV_MV	1.4889	1.242	152	1.198	1
	MV_HV - MV_MV	0.64	0.836	118	0.765	1
	MV_HV - LV_LV	0.8848	1.247	150	0.71	1
	LV_HV - HV_MV	1.0789	1.258	149	0.858	1
	LV_HV - MV_MV	0.23	1.249	155	0.184	1
	LV_HV - LV_LV	0.4748	0.843	116	0.563	1
	HV_MV - MV_MV	-0.8489	1.229	149	-0.691	1
	HV_MV - LV_LV	-0.6041	1.242	142	-0.486	1
	MV_MV - LV_LV	0.2448	1.233	147	0.199	1
6mo*heat	HV_HV - MV_HV	-1.7352	1.323	154	-1.311	1
	HV_HV - LV_HV	-1.5922	1.292	146	-1.232	1
	HV_HV - HV_MV	0.2958	0.855	110	0.346	1
	HV_HV - MV_MV	-1.2871	1.287	146	-1	1
	HV_HV - LV_LV	-1.5417	1.306	151	-1.181	1
	MV_HV - LV_HV	0.143	1.279	150	0.112	1

MV_HV - HV_MV	2.031	1.31	153	1.551	1
MV_HV - MV_MV	0.4482	0.847	114	0.529	1
MV_HV - LV_LV	0.1936	1.295	157	0.15	1
LV_HV - HV_MV	1.888	1.279	145	1.477	1
LV_HV - MV_MV	0.3052	1.242	142	0.246	1
LV_HV - LV_LV	0.0506	0.844	116	0.06	1
HV_MV - MV_MV	-1.5829	1.273	145	-1.243	1
HV_MV - LV_LV	-1.8374	1.292	150	-1.422	1
MV_MV - LV_LV	-0.2546	1.258	150	-0.202	1

Table A8 Ofu Pool Natural Bleaching

A. LMER

Model: lmer(totalchl ~ site* sample + (1|colony))

Type III Analysis of Variance Table with Satterthwaite's method

	Sum Sq	Mean Sq	NumDF	DenDF	F value	Pr(>F)
site	3.76E+00	1.88E+00	2.00E+00	2.54E+01	3.28E-01	0.72330
sample	1.74E+02	8.72E+01	2.00E+00	5.29E+01	1.52E+01	**0.00001**
site:sample	7.08E+00	1.77E+00	4.00E+00	5.28E+01	3.09E-01	0.87070

contrast	estimate	SE	df	t.ratio	p.value
donor - heat	3.54	0.642	52.8	5.515	**<.0001**
donor - cont	1.69	0.629	52.6	2.682	**0.0293**
heat - cont	-1.85	0.657	56.1	-2.82	**0.0199**

B. Pearson's product-moment correlation

donor vs. control

t = -1.290 df = 23 p-val = 0.210 cor = -0.260

C. Correlation test p-values of chl values and days over Bleaching Threshold

	heatchl	contchl	donorchl	days.31	days.32	days.33
heatchl	-	**0.000**	0.637	0.681	0.501	0.488
contchl	**0.000**	-	0.210	0.755	0.841	0.850
donorchl	0.637	0.210	-	0.952	0.884	0.878
days.31	0.681	0.755	0.952	-	**0.000**	**0.000**
days.32	0.501	0.841	0.884	**0.000**	-	**0.000**
days.33	0.488	0.850	0.878	**0.000**	**0.000**	-

Table A9 *P. lobata* traits and Ofu Temperature Metrics

Correlation matrix of *P. lobata* traits and temperature metrics of Ofu Island (sites combined)

	time	trt	wkgrate	mqy	totalchl	mean	min	mmm	dtr	maxdtr	dr90	days31	days32
time	1.00	0.00	0.23	-0.05	-0.37	1.00	0.96	0.93	0.89	0.77	0.24	0.96	0.93
trt		1.00	-0.01	-0.74	-0.45	0.00	-0.01	0.01	0.01	0.02	0.02	0.00	0.01
wkgrate			1.00	-0.13	-0.16	0.23	0.22	0.22	0.23	0.20	0.07	0.25	0.25
mqy				1.00	0.47	-0.05	-0.06	-0.03	-0.03	-0.03	0.02	-0.04	-0.04
totalchl					1.00	-0.37	-0.37	-0.32	-0.31	-0.26	-0.04	-0.37	-0.36
mean						1.00	0.96	0.94	0.89	0.77	0.26	0.97	0.93
min							1.00	0.80	0.78	0.68	-0.03	0.90	0.84
mmm								1.00	0.94	0.83	0.56	0.93	0.92
dtr									1.00	0.96	0.51	0.92	0.93
maxdtr										1.00	0.45	0.80	0.82
dr90											1.00	0.33	0.41
days31												1.00	0.99
days32													1.00

P-value matrix of correlations between *P. lobata* traits and temperature metrics of Ofu Island (sites combined)

	time	trt	wkgrate	mqy	totalchl	mean	min	mmm	dtr	maxdtr	dr90	days31	days32
time	0	1.00000	**0.00032**	0.42164	**0.00000**	**2.466e-31**	**1.438e-13**	**0.00000**	**0.00000**	**0.00000**	**0.00015**	**0.00000**	**0.00000**
trt		0	0.89027	**0.00000**	**0.00000**	0.99747	0.9371	0.91191	0.81744	0.75563	0.76119	0.95287	0.91248
wkgrate			0	**0.03843**	**0.01691**	**0.00028**	**0.0006**	**0.00056**	**0.00041**	**0.00178**	0.26022	**0.00008**	**0.00008**
mqy				0	**0.00000**	0.44240	0.3688	0.60281	0.62572	0.68468	0.75751	0.53416	0.57898
totalchl					0	**0.00000**	**3.936e-09**	**0.00000**	**0.00000**	**0.00005**	0.55723	**0.00000**	**0.00000**
mean						0	**4.328e-12**	**0.00000**	**0.00000**	**0.00000**	**0.00006**	**0.00000**	**0.00000**
min							0	**0.00000**	**0.00000**	**0.00000**	0.59485	**0.00000**	**0.00000**
mmm								0	**0.00000**	**0.00000**	**0.00000**	**0.00000**	**0.00000**
dtr									0	**0.00000**	**0.00000**	**0.00000**	**0.00000**
maxdtr										0	**0.00000**	**0.00000**	**0.00000**
dr90											0	**0.00000**	**0.00000**
days31												0	**0.00000**
days32													0

Table A9 *P. lobata* traits and Ofu Temperature Metrics

PERMANOVA of log-transformed *P. lobata* traits and temperature metrics of Ofu Island (sites combined)

Block=colony,method=Eucledian, Permutations=999

Time*Origin_Destination*Treatment

	Df	SumsOfSqs	MeanSqs	F.Model	R2
origin_dest	5	343.15	68.63	7.935	0.15457
Residuals	217	1876.85	8.649	0.84543	
Total	222	2220	1		

Pairwise Adonis

contrast	Df	SumsOfSqs	F.Model	R2	p.value
HV_HV vs HV_MV	1	162800.8145	281.316821	0.791735162	0.3000
HV_HV vs MV_HV	1	-1200.7095	-5.9938693	-0.08813719	0.5830
HV_HV vs MV_MV	1	1039250.227	1130.675413	0.942484443	0.2530
HV_HV vs LV_HV	1	47263.0709	64.7444868	0.4769585	0.1800
HV_HV vs LV_LV	1	-236.6987	-2.1951251	-0.03100246	0.5990
HV_MV vs MV_HV	1	-18632.1896	-29.9339812	-0.64980613	0.8510
HV_MV vs MV_MV	1	-46010.843	-34.0634531	-0.92221542	0.9780
HV_MV vs LV_HV	1	529618.1935	458.5639698	0.862669398	0.1350
HV_MV vs LV_LV	1	38912.3692	72.3219327	0.490910833	0.2370
MV_HV vs MV_MV	1	6936.5751	7.2530689	0.092687341	0.4630
MV_HV vs LV_HV	1	1434.8103	1.8600585	0.024847142	0.4920
MV_HV vs LV_LV	1	20404.1989	123.885501	0.622898604	0.2050
MV_MV vs LV_HV	1	-29474.9698	-19.1053802	-0.39074606	0.8050
MV_MV vs LV_LV	1	576.7593	0.6624034	0.009374198	0.4990
LV_HV vs LV_LV	1	-21899.3141	-31.944985	-0.79752773	0.8580

Time

	Df	SumsOfSqs	MeanSqs	F.Model	R2
time	1	1135.5	1135.53	231.4	0.5115
Residuals	221	1084.5	4.91	0.4885	
Total	222	2220	1		

Origin_Destination*Treatment

	Df	SumsOfSqs	MeanSqs	F.Model	R2
grptrt	11	503.1	45.736	5.6208	0.22662
Residuals	211	1716.9	8.137		0.77338
Total	222	2220			1

Pairwise Adonis

contrast	Df	SumsOfSqs	F.Model	R2	p.value
HV_HV.Control vs HV_HV.Heat	1	3.22E+03	57.89588	0.6232341	0.186

HV_HV.Control vs HV_MV.Control	1	-7.55E-01	-2.09531	-0.05835755	0.878
HV_HV.Control vs MV_HV.Control	1	3.57E+00	8.395861	0.18096141	0.116
HV_HV.Control vs MV_MV.Control	1	-7.62E+02	-17.920832	-1.04928011	0.994
HV_HV.Control vs LV_HV.Control	1	1.99E+02	45.312864	0.57131797	0.192
HV_HV.Control vs LV_LV.Control	1	2.13E+03	739.296273	0.94989055	0.125
HV_HV.Heat vs HV_MV.Heat	1	-1.03E+03	-15.157797	-0.80445992	0.895
HV_HV.Heat vs MV_HV.Heat	1	1.75E+03	23.430754	0.4079827	0.268
HV_HV.Heat vs MV_MV.Heat	1	5.79E+05	848.780358	0.96366858	0.383
HV_HV.Heat vs LV_HV.Heat	1	4.40E+04	596.9118	0.94461252	0.221
HV_HV.Heat vs LV_LV.Heat	1	-9.27E+02	-14.460067	-0.82440832	0.704
HV_MV.Heat vs HV_MV.Control	1	3.73E+04	3685.507827	0.99006046	**0.001**
HV_MV.Heat vs MV_HV.Heat	1	3.36E+03	126.608681	0.77860961	0.21
HV_MV.Heat vs MV_MV.Heat	1	-9.85E+03	-16.548449	-0.94825088	0.797
HV_MV.Heat vs LV_HV.Heat	1	-2.01E+02	-7.437364	-0.25157989	0.624
HV_MV.Heat vs LV_LV.Heat	1	1.90E+02	13.694038	0.28712264	0.304
HV_MV.Control vs MV_HV.Control	1	9.84E+01	170.839136	0.81804177	**0.028**
HV_MV.Control vs MV_MV.Control	1	-7.89E+02	-18.494028	-1.1204447	1
HV_MV.Control vs LV_HV.Control	1	4.00E+01	8.757446	0.20481686	0.305
HV_MV.Control vs LV_LV.Control	1	4.20E+01	13.858034	0.2621746	0.219
MV_HV.Control vs MV_HV.Heat	1	9.05E+03	553.954731	0.93738945	**0.014**
MV_HV.Control vs MV_MV.Control	1	-7.11E+02	-16.640477	-0.90636762	0.982
MV_HV.Control vs LV_HV.Control	1	9.48E+02	204.473959	0.85742678	0.107
MV_HV.Control vs LV_LV.Control	1	3.26E+04	10536.2356	0.99631214	**0.029**
MV_HV.Heat vs MV_MV.Heat	1	-6.03E+03	-10.021514	-0.41793772	0.697
MV_HV.Heat vs LV_HV.Heat	1	1.40E+03	42.248519	0.5331143	0.327
MV_HV.Heat vs LV_LV.Heat	1	-2.40E+02	-11.672602	-0.52279276	0.949
MV_MV.Heat vs MV_MV.Control	1	3.69E+04	55.272671	0.6333331	0.302
MV_MV.Heat vs LV_HV.Heat	1	-8.21E+03	-14.006944	-0.66721793	0.668
MV_MV.Heat vs LV_LV.Heat	1	1.76E+04	28.19827	0.46842326	0.317
MV_MV.Control vs LV_HV.Control	1	-1.97E+02	-3.746183	-0.13745534	0.638
MV_MV.Control vs LV_LV.Control	1	-8.68E+01	-1.961728	-0.05763302	0.597
LV_HV.Heat vs LV_HV.Control	1	4.59E+04	2002.713047	0.98330644	0.117
LV_HV.Heat vs LV_LV.Heat	1	-2.23E+02	-10.548176	-0.43138607	0.586
LV_HV.Control vs LV_LV.Control	1	-2.18E+01	-3.008908	-0.09405454	0.752
LV_LV.Heat vs LV_LV.Control	1	2.48E+03	412.95531	0.91981385	**0.001**

A10 *Porites lobata* mtDNA

	Source of variation	% variation	df	σ^2	P-value	φST	Nucleotide Diversity
PCr							
	Among populations	12.32713	2	0.148	0.061	0.12327	π = 0.0030
	Within populations	87.67287	23	1.054			
NAD5							
	Among populations	1.02421	2	0.005	0.353	0.01024	π = 0.0015
	Within populations	98.97579	25	0.496			
COI							
	Among populations	2.03547	2	0.01	0.351	0.02035	π = 0.0011
	Within populations	97.96453	21	0.495			

Based on an Analysis of Molecular Variance (AMOVA) calculated assuming an F-distribution with 10 000 permutations.

A11 Symbiodiniaceae Clade Proportion

Origin	Destination	Treatment	Clade A	Clade B	Clade C	Clade D	Total
HV	HV	control	0.0280	0.3298	0.6177	0.0210	0.9965
		heat	0.0375	0.6233	0.3087	0.0265	0.9960
	MV	control	0.0288	0.3395	0.6112	0.0215	1.0010
		heat	0.0347	0.1853	0.7528	0.0264	0.9992
MV	HV	control	0.0386	0.1854	0.7446	0.0213	0.9899
		heat	0.0542	0.3926	0.5140	0.0350	0.9958
	MV	control	0.0306	0.0390	0.9082	0.0220	0.9998
		heat	0.0388	0.4006	0.5326	0.0307	1.0027

A12 *P. lobata* DESeq Results (FDR 5%)

ORIGIN_DEST+TRT	Upreg DEG	% Up	Down DEG	% Down	Total DEG
	3116	39%	2716	34%	5832
ORIGIN_DEST					
HV_HV HEATvsCONT	2281	28%	1667	21%	3948
HV_MV HEATvsCONT	2327	29%	1759	22%	4086
MV_HV HEATvsCONT	1940	24%	1546	19%	3486
MV_MV HEATvsCONT	1886	23%	1611	20%	3497
HEAT ORIGINvsDEST					
HV_MVvsHV_HV	38	0.51%	97	1.30%	135
MV_MVvsHV_MV	38	0.51%	60	0.80%	98
HV_HVvsHV_MV	0	0%	0	0%	0
MV_HVvsMV_MV	0	0%	0	0%	0
CONTROL ORIGINvsDEST					
HV_MVvsHV_HV	1	0.01%	2	0.03%	3
MV_MVvsHV_MV	2	0.03%	0	0%	2
HV_HVvsHV_MV	0	0%	0	0%	0
MV_HVvsMV_MV	0	0%	2	0.03%	2

A13 PCA Adonis for *P. lobata* (free permutation =999)

Origin_Destination*Trt	Df	SumsOfSqs	MeanSqs	F.Model	R2	Pr(>F)
	7	138263	19751.9	3.4071	0.39849	**0.001**
Residuals	36	208704	5797.3		0.60151	
Total	43	346967			1	

Paiwise Contrasts	SumsOfSqs	F.Model	R2	p.value	p.adjusted
HV_HV.C vs HV_HV.H	-178.400	-2.332	-0.304	0.922	1.000
HV_HV.C vs HV_MV.C	-6556.643	-4.827	-0.933	0.685	1.000
HV_HV.C vs MV_HV.C	-99.530	-4.091	-0.833	0.839	1.000
HV_HV.C vs MV_MV.C	54.849	2.254	0.200	0.387	1.000
HV_HV.H vs HV_MV.H	3909.528	47.518	0.826	0.195	1.000
HV_HV.H vs MV_HV.H	2061.965	31.096	0.776	0.426	1.000
HV_HV.H vs MV_MV.H	9767.085	158.202	0.946	0.360	1.000
HV_MV.C vs HV_MV.H	-6484.320	-4.754	-0.906	0.672	1.000
HV_MV.C vs MV_HV.C	-5899.819	-3.973	-0.790	0.592	1.000
HV_MV.C vs MV_MV.C	-5537.894	-3.730	-0.708	0.604	1.000
HV_MV.H vs MV_HV.H	682.786	18.764	0.676	0.177	1.000
HV_MV.H vs MV_MV.H	290.536	9.131	0.504	0.203	1.000
MV_HV.H vs MV_HV.C	5520.983	870.046	0.991	0.121	1.000
MV_HV.H vs MV_MV.H	40.472	5.361	0.401	0.400	1.000
MV_HV.C vs MV_MV.C	0.000	NaN	NaN	NA	NA
MV_MV.C vs MV_MV.H	1.434	1.192	0.130	0.481	1.000

Trt	Df	SumsOfSqs	MeanSqs	F.Model	R2	Pr(>F)
	1	112135	112135	20.055	0.32319	**0.001**
Residuals	42	234832	5591		0.67681	
Total	43	346967			1	
Total	43	346967			1	

Paiwise Contrasts	SumsOfSqs	F.Model	R2	p.value	p.adjusted
HV_HV vs HV_MV	1177.166	3.345	0.132	0.408	1.000

HV_HV vs MV_HV	-508.995	-1.653	-0.090	0.624	1.000
HV_HV vs MV_MV	5896.321	197.320	0.908	**0.031**	0.465
HV_MV vs MV_HV	19255.270	30.257	0.602	0.414	1.000
HV_MV vs MV_MV	516.844	1.442	0.067	0.441	1.000
MV_HV vs MV_MV	-2693.546	-8.684	-0.932	0.689	1.000

HEAT Origin_Destination	Df	SumsOfSqs	MeanSqs	F.Model	R2	Pr(>F)
	3	16775	5591.6	0.65923	0.099	0.969
Residuals	18	152674	8481.9		0.901	
Total	21	169449			1	

CONTROL Origin_Destination	Df	SumsOfSqs	MeanSqs	F.Model	R2	Pr(>F)
	3	18457	6152.4	0.73344	0.10892	0.905
Residuals	18	150992	8388.4		0.89108	
Total	21	169449			1	

A14 Gene Ontology (GO) Functional Enrichment of Filtered 8069 Genes in *P. lobata's* Response to Heat Stress

Run paramete largest GO category as fraction of all genes (largest) : 0.1
smallest GO category as # of genes (smallest) : 5
clustering threshold (clusterCutHeight) : 0.25

Molecular Functions (MF)	**Biological Processes**	**Cellular Components**
2923 categories, 5366 genes; size range 5-536.6	11302 categories, 5607 genes; size range 5-560.7	1534 categories, 6021 genes; size range 5-6(
29 too broad	106 too broad	23 too broad
1912 too small	6386 too small	804 too small
982 remaining	4810 remaining	707 remaining
	Removing redundancy:	
775 non-redundant GO categories of good size	3473 non-redundant GO categories of good size	578 non-redundant GO categories of good s
	Secondary clustering:	
	MWU test	
35 GO terms at 10% FDR	**199 GO terms at 10% FDR**	**45 GO terms at 10% FDR**
GO terms dispayed: 23	GO terms dispayed: 102	GO terms dispayed: 32
Good genes accounted for: 1376 out of 4580 (30%)	Good genes accounted for: 3068 out of 5001 (61%)	Good genes accounted for: 1396 out of 443

A15 Discriminant Analysis of Principal Components for *P. lobata* HV and MV Reciprocal Transplant Experiment

Iterations = 5001:74976

Thinning interval = 25

Sample size = 2800

Location effects: LD1 ~ ori + ori:away

MCMCglmm Heat	post.mean	l-95% CI	u-95% CI	eff.samp	pMCMC
(Intercept)	1.3499	0.5593	2.1395	2800	**0.00214**
oriMV	-2.9791	-4.2126	-1.8297	2800	**< 4e-04**
oriHV:away	-0.219	-0.866	0.3977	2800	0.44643
oriMV:away	0.1238	-0.6158	0.7854	2616	0.70143

Difference in Magnitudes	p-value
oriHV vs. oriMV	1
oriHV:away vs. oriMV:away	0.47

MCMCglmm Control	post.mean	l-95% CI	u-95% CI	eff.samp	pMCMC
(Intercept)	0.85173	0.01646	1.71634	2800	0.05357
oriMV	-1.86191	-3.10729	-0.65134	2800	**0.00857**
oriHV:away	-0.15756	-0.61496	0.26086	2800	0.45643
oriMV:away	0.36087	-0.12795	0.85618	2800	0.13143

Difference in Magnitudes	p-value
oriHV vs. oriMV	0.98
oriHV:away vs. oriMV:away	0.73

A16 Frontloaded Gene Exploration in *P. lobata*

Comparing Unique DEGs Among Native HV_HV and Transplant HV_MV

537 Unique DEGs in HV_MV not in HV_HV

Log2Fold Change Summay

	Min.	1stQ	Median	Mean	3rdQ	Max.	Variance	StdDev
HV_MV	-4.9406	-0.6986	0.1048	0.2279	1.0171	9.8128	2.0135	1.4190
HV_HV	-4.5797	-0.6680	0.1068	0.2490	0.9933	11.1025	1.9162	1.3843

Chi-Square Goodness-of-Fit Test between 537 Unique DEG in HV_MV not in HV_HV

	Observed	Expected	X-squared	df	p-value
Upreg	249	1	246.02	1	**<2.2e-16**
Downreg	0	287	287	1	**<2.2e-16**

Regression of BaseMean ratio against Log2FoldChange ratio between 247 Upreg Control HV_HV to HV_MV

lm(y~x)

	Estimate	Std.Error	t value	Pr(>|t|)
(Intercept)	0.87066	2.31E-02	37.72	**<2e-16**
x	-0.75272	0.04029	-18.68	**<2e-16**
Multiple R-squared:	0.5876			
Adjusted R-squared:	0.5859			
F-statistic:	349.1 on 1 and 245 DF			

Frontloading DESeq Comparison between HV_HV and HV_MV Controls

adjusted p-value < 0.05	Upreg DEG	Up %	Down DEG	Down %
	0	0%	0	0%

366 Unique DEGs in HV_HV not in HV_MV

Chi-Square Goodness-of-Fit Test between 366 Unique DEG in HV_HV not in HV_MV

	Observed	Expected	X-squared	df	p-value
Upreg	196	0	196	1	**<2.2e-16**
Downreg	0	170	170	1	**<2.2e-16**

Regression of BaseMean ratio against Log2FoldChange ratio between 195 Upreg Control HV_MV to HV_HV

lm(y~x)

	Estimate	Std.Error	t value	Pr(>|t|)
(Intercept)	1.0248	1.60E-02	63.9	**<2e-16**
x	-0.32061	0.03202	-10.01	**<2e-16**
Multiple R-squared:	0.3419			
Adjusted R-squared:	0.3385			
F-statistic:	100.3 on 1 and 193 DF			

Frontloading DESeq Comparison between HV_MV and HV_HV Controls

adjusted p-value < 0.05	Upreg DEG	Up %	Down DEG	Down %
	0	0%	0	0%

Chi-Square Goodness-of-Fit Test between 430 Unique DEG in MV_MV not in MV_HV

	Observed	Expected	X-squared	df	p-value
Upreg	160	0	160	1	**<2.2e-16**
Downreg	0	270	270	1	**<2.2e-16**

Regression of BaseMean ratio against Log2FoldChange ratio between 160 Upreg Control MV_HV to MV_MV

lm(y~x)

	Estimate	Std.Error	t value	Pr(>|t|)
(Intercept)	1.01705	2.56E-02	39.71	**< 2e-16**
x	-0.42472	0.05606	-7.576	**2.82E-12**
Multiple R-squared:	0.2665			
Adjusted R-squared:	0.2618			
F-statistic:	57.39 on 1 and 158 DF			

Frontloading DESeq Comparison between MV_HV and MV_MV Controls

adjusted p-value < 0.05	Upreg DEG	Up %	Down DEG	Down %
	0	0%	2	0.03%

384 Unique DEGs in MV_HV not in MV_MV

Chi-Square Goodness-of-Fit Test between 384 Unique DEG in MV_HV not in MV_MV

	Observed	Expected	X-squared	df	p-value
Upreg	208	0	208	1	**<2.2e-16**
Downreg	0	176	176	1	**<2.2e-16**

Regression of BaseMean ratio against Log2FoldChange ratio between 205 Upreg Control MV_MV to MV_HV

lm(y~x)

	Estimate	Std.Error	t value	Pr(>|t|)
(Intercept)	0.69323	4.03E-02	17.22	**<2e-16**
x	-1.50909	0.05911	-25.53	**<2e-16**
Multiple R-squared:	0.7625			
Adjusted R-squared:	0.7614			
F-statistic:	651.9 on 1 and 203 DF			

Frontloading DESeq Comparison between MV_MV and MV_HV Controls

adjusted p-value < 0.05	Upreg DEG	Up %	Down DEG	Down %
	2	0.03%	0	0%

A17 DESeq results for Symbiodiniaceae (FDR 5%)

ORIGIN_DEST+TRT	Upreg DEG	Up %	Down DEG	Down %	Total
	2659	17	3349	22%	6008
ORIGIN_DEST					
HV_HV HEATvsCONT	546	4%	558	4%	1104
HV_MV HEATvsCONT	1115	7.30%	1540	10%	2655
MV_HV HEATvsCONT	1	0.01%	0	0%	1
MV_MV HEATvsCONT	4	0.03%	0	0%	4
HEAT ORIGINvsDEST					
HV_MVvsHV_HV	0	0.00%	0	0.00%	0
MV_MVvsHV_MV	0	0.00%	0	0.00%	0
HV_HVvsHV_MV	0	0%	0	0%	0
MV_HVvsMV_MV	0	0%	0	0%	0
CONTROL ORIGINvsDEST					
HV_MVvsHV_HV	0	0.00%	0	0.00%	0
MV_MVvsHV_MV	0	0.00%	1	0%	1
HV_HVvsHV_MV	0	0%	0	0%	0
MV_HVvsMV_MV	0	0%	0	0.00%	0

A18 PCA Adonis for Symbiodiniaceae (free permutation =999)

Origin_Destination*Trt	Df	SumsOfSqs	MeanSqs	F.Model	R2	Pr(>F)
	7	145791	20827	1.4278	0.2173	**0.02**
Residuals	36	525138	14587		0.7827	
Total	43	670929			1	

Paiwise Contrasts	SumsOfSqs	F.Model	R2	p.value	p.adjusted
HV_HV.C vs HV_HV.H	-30186.156	-4.723	-0.895	0.650	1.000
HV_HV.C vs HV_MV.C	5485.076	1658.251	0.994	0.272	1.000
HV_HV.C vs MV_HV.C	137.578	10.961	0.549	0.144	1.000
HV_HV.C vs MV_MV.C	-34376.783	-4.839	-1.163	0.945	1.000
HV_HV.H vs HV_MV.H	-16519.183	-2.573	-0.346	0.806	1.000
HV_HV.H vs MV_HV.H	#########	15.206	0.628	0.388	1.000
HV_HV.H vs MV_MV.H	-29082.926	-4.035	-0.813	0.778	1.000
HV_MV.C vs HV_MV.H	20265.352	599.567	0.984	**0.019**	1.000
HV_MV.C vs MV_HV.C	-28.651	-3.228	-0.559	0.961	1.000
HV_MV.C vs MV_MV.C	-34324.163	-4.835	-1.161	0.892	1.000
HV_MV.H vs MV_HV.H	12071.384	203.061	0.958	0.192	1.000
HV_MV.H vs MV_MV.H	83146.222	560.382	0.984	0.445	1.000
MV_HV.H vs MV_HV.C	539.395	15.583	0.661	0.429	1.000
MV_HV.H vs MV_MV.H	-107.908	-0.723	-0.099	0.768	1.000
MV_HV.C vs MV_MV.C	-31760.917	-3.971	-0.986	0.917	1.000
MV_MV.C vs MV_MV.H	-31557.832	-3.890	-0.947	0.789	1.000

Trt	Df	SumsOfSqs	MeanSqs	F.Model	R2	Pr(>F)
	1	65326	65326	4.5305	0.09737	**0.002**
Residuals	42	605603	14419		0.90263	
Total	43	670929			1	

Origin_Destination	Df	SumsOfSqs	MeanSqs	F.Model	R2	Pr(>F)
	3	32854	10951	0.68653	0.04897	0.942
Residuals	40	638075	15952		0.95103	

Total	43	670929			1
Paiwise Contrasts	SumsOfSqs	F.Model	R2	p.value	p.adjusted
HV_HV vs HV_MV	13101.149	5.305	0.194	0.405	1.000
HV_HV vs MV_HV	92756.047	53.710	0.729	0.139	1.000
HV_HV vs MV_MV	-32529.418	-9.702	-0.942	0.928	1.000
HV_MV vs MV_HV	35898.888	33.520	0.626	0.128	1.000
HV_MV vs MV_MV	15114.264	5.604	0.219	0.492	1.000
MV_HV vs MV_MV	-16385.337	-8.636	-0.922	0.973	1.000

HEAT Origin_Destination	Df	SumsOfSqs	MeanSqs	F.Model	R2	Pr(>F)
	3	38295	12765	0.79404	0.11687	0.819
Residuals	18	289368	16076		0.88313	
Total	21	327663			1	

CONTROL Origin_Destination	Df	SumsOfSqs	MeanSqs	F.Model	R2	Pr(>F)
	3	37197	12399	0.76837	0.11352	0.839
Residuals	18	290466	16137		0.88648	
Total	21	327663			1	

A19 Gene Ontology (GO) Functional Enrichment of Filtered 7502 Genes in Response to Heat Stress

Run parameters: largest GO category as fraction of all genes (largest) : 0.1
smallest GO category as # of genes (smallest) : 5
clustering threshold (clusterCutHeight) : 0.25

Molecular Functions (MF)	**Biological Processes**	**Cellular Components**
2036 categories, 4336 genes; size range 5-433.6	6498 categories, 3960 genes; size range 5-396	934 categories, 4073 genes; s
30 too broad	45 too broad	16 too broad
1399 too small	4318 too small	557 too small
607 remaining	2135 remaining	361 remaining
	Removing redundancy:	
464 non-redundant GO categories of good size	1339 non-redundant GO categories of good size	268 non-redundant GO categ
	Secondary clustering:	
	MWU test	
22 GO terms at 10% FDR	**15 GO terms at 10% FDR**	**28 GO terms at 10% FDR**
GO terms dispayed: 16	GO terms dispayed: 10	GO terms dispayed: 22
Good genes accounted for: 1020 out of 2874 (35%)	Good genes accounted for: 776 out of 2629 (30%)	Good genes accounted for: 5

A20 Discriminant Analysis of Principal Components for Symbiodiniaceae HV and MV Reciprocal Transplant Experiment

Iterations = 5001:74976
Thinning interval = 25
Sample size = 2800
Location effects: LD1 ~ ori + ori:away

MCMCglmm Heat	post.mean	l-95% CI	u-95% CI	eff.samp	pMCMC
(Intercept)	1.34441	0.29978	2.17416	2800	**0.01**
oriMV	-2.91915	-4.31507	-1.57974	2800	**0.00214**
oriHV:away	-0.79559	-1.55276	0.08698	2800	0.06643
oriMV:away	0.50956	-0.34523	1.45268	2800	0.24143

Difference in Magnitudes	p-value
oriHV vs. oriMV	1
oriHV:away vs. oriMV:away	0.32

MCMCglmm Control	post.mean	l-95% CI	u-95% CI	eff.samp	pMCMC
(Intercept)	1.01094	0.09321	1.85141	3035	**0.02857**
oriMV	-2.20778	-3.46714	-0.92148	2800	**0.00214**
oriHV:away	-0.20387	-0.67665	0.22481	2800	0.34643
oriMV:away	0.25377	-0.23118	0.72062	3058	0.28714

Difference in Magnitudes	p-value
oriHV vs. oriMV	0.95
oriHV:away vs. oriMV:away	0.55

A21 Comparing Unique DEGs Among Native HV_HV and Transplant HV_M

1831 Unique DEGs in HV_MV not in HV_HV

Log2Fold Change Summay

	Min.	1stQ	Median	Mean	3rdQ	Max.	Variance
HV_MV	-2.512286	-0.331967	0.001938	-0.053655	0.279791	1.575691	0.2161658
HV_HV	-2.29658	-0.28745	-0.01576	-0.03384	0.23312	1.48901	0.1466408

Chi-Square Goodness-of-Fit Test between 1831 Unique DEG in HV_MV not in HV_HV

	Observed	Expected	X-squared	df	p-value
Upreg	715	21	654.4	1	**<2.2e-16**
Downreg	27	1068	989.66	1	**<2.2e-16**

Regression of BaseMean ratio against Log2FoldChange ratio between 731 Upreg Control HV_HV to HV_MV

lm(y~x)

	Estimate	Std.Error	t value	Pr(>|t|)
(Intercept)	1.02266	5.57E-03	183.6	**<2e-16**
x	-0.45843	0.02106	-21.77	**<2e-16**
Multiple R-squared:	0.394			
Adjusted R-squared:	0.3932			
474 on 1 and 729 DF				

Frontloading DESeq Comparison between HV_HV and HV_MV

adjusted p-value < 0.05	Upreg DEG	Up %	Down DEG	Down %
	0	0%	0	0%

280 Unique DEGs in HV_HV not in HV_MV

Chi-Square Goodness-of-Fit Test between 280 Unique DEG in HV_HV not in HV_MV

	Observed	Expected	X-squared	df	p-value
Upreg	167	0	167	1	**<2.2e-16**
Downreg	0	113	113	1	**<2.2e-16**

Regression of BaseMean ratio against Log2FoldChange ratio between 165 Upreg Control HV_MV to HV_HV

lm(y~x)

	Estimate	Std.Error	t value	Pr(>|t|)
(Intercept)	0.96124	1.39E-02	69.254	**< 2e-16**
x	-0.38835	0.0509	-7.629	**1.87E-12**
Multiple R-squared:	0.2631			
Adjusted R-squared:	0.2586			
F-statistic:	58.2 on 1 and 163 DF			

Frontloading DESeq Comparison between HV_MV and HV_HV

adjusted p-value < 0.05	Upreg DEG	Up %	Down DEG	Down %
	0	0%	0	0%

VITA

Courtney Nicole Klepac
Department of Biological Sciences
Old Dominion University, Norfolk, VA 23529

EDUCATION

Old Dominion University	Ecological Sciences	
Florida Atlantic University	Biological Sciences	MS, 2014
Texas A&M University at Galveston	Marine Biology	BS, 2008

SELECTED PUBLICATIONS

Klepac C.N., Beal J., Kenkel C.D., Sproles A., Polinski J.M., Williams M.A., Matz M.V., Voss J.D. (2015) Seasonal stability of coral-*Symbiodinium* associations in the subtropical coral habitat of St. Lucie Reef, Florida. Marine Ecology Progress Series 532:137-151.

Klepac, C.N., Barshis D.J. (2020) Reduced thermal tolerance of massive coral species in a highly variable environment. Proceeding of the Royal Society B 287: 20201379. http://dx.doi.org/10.1098/rspb.2020.1379.